PERFORMANCE OF THE VERTICAL ROLLER MILL IN A MINERAL PROCESSING APPLICATION WHEN COUPLED WITH INTERNAL AND EXTERNAL CLASSIFIERS

Warren Little

A thesis submitted to the University of Cape Town
in fulfilment of the requirements for the degree of

DOCTOR OF PHILOSOPHY

05 November 2020

Centre for Minerals Research

Department of Chemical Engineering

UNIVERSITY OF CAPE TOWN

SYNOPSIS

Comminution is applied in all mineral processing plants where mineral liberation is needed for separation and concentration of valuable minerals. The process is energy intensive and is predominantly carried out in tumbling mills which are known to be highly inefficient. Comminution technologies utilised in other industries, such as the vertical roller mill (VRM), a high compression dry grinding device, have the potential to contribute towards enhancing the energy efficiency of comminution and the sustainability of mineral processing.

The vertical roller mill is used extensively in cement and coal grinding applications, where it is known to be more energy efficient than traditional tumbling mills. The VRM has a larger reduction ratio and greater flexibility in terms of product quality control and throughput. However, in the majority of operations where the vertical roller mill is applied, the device is coupled with an internal dynamic air classifier. These classifiers are significantly more energy intensive than other classifiers typically used in the mineral processing industry. Operating the vertical roller mill with less energy intensive classification devices could have the potential to further reduce the total comminution circuit energy. Reducing the comminution energy usage in mineral processing is important, however there are other factors which also need to be considered before the vertical roller mill can be considered as a viable alternative to tumbling mills. The effect of grinding with the vertical roller mill on product quality and mineral liberation, and their impact on downstream processing is of critical importance and has not yet been extensively investigated.

This study investigates the grinding of the platinum group mineral (PGM) bearing Platreef ore, in a pilot scale vertical roller mill. The research explores the effects of milling variables and methods of classification on the mill performance, energy consumption, throughput, product characteristics and flotation response. The energy efficiency of the vertical roller mill and product flotation response is also compared with that of a traditional ball milling circuit.

Vertical roller mill products of three target grinds, typical to primary, secondary and tertiary grinds in PGM circuit, were generated with the VRM operated in the standard airflow mode, with the internal dynamic air classifier, for a variety of grinding pressures (an online control used for maintaining product quality), and dam ring heights (a design variable affecting

residence time on the grinding table). The specific grinding energy for the vertical roller mill was found to increase as the target grind became finer, conforming to general comminution theory. Vertical roller mill specific grinding energies were lower than those for a ball mill at all product sizes, and when estimates of classification energy and scale-up of the VRM are included, the specific energy for the vertical roller mill is up to 35% lower than for a ball mill in closed circuit. Grinding at higher pressures yielded greater throughputs and was found to generate products of less steep particle size distribution (PSD), but did not affect specific grinding energy. The effect of varying dam ring height was found to be target grind dependent. Higher dam rings yielded products with a greater proportion of fines, for higher specific grinding energies with the differences more pronounced at coarser target grinds.

The grinding component of the vertical roller mill was operated in conjunction with three classification devices - the internal dynamic air classifier, external hybrid air classifier and an external vibrating screen. The external air classification circuit had a lower throughput than the internal air classification circuit, and operated with a 20 - 40% higher specific grinding energy. When including pilot scale estimations for classification energy, the external air classification circuit overall specific energy is lower at intermediate and coarse grinds, and comparable at finer target grinds, to that of the internal air classification circuit. The specific grinding energy in the VRM - external screening system was higher than both air classification circuits, however when considering the lower energy intensity of screening, this circuit may prove more efficient.

The flotation response of the tumbling mill product and the vertical roller mill product prepared under different operating conditions in circuits with different classification devices was assessed using a standard reagent suite, in terms of platinum, palladium, gold (3E PGE), and copper, nickel (Cu, Ni) concentrate grades and recoveries. Both vertical roller mill and tumbling mill products yielded greater recoveries as the products became finer and valuable mineral liberation increased. The vertical roller mill products however had substantially higher recoveries, which was linked to higher froth recoveries and differences in oxidation potential within the flotation pulp.

Increasing the compressive force in the VRM through the application of higher grinding pressures led to an increase in fines causing a decrease in froth stability during flotation, which corresponded with lower valuable metal recoveries. Variation in dam ring height caused small decreases in discrete PGM liberation but an increase in effective PGM liberation (considering PGMs liberated and locked in floatable base metal sulphide minerals). Flotation recoveries followed changes in froth stability with products prepared at the highest dam ring height, which had greater fines contents, yielding lower valuable metal recoveries. An optimised reagent suite

for VRM products should be developed to address issues with froth stability caused by the increase in fines component at higher grinding pressure and dam ring heights. This will allow for the improvements in valuable mineral liberation with these grinding conditions to be realised as increased flotation recoveries.

When operating the VRM grinding components with different classification devices, flotation performance was influenced by variation in the particle size distributions of products. External and internal air classification products with closely comparably particle size distributions yielded similar 3E PGE flotation recoveries. Flotation recoveries were however lower for the finest external air classifier product, which had a less steep PSD. A similar difference in PSD was observed for the screening vertical roller mill circuit products, which also had lower flotation recoveries than products generated with the internal dynamic air classifier.

The research indicates that the vertical roller mill is able to efficiently prepare material for valuable mineral concentration through flotation. The effects that the vertical roller mill variables grinding pressure and dam ring height have on operation and the comminution product has been investigated. Furthermore the VRM has been successfully coupled with different classification devices to generate a product with flotation response better than that of tumbling mill products.

Statement of Originality

The novelty of this study lies in that this research is the first comprehensive study, coupling an investigation of downstream valuable mineral recovery with grinding and classification in the vertical roller mill in a minerals processing context. The thesis includes the following original contributions to this field of knowledge:

- Research on the comminution of a PGM ore (Platreef) in the vertical roller mill.
- The coupling of a vertical roller mill with a vibrating screen to generate a suitable product for downstream processing.
- A comparison of the operation, product quality and product flotation response of a vertical roller mill coupled with different classification devices (internal dynamic air classifier, external hybrid air classifier and external vibrating screen).
- Comparison of the vertical roller mill with a tumbling mill in terms of specific energy, product quality, and product flotation response for a PGM bearing ore.

Plagiarism Declaration

I, Warren Little, declare that this thesis being submitted for the degree of Doctor of Philosophy (PhD) at the University of Cape Town (UCT) is my own work and that the thesis has not been submitted before for any degree or examination at any other institution.

Signed Signed by candidate Date 05/11/2020

Acknowledgements

I would like to acknowledge the support received from the following people and institutions without which I would not have been able to complete this PhD thesis. There are also numerous people not mentioned here who have encouraged and supported me throughout this project and also have my gratitude.

Thank you to the following people:

- My excellent supervisors Prof Aubrey Mainza and A/Prof Megan Becker, thanks for the support, guidance and opportunities given to me throughout the project, as well as the patience as we navigated through obstacles which this study seemed determined to throw our way
- Dr Carsten Gerold for the support I received while I conducted the VRM test work at the Loesche Test Facility and for all the knowledge you contributed then and at other times during this thesis
- Shireen Govender, Kenneth Maseko, Gilmour Zimri, Refilwe Moalosi and Monde 'the Cleaner' Bekaphi for assistance and entertainment in the numerous hours spent together in the Centre for Mineral Research (CMR) laboratories
- Sandip Naik, Hartmut Brodner and Kaja Tshimanga for assistance with all the sample processing, transportation and assaying you facilitated through Anglo American
- Gaynor Yorath and Lorraine Nkemba for assistance with QEMSCAN analysis and sample preparation at UCT
- Markus Stapelmann, Christian Schmitz, Jörg Langel and the rest of the Loesche Test Facility team for the assistance I received while in Düsseldorf
- Adj. Prof Jeremy Mann and Prof Kari Heiskanen for the direction and guidance during various stages of the project
- Dr Deniz Altun, Prof Hakan Benzer and Dr Hakan Dündar for the introduction to vertical roller mills at the Hacettepe University and input into my thesis I received from you during its completion
- And of course to my loving wife Lucy and our fantastic and wonderful family

Thanks also to the following companies and institutions:

- Loesche GmbH for their contributions towards sponsoring the project and conducting the grinding test work
- Anglo American for their contributions towards sponsoring the project, supplying and transporting the ore and various assay analyses
- Centre for Mineral Research and MPtech through which I was able to expose myself to a broad range of minerals processing projects, gaining invaluable knowledge
- Global Commintion Collaborative (GCC) and all its partner institutions through which I had to access many of the most knowledgeable people in this research field
- The University of Cape Town and the Department of Chemical Engineering, and
- The National Research Foundation of South Africa (NRF)

The financial assistance of the National Research Foundation of South Africa (NRF) towards this research is also hereby acknowledged. This included direct financial support as well as indirect research support through Grant Numbers 86054 & 93189. Any opinions, findings and conclusions or recommendations expressed in any publication generated by the NRF supported research is that of the author(s), and the NRF accepts no liability whatsoever in this regard.

CONTENTS

List of Figures

List of Tables

List of Abbreviations and Acronyms

Acronym	Definition
AG mill	Autogenous grinding mill
Auto-SEM-EDS/ Auto-SEM	Automated scanning electron microscopy with energy dispersive X-ray spectrometry (e.g. QEMSCAN, MLA, TIMA, Mineralogic)
BMS	Base metal sulphides
BSE	Back scattered electrons
d_{50}	Size corresponding to 50th percentile of a particle size distribution
E	Mechanical energy input
E_h	Pulp potential/redox potential
F_{80}	Size corresponding to 80th percentile of the feed particle size distribution
HPGR	High pressure grinding rolls
ICP-AES/OES	Inductively coupled plasma atomic emission spectroscopy/ optical emission spectrometry
MIG	Mainstream inert grinding
n	Rotational frequency
P	Power
PGE	Platinum group elements
3E PGE (assay)	Includes the elements platinum, palladium and gold
4E PGE (assay)	Includes the elements platinum, palladium, rhodium and gold
PGM	Platinum group minerals
PMA	Particle mineral analysis (QEMSCAN measurement type)
PSD	Particle size distribution
P_{80}	Size corresponding to 80th percentile of the product particle size distribution
QEMSCAN	Quantitative evaluation of minerals by scanning electron microscopy
SAG mill	Semi-autogenous grinding mill
SIBX	Sodium iso-butyl xanthate
SPW	Synthetic plant water
TMS	Trace mineral search (QEMSCAN measurement type)
ToF-SIMS	Time of flight secondary ion mass spectrometry
Acronym	Definition

UG2	Upper Group 2 chromitite
XPS	X-ray photoelectron spectroscopy
XRD	X-ray diffraction
XRF	X-ray florescence spectrometry

Glossary of Terms

Term	Definition
Abrasion	Breakage caused by tangential applied shear forces
Blaine's fineness	A quantification of a powder's 'fineness' determined by measuring pressure drop and volumetric flow rate through a packed bed
Bushveld Complex	A large rock complex in South Africa containing a significant portion of the world's platinum group metal reserves
Bypass	The portion of the feed which is not classified and passes to the coarse product
Classification	The separation of solid particles by size
Closed side setting	A measurement of minimum distance between liners during crusher motion
Comminution	The reduction in size of ore by crushing and grinding, to increase surface area and liberate valuable minerals
Compression breakage	Breakage caused by normal or almost normally applied forces
Cut size (d_{50})	Size of a particle from partition curve, which is equally likely to report to the coarse or fines fraction
Dry-screening	Process by which a sample in split into various size fractions through the use of a series of decreasing aperture meshes without the use of water
Entrainment	An unselective process in flotation, through which particles suspended in the water film between bubbles enter the froth from the pulp causing dilution of the concentrate grade
Effective PGM liberation	Summation of liberated PGMs and PGMs associated with liberated BMS
Froth stability	A quantitative concept established on the lifetime of a froth
Gangue	Minerals within an ore body that are of no commercial value
Grain	A three dimensional entity consisting of only one mineral (Barbery, 1991)

Term	Definition
Impact breakage	Breakage caused by forces resulting from the kinetic energy of the grinding media (Lynch, 2015)
Interparticle breakage	Breakage occurring when a bed of particles experiences compression
Liberation	State of a particle consisting of no more than one phase (Barbery, 1991)
Malvern Mastersizer	A machine that uses laser diffraction to measure the volume of particles
Merensky Reef	One of the major reefs in the Bushveld Complex carrying enrichment in platinum group minerals and base metal sulphides
Minerals processing	The processes by which valuable minerals are extracted from ore by separation of them from gangue minerals
Platreef ore	A PGE bearing ore in the Bushveld Complex associated with the Northern Limb
Pulp potential	Measure of the redox potential in a mineral slurry
Open/closed circuit	If a mill is run in open circuit it means that particles only pass through the mill once. In closed circuit the coarse particles in the mill product are separated from the fines by a classifier and recycled to the mill
Particle size distribution	The frequency distribution of a rock/soil sample in terms of a physical measure (mass, volume, etc) falling into each size class bin
Sharpness (α)	A separation parameter defined from the linear section of a partition curve. The greater α, the steeper the slope and more ideal the separation.
Specific (energy)	"Specific" implies that the quantity is expressed per unit mass
Thiol collector	Flotation collectors with the form $R\text{-}S^{-}(X^{+})$, where R is an organic compound and X^{+} is Na^{+} or K^{+}
Torque	The tangential portion of a force that causes rotation multiplied by the distance to the central axis

Chapter 1

INTRODUCTION

In this chapter the purpose of the thesis is introduced. A brief background of mineral processing is provided and challenges faced in the industry are highlighted. High compression grinding technology is presented as a potential solution to tackling some of the challenges, and the vertical roller mill, a high compression grinding device which is the focus of this thesis, is introduced. Following this, the objectives, scope and limitations of the thesis are presented and the contents of each chapter contained in the thesis are outlined.

This thesis focuses on evaluating the performance of the vertical roller mill (VRM) in a minerals processing application when operated with different classification systems. The areas of interest with regards to VRM performance are energy efficiency, product properties and flotation response. The thesis also considers the impacts of three grinding parameters on the VRM performance: product size, grinding pressure and dam ring height, and three classification circuits: internal air classification, external screening and external air classification.

1.1 Background

The purpose of a concentrator circuit in a minerals processing application is to recover the valuable components received in a low grade feed, to produce a concentrate of higher grade and quality, applicable for direct use or further treatment. Concentrator circuits usually consist of multiple sections for which there are different objectives. These sections can be broadly grouped into stages focusing on mineral liberation and valuable mineral separation. Comminution circuits focus on attaining mineral liberation through size reduction by applying energy to material within the system to cause particle breakage. The minerals liberated in this

process are then able to be separated based on differences in their material properties such as density (gravity separation), hydrophobicity (flotation), and electrostatic or magnetic susceptibility.

The comminution circuit comprises comminution (crushing and grinding) and classification (size separation) devices. The role of comminution devices is to liberate the valuable minerals from the gangue/unwanted minerals, while classification devices control particle size of the material leaving the comminution circuit as product (Lynch, 2015; Mainza, 2017, 2016; Mainza et al., 2013; Wills and Napier-Munn, 2006). A conventional comminution circuit usually contains a number of grinding and classification stages. Initial size reduction is carried out as a dry process with a series of crushers which operate in conjunction with vibrating screens to produce a feed for primary milling. Rod, autogenous grinding (AG), Semi-autogenous grinding (SAG) or ball mills are used for primary wet milling, a further size reduction step and liberation stage. Hydrocyclones and occasionally screens and spiral classifiers are used in combination with these mills to classify the milled material and control the quality of the feed to subsequent separation processes for valuable mineral recovery. Where further liberation of valuable minerals is required, secondary milling in ball mills or stirred mills can be employed.

The comminution process is highly energy intensive, consuming 70% of the energy on a mineral processing plant or 30% of most mining operations, and conventional comminution circuits are notoriously inefficient (Fuerstenau et al., 1999; Office of Energy Efficiency and Renewable Energy (EERE), 2007; Tromans, 2008). Improving the energy efficiency of comminution is of increasing importance due to the depletion of simple, high grade ores and the consequent move towards processing ores which are lower grade, with more disseminated, fine grained mineralization (Bhardwaj et al., 1985; Mudd, 2012; Phala, 2012; Powell and Mainza, 2012). These ores require greater volumes of ore to be ground to finer sizes in order to maintain metal production targets, and are often more competent (harder to grind) and difficult to process. These principles are illustrated separately with data from Kansanshi Copper Mine in Zambia and Mt Isa in Australia. At Kansanshi Copper Mine (Figure 1-1) the feed copper grade has decreased over time and the plant has had to increase mill throughput in order to maintain copper production (Chongo et al., 2018). At Mt Isa (Figure 1-2) additional grinding power was required to combat the trend of declining zinc recovery through an increase in sphalerite liberation (Young et al., 1997).

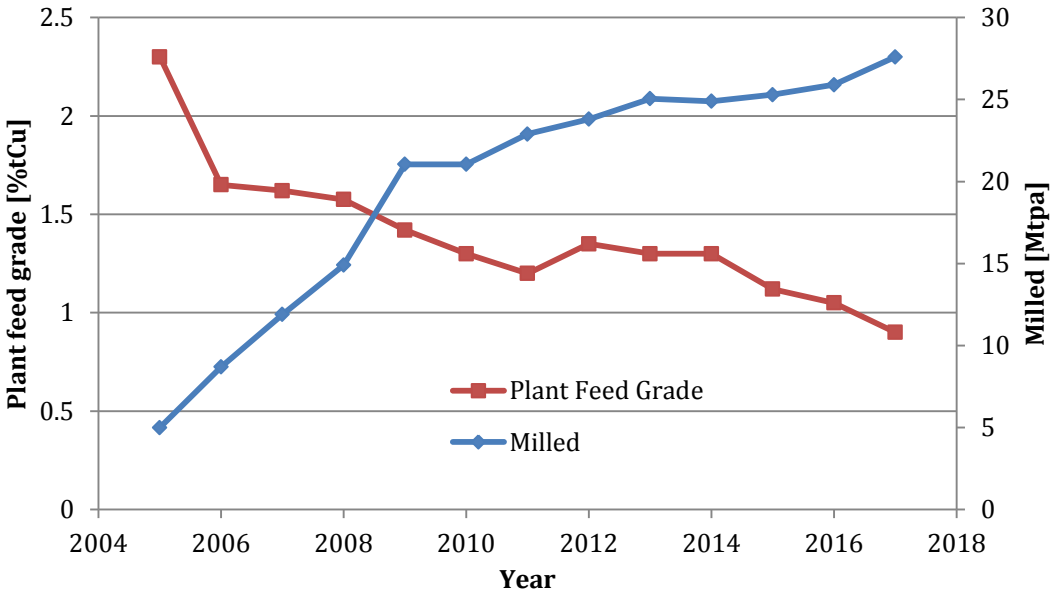

Figure 1-1: General trend of declining ore grades at First Quantum's Kansanshi Copper Mine and associated increase in tonnes milled, after Chongo et al. (2018).

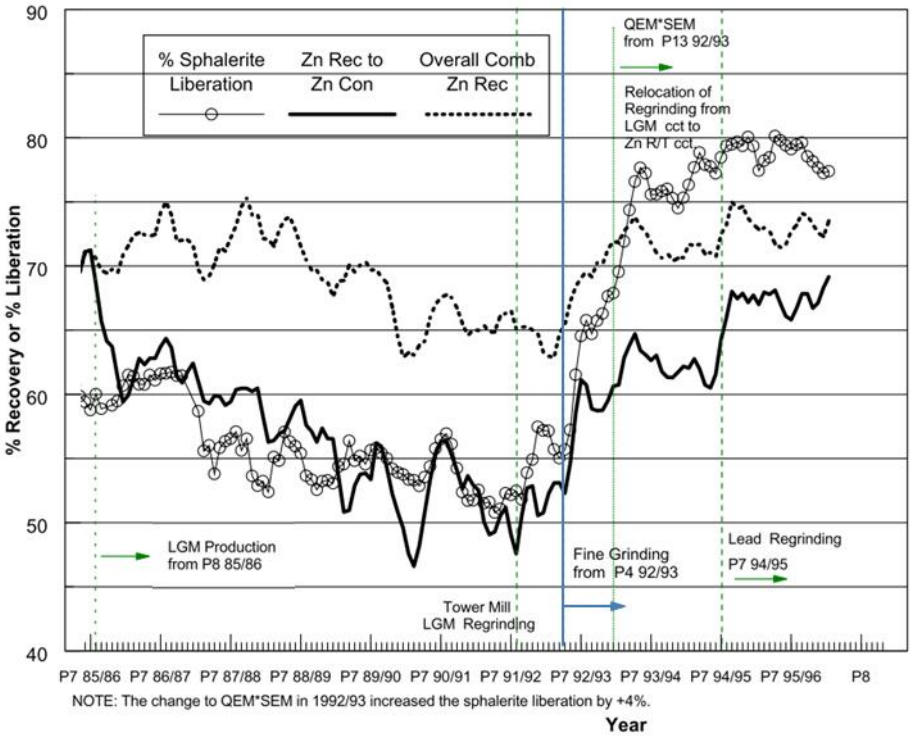

Figure 1-2: The percentage liberation - zinc recovery relationship at Mt Isa from 1985 to 1996 showing the impact of increased grinding power [blue] and introduction of regrinding [green] on flotation (Young et al., 1997).

To reduce the associated rise in required energy input in comminution, more energy efficient equipment from other industries is being adopted for minerals processing applications. The

cement industry makes extensive use of high compression grinding technology, which is accepted to be significantly more energy efficient than grinding in tumbling mills (Schönert, 1988). High pressure grinding rolls (HPGRs) form part of this group and in addition to better energy efficiency (Patzelt, 1992; Wüstner, 1986), their incorporation into circuits can increase throughput (Rule et al., 2008). The successful implementation of HPGRs in a number of mineral processing circuits, including application in the comminution of Platreef, a competent PGM bearing ore in South Africa, has encouraged the investigation of other high compression grinding technologies, such as the vertical roller mill.

The Loesche vertical roller mill was adapted for use in the cement industry in the early nineteen hundreds (Loesche, 1964). It is a dry grinding device that has seen limited implementation for mineral processing applications, with a single industrial mill in phosphate production, and pilot scale testing conducted on gold, copper, zinc and iron ores (Brundiek, 1995; Erkan et al., 2012; Gerold et al., 2012a, 2012b; Nyakunuhwa, 2019; Schaefer, 2001; van Drunick et al., 2010). In these applications the VRM has been observed to have a lower energy requirement than that expected from traditional tumbling mills. The VRM is a versatile device that can achieve significantly higher reduction ratios than HPGRs, processing feeds of top size 150 mm down to products of top size 20 μm. This gives the vertical roller mill the potential to replace later stages of crushing and traditional milling with a single unit to produce a product suitable for separation processes such as flotation and leaching.

Classification in the VRM, an important part of any comminution circuit, typically occurs in an internal dynamic air classifier situated within the grinding chamber above the table and rollers (Aydoğan and Benzer, 2011). Dynamic air classification is however energy intensive, and in previous pilot studies it was reported that the energy consumption of classification was comparable to that of the grinding components (van Drunick et al., 2010). In industrial applications the ratio of classification to grinding energy is reduced, however the perception created from reports on pilot plant studies, regarding the large ratio of classification energy, has adversely affected the appeal of the device. Concerns regarding the unknown potential influence of the different comminution methods on the performance of downstream separation processes such as flotation, constitute an additional barrier towards the acceptance of the VRM as a potentially energy efficient grinding technology for minerals processing applications. Because of this, the work in this thesis is aimed at assessing the performance of the vertical roller mill operated in conjunction with different classification devices, with specific focus on the effect of these changes on flotation response. Figure 1-3 illustrates how the VRM will be compared with that of conventional milling. The figure shows the relation between grinding and classification

in both the tumbling mill and vertical roller mill circuits, and illustrates the dependency of downstream recovery on both grinding and classification.

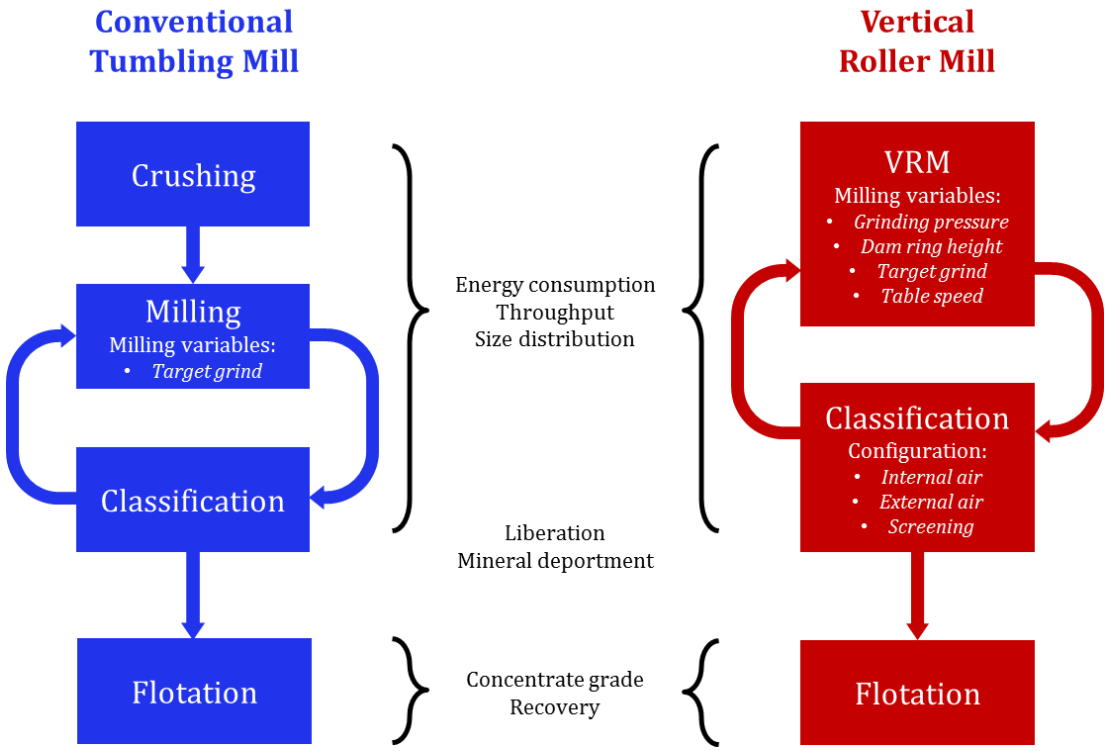

Figure 1-3: An overview of the scope of the thesis highlighting the links between comminution, classification and separation in a minerals processing application.

1.2 Problem Statement

The feasible exploitation of remaining low grade, disseminated mineral deposits will require increased energy input during comminution as greater volumes of ore are milled finer. The adoption of applicable technologies utilised in other industries could contribute towards enhancing the energy efficiency of comminution. The vertical roller mill, a high compression dry grinding device used extensively in cement and coal grinding applications (Altun et al., 2016, 2015; Gerold et al., 2012a, 2012b; Harder, 2010; Reichert et al., 2015), has the potential to contribute towards realising this goal. Before the benefits of the device can be harnessed, there is a need to understand how the vertical roller mill will perform when grinding a hard rock ore, as well as the affects the different operational parameters will have on mill performance. Furthermore it is important to understand how grinding in a vertical roller mill will affect downstream separation processes and how recovery performance may change.

1.3 Objectives

The main objectives of this study are to:

1. Investigate the influence of VRM operating parameters on energy, mineral liberation and downstream flotation response.
2. Compare the performance of VRM in standard operation with internal air classification, to that with external classification and assess performance of downstream processes.

1.4 Scope and Limitations

Test work with a pilot scale vertical roller mill was carried out to study the effects of milling variables and methods of classification on the mill performance, investigating energy consumption, throughput and product characteristics. Three main mill variables were investigated: grinding pressure, dam ring height and target grind, and three classification configurations: an internal dynamic air classifier, an external air classifier and an external dry screen. The data from the internal dynamic air classifier testing was used to develop empirical correlations describing the relationships between the operating variables and the grinding performance for the ore type. The correlations were developed for use in analysing the performance of the VRM under the broad range of conditions.

The research was confined to understanding the comminution and flotation response of a single ore, the PGM bearing Platreef. The high competency of Platreef, fine target grind size required for PGMs separation and the ore's amenability to processing with high compression grinding, made it a suitable ore choice for conducting the vertical roller mill test work. The air classification VRM tests targeted grinds of P_{80} ~ 240, ~ 75, and ~ 45 µm (later 60 µm), typical of the staged grinding circuits employed in the platinum and base metal industries. Operation of the VRM with an external dry screen however was restricted to the coarse product grind as continuous dry screening is unfeasible at the intermediate and fine grind. Flotation response of VRM products was determined in batch flotation tests and compared to that for tumbling mill products of equivalent grinds, prepared using the same ore. Mineralogical studies of both the gangue and platinum group minerals were carried out to gain understanding towards the link between grinding and flotation.

1.5 Outline of the Thesis

Chapter 1 - Introduction - A brief background into mineral processing is provided and some of the challenges faced by the industry are highlighted. The vertical roller mill is introduced as a technology capable of addressing these challenges, and base on this the objectives of the thesis are established. This is followed by the scope and limitations of the research and an outline of the thesis.

Chapter 2 - Literature Review - A review of the relevant literature is presented. The comminution process is described within the context of minerals processing and the inherent inefficiency of traditional grinding methods is highlighted. High compression grinding and compression breakage are introduced and a detailed review of the vertical roller mill is presented. How this comminution technology integrates with classification and separation processes is then considered and finally, literature pertaining to process mineralogy, flotation and the processing of PGM ore is presented. The literature review is summarised and key questions and hypothesis proposed.

Chapter 3 - Description of Experimental Apparatus - The experimental apparatus and its operation are described in the context of this study. The classification processes are outlined for the different classifiers used and how they were integrated in circuits with the vertical roller mill is explained. The reasoning for the selection of certain variables is explained and observations from literature relating to these variables are highlighted. The flotation equipment used for the batch flotation tests and laboratory scale tumbling mill are also described.

Chapter 4 - Materials and Methods - Experimental work conducted as part of the thesis is outlined. A description of the preparation of the ore used for this research is presented. This is followed by an account of the pilot scale vertical roller mill test work conducted, together with detailed explanations of the operating and sampling procedures for the different classifier circuits. The process used to generate flotation feed in the batch tumbling mill is explained and the sample processing, mineralogical analysis and flotation test procedures are described.

Chapter 5 - Airflow Operation - The results generated from the internal air classification vertical roller mill grinding test work are analysed alongside mineralogical and batch flotation data generated for the grinding products.

Chapter 6 - VRM & Classification - The results from the test work carried out for the vertical roller mill operated in conjunction with various methods of classification are assessed and compared with batch tumbling mill grinding and flotation data.

Chapter 7 - Concluding Discussion - This chapter contains a summary of the work undertaken as part of this thesis, the important results and key findings obtained and recommendations for future work based on questions that arose during this thesis.

Chapter 2

LITERATURE REVIEW

Bodies of work in the literature that were considered relevant to the work carried out in this thesis are critically reviewed in this chapter. The comminution process is described within the context of minerals processing and the inefficiency of traditional grinding methods is highlighted. High compression grinding and the vertical roller mill are introduced as technologies with the potential to increase comminution efficiencies. The background into classification in a minerals processing context is presented and how VRM technology integrates with classification processes is considered. The flotation process is described, process mineralogy is introduced and specifics regarding the processing of Platreef, a platinum group element bearing ore, are highlighted. Lastly, the literature is summarised and the hypotheses and key questions presented.

2.1 Comminution Theory

The comminution process forms a principle part of many bulk commodity and minerals processing circuits. The process focuses on generating new surface area or attaining mineral liberation through size reduction, by applying energy to material within the system to cause particle breakage (Lynch, 2015; Wills and Napier-Munn, 2006). The relationship between energy input and the change in particle size through breakage is the basis of comminution theory and is described by the general equation:

$$dE = -K\, {dx}/{x^n} \qquad \textit{Equation 2-1}$$

Three versions of this general relationship have been proposed, in which energy consumed by breakage is proportional to the production of new surface area, reduction in particle volume, and decrease in particle size respectively (Lynch, 2015).

Von Rittinger (1867) $E = k\left(\frac{1}{x_2} - \frac{1}{x_1}\right)$ *Equation 2-2*

Kick (1885)	$E = k\ ln\left(\frac{x_1}{x_2}\right)$	*Equation 2-3*
Bond (1952)	$E = 2k\left(\frac{1}{\sqrt{x_2}} - \frac{1}{\sqrt{x_1}}\right)$	*Equation 2-4*

Together these theories can be applied to different parts of the size reduction curve (Figure 2-1) as proposed by Hukki (1961).

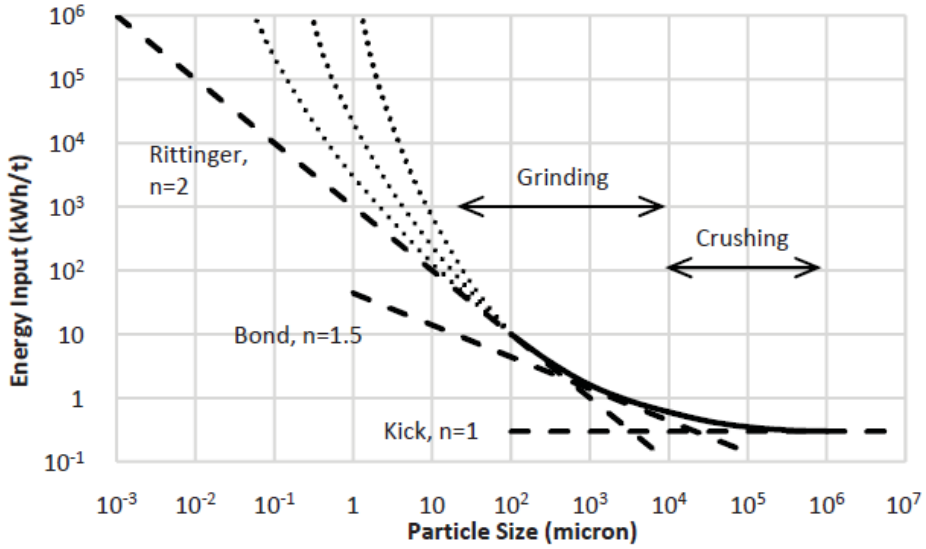

Figure 2-1: Comparison of the comminution theories proposed by Von Rittinger, Kick and Bond to operating practice (Lynch, 2015).

2.2 The Comminution Process

In minerals processing the concentration of valuable components in a mined ore is often required before further extraction of valuable constituents can occur. The concentration process can be broadly divided into stages focusing on either mineral liberation or valuable mineral separation. The comminution process is focused on attaining mineral liberation through size reduction and enables the separation and concentration of valuable minerals in subsequent stages.

A comminution circuit typically comprises comminution and classification devices. The role of comminution devices is to liberate the valuable minerals from the gangue/unwanted minerals (Wills and Napier-Munn, 2006), while classification devices regulate the material fed to later comminution stages and control the quality of material fed to subsequent valuable mineral separation processes. A conventional comminution circuit usually contains a number of grinding and classification stages (Mainza, 2016). Initial size reduction is carried out by a series of crushers often operating in conjunction with vibrating screens for size classification. Size reduction in crushers occurs through the compression of particles between two surfaces, either

individually or as a bed of particles. Material produced by the crushing circuit is fed to the primary mills which further reduce the particle size and liberate minerals for separation (Lynch, 2015; Wills and Napier-Munn, 2006). Autogenous Grinding (AG), Semi-Autogenous Grinding (SAG), rod and ball mills are used for primary milling and together are grouped as tumbling mills. These grinding units rely on the transfer of energy to the charge through rotation of the mill shell. The charge, made up of material being comminuted and grinding media (steel balls, rod or the material itself), is lifted by the rotating shell of the mill and after reaching a maximum height falls in a cascading or cataracting motion (Figure 2-2) during which energy is transferred to the material causing particle breakage through impact, abrasive and compressive forces (Wills and Napier-Munn, 2006). Some mineral processing applications require further size reduction steps. These finer grinding steps are carried out in ball or stirred mills. Stirred mills, similarly to tumbling mills, contain material and grinding media within a shell, in these mills however the shell is stationary and an internal stirrer imparts energy to the charge. The grinding media is smaller than that used in ball mills, making stirred mills more suitable for fine grinding applications (Wills and Napier-Munn, 2006).

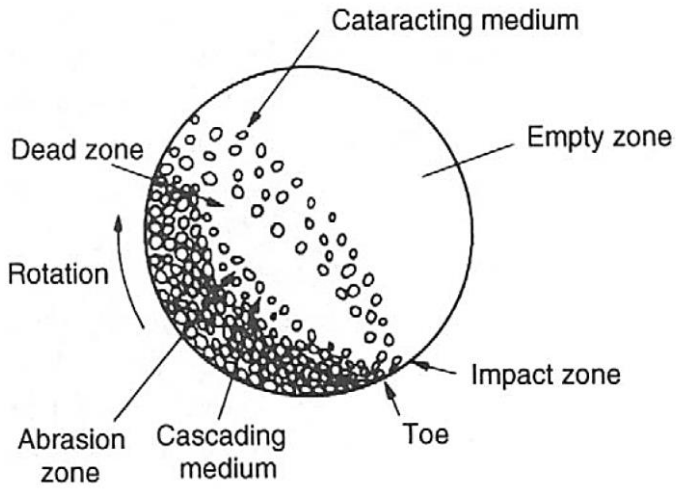

Figure 2-2: Schematic representation of a tumbling mill (Wills and Napier-Munn, 2006).

The comminution process is highly energy intensive, consuming 70% of the energy on a mineral processing plant or 30% of that in a mining operations (Ballantyne et al., 2012; Fuerstenau et al., 1999; Office of Energy Efficiency and Renewable Energy (EERE), 2007; Tromans, 2008). The high proportion of energy used in minerals processing by the comminution process has led to a significant amount of research focused on investigating and implementing more energy efficient grinding technologies. High compression grinding, which is recognised in the cement industry as more energy efficient than conventional tumbling mills, has the potential to assist in realising an increase in comminution energy efficiency in minerals processing.

2.3 High Compression Grinding Technology

The precursor to a modern day high compression grinding device is the traditional edge roller mill. These mills relied on the weight of the roller to achieve breakage and were used as early as the 2nd century in China for the grinding of pigment (Lynch and Rowland, 2005). Advances in design, included the use of hydraulic and pneumatic systems to enable higher grinding pressures, culminated in a variety of modern day high compression devices. While design can vary considerably between different devices, the principle of applying a compressive force to a bed of particles is observed throughout. This technology, in the form of high pressure grinding rolls, vertical roller mills and Horomills, has seen widespread use within the cement industry for the grinding of clinker, slag and raw materials, where they are acknowledged to be more energy efficient than tumbling mills (Batra et al., 2005; Cordonnier, 1996; Jørgensen, 2005; Schaefer, 2001). This increase in energy efficiency is one of the reasons the minerals processing industry has introduced high compression grinding in some circuits.

Breakage Mechanisms

The enhanced energy efficiency realised in high compression grinding is related to the dominant breakage mechanisms associated with the technology. Compression, impact and shear are the three main breakage mechanisms occurring in grinding (Lynch, 2015; Wills and Napier-Munn, 2006) and although a combination of these mechanisms are present in most comminution devices, one or more of the mechanisms will dominate (Figure 2-3). Tumbling mills are associated with impact and shear, stirred mills with shear/abrasion, and roller mills and crushers are associated with compression (Gao and Forssberg, 1995; Lynch, 2015; Ye et al., 2010).

In compression devices, breakage is caused when particles are stressed through the application of opposed forces. Energy is applied directly to the material being ground by the opposing grinding surfaces, unlike in other comminution devices where energy is directed to the grinding media (Fuerstenau et al., 1996). Fundamentally, single particle compression breakage is the most efficient means of causing breakage and interparticle or bed breakage, characteristic of high compression grinding devices, is the next most energy efficient (Fuerstenau et al., 1999). Single particle compression breakage is not practically achievable in industrial-scale comminution devices at fine particle sizes. Interparticle breakage occurs when a particle has contact points shared with surrounding particles in a bed of particles, and the bed experiences compression (Figure 2-4). Each particle encounters multiple forces applied from the surrounding particles or walls, which lead to breakage (Kou et al., 2001; Liu et al., 2005; Viljoen et al., 2001).

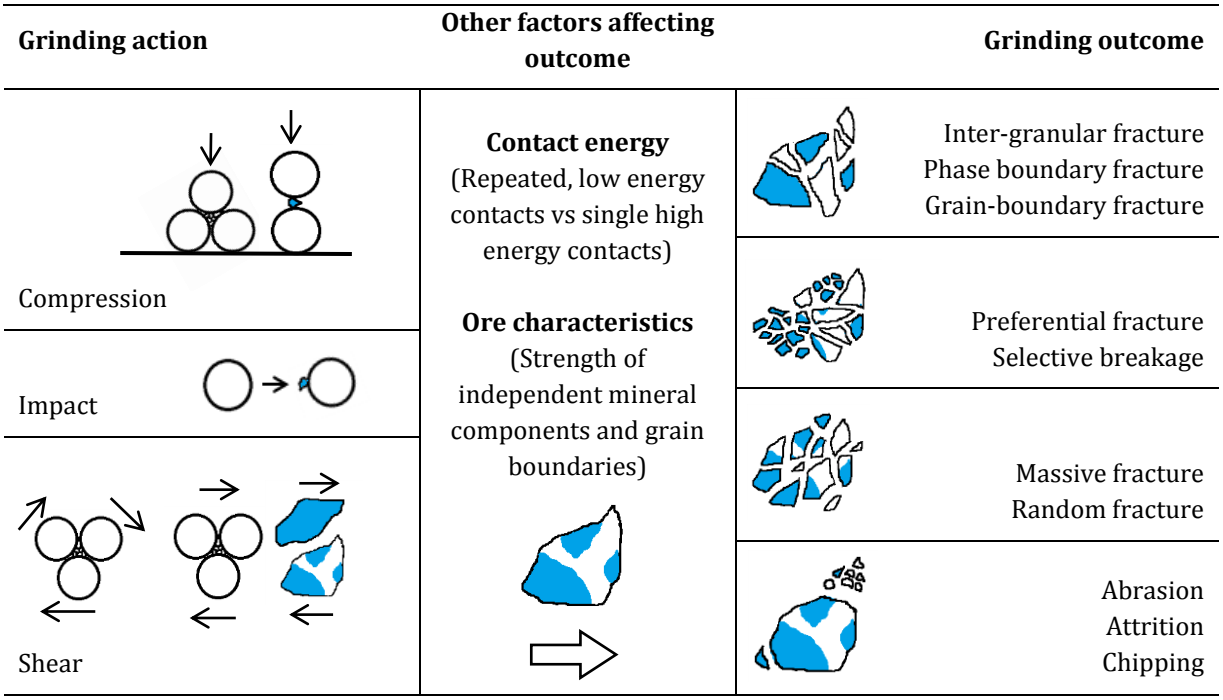

Figure 2-3: Illustration of the different breakage mechanism and associated grinding outcomes (Little et al., 2016).

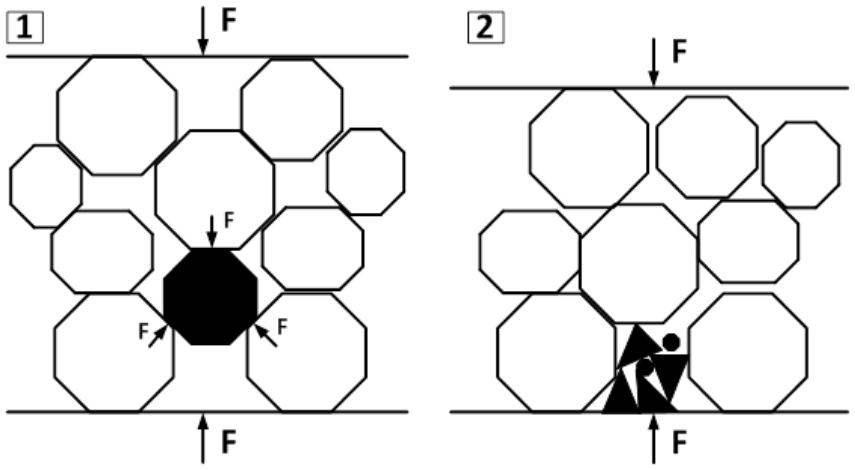

Figure 2-4: Schematic representation of bed compression and interparticle breakage (Viljoen et al., 2001).

Breakage in the particle bed is governed by the energy absorbed during a compression event which is affected by the magnitude of the compressive force, feed particle size, bed depth, moisture content and confinement of the bed. Both increased compressive force and degree of confinement increase the mass specific energy absorbed by the particle bed (Figure 2-5) (Nguyen et al., 2002; Oettel et al., 2001; Schönert, 1996), while deeper particle beds are associated with lower specific energy absorptions (Kanda et al., 1990; Schönert, 1996). Oettel et

al. (2001) further demonstrated that production of new surface area was greater at higher degrees of confinement (Figure 2-6).

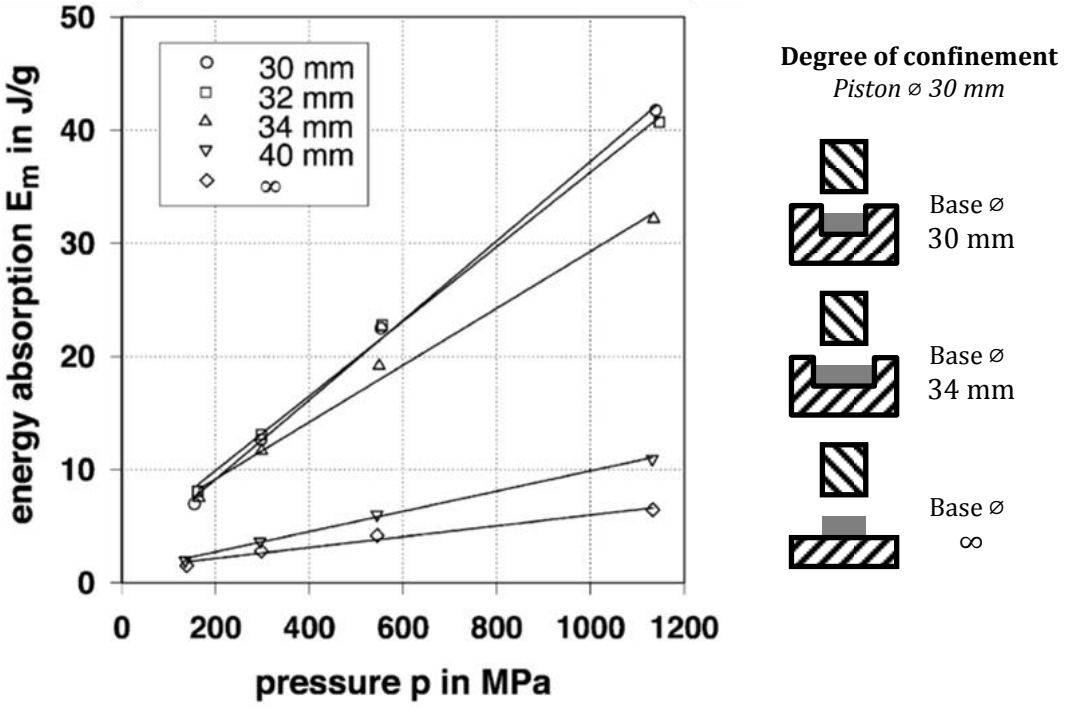

Figure 2-5: Energy absorption as a function of applied pressure, differentiating between mould diameter/degree of confinement (Oettel et al., 2001).

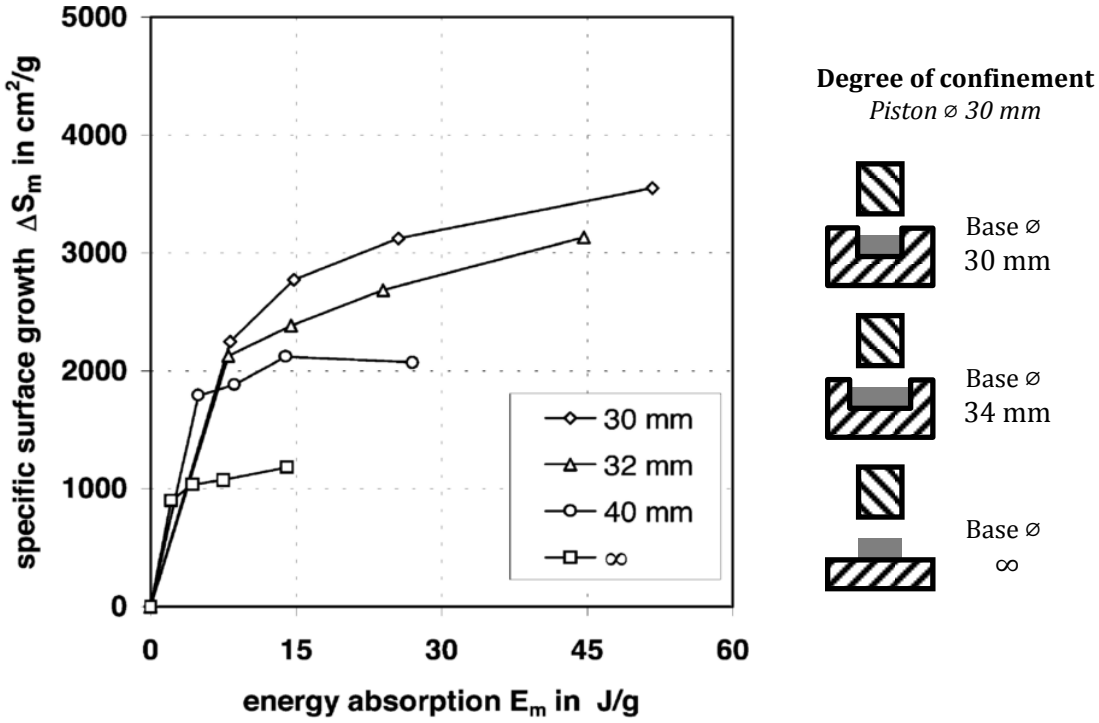

Figure 2-6: Increase in specific surface area as a function of energy absorption, differentiating between mould diameter/degree of confinement (Oettel et al., 2001).

Breakage mechanisms do not only affect energy efficiency of grinding but they also affect product size distribution, mineral liberation and the particle shape and surface properties of the product (Avimanyu and Subrata, 2007; Gao and Forssberg, 1995). These factors together will have an effect on the downstream processing of the ore (Ye et al., 2010).

High Pressure Grinding Rolls

High pressure grinding rolls (HPGRs) are a high compression grinding technology developed in the late 1970s by Schönert after research into the most efficient method of grinding (Apling and Bwalya, 1997; Aydoğan et al., 2006; Benzer et al., 2011). The HPGR has seen wide spread application in both the cement and minerals processing industries (Aydoğan et al., 2006; Kellerwessel, 1990; Morley, 2010; Tavares, 2005; van der Meer and Maphosa, 2012).

Design and Operation

The mill design consists of a set of counter-rotating horizontal rolls between which material is compressed (Rule et al., 2008). One of the rolls is fixed while the other floats on a set of rails with its position controlled by pneumo-hydraulic springs (Morley, 2010). Fresh material is choke fed into the gap between rollers, where a bed of material is compressed. After compression the comminuted product leaves the device, often as flakes requiring de-agglomeration (Lynch, 2015).

In the cement industry these units have been widely adopted for use across the production chain. Units are used for finish grinding of various raw materials, however, because of the steeper PSD produced by the HPGR which reduces cement strength, for the grinding of clinker for cement the units are predominantly used before or alongside ball mills (Figure 2-7) in a closed or semi-finish grinding circuit (Aydoğan et al., 2006; Lynch, 2015; Patzelt, 1992). In minerals processing the HPGR has been incorporated in a variety of comminution circuits including diamonds, gold, iron, copper and platinum group minerals (Aydoğan et al., 2006; Morley, 2010; van der Meer and Maphosa, 2012). The unit commonly replaces tertiary crushing, operating in combination with a screen to provide mill feed (Figure 2-8). HPGR product contains more fines than typical crushing, allowing for increased throughput in subsequent milling (Rule et al., 2008).

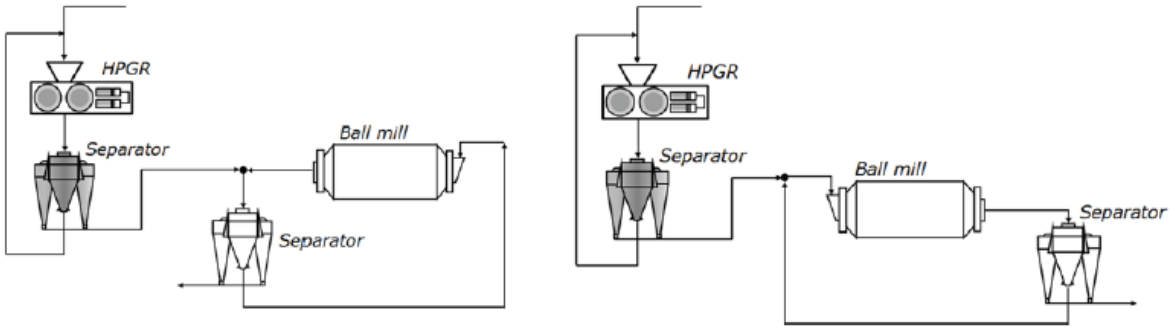

Figure 2-7: HPGR cement grinding flowsheets: semi-finish [left] and closed circuit grinding [right] (Lynch, 2015).

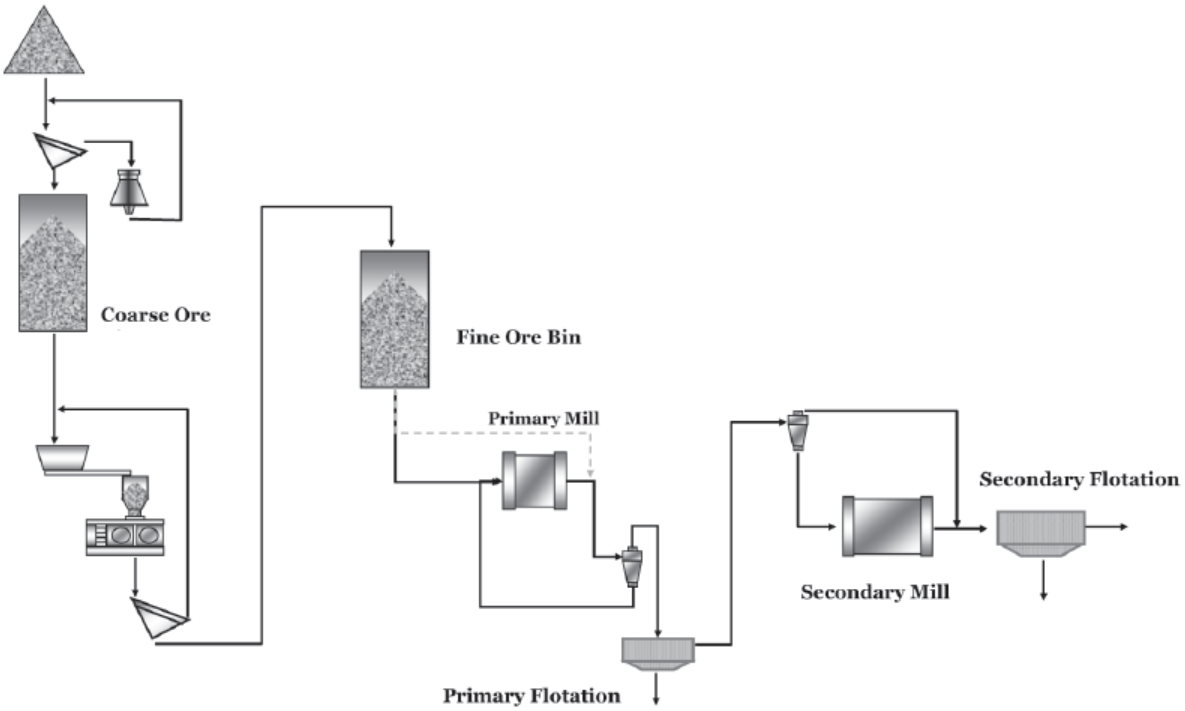

Figure 2-8: Mogalakwena North flowsheet with an HPGR for the processing of a platinum ore (Rule et al., 2008).

Horomill

The FCB Horomill® is a high compression device developed with a particular focus on the finish grinding of cement. The mill comprises a single roller inside a rotating cylindrical shell. The shell is driven in a similar way to that of a tumbling mill, with hydraulic grinding force transmitted to material resting at the base of the shell via the roller. Milled material is transported for size classification in an external classier by a stream of air, with oversize material returning to the mill for further grinding (Aydoğan et al., 2006; Cordonnier, 1996; Folsberg and Smidth, 1997; Marchal, 1997).

Vertical Roller Mill

Vertical roller mills are a type of high compression grinding technology which has been predominantly used in cement and coal grinding applications. In the cement industry the units are viewed as more energy efficient than tumbling mills, and as such, the number of their installations has overtaken that of ball mills (Harder, 2010). There are a number of VRM manufacturers, and although there are some key differences between their mill designs, the basic structure is similar.

The Loesche vertical roller mill is a dry grinding device that incorporates both comminution and classification. The device can be fed particles up to 150 mm in size and achieve grinds of down to 20 μm (Erkan et al., 2012), thereby performing the function of two units in traditional circuits: either the tertiary crusher and ball mill or the SAG mill and ball mill from conventional circuits. Loesche's first vertical roller mill, an LM 11, was supplied to Joao Pessao, Brazil in 1935 for the grinding of cement clinker. The mill was part of a cement plant and incorporated an internal dynamic classifier and spring loaded roller mill into a single unit (Brundiek, 1995; Loesche GmbH, 2014a). For some time this design remained unchanged, with larger units being constructed as required by the industry. In 1961, Loesche designs had reached the limit of the spring assembly's safe operation, and the hydro-pneumatic spring assembly found in their current mills was adopted (Loesche GmbH, 2006). Further differences between the current VRM and original mills include the replacement of the earlier classifiers with higher efficiency separators, changes in the mill and roller design to reduce mill vibrations and advances in wear resistance in the mills (Harder, 2010).

Within the South African mining sector the vertical roller mill was only introduced in the 1990s. In 1998, an LM 50.4, which was the largest Loesche mill at the time, was installed for Foskor in Phalaborwa for the dry grinding of a phosphate carrying pyroxenite (Jacobs et al., 2016; Schaefer, 2001).

Circuit

In order to control product quality the vertical roller mill is operated in conjunction with a classification stage. In most applications the VRM is operated with an internal dynamic air classifier situated within the grinding chamber housing, above the grinding components. Comminuted material is transported to the classifier from the grinding section by suspending particles in an air stream passing through the grinding chamber (Schaefer, 2001; Jensen et al., 2010; Jensen et al., 2011). A flow sheet for this manner of operation, termed 'airflow mode', is presented in Figure 2-9. In operation with external classification the VRM runs in 'overflow

mode' and there is no suspension of particles within the unit and all material falls from the grinding table and is transported mechanically to a classifier.

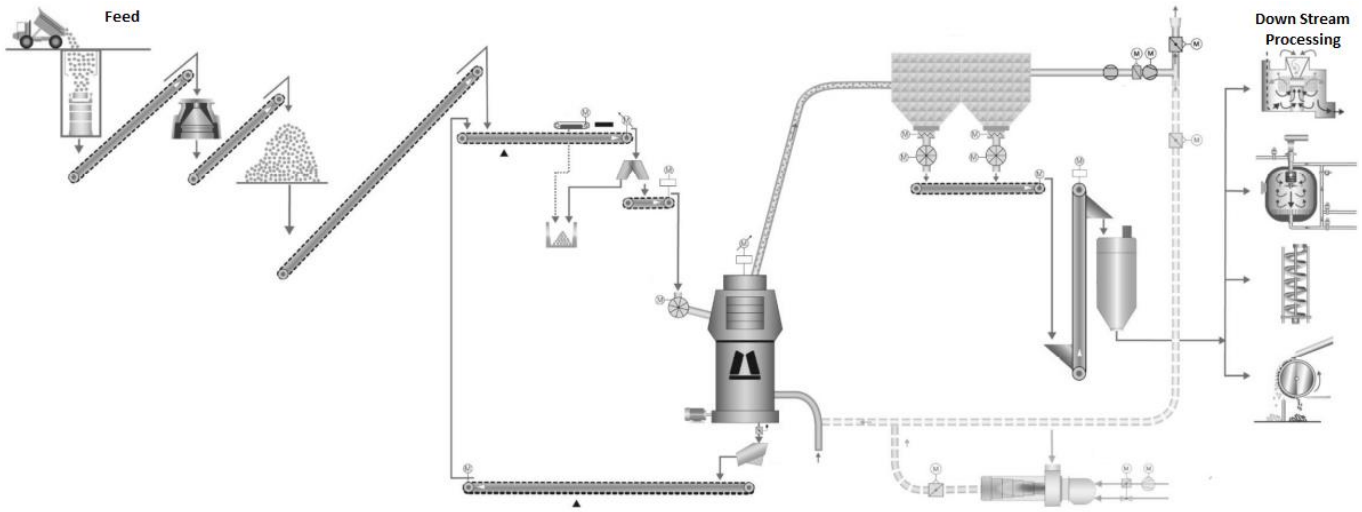

Figure 2-9: Loesche flow sheet for the VRM operating in airflow mode (Gerold et al., 2012b).

In Figure 2-10, the vertical roller mill is operated in overflow mode with both a static and a dynamic air classifier. Initially material passes through a static air classifier, which separates off the coarse component for return to the mill. The static separator undersize proceeds to a dynamic classifier where most of the particles finer than the target cut size are separated off as comminution product. The oversize fraction is combined with the static separator coarse material which is recycled.

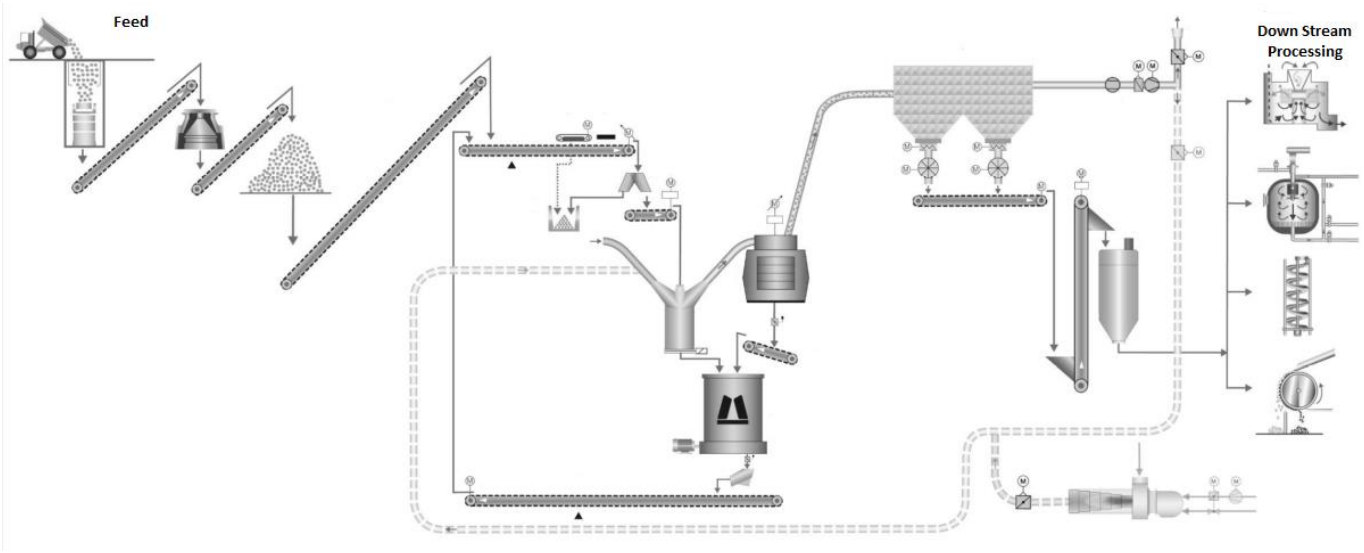

Figure 2-10: Loesche flow sheet for the VRM operating in overflow mode (Gerold et al., 2012b).

Roy (2002) suggested that the VRM could also function without the classification component, as a pregrind stage prior to tumbling milling to increase capacity of existing circuits. Applications in this configuration are however not common.

Grinding Components

The grinding components of the vertical roller mill as illustrated in Figure 2-11 are situated in the lower section of the unit and consist of a number of conical rollers [1] positioned on a grinding track at the rim of a rotating circular table [2]. The dynamic air classifier [3] used for airflow mode operation is situated above the grinding components. Material is added to the centre of the rotating grinding table and forms a bed of particles which proceeds outwards due to the centrifugal force experienced by the particles. As the particles near the edge of the table, they pass under the rollers and comminution takes place. The material is compressed as a bed of particles and interparticle breakage occurs. The necessary grinding pressure required for compression of the bed is greater than the weight of the rollers and is exerted by a hydro-pneumatic spring system (Reichert et al., 2014; Schaefer, 2001).

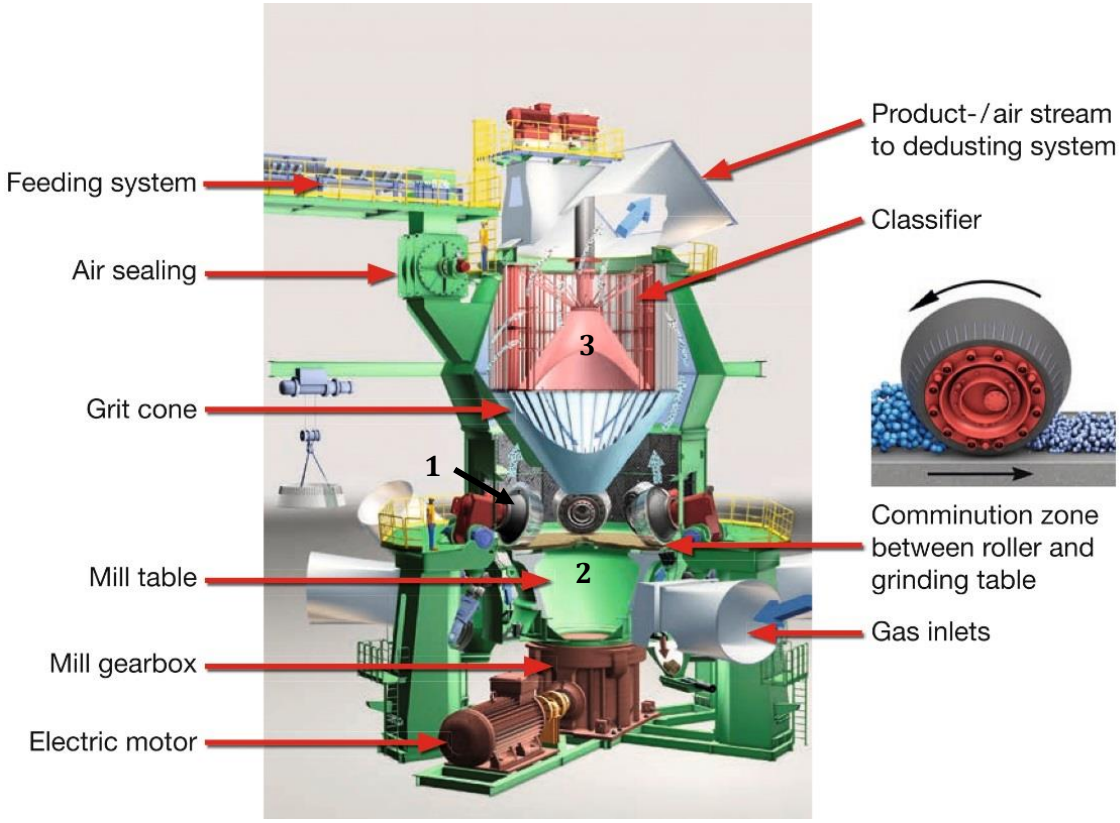

Figure 2-11: Schematic of the operation of the VRM (C. Gerold, Personal Communication, 2016).

The bed is formed from the addition of fresh feed and recycling of oversized material. Fresh feed enters the grinding chamber through a chute, passing through an airlock. In airflow mode the recycled oversized particles, which do not exit the grinding chamber, either settle from

suspension or fall as the classifier reject stream, guided back to the table through the grit cone. When an external classifier is used the classification oversize/recycle is returned with the fresh feed. Particles that pass through the louver ring are collected below the table. In airflow mode, generation of this material is negligible and it may be recombined with the feed. In operation with external classification this material is the feed to the classifier (Brundiek and Poeschl, 1995; Hackländer-Woywadt, 2005). The retention of material on the table is controlled through the table speed, and hence centrifugal force on the particles, as well as the manipulation of the dam ring height. The dam ring, situated around the rim of the table, can be varied in height to manipulate the depth of the grinding bed as well as the table residence time (Hackländer-Woywadt, 2005; Jørgensen, 2005). In scenarios where there is potential for a build-up of foreign particles in the grinding bed, small holes are placed in the grinding table near the dam ring. Contaminants can pass through these holes, preventing their build-up, which would reduce mill efficiency and limit damage caused to the grinding components (Hackländer-Woywadt, 2005; Knoflicek and Wentzel, 1994).

Loesche's LM series provides vertical roller mills with tables 1.2 - 6.9 m in diameter. Each table is accompanied by either 2, 3, 4 or 6 rollers, larger table diameters having more rollers (Hackländer-Woywadt, 2006; Loesche GmbH, 2014b). Each of the rollers is individually supported on a rocker arm, which is mechanically buffered to limit the downwards motion of the rollers inhibiting contact with the grinding track (Ahluwalia et al., 2006). The pressure required for comminution is supplied to the rollers by a series of hydraulic cylinders in the hydro-pneumatic spring assembly. This system also includes a number of accumulators to smooth irregularities in movement, reducing vibrations that destabilise production (Schaefer, 2001).

The rollers themselves have a number of variations. In certain applications Loesche's alternating support and master roller configuration is used (Figure 2-12). The support rollers are smaller and apply less force to the particle bed, de-aerating and compacting the material, making it more stable for the master roller (Hackländer-Woywadt, 2006; Salewski, 2005). This is necessary for fine grinding and other cases of high bed fluidity in order to achieve efficient grinding (Brundiek and Poeschl, 1995; Oesch and Jurko, 2002). In addition, rollers can either be high shear (standard) or low shear (Figure 2-13). Rollers of standard geometry (high shear) are tapered and set at an inclination such that there are differences in rotational velocity between points on the roller surface and the rotating grinding table. This leads to the rollers exerting both compressive and shear forces on the particle bed. The high shear environment promotes fines production but also leads to greater wear rates. By altering the angle of the roller, shear forces exerted on the particle bed can be minimised (Gerold et al., 2012b).

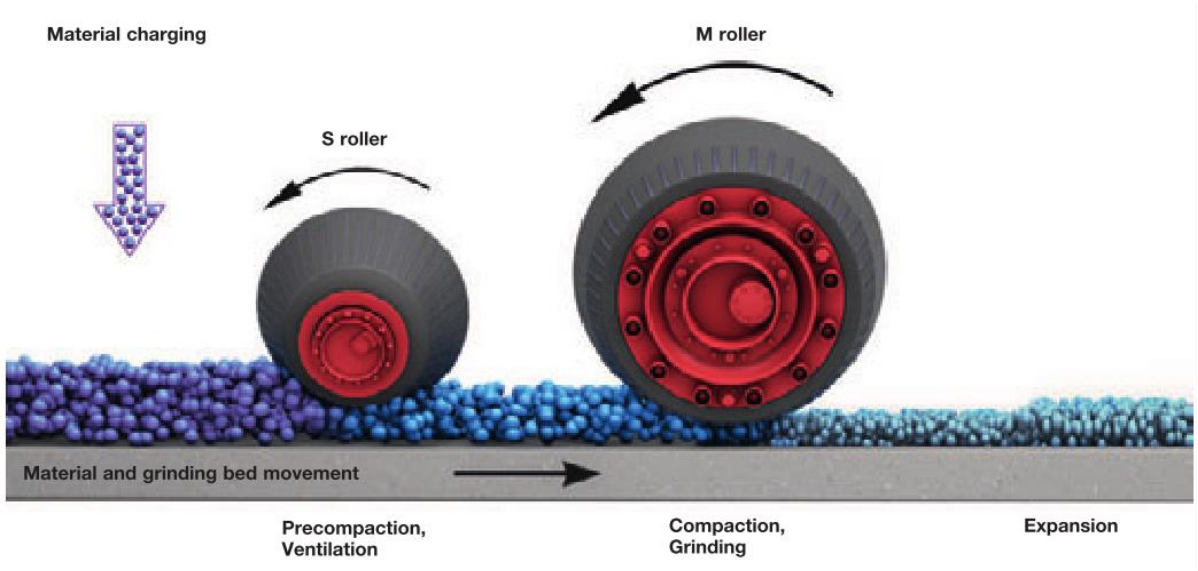

Figure 2-12: Vertical roller mill support roller [S] and master roller [M] (Loesche GmbH, 2014a).

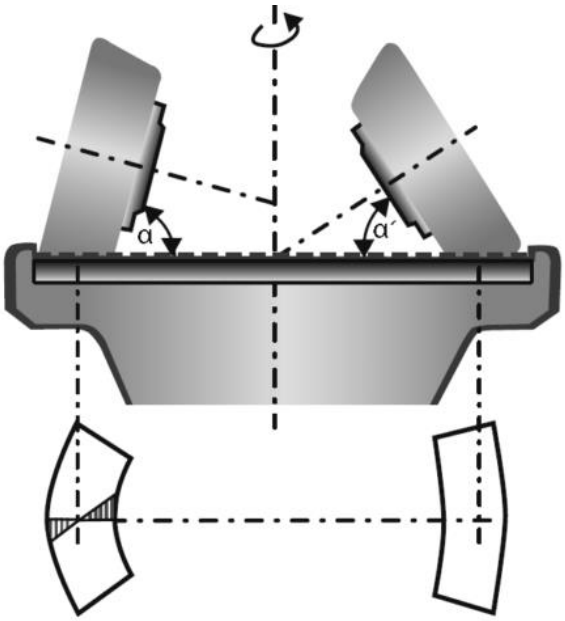

Figure 2-13: Vertical roller mill high shear or standard [left] and low shear [right] roller orientation (Gerold et al., 2012b).

Wear rates in the vertical roller mill in current clinker and blast furnace slag applications are lower per tonne than that of a ball mill, typically 3 - 7 g/t (Ahluwalia et al., 2006; Erkan et al., 2012; Hackländer-Woywadt, 2005). Although wear rates are lower for the VRM, the cost of wear is higher. VRM wear rates above 10 g/t are said to make the implementation of mill uneconomical when compared to other technology (Jensen et al., 2011). Current grinding surfaces in the VRM are either heat treated high chromium carbide cast alloys or chrome carbide hard facings (Hackländer-Woywadt, 2006; Jensen et al., 2010). Some segments in larger mills weigh more than 1200 kg and make the casting process unfavourable, as it leads to large

primary carbides, which are unfavourable to wear (Jensen et al., 2010). For this reason in situ resurfacing of new as well as old rollers often takes place (Ahluwalia et al., 2006; Wahl, 1994). The resurfaced faces show lower wear than the cast alloys prolonging grinding component life span (Jensen et al., 2010; Simmons et al., 2005). Experience form operations has found negligible wear on the support rollers as well as low mill housing wear (Brundiek and Poeschl, 1995; Hackländer-Woywadt, 2006). A list of all the wearing parts including classifier components can be found in Hackländer-Woywadt (2005).

Application

Manipulation and control of the grind in the vertical roller mill is achieved by changing various online variables such as: grinding pressure, table speed, feed rate and if operating with air classification: classifier rotor speed, air flow rate, and pressure drop across the unit (Figure 2-14). The ability to adjust variables allows for the mill to be adapted quickly to changes in feed, to maintain product quality. Design variables such as dam ring height, roller geometry and type, and classifier design can be altered to adapt the mill performance (Reichert et al., 2014).

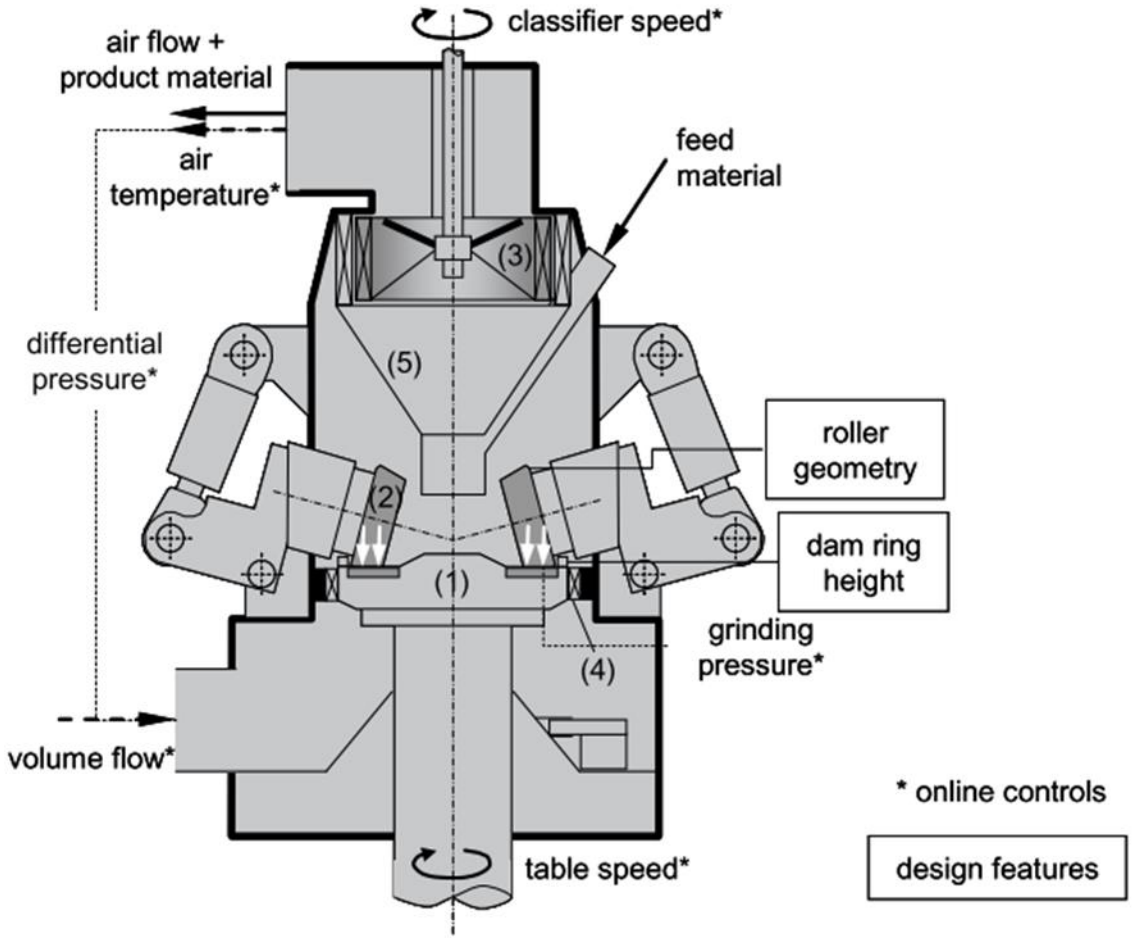

Figure 2-14: Schematic of the operation of a vertical roller mill in airflow mode (Reichert et al., 2014).

As with all comminution circuits the characteristics of the feed to the vertical roller mill has a large effect on overall performance. General material properties such as hardness, particle size distribution, and moisture contents for each application are taken into account during the selection and design of the mill. Depending on the final design, the mill will be able to operate within a certain operating range of feed rates/ throughputs. If throughput is outside of this range either production will no longer meet the target requirements or the unit will be operating ineffectively. Variations in other feed characteristics will also have an effect on output. Within a single deposit, ore hardness can vary considerably, and mill power draw and throughput are manipulated in response in order to maintain product quality (Thiel and Schössow, 2001). The steepness of the feed particle size distribution can affect the energy absorbed by the grinding bed with wider particle size distribution resulting in lower specific energy absorptions (Hosten and Cimilli, 2009). Changes in the moisture content of the feed could lead to higher wear rates of the grinding components (Schaefer, 2001; Schönert and Sander, 2002). Slight changes in these can be overcome as long as they do not move throughput out of the operational range.

In airflow mode the VRM is able to act as a dryer as well as a comminution and separation device. In the cement industry, raw materials with moisture contents of up to 20% can be dried by using heated air in the mill (Brundiek and Poeschl, 1997; Jensen et al., 2010; Reichert et al., 2014). While drying and dry grinding are not of clear significance in the largely flotation dependent minerals industry, the advantages of not using process water in comminution and only adding water where it is needed may be beneficial to the industry (Norgate et al., 2010). Furthermore this may prove advantageous as the grinding operations can be run independently of up and downstream processes. Having a dry product allows for better control of pulp density, a key aspect of flotation performance (Schaefer, 2001). There are however concerns that the dry grinding environment may affect the pulp potential and mineral surface properties, influencing flotation recoveries (Palm et al., 2010).

The dominant use of the vertical roller mill is in airflow mode, in conjunction with a dynamic air classifier. Dynamic air classification is however an energy intensive process with substantial power required by the fan to overcome the large pressure drop across the classifier (Schonbach, 1988). The energy requirements for industrial mills is close to 50% of that required in grinding components (Roy, 2002; Simmons et al., 2005). External air classification incorporates a static classifier and allows for the installation of a lower duty fan, thus increasing the energy efficiency of the circuit with reductions of 40% achieved in pilot scale testing (van Drunick et al., 2010). Application of the VRM with other external classification devices is limited and potential for operation with low energy intensity classifiers has not been investigated.

High Compression Grinding Comparison to Tumbling Mills

With high compression grinding technology experiencing adoption in the minerals processing industry, it is important to understand the impact that the inclusion of these devices may have on comminution circuits as well as on the performance of downstream processing.

Energy Efficiency

In cement and coal applications these devices have widely been adopted due to their better energy efficiency compared to equivalent tumbling mills (Altun et al., 2011; Batra et al., 2005; Cordonnier, 1996; Jørgensen, 2005; Schaefer, 2001). This is the principal appealing factor for the inclusion of high pressure grinding technology in minerals processing.

The HPGR is a high compression grinding device which has seen significant use in hard rock mineral processing applications. This device has been incorporated into a number of copper, gold and platinum circuits (Morley, 2010). In the platinum industry, an HPGR retrofitted at Northam Platinum UG2 plant yielded a 20 to 30% reduction in total comminution energy consumption when the target grind was maintained, and the implementation of the HPGR-ball mill circuit over the conventional crusher-ball mill configuration at the Mogalakwena North concentrator was estimated to achieve a 19% saving in energy consumption (Rule et al., 2008).

Aydoğan et al. (2006) performed an investigation into the grinding of cement in circuits incorporating high compression devices. The HPGR-ball mill, VRM, Horomill and conventional ball mill circuits were considered. Findings from the pilot scale study indicated that the high compression grinding circuits exhibited a 15 to 40% lower specific grinding energy than the conventional tumbling mill circuit. The study further highlighted the high energy consumption of the classifier, one of the reasons why the unit is yet to see significant acceptance and industrial application in minerals processing.

A series of pilot scale trials on a Gamsberg sphalerite ore were conducted by van Drunick et al. (2010) using circuits incorporating high compression devices. One of the aspects of the study was to compare the overall specific energy required by the circuits (Table 2-1). It was observed that the high compression circuits performed better than the AG/SAG mill - ball mill circuit, with the VRM in overflow mode achieving the lowest energy requirement. Benzer et al. (2018) similarly reported a reduced energy consumption for the VRM of 8 to 15% over other conventional circuits.

Table 2-1: Overall specific energy comparison for the comminution of a Gamsberg ore in various circuits (van Drunick et al., 2010).

		Circuit 1	Circuit 2	Circuit 3		Circuit 4	
		AG/SAG mill - ball mill	**Crusher - HPGR - ball mill**	**VRM - airflow**		**VRM - overflow**	
				Cone crusher fed	**HPGR fed**	**Cone crusher fed**	**HPGR fed**
AG/SAG mill	kWh/t	11.26					
Ball mill		8.85	11.17				
Crusher			0.57	1.14	0.57	1.14	0.57
HPGR			2.56		2.56		2.56
VRM				6.92	5.69	7.80	8.05
VRM classifier				5.59	5.40	2.46	2.22
Total	kWh/t	20.11	14.30	13.66	14.21	11.40	13.40

Particle Size Distribution

Different grinding circuits containing different comminution devices and classification methods will likely yield products with different particle size distributions. In a study conducted by Solomon et al. (2011) in which flotation feeds were prepared with both a ball mill and HPGR, it was observed that the HPGR produced a less steep size distribution with more material contained in the fines and coarse fractions. Palm et al. (2010) observed a similar increase in proportion of fines when grinding a Gamsberg sphalerite ore in a circuit incorporating an HPGR.

Products generated with a vertical roller mill in airflow configuration, where an internal air classifier is coupled with the mill and there is a high rate of recirculation, have a steeper particle size distribution than that for the equivalent grind from a ball mill (Erkan et al., 2012; Jørgensen, 2005). Crosbie et al. (2005) however notes that the optimal grind may be different for the different devices and a comparison base on a target P80 may not be equitable.

Liberation and Recovery

Literature displays a variety of liberation and recovery results for comminution with high compression grinding devices. The flotation recoveries from Crosbie et al. (2005), Katzmarzyk et al. (2019), and Nyakunuhwa (2019) for vertical roller mill products and those by Palm et al. (2010), Chapman et al. (2011) and Solomon et al. (2011) on the HPGR products were inconsistent in their comparison to flotation after conventional milling. The findings from these studies are examined in more detail in Section 2.5. A further advantage of high compression grinding is improved leachability of the comminuted product. Leach tests conducted by

Ghorbani et al. (2013), Apling and Bwalya (1997) and Patzelt et al. (1995) indicate improvements in leach recoveries for HPGR over conventional crushing. These observations are attributed to microfracturing (illustrated in Figure 2-15) and are most significant in the larger size fractions (Michaelis, 2005).

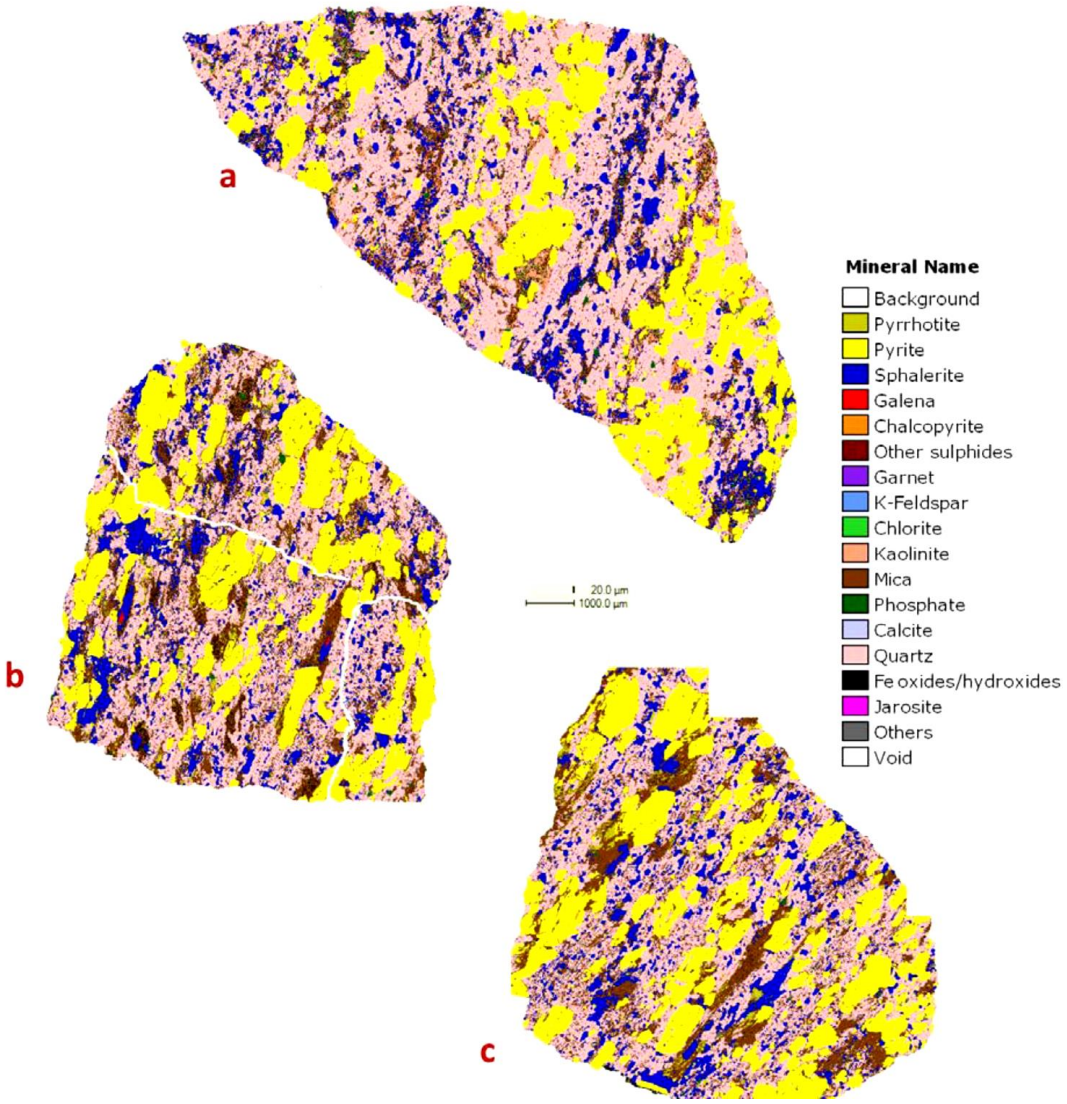

Figure 2-15: Ore crushed with the jaw crusher [a], HPGR [b] and cone crusher [c] (Ghorbani, 2012).

2.4 Classification

Classification is an essential part of all comminution applications and is crucial in controlling product characteristics as well as maintaining the efficient operation of the grinding devices. In minerals processing numerous classification devices including screens, screw classifiers, hydrocyclones, and air classifiers are operated. The method of classification, and hence the

classifier utilised for an application is determined by both the grinding process and the required cut size of separation (Mainza, 2016; Mwale, 2015).

Poor classification in grinding circuits leads to energy inefficient comminution as some fine (product size) material is retained within the grinding circuit causing overgrinding and reducing the circuit's ability to reach optimal throughputs. In addition, poor classification can lead to discharge of low quality product, both too coarse and unliberated as well as too fine, which will affect subsequent valuable mineral recoveries (Albuquerque et al., 2013; Becker et al., 2008; Bhardwaj et al., 1985; Jankovic and Valery, 2012; Mainza et al., 2004).

Classification efficiency can be assessed with the use of partition curves, which yield parameters such as the diameter of a particle equally likely to report to the coarse or fines fractions (cut size), the fraction of fine product size material reporting to the coarse fraction (bypass) and the efficiency of separation (sharpness), which allow for comparison of classification devices or separations (Lynch, 2015).

Hydrocyclones

Hydrocyclones form a core part of classification in wet grinding circuits. Within these devices, slurry flowing under high pressure enters the cyclone tangentially which generates a vortex enabling particle size classification through centrifugally enhanced settling (Figure 2-16). Fine particles flow to the centre of the vortex and exit through the vortex finder, a pipe in the centre of the cylinder, while coarse particles are discharged at the apex of the cone. The separation is affected by the density of the individual particles, with material of a higher specific gravity needing to be finer to report to the vortex finder (Padhi et al., 2019). Hydrocyclones are simple, have a high capacity, have relatively low energy requirements and are able to operate over a wide particle size range (Jankovic and Valery, 2012; Mainza, 2017, 2016; Wills and Napier-Munn, 2006).

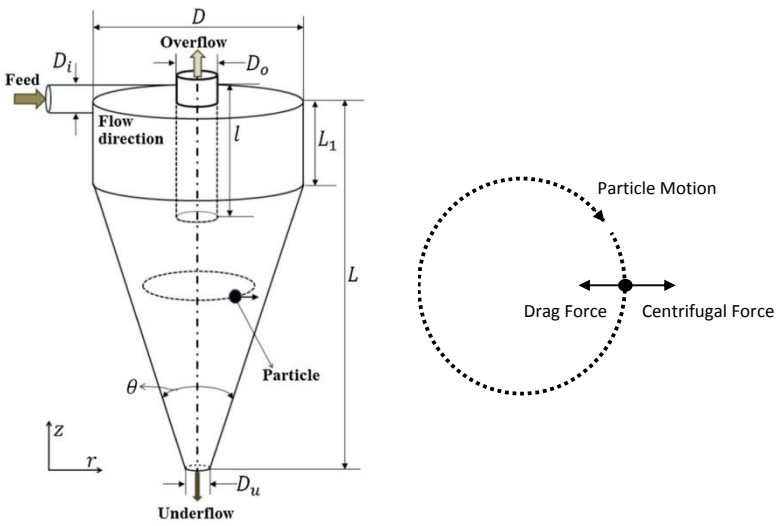

Figure 2-16: The principles of operation of a cyclone (Sabbagh et al., 2016).

Screening

Size separation of material by screening is commonly used in the mineral processing industry. The process takes place on a vibrating surface with multiple apertures (Figure 2-17) and the dimensions of the particles with respect to the apertures determine whether they will pass through (Mwale, 2015; Wills and Napier-Munn, 2006). The separation is made only based on the size of the particle and factors such as density do not affect the classification process significantly. Screening applications can be either dry or wet processes and they are not energy intensive but have historically been limited to coarser size separations (>200 μm) because of throughput restrictions. Recent improvements in design allow for screening at an aperture of close to 45 μm (Hayes, 2003; Mainza, 2017, 2016; Valine et al., 2009).

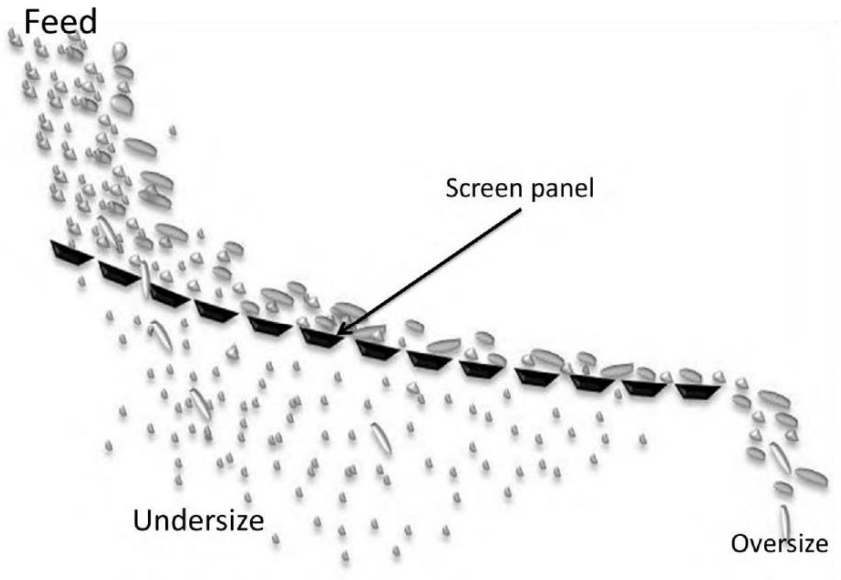

Figure 2-17: The basic screening operation principle (Mwale, 2015).

Air Classifiers

Air classifiers are used extensively in dry grinding applications achieving separation of material suspended in air. Like hydrocyclones, size separation is achieved by balancing the drag forces experienced by particles with gravitational or centrifugal forces. Particles of different size experience these forces in varying magnitudes and this enables separation around a cut size (Altun and Benzer, 2014; Muscolino, 2010; Shapiro and Galperin, 2005). Air classifiers can be broadly split into two different types; static and dynamic (Figure 2-18). Static air classifiers contain no moving parts and the forces on the particles are either generated through the flow of air or induced by gravity (Cepuritis et al., 2015; Lynch, 2015; Lynch and Rowland, 2005), while dynamic classifiers incorporate a rotor which imparts a centrifugal force on the particles.

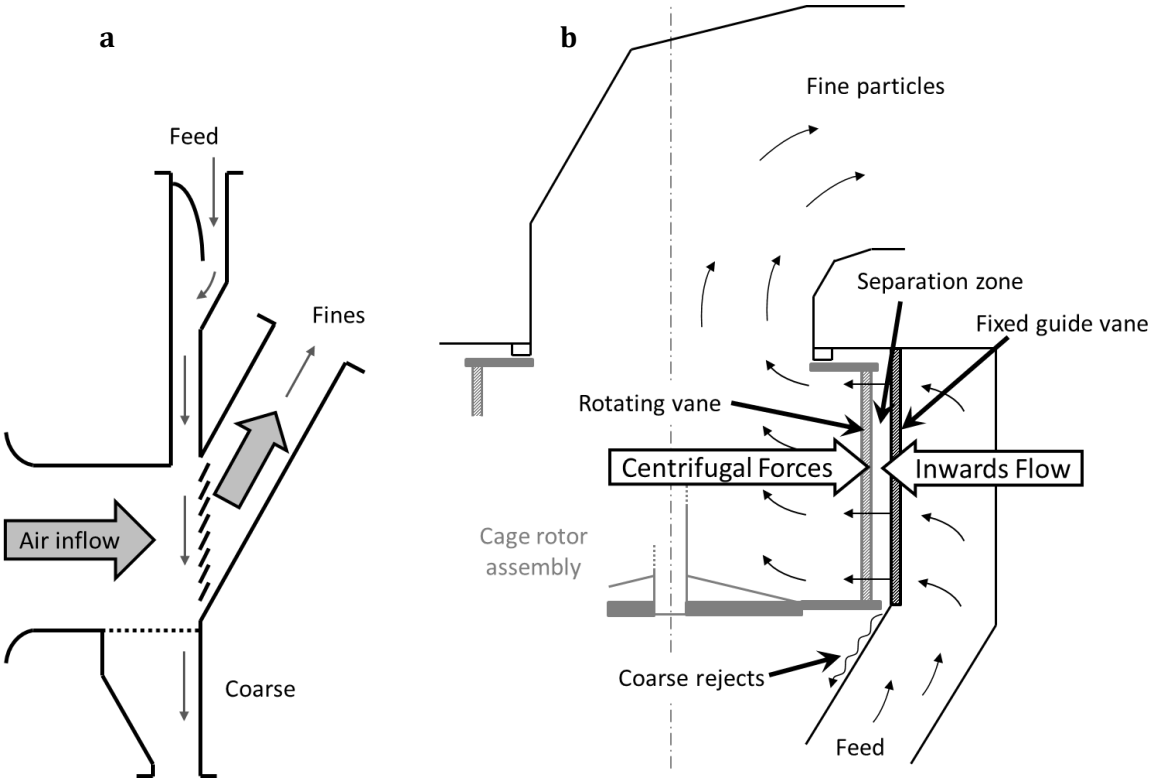

Figure 2-18: The principles of operation of a gravitationally fed static [a] and 3rd generation dynamic [b] air classifier, after Cepuritis et al. (2015) and Schonbach (1988) respectively.

Static classifiers can be grouped into two categories, those with a gravitational feed, including zigzag and V-separators, and those such as conical static separators (Figure 2-19) which are pneumatically fed. The gravity fed classifiers achieve separation through the differential falling rates of particles in a moving air stream, while the conical air classifier relies on centrifugal forces imparted to the material as it passes through a series of guide vanes. The cut sizes and efficiencies of both of these categories are controlled through manipulation of the velocity and direction of the airflow. Unlike dynamic air classifiers, they contain no moving parts so they are relatively inexpensive to operate (Lynch, 2015).

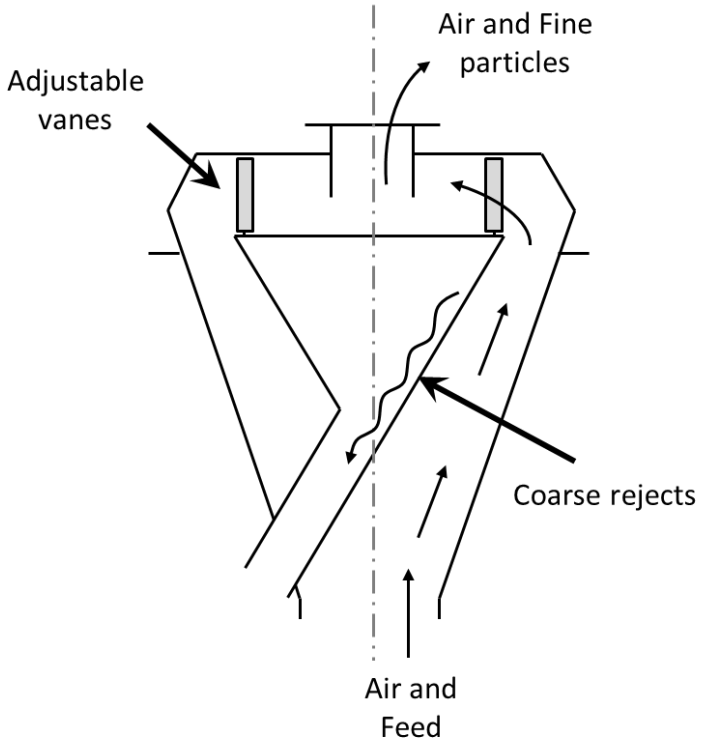

Figure 2-19: The principles of operation of a conical static air classifier, after Lynch and Rowland (2005).

Dynamic classifiers contain rotating parts to facilitate material distribution and airflow in the devices, which reduces the bypass fraction and enables a better separation to be achieved (Table 2-2). The inclusion of these parts however results in the dynamic devices requiring more energy to operate than their static counterparts. A series of generations of dynamic air classifiers have been developed (Figure 2-18 and Figure 2-20). Between generations, advances made by way of the inclusion of external fans, to decouple separator speed from air circulation, and the addition of rotor speed control have allowed improved manipulation of the classifier. The developments have also lead to better classification separations, reduced bypasses and operation at finer minimum cut sizes (Table 2-2 and Figure 2-21).

Table 2-2: Improvements in air classification performance (Lynch, 2015).

	Static	**First generation (1890)**	**Second generation (1960)**	**Third generation (1980)**
d50 [µm]	-	20+	15 - 20	10 - 15
Bypass [%]	60+	50+	15 - 35	5 - 15
Sharpness *(from efficiency curve)*	0.65 - 0.75	0.80 - 0.85	0.85 - 0.90	0.95 - 1.20

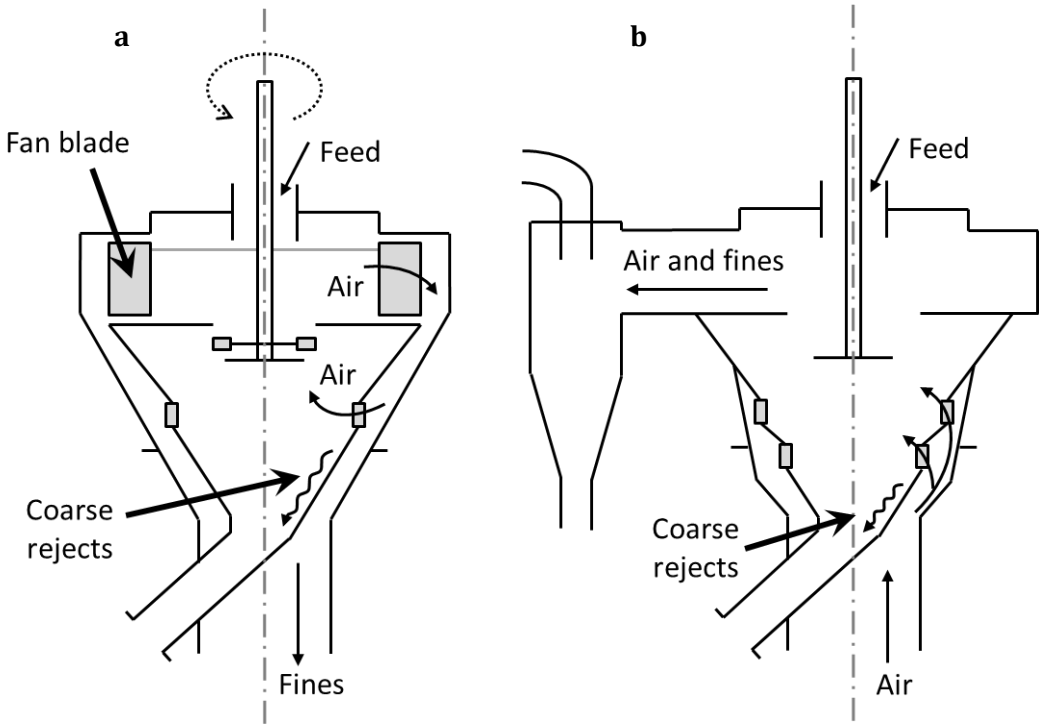

Figure 2-20: The principles of operations of a 1st [a] and 2nd [b] generation dynamic air classifier, after Lynch (2015).

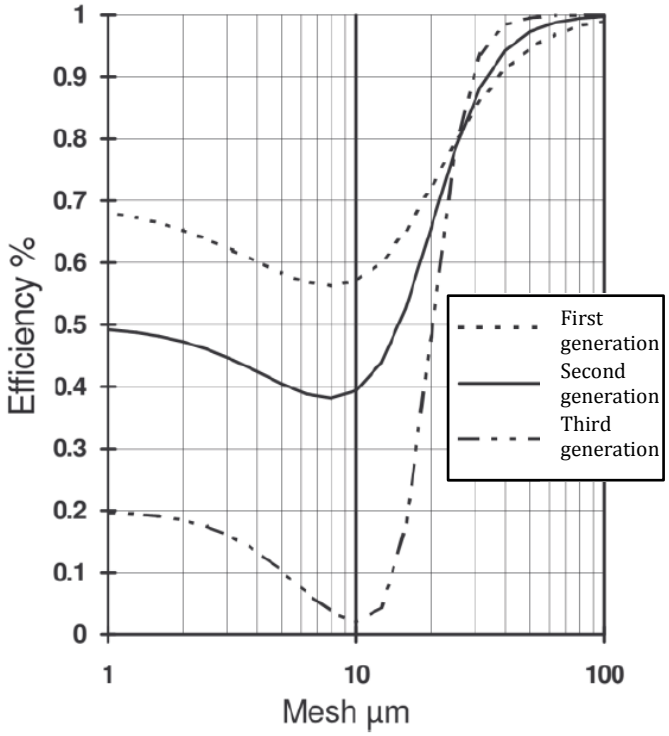

Figure 2-21: Typical partition curves for the three generations of dynamic air classifiers (Lynch, 2015).

Current 3rd generation dynamic air classifiers incorporate a rotor which is used to generate a centrifugal force in the opposite direction to that of the air flow. In the classifier, larger heavier

particles experience a greater centrifugal force, while smaller lighter particles are subject to a greater drag force resulting in a size separation. These classifiers remain energy intensive with substantial power required by the fan to overcome the large pressure drop across the classifier (Loesche GmbH, 2013; Muscolino, 2010; Schonbach, 1988).

Both static and dynamic air classifiers are negatively affected by surface moisture. High moisture levels lead to smaller particles agglomerating or sticking to large particles, which can cause recirculation of product size material and inefficient separations. Density is also seen to have an effect on the classifier's operation. When smaller dense particles are classified they may report to the coarse product despite being of the desired product size because they have a similar weight to less dense larger particles. This impacts the efficiency of classification, reducing grinding capacity, and it can lead to over comminution of denser material (Muscolino, 2010).

2.5 Flotation

The objective of comminution and classification processes is to efficiently prepare feed material for subsequent valuable mineral concentration. Because of this, when testing a comminution device, it is important to also assess the impact the device has on the valuable mineral concentration process.

Principles of Flotation

Flotation is used in multiple mineral processing industries, utilising differences in mineral surface properties to concentrate valuable minerals. The process relies on the natural or induced affinity of different minerals for either water (hydrophilic) or air (hydrophobic) (Ata, 2012). The process is carried out in a series of agitated cells filled with slurry (pulp) containing both the hydrophobic and hydrophilic species. Air is introduced to the system as small bubbles, to which the hydrophobic particles attach (Figure 2-22) and travel to the surface of the pulp. The bubbles reaching the surface form a froth layer, which is collected as it overflows the top of the cell into the launder (Ata, 2012; Wang et al., 2015; Wills and Napier-Munn, 2006).

The separation process can be utilised in two ways, with either the valuable minerals reporting to the froth, which is known as direct flotation, or the unwanted gangue minerals reporting to the froth, known as reverse flotation (Wills and Napier-Munn, 2006). For flotation in the platinum industry, the valuable minerals targeted for concentration are hydrophobic and recovered to the froth. Because of this, further mention of flotation in this study refers to direct flotation.

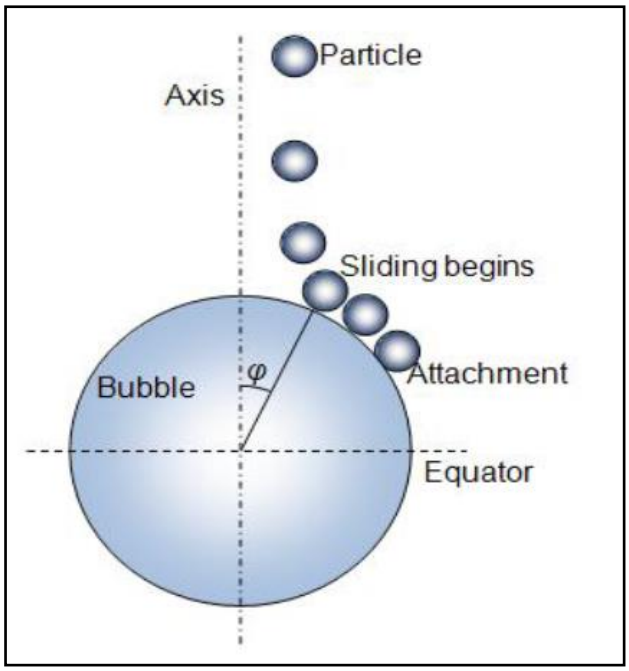

Figure 2-22: Schematic of a particle interacting with and attaching to a bubble (Verrelli et al., 2012).

The recovery of minerals to the concentrate has been described by three main sub-processes: true flotation, entrainment and entrapment. True flotation is the recovery of hydrophobic particles through their attachment to air bubbles and represents the dominant method through which valuable minerals are recovered to the froth (Wills and Napier-Munn, 2006). Entrainment and entrapment are unselective processes, recovering both gangue and valuable minerals to the froth, resulting in dilution of concentrate grades. Entrainment is the mechanical transfer of particles suspended in water entering the froth and is generally the dominant means by which gangue is recovered (Ata, 2012; Wills and Napier-Munn, 2006).

Operational Factors

The flotation process is affected by numerous factors including flotation equipment design and operation, reagent addition, pulp chemistry, and feed particle properties (Klimpel, 1984).

Reagents

Separation in flotation is enhanced through the addition of reagents such as frothers, collectors and regulators. Frothers are added to promote bubble formation in the pulp, reduce bubble coalescences and provide a stable froth phase (Laskowski, 2004). The froth phase functions to enhance the overall selectivity of flotation, with froth stability central in achieving this. Within the froth phase, water is continually draining back to the pulp phase, carrying with it entrained gangue, improving grade of the recovered froth. Too stable froths have low liquid drainage and yield greater recoveries of the unwanted gangue minerals causing low grades (Ata, 2012; Wills

and Napier-Munn, 2006). Too low a froth stability can lead to lower recoveries, as valuable minerals are lost back to the pulp (Wiese et al., 2011). Collectors are compounds added to the pulp to induce hydrophobicity for valuable minerals. The collectors are organic compounds with a polar head and non-polar hydrocarbon tail. The polar head of the collector adsorbs onto the mineral surface, leaving the non-polar tail orientated outward, thereby inducing hydrophobicity (Wills and Napier-Munn, 2006). Regulators can be grouped into activators, depressants and pH modifiers. Activators are generally soluble salts, which dissolve in the pulp and react with mineral surfaces making them more susceptible to collector adsorption. Depressants act to reduce true flotation recovery of naturally hydrophobic gangue species by rendering the minerals hydrophilic, and pH modifiers alter the pulp alkalinity to favour certain reactions and flotation of certain sulphides minerals (Bruckard et al., 2011; Wills and Napier-Munn, 2006).

Pulp Potential

The interaction of mineral surfaces and collectors is also influenced by the redox potential of the pulp (pulp potential). Pulp potential is dependent on the pulp pH and dissolved oxygen, and influences the formation of surface species on minerals (Hu et al., 2020; Zanin et al., 2019) and the adsorption of collectors (Bruckard et al., 2011; He et al., 2005). Sulphide minerals have been shown to be made recoverable without collectors through oxidation of the minerals to form a hydrophobic sulphur-rich, metal-deficient sulphide surface (Wills and Napier-Munn, 2006). Conversely, in reducing pulp environments the precipitation of metal cations as hydroxide species on the mineral surface can render the surface hydrophilic and disrupt collector adsorption (Bruckard et al., 2011; Wills and Napier-Munn, 2006). Pulp potential also plays a role in thiol collector adsorption, with the anodic collector-mineral surface reaction favoured in more oxidising pulps (Bruckard et al., 2011; Koleini et al., 2012). Because of this, it is important to control the pulp potential in flotation so that desired reactions are promoted and unwanted reactions limited (Hu et al., 2020; Zanin et al., 2019). The pulp potential is however not only dependent on reactions occurring in the flotation process, but also those which occur in the grinding environment. Preparation of feed material for flotation typically involves grinding ore as a slurry in mills containing steel grinding media. During this time galvanic interactions occur between the media and sulphide minerals, increasing iron levels in the slurry and lowering the dissolved oxygen concentration. These interactions result in corrosive wear of the grinding media and can lead to the formation of iron hydroxides on the sulphide mineral surfaces, limiting accessibility for collector adsorption (Bruckard et al., 2011). The consumption of dissolved oxygen also results in lower pulp potentials and limits collector activity by inhibiting thiol oxidation and adsorption onto sulphide minerals (Gonçalves et al., 2003). Products

comminuted in dry grinding environments, where galvanic interactions are limited, have shown higher pulp potentials (Chapman et al., 2011; Koleini et al., 2012; Palm et al., 2010; Seke and Pistorius, 2006; van Drunick et al., 2010), corresponding to higher amounts of dissolved oxygen.

Particle Size Distribution and Liberation

Particle size and liberation of the comminution product have a significant influence on the recovery of valuable minerals during flotation. These factors are influenced during comminution, and hence differences in the grinding environment can lead to changes in flotation response.

Particle size is highly important to flotation, affecting particle-bubble attachment/detachment, entrainment and froth stability (Ata, 2012). Attachment of hydrophobic particles is dependent on the energy involved in the collision between the particle and bubble. Sufficient energy is required for attachment to occur, with attachment of finer particles limited because of their lesser inertia (Pease et al., 2006; Prakash et al., 2018; Wang et al., 2016). Detachment is also a function of particle size, with larger particles more exposed to disturbances in the adjacent liquid and hence more likely to detach (Feng and Aldrich, 1999; Wang et al., 2016). Particle size has a marked effect on entrainment in flotation, with finer particles significantly more likely to be entrained (Wang et al., 2015). Figure 2-23 demonstrates the relationship between particle size and recovery through entrainment, with entrainment the primary mechanism for fine gaunge particle recovery (Wang et al., 2015). The presence of particles in the froth has an effect on froth stability. Livshits and Dudenkov (1965) (as referenced in Ata (2012)) showed that there is an optimum particle size which promotes froth stability. The hydrophobic particles stabilise the froth through bubble film stabilisation, reducing bubble coalescence (Ata, 2012), and providing resistance to physical drainage in the lamella (Wiese et al., 2011). The presence of highly hydrophobic particles however can destabilise froths by bridging the froth film and causing bubble coalescence (Johansson and Pugh, 1992; Wiese et al., 2011).

The relationship between true flotation recovery and particle size is illustrated in Figure 2-24. The reduction in recovery for finer particles is due to finer particles displaying slower recovery rates, due to decreased efficiency of particle-bubble collisions, and having higher surface areas requiring excessive reagent dosages. The loss of coarse fractions is due to high detachment rates in the pulp and decreased buoyancies of the particle-bubble aggregates (Feng and Aldrich, 1999; Prakash et al., 2018; Runge et al., 2013; Trahar, 1981). The diagram shows that there is an optimum size range in which flotation recovery of particles is maximised. This range has been typically found to be 10 - 100 μm for a wide variety of minerals, reagents, and flotation machines (Prakash et al., 2018; Trahar, 1981; Wills and Napier-Munn, 2006).

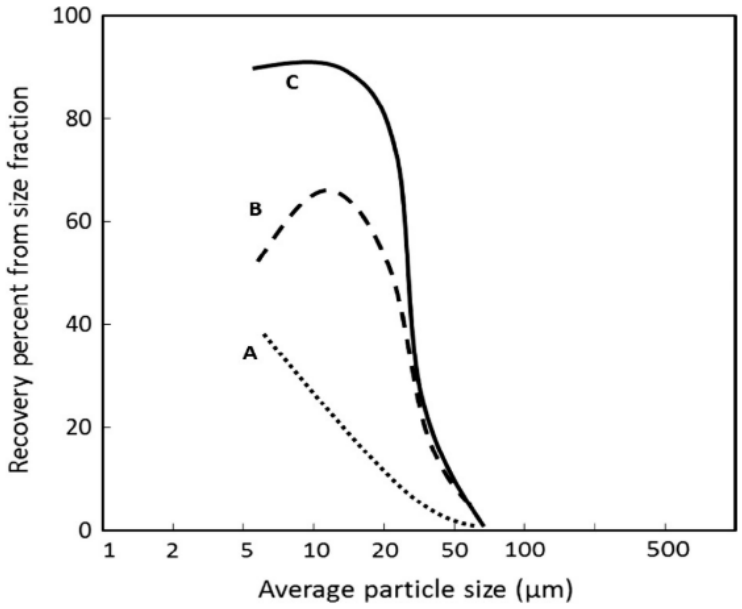

Figure 2-23: Recovery of siderite as a function of the average particle size, showing recovery by entrainment [A], recovery by true flotation [B] and recovery by entrainment & true flotation [C] (Wang et al., 2015), after Trahar (1981).

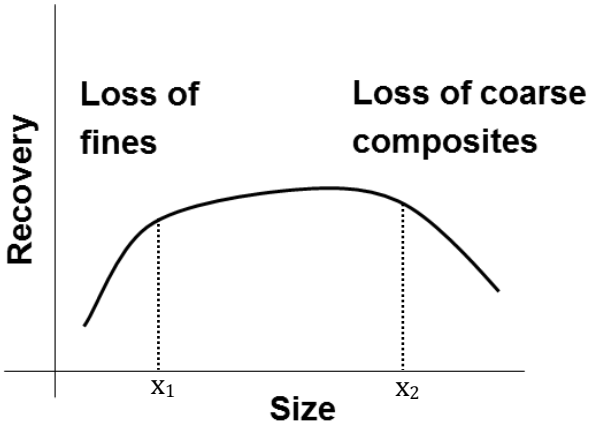

Figure 2-24: Diagram illustration the variation of flotation recovery with particle size, after Trahar (1981).

Particle size is also directly linked with mineral liberation. Finer products, which have a higher valuable mineral liberation, are more likely to have higher flotation recoveries as there are fewer unliberated, unrecoverable valuable mineral particles. For coarser products, there may be insufficient valuable mineral liberation, which will correspond to lower flotation recoveries.

Influence of High Compression Grinding

In literature, the response of liberation to comminution in high compression grinding devices was shown to be variable. Several researchers have investigated the effect of comminution with an HPGR on valuable mineral liberation. The conducted research spans ores from a variety of

mineral processing applications and results indicate that a similar or greater extent of valuable mineral liberation can be achieved when grinding with an HPGR as opposed to a tumbling mill/crusher (Chapman et al., 2011; Palm et al., 2010; Solomon et al., 2011). The flotation response for products incorporating high compression grinding has been compared in a series of studies which yielded variable results. Michaelis (2005) found that for a Chilean copper ore, the HPGR product gave better copper recoveries than the ball mill product. Palm et al. (2010) related pulp potential and mineral surface properties to grinding environment and found that flotation grade and recovery did not change when a dry grinding ball mill was fed with either cone crush or HPGR product. Research conducted by Solomon et al. (2011) and Chapman et al. (2011) found better grade-recovery curves for wet ball milling products. In the HPGR papers by Saramak et al. (2014) and Michaelis (2005), results indicated that increases in grinding pressure improved flotation recoveries to a point, after which recoveries dropped. The increase in recovery was due to better liberation and the decrease caused by over-grinding (Michaelis, 2005).

There are few VRM applications in mineral processing and hence minimal literature is available on its effect on downstream processing. Products from the VRM are expected to have a better flotation response than those for conventional tumbling mills, with higher valuable mineral recoveries and grades because of their steeper particle size distribution (Crosbie et al., 2005; Erkan et al., 2012; Gerold et al., 2012b). Gerold et al. (2012b) also argued that the lower wear rates will reduce the metal input into flotation, limiting the formation of iron hydroxides on the sulphide mineral surfaces, improving the flotation chemistry. van Drunick et al. (2010) performed flotation tests in which a zinc ore prepared in either a crusher or HPGR was comminuted in the VRM with different roller configurations. No comparison to ball mill flotation response was made, however flotation tests did indicate that the combination of HPGR and two roller VRM produced the highest grade-recovery curve, with the improvements attributed to greater valuable mineral liberation. Results presented by Crosbie et al. (2005) for a copper sulphide ore indicated that inter-particle breakage, generated with a VRM, yielded a superior grade-recovery curve compared to that obtained for tumbling mill product (Figure 2-25). This increase in recovery was linked to a higher proportion of the copper sulphides in the VRM product reporting to size classes optimal for flotation recovery. Flotation data for the same test work, further demonstrated increased flotation kinetics for the VRM product (Figure 2-26). In work carried out by Nyakunuhwa (2019) on a copper/lead/zinc ore, no difference was observed in valuable mineral recoveries when varying the vertical roller mill grinding pressure and VRM recoveries were comparable to those obtained for a product prepared in a wet rod mill. In a study by Katzmarzyk et al. (2019), grade-recovery curves for VRM product were

observed to be better than those for a wet rod mill product. The results were consistent for a range of flotation alkalinity and the difference between comminution devices was correlated to pulp potentials.

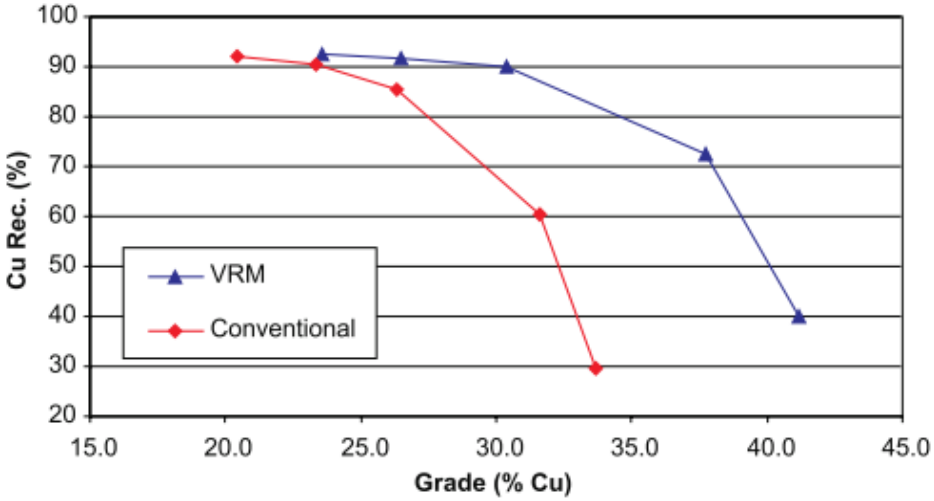

Figure 2-25: Comparative copper sulphide ore grade-recovery curves for VRM and conventional tumbling mill products (Crosbie et al., 2005).

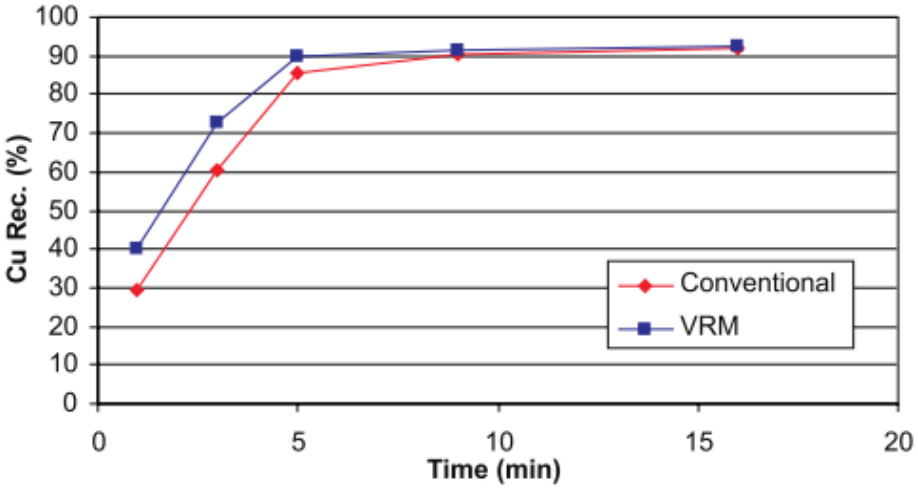

Figure 2-26: Rates of VRM and conventional tumbling mill product flotation recoveries for a copper sulphide ore (Crosbie et al., 2005).

The effect on pulp potential is a further aspect which must be considered when comparing the flotation response of high compression grinding and conventional milling products. High compression grinding is carried out in a dry environment and this can affect both the mineral surfaces and electrochemistry of the pulp in flotation. Zhu et al. (2015) and Farrokhpay and Manouchehri (2012) observed lower collector adsorption for dry grinding products, resulting in lower flotation recoveries. Greater surface oxidation was proposed by Farrokhpay and Manouchehri (2012) as the reason for the lower collector adsorption. Chapman et al. (2011)

similarly found better flotation recoveries for wet grinding products and studied the ground product surfaces with XPS. Results indicated higher levels of metal oxides for dry grinding samples, however wet ground samples displayed greater surface levels of hydroxides species. Katzmarzyk et al. (2019), Koleini et al. (2012), Palm et al. (2010) and Seke and Pistorius (2006) all obtained higher valuable mineral recoveries for dry milled products and attributed this to increased pulp potentials for products from the dry grinding environments. Chelgani et al. (2019) reviewed the effects of dry and wet grinding on flotation, and summarised that dry grinding products yielded higher flotation pulp potentials and dissolved oxygen levels. The effect of these conditions on flotation was dependent on mineral type, with sphalerite and chalcopyrite benefiting, while recoveries of pyrite, PGMs and galena are depressed. This however does not align with chalcopyrite and galena recoveries presented by Farrokhpay and Manouchehri (2012).

2.6 Process Mineralogy

Historically the performance of processing circuits has been characterised by comminution size reduction and elemental metal recoveries, however the need to understand mineral behaviour during processing is being increasingly recognised as important as the industry exploits more complex ore bodies (Becker et al., 2016; Bradshaw, 2014; Petruk, 2000; Rule and Schouwstra, 2011; Solomon et al., 2011; Young et al., 1997). Characterising and understanding the mineralogical information allows for better plant design and circuit optimisation (Gu et al., 2014; Lotter, 2011; Rule and Schouwstra, 2011). Process mineralogy looks at factors such as ore constituents, valuable mineral grades, grain sizes, liberation and associations, using the information to predict, understand and solve "problems encountered during the processing of ores, concentrates, smelter products and related materials" (Petruk, 2000). Amongst other applications, process mineralogy can be used to analyse tail samples from concentration processes, determining mineral specific losses, and to characterise ore textures, helping inform decisions on comminution throughput, required target grinds and grinding energy consumption (Cropp and Goodall, 2013).

Mineralogical characterisation can be carried out with a number of methods, the most common of which are optical microscopy, quantitative X-ray diffractometry (XRD) and quantitative automated scanning electron microscopy with energy dispersive X-ray spectrometry (Auto SEM-EDS). Optical microscopy uses visible light for the identification of minerals and ore textures, quantifying mineral composition through point counts. XRD makes use of X-ray diffraction patterns for crystalline phase identification and thereby determination of mineral

composition. For Auto SEM-EDS, mineral surfaces are scanned with a focused electron beam, and the resulting backscattered electrons and X-ray spectra are analysed to give mineralogical information about the sample (Becker et al., 2016; Xiao and Laplante, 2004). Auto SEM-EDS systems, such as Quantitative Evaluation of Minerals with Scanning Electron Microscopy (QEMSCAN) and the Mineral Liberation Analyser (MLA) are widely used in the mining industry and have enabled for the routine, quantitative mineralogical characterisation of ores (Gu et al., 2014). For the QEMSCAN, results generated in the analysis are processed to give false colour mineral maps which describe mineral texture and association. The data can be further processed to obtain quantitative measures of bulk mineralogy, mineral liberation, association and grain size, and mineral and particle deportment to different size classes and shape profiles (Little, 2016).

Mineral liberation is a characteristic which is fundamental for achieving effective separation in flotation circuits. It is a measure of the exposure of a mineral/mineral grouping in a particle and is often broadly split into categories like those seen in Figure 2-27. For flotation, sufficient comminution/size reduction is required to liberate valuable minerals, exposing mineral surfaces to enable collector adsorption, allowing for subsequent concentration. Valuable minerals which are 'locked' in particles, surrounded by other minerals with little or no exposure at the particle surface, are unlikely to be recovered.

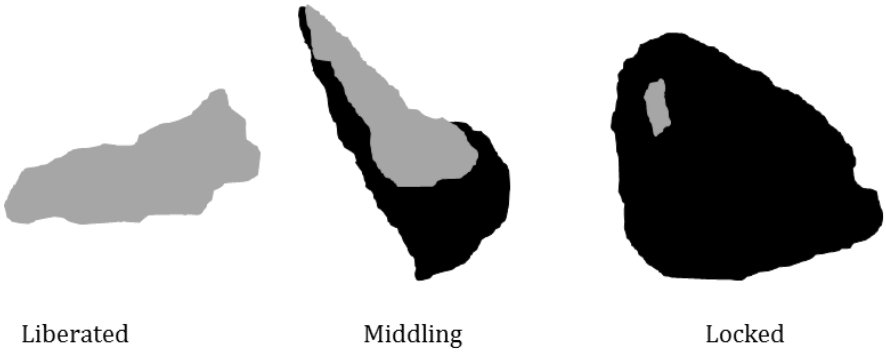

Figure 2-27: Diagram illustrating the different degrees of liberation.

2.7 Mineralisation and Processing of PGMs

Most of the world's supply of platinum group elements (PGE) are extracted from ores mined in four major layered igneous intrusions; the Bushveld Complex in South Africa, the Great Dyke in Zimbabwe, the Stillwater Complex in the U.S.A., and the Norilsk/Talnakh Complexes in Russia (Schouwstra et al., 2000).

The Bushveld Complex (Figure 2-28) in South Africa is the world's largest layered intrusion, extending over 65 000 km^2 and reaching a thickness of 7 km. The complex is a key resource of the PGEs: ruthenium, osmium, rhodium, iridium, palladium and platinum, which are mined in three ores: Merensky reef, Upper Group 2 chromitite reef (UG2), and Platreef. Together, these contain ~75% of the global PGE reserves, as well as significant traces of chromite and base metal sulphides (Mudd, 2010). The Merensky and UG2 are hosted in the critical zone in both the western and eastern limbs of the complex while the northern limb contains the Platreef ore (Cawthorn, 1999; Clarke et al., 2009; Mudd, 2012; Naldrett et al., 2008).

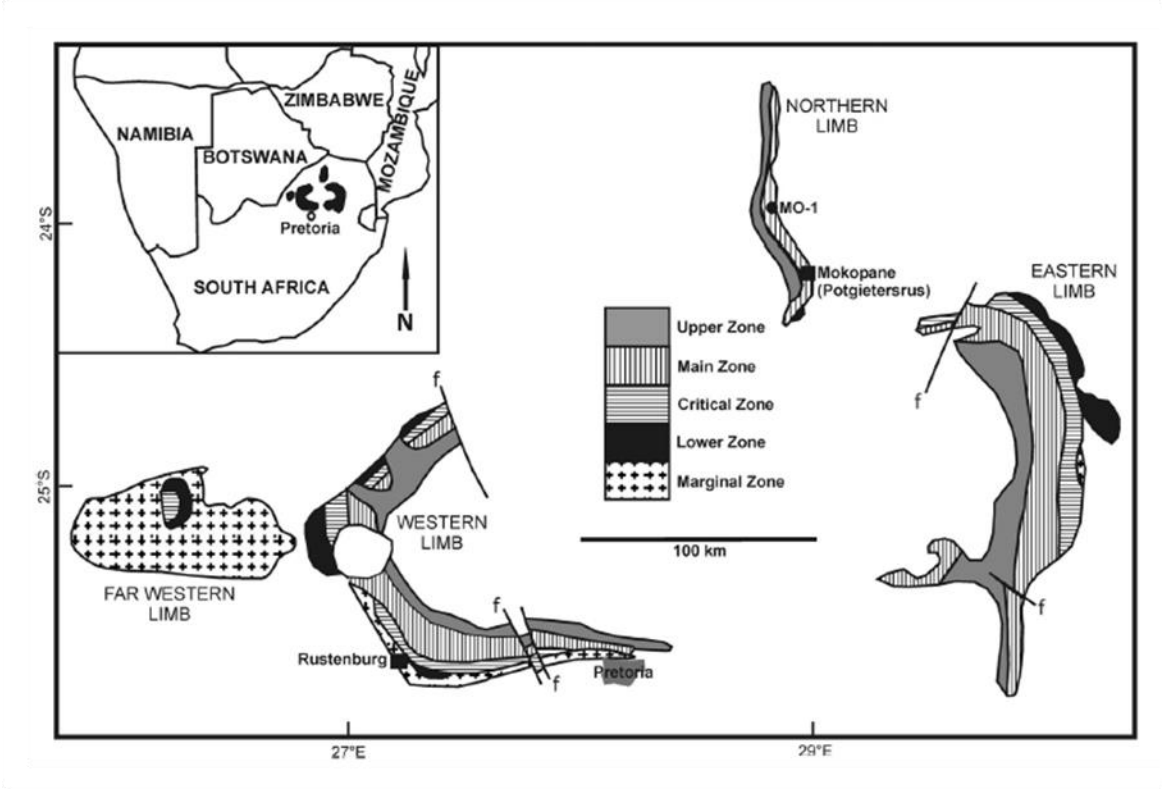

Figure 2-28: Geological map of the Bushveld Complex with an inset showing its position in South Africa (Lehloenya and Roelofse, 2013).

The Merensky reef was the first economic PGM reef type to be discovered and successfully processed in South Africa (Cawthorn, 1999). The reef is regarded as having the simplest mineralogy of the three reef types, with typical 4E grades of 4.2 and 6.0 g/t in the Eastern and Western limbs respectively (Mudd, 2012). The reef typically consists of orthopyroxene (~60%), plagioclase feldspar (~20%), clinopyroxene (~15%) and base metal sulphides (1-3%), with most of the PGMs associated with the BMS (Schouwstra et al., 2000). UG2 ore was considered more difficult to process and as a result it was not mined until technology advances in the 1980s which allowed for feasible PGM extraction (Mudd, 2012; Naldrett et al., 2008).

UG2 from the Eastern and Western limbs of the Bushveld Complex contains 4E grades of 5.1 and 4.9 g/t respectively with the predominant mineral components being chromite (60-90%), pyroxene (5-30%) and plagioclase (1-10%) (Mudd, 2012; Schouwstra et al., 2000). The reef is found as a 0.4 to 2.5 m thick layer 40 to 400 m below the Merensky reef (Cawthorn, 1999; Schouwstra et al., 2000). Within the UG2 ore, PGMs are typically finer grained and associated less with the base metal sulphides than in the Merensky reef (Rule and Schouwstra, 2011).

Platreef is the most variable of the three ore types and of the three ores it has the shortest history of being exploited. The reef is found in the Northern limb of the Bushveld Complex and consists of an upper orthopyroxene cumulate, transitioning to a lower zone of pyroxenite, feldspathic pyroxenite and norite that has interacted strongly with the footwall sediments (Naldrett et al., 2008; Schouwstra et al., 2013). The Platreef layer can reach thicknesses of 10 to 40 m, and as opposed to the thinner Merensky and UG2 reefs it has been mined in open-pit fashion by means of the Mogalakwena North, Mogalakwena Central, Sandsloot and Zwartfontein pits (Cramer, 2001; Holwell et al., 2007; McDonald et al., 2017; Schouwstra et al., 2000). The base metal mineralisation and PGE concentration are found to be highly variable (Cramer, 2001; Mudd, 2012; Naldrett et al., 2008). The platinum group minerals consist mainly of PGE tellurides, platinum arsenides and platinum sulphides. These are found either as fine grained PGMs, typically less than 10 μm (Nel et al., 2005) disseminated in the silicates, or enclosed in or on the grain boundaries of base metal sulphides, which include pyrrhotite, pentlandite, chalcopyrite and pyrite (Schouwstra et al., 2000, 2013). Platreef has a higher ratio of palladium to platinum than that of the Merensky and UG2 deposits, but is of overall lower PGE grade (Mudd, 2012). The Platreef is considered challenging to process with considerable variation in hardness and recovery potential due to variation in rock type associated with the interaction of the footwall and lower zone (Schouwstra et al., 2013). Bond work indices of greater than 25 kWh/t are frequently encountered for the ore (Cramer, 2001; Humphries et al., 2006; Mainza and Powell, 2006; Schouwstra et al., 2013).

Processing of PGE Ores

After crushing, the three PGE bearing ores are treated with a similar staged comminution-flotation process, commonly referred to as an mill-float-mill (MF2) circuit (Humphries et al., 2006; Mainza et al., 2004). A primary tumbling mill targets liberation of coarse valuable minerals and base metal sulphides, with which PGMs are often associated, for recovery in primary rougher flotation, and a secondary ball mill achieves a finer grind, liberating previous unrecoverable valuable minerals before the secondary roughers or scavengers (Cramer, 2001). After the rougher and scavenger flotation sections, which target recovery of the PGMs and base metal sulphide minerals, concentrate is fed to the cleaner flotation circuit for further upgrading

(Figure 2-29). Several cleaner flotation stages are used to reduce naturally floating gangue minerals such as talc, a mineral present in the PGE bearing ores, and in the case of UG2 ore, to reduce chromite levels in the concentrate sent to pyrometallurgy. In certain applications, additional grinding capacity has been installed in the form of high intensity stirred mills. These mills are incorporated either after the secondary mill to achieve further liberation prior to secondary flotation or for grinding of rougher concentrate prior to cleaner flotation. The overall process typically achieves a PGM recovery of 80-90% for the three ore types (Cramer, 2001). The efficiency of comminution in these and other minerals processing circuits is constrained by the indirect method of applying energy to particles in the grinding environment of tumbling mills. In these devices only a small fraction of the energy is available for breakage.

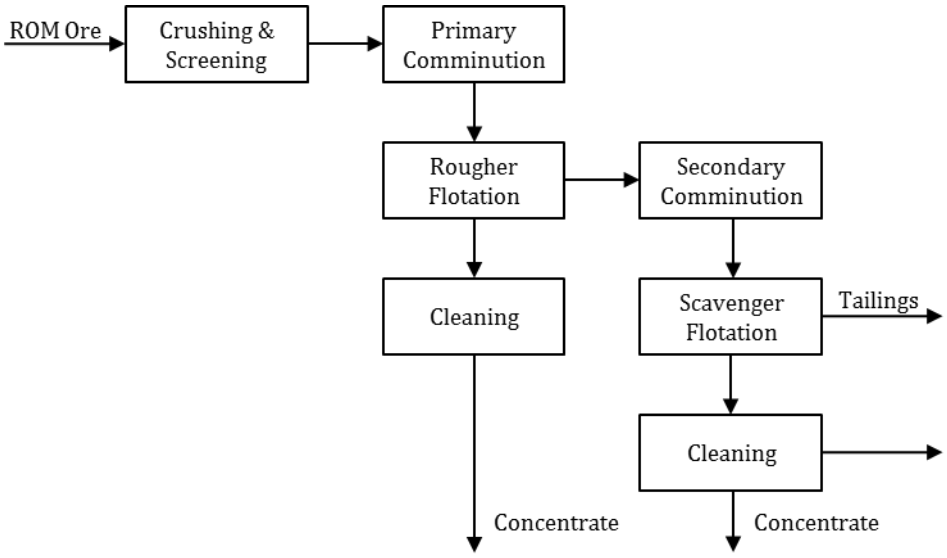

Figure 2-29: Typical PGM concentrator flowsheet (Cramer, 2001).

With the increasing cost of energy and continual shift to processing of finer grained, lower grade, mineralogically more complex ores, it has become essential for the industry to look at more efficient means of grinding. Large amounts of research have been conducted into investigating and implementing more energy efficient comminution technologies for the processing of PGMs (Chapman et al., 2011; Drozdiak et al., 2011; Little, 2016; Rule, 2008, 2011; Rule et al., 2008; Solomon et al., 2011; van Drunick et al., 2010). One of the more recently constructed plants processes Platreef with the inclusion of stirred milling as well as incorporating high pressure grinding rolls (HPGR) in closed circuit prior to the primary mill in place of tertiary crushing (Humphries et al., 2006; Rule et al., 2008). In this and other applications the adoption of the HPGR resulted in improved overall comminution energy efficiency (Patzelt, 1992; Wüstner, 1986) and increased throughput (Rule et al., 2008).

Critical Review of the Literature

Research in comminution is typically focused on gaining understanding and increasing efficiencies of comminution devices and the comminution process. The majority of this research has been conducted for well-known and widely implemented technologies. Significantly less research has been conducted for the less used technologies and devices (Figure 2-30). The lack to research into other technologies is a result of the industry's conservative nature, the preferring of 'tried and tested' design over other, potentially better technologies (Rule et al., 2008). It is however important in an industry continually faced with increasing throughput and energy requirements because of declining ore grades and increasing mineralogical complexity that technologies with potential to reduce energy use be sufficiently investigated. This is particularly significant as the minerals processing industry proceeds to finer grinds, progressing towards the unknown and potentially exponential trends in the particle size-energy relationship illustrated by Lynch (2015) in Figure 2-1.

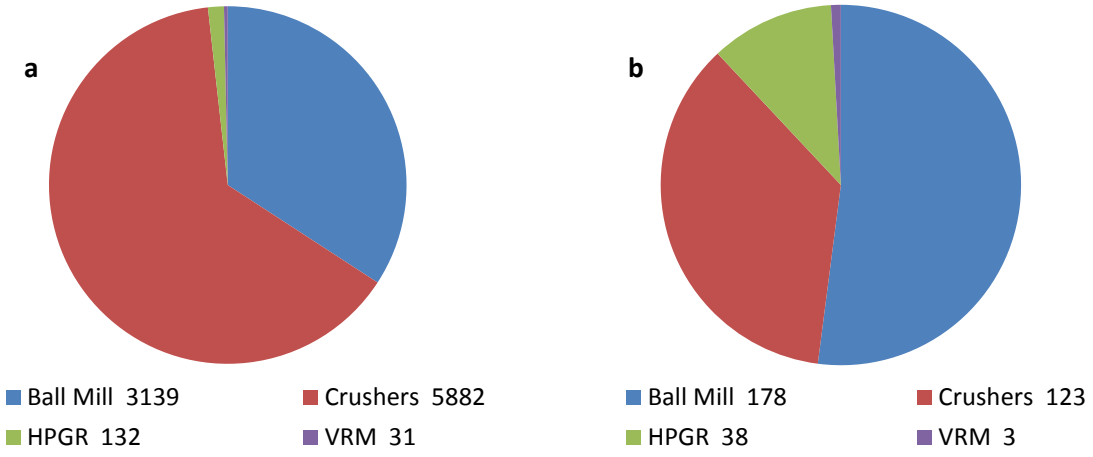

Figure 2-30: Search hits for the terms 'ball mill', 'high pressure grinding rolls' or 'vertical roller mill' in conjunction with the term 'minerals processing' in the ScienceDirect [a] and OneMine®.org [b] databases March 2020.

Literature indicates that high compression grinding is an energy efficient method of achieving size reduction. High compression devices such as the HPGR have seen implementation in minerals processing circuits and have become accepted technologies. Other high compression devices such as the VRM however have not been adequately investigated but could have potential to benefit the minerals processing industry.

Vertical roller mills are widely used in the production of cement and for the pulverisation of coal for power plants and furnaces. In these applications the objective is to efficiently reduce particle size (increase surface area) to a desired range and this is evident in the summary for vertical roller mill literature given in Table 2-3. Vertical roller mill studies in cement and coal grinding applications have largely focussed on the comparison of energy efficiency and product quality to

tumbling mills equivalents, with some of the research investigating how online and design variables such as grinding pressure and classifier rotor speed affect mill performance and product quality. In the work by Özer (2011), a novel method was developed for the sampling of the internal VRM streams, enabling the transport of material within the mill chamber to be studied. This information presented is useful in designing experiments and isolating which machine variables are important, however it cannot be applied directly to minerals processing applications that include downstream recovery steps, in which liberation has to be considered.

A few studies have been conducted on the operation of the vertical roller mill in a minerals processing environment. Table 2-4 summarises VRM test work carried out on a number of ores. Various online and design variables have been investigated and comparisons to tumbling mills have been made. The literature has predominantly been focused on energy usage and throughput, with certain studies examining product mineralogy and downstream valuable mineral recoveries. The paper by van Drunick et al. (2010) contains a grade-recovery curve showing select results from testing on a sphalerite ore. Work presented by Nyakunuhwa (2019) and Katzmarzyk et al. (2019) compared flotation performance of wet conventionally milled products with those generated by the VRM, and in both studies valuable mineral recoveries were similar for the comminution products. Nyakunuhwa (2019) went further in recommending that future studies be done on other ore types, particularly focusing on those with a finer mineral grain size, where difference in flotation response between the comminution products may appear. The paper by Crosbie et al. (2005) alludes to a significant unpublished body of work carried out at Anglo American Research Laboratories that cannot be cited since it is kept confidential. The selection of data which has been published by Crosbie et al. (2005) indicates that vertical roller mill products can achieve comparable flotation recoveries to conventional tumbling mills, however the impact of grinding in the vertical roller mill on downstream processes was not presented. Furthermore, only exploratory investigations by Altun et al. (2015) and van Drunick et al. (2010) have been conducted into operation of the VRM with different classification methods and in both studies the effect on downstream processing was not considered. In line with this, the field would benefit from a comprehensive study investigating the effects of different vertical roller mill variables and different classification configurations on milling performance and downstream recovery methods.

This thesis aims to achieve this, consolidating the aspects investigated in the individual studies into a single body of work. In doing this, a study was undertaken for the comminution of a platinum group mineral ore, Platreef, in a vertical roller mill operated with different classification methods (internal and external air classification, and external screening) and varying design (dam ring height) and operational (grinding pressure, classifier rotor speed)

variables. The effect of comminution on downstream processes was established by analysing flotation response of the comminution products and comparing these to the flotation performance of products comminuted in a tumbling mill.

Table 2-3: Summary of vertical roller mill grinding studies in literature.

	Authors	Online Variables				Design Variables		Feed	Tumbling mills comparison
		Grinding pressure	Table speed	Airflow rate	Classifier rotor speed	Dam ring height	Means of classification		
Cement	Roy (2002)	PSD	-	-	-	PSD	-	-	SE, PSD
Cement	Simmons et al. (2005)	-	-	-	-	-	-	-	SE, PSD
Cement	Tamashige et al. (1991)	SE, tph, PSD	-	-	PSD	SE, tph, PSD	-	-	Wear
Cement	Jørgensen (2005)	Bed height	-	-	-	-	-	Cement blends	SE, Fineness, Cement strength
Cement	Aydoğan & Benzer (2011)	-	-	-	-	-	-	-	SE, PSD
Cement	Panigrahy et al. (2003)	-	-	-	-	-	-	-	Cement setting time
Coal	Thiel & Schössow (2001)	tph	-	-	-	-	-	Hardness on tph	-
Coal	Özer (2011)	-	-	PSD, tph, Circulating load	-	-	-	-	-
Marble, Siderite, Hematite	Boehm et al. (2014)	-	-	-	-	-	-	-	Energy and surface area generation

Where SE, tph, PSD stand for comparisons made in terms of specific energy, throughput and particle size respectively.

Table 2-4: Summary of vertical roller mill grinding studies in literature continued.

	Authors	Online Variables				Design Variables			Feed	Tumbling mills comparison
		Grinding pressure	Table speed	Air temp.	Classifier rotor speed	Dam ring height	Means of classification	2 vs 4 roller		
Copper/ lead/zinc ore	Nyakunuhwa (2019)	SE, tph, PSD, Flotation	-	PSD	SE, tph, PSD, Flotation	-	-	-	-	PSD, Min, Flotation
Copper ore	Katzmarzyk et al. (2019)	-	-	-	-	-	-	-	-	Min, Flotation
Copper/ gold ore	Benzer et al. (2018)	SE, tph, Wear	-	-	-	-	-	-	-	SE, Wear
Gold ore	Altun et al. (2017)	tph	tph	-	tph, PSD	-	-	-	-	-
Gold ore	Erkan et al. (2012)	-	-	-	-	-	-	-	-	SE, PSD, leach, wear
Copper ore	Altun et al. (2015)	-	-	-	-	-	SE, PSD	-	-	SE
Zinc ore	van Drunick et al. (2010)	-	-	-	-	-	SE	Flotation, Min	HPGR vs cone fed on flotation	SE
Iron ore	Reichert et al. (2015)	SE, tph, PSD, Min	-	-	SE, tph, PSD, Min	SE, tph, PSD, Min	-	-	-	-
Mineral sands	Philander & Rozendaal (2011)	-	-	-	-	-	-	-	-	SE, Min, Spiral recovery
Copper ore, Nickel ore	Crosbie et al. (2005)	-	-	-	-	-	-	-	-	PSD, Flotation, Min
PGE ore	This thesis	SE, tph, PSD, Flotation	-	-	SE, tph, PSD, Min, Flotation	SE, tph, PSD, Min, Flotation	SE, tph, PSD, Flotation	-	-	PSD, Flotation

Where SE, tph, PSD and Min stand for comparisons made in terms of specific energy, throughput, particle size and mineralogy respectively.

Hypotheses

For the work conducted as part of this research into the operation of the vertical roller mill with different classification devices, and under different operating conditions, the following hypotheses have been proposed:

1. The VRM will be able to efficiently generate a suitable comminution product because the method of achieving breakage in this device is through the direct application of a force to a bed of particles.
2. Using a VRM in conjunction with an external classifier will improve the unit's overall energy utilisation because the energy used for material transportation and separation mechanisms will reduce, while energy contributed towards breakage in the system is not altered.
3. During comminution in the vertical roller mill, increasing the compressive forces acting on the particle bed and the degree of confinement of the particles in a bed will improve the flotation recovery for products, because energy absorbed by the particles increases, leading to higher breakage rates within the system, which increases liberation of particles.
4. Changing the classification method used in conjunction with the VRM will affect the flotation response of the ore because different classifiers yield comminution products of different particle size distribution. Classifiers which yield a narrower particle size distribution, at the same grind, will have an increased proportion of valuable minerals in the optimum flotation range.

Key Questions

The following questions have been constructed to test each respective hypothesis.

1. How does performance of the VRM vary when grinding pressure alters the compressive forces particles experience and adjusting the dam ring height changes residence time on the grinding table?
2. What effects does changing the classification device used in conjunction with the vertical roller mill have on circuit performance and the particle size distribution of the product?
3. Do the liberation profiles and flotation performance of products vary depending on the compressive force and degree of bed confinement experienced during comminution in the VRM?
4. Does the flotation response for particles comminuted with the VRM change when the classification method is altered? Are changes in flotation response due to differences caused by the different classifiers employed?

Chapter 3

DESCRIPTION OF EXPERIMENTAL APPARATUS

This chapter delves into the operation of the vertical roller mills used in this study. The classification processes associated with each of the classifiers is outlined and how they were integrated with the VRM to form comminution circuits is explained in terms of transport of material within the systems. The factors that affect the operation and performance of the vertical roller mill are considered. Observations from literature relating to these variables and the motivation for their selection in this study are outlined. The flotation equipment used for the batch flotation tests and laboratory scale tumbling mill are also described.

3.1 Loesche Vertical Roller Mill

The vertical roller mill has been introduced in Section 2.3 of the Literature Review. The mill is incorporated into the comminution circuit after either a secondary or tertiary crushing stage, replacing the tumbling mill section of the traditional comminution circuit (van Drunick et al., 2010). The unit receives crusher product, at a feed size of up to 80-150 mm (Erkan et al., 2012; Schaefer, 2001) and depending on the application, produces particles for further processing as fine as 20 μm (Erkan et al., 2012). The VRM circuit comprises grinding and classification components, with the choice of the method of classification playing a key role in determining how the components operate together in a circuit.

3.2 Classification

Airflow

In the conventional design the VRM is operated with two different classification configurations. The first classification configuration makes use of a dynamic air classifier mounted directly above the grinding section within the vertical roller mill. This is referred to as ‘airflow mode’

and is the standard mode for operation of the VRM with a schematic of the setup is provided in Figure 3-1. The grinding table, grinding rollers and dam ring form the grinding components of the system and are located in the lower section of the vertical roller mill. Elements such as the feed chute, grit cone and louver rings (a series of vanes below the grinding table which direct air as a vortex through the mill chamber), facilitate transport within the grinding chamber and the transfer of material to and from the dynamic air classifier.

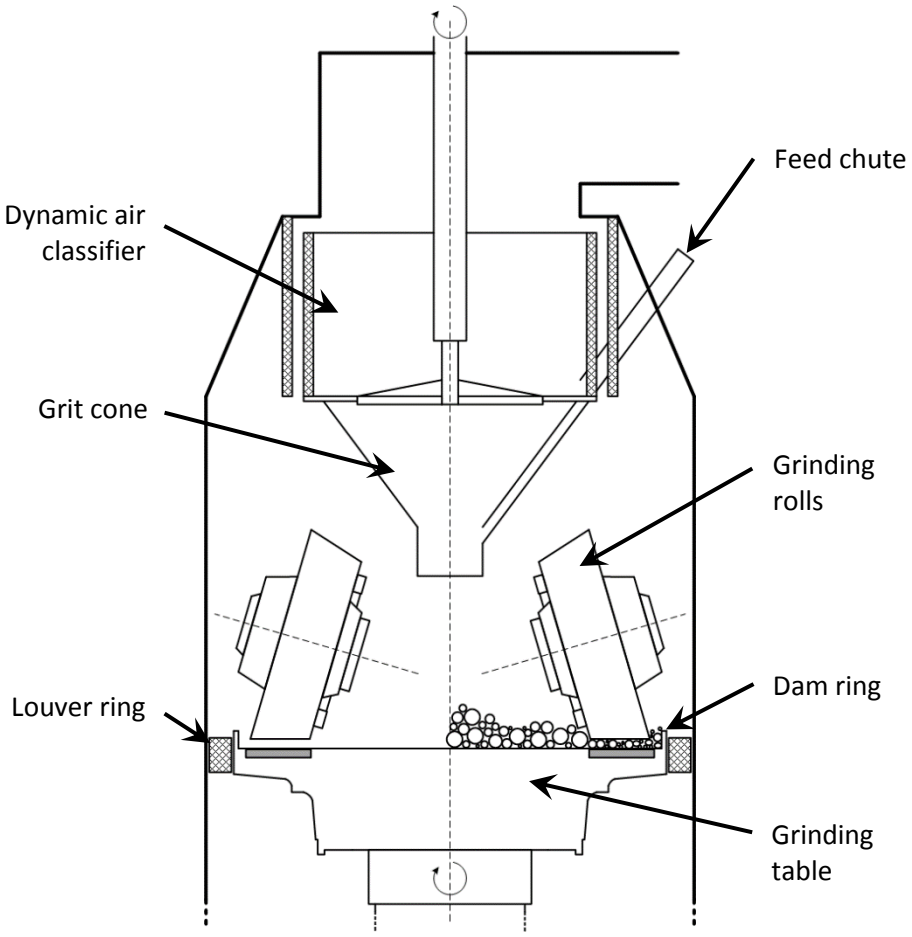

Figure 3-1: Schematic illustrating components of the Loesche VRM operated in airflow mode.

In airflow mode there are three ways material recirculates, depending on particle size (Figure 3-2). Large particles [1] fall in the air stream and pass through the louver ring where they are collected by a scraper and added to the new feed via a bucket elevator. Smaller particles [2] are transported by the air stream upwards through the grinding chamber to the dynamic air classifier. Particles that travel to the classifier are split based on particle size, with bigger particles rejected and returned to the grinding bed via the grit cone, and fine, product sized material passing through the classifier and continuing to a filter where the solids component is collected and discharged as product. Intermediate sized particles [3] are initially lifted in the air stream but because their weight is similar to the buoyancy of the air stream, they circulate

within the chamber (Jensen et al., 2010; Robinson, 1985; Zhou et al., 2000). Zhou et al. (2000) describes the classification process within the grinding chamber as a multi-zoned system, as proposed by Robison (1985). A similar simpler representation is shown in Figure 3-3 for a ring-roller mill after Shoji et al. (1998) where the settling of intermediate size particles is included in what is termed "primary classification".

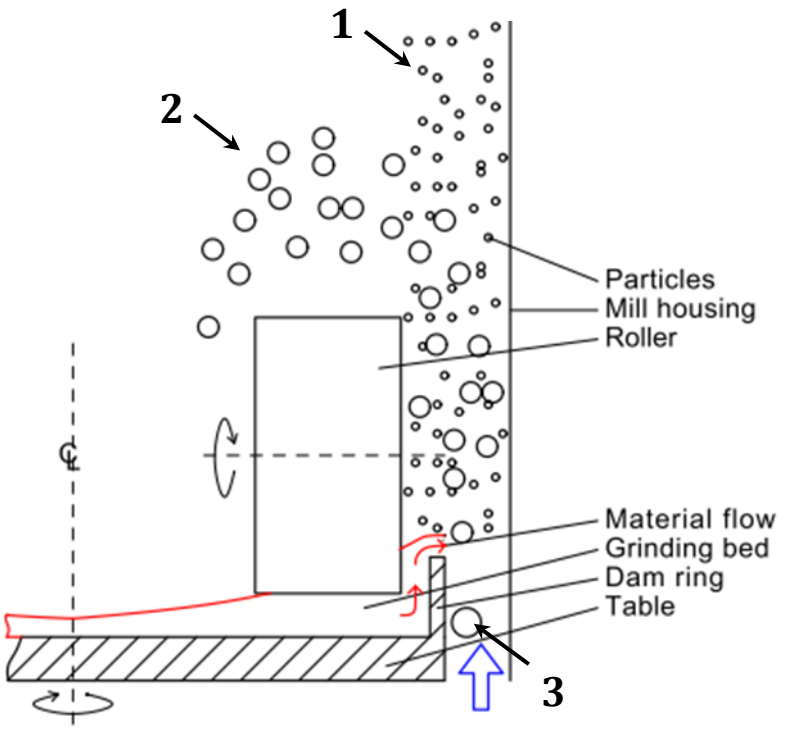

Figure 3-2: Illustration the grinding components of the VRM showing the suspension of particles in the air stream passing the edge of grinding table (Jensen et al., 2010). Fine [1], intermediate [2] and coarse [3] particles react in different ways to the air stream.

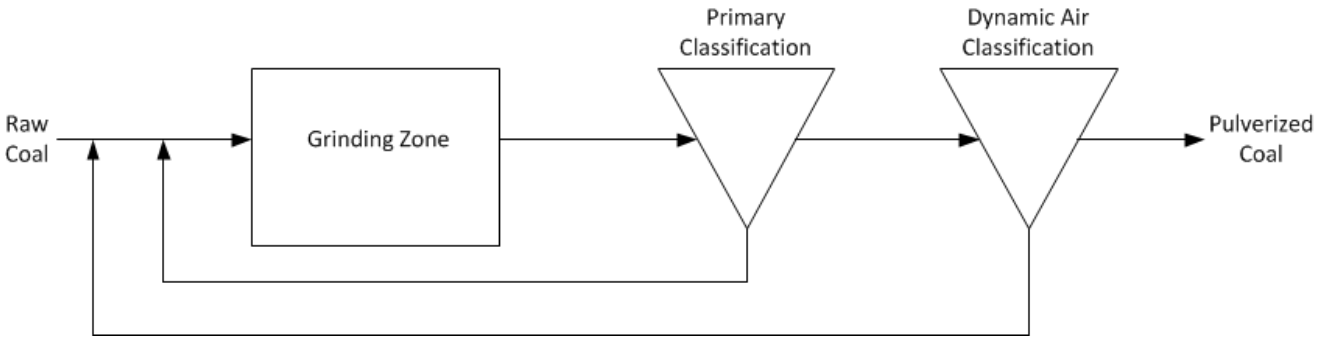

Figure 3-3: Ring-roller mill classification zones in airflow mode, after Shoji et al. (1998).

Overflow

The VRM overflow mode differs from the airflow mode in that there is no suspension of particles within the unit. Fresh material falls into the centre of the grinding table, moving outwards and under the rollers much like in the airflow configuration. However, on reaching the perimeter of the table, particles are not exposed to an upward stream of air and fall to the base

of the mill (Figure 3-4). From the base of the mill they are transported to the external classifier via a bucket elevator.

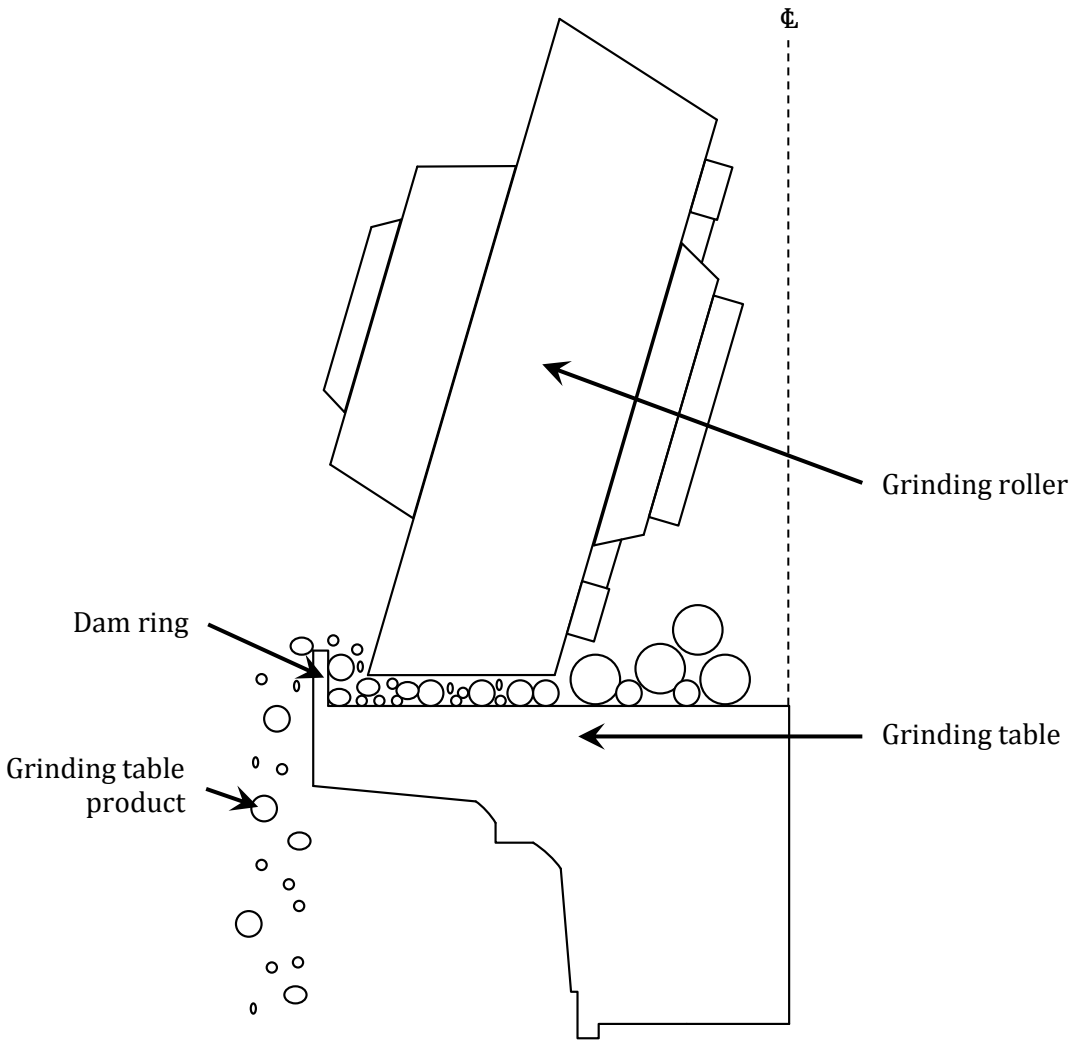

Figure 3-4: Diagram of the table and roller of vertical roller mill operating in overflow mode, with material falling from the perimeter of the table.

The grinding table product can be fed to a hybrid air classifier, a device containing both static and dynamic air classification elements (Figure 3-5). For this configuration the hybrid classifier is fed via a vibrating feeder which distributes material onto a rotating plate above the dynamic classification component of the classifier. Material migrates outwards on the plate, falling at the circumference of the plate into the air stream flowing towards the dynamic classifier. Coarse particles fall with gravity, shown as [1] in Figure 3-5, while fine and intermediate particles are transported inwards to the dynamic classifier, indicated by [2]. At the dynamic air classifier, product size material passes through the classifier suspended in an air stream, while the larger intermediate fraction is rejected, represented by [3] in Figure 3-5. The fine material is collected in a bag house as final comminution product and the coarse and intermediate streams are

recycled with the fresh feed for further comminution. Operation of the VRM in overflow mode with external air classification allows for the installation of a lower duty fan, thus increasing the energy efficiency of the circuit (Gerold et al., 2012b; van Drunick et al., 2010). However it has been observed that utilizing the VRM with an external air classifier results in a less steep product particle size distribution (Altun et al., 2015).

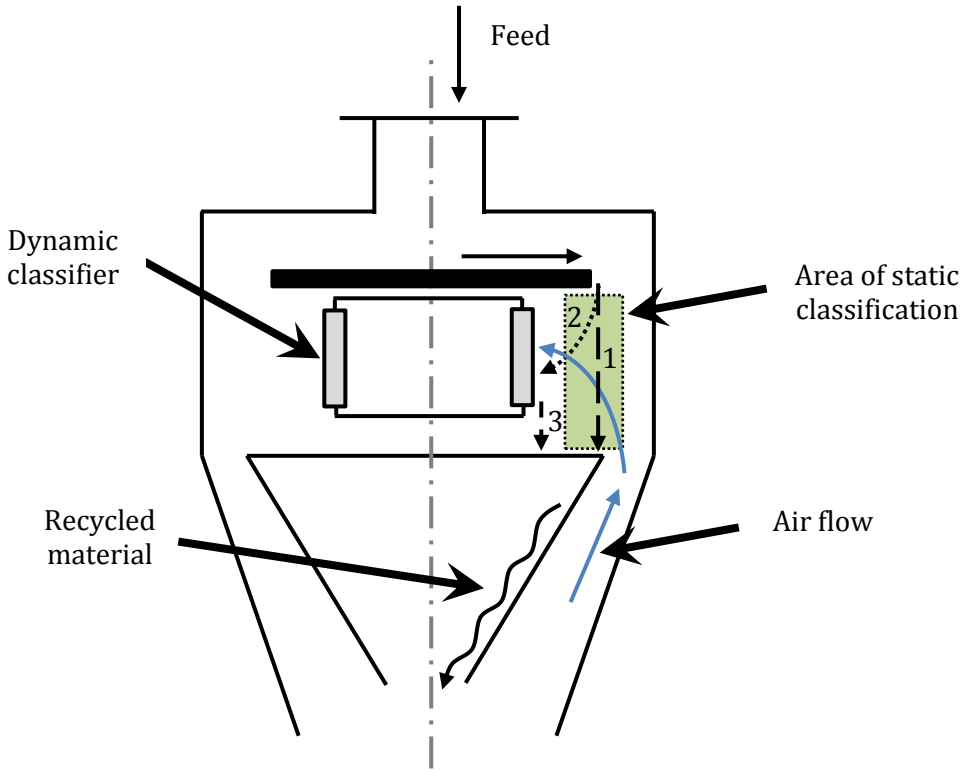

Figure 3-5: Schematic of the hybrid air classifier showing flow of material and air, and highlighting the area of static classification.

The grinding product generated in overflow mode is not suspended in a stream of air and as such could also be fed to external classifiers. The classification techniques suitable are however limited by the requirement for dry grinding in the vertical roller mill. One possible configuration is the operation of the VRM in conjunction with a vibrating screen. The low energy usage of screening makes this an attractive alternative to the standard highly energy intensive air classification. Grinding table product, transported from the base of the mill via the bucket elevator, can be fed to the screen and the screen oversize returned to the grinding table with the fresh feed. Screen undersize can be collected directly as the circuit product and filter systems like those used for air classification are not required. The screening equipment used for the external classification test work is shown in Figure 3-6, a cover was fitted to the screen during operation to minimise the generation of dust. Factors such as screen feed rate and aperture size would affect the product particle size and efficiency of separation. Monitoring feed rate to the screen is important as at high feed rates a thick bed of material forms. Fine product size

material must pass through the bed before being able to pass through the screen surface. Too deep a screening bed can cause a drastic drop in screening efficiency as product size material does not reach the screen, remaining in the bed and reporting to the screen oversize. This material is recycled back to the mill, leading to the over grinding of product size material and a reduction in throughput.

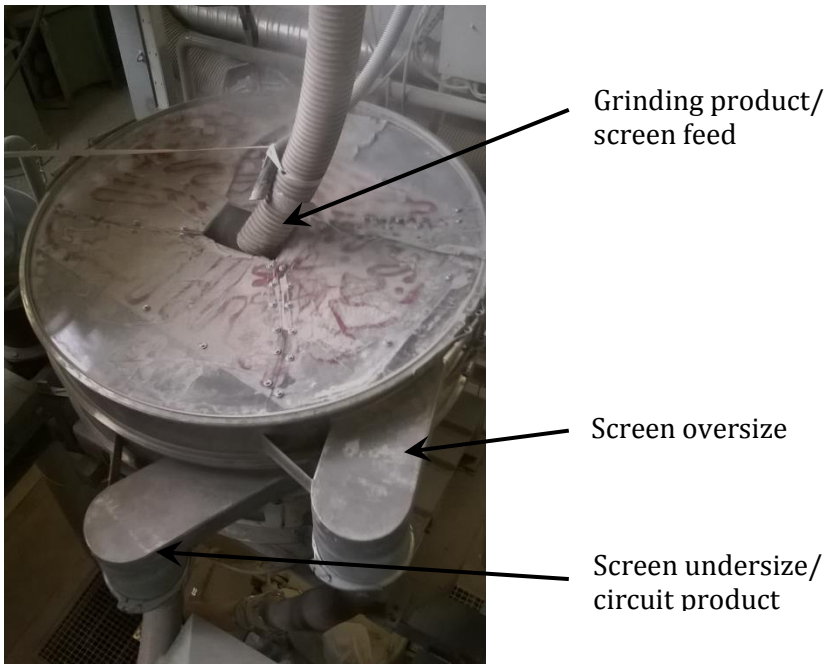

Figure 3-6: Screening equipment used for the external classification test work.

3.3 Grinding

Two pilot scale Loesche vertical roller mills of table diameters above 0.300 m were used for the vertical roller mill grinding test work at the Loesche Test Centre in Germany. These mills were each equipped with a pair of standard geometry, high shear rollers with diameters close to 0.3 m. The VRMs used in the test work were able to process feed material at throughputs ranging from 100 - 1000 kg/h depending on the circuit configuration, product size requirements and operating conditions. The vertical roller mills were integrated into different circuits as required in the test plan. The VRM pilot plants used were equipped with an automated control system that allows for the control and monitoring of important grinding and classification parameters.

Variables

Altering design and operation variables has an effect on throughput for the device, the specific grinding and overall energy consumptions, the quality of the product and other factors such as bed depth, circulation rate, and wear of different components. The parameters classifier speed, grinding pressure and dam ring height were selected as independent variables for the airflow

test programme. Classifier speed is used to adjust the product size to a desired target and product size is used in grinding applications as a proxy for liberation of minerals, which influences downstream valuable mineral recoveries. Grind pressure affects the level of compressive force applied by the rollers to the particle bed on the grinding table and is used as an online operating variable to control throughput and product quality. Dam ring height is a design variable which affects bed characteristics, influencing the retention time of material on the grinding table, affecting the material presented to the classifier.

Classifier Speed

The rotational speed of the classifier rotor in a dynamic air classifier is used together with airflow rate as the primary control for manipulating the particle size of material reporting to product in the vertical roller mill. The classifier rotor speed and the product size are inversely proportional (Altun et al., 2017; Nyakunuhwa, 2019; Reichert et al., 2015; Tamashige et al., 1991); an increase in rotor speed increases the centrifugal force experienced by a particle, increasing the likelihood of the particle being rejected by the classifier and recycled for further comminution. Manipulation of classifier rotor speed not only has an effect on the product size but also affects the recycle of material within the grinding and classification system. Increasing the classifier rotor speed reduces the classifier cut size and hence more material is retained within the grinding-classification circuit due to increased circulating load. In retaining more material within the system, production rate decreases as is seen in the work by Altun et al. (2017) for a gold and Reichert et al. (2015) for iron ore. Reichert et al. (2015) goes further to show the increasing relationship between classifier speed and specific energy consumption.

Grinding Pressure

Grinding pressure can be varied online during operation and is used as a method of maintaining product quality when feed to the grinding system is changed. Increasing the grinding pressure increases the throughput of the device (Altun et al., 2016; Nyakunuhwa, 2019; Tamashige et al., 1991; Thiel and Schössow, 2001). The rise in throughput with an increase in pressure can be attributed to more energy being imparted to the material on each pass under the rollers. Particles presented to the classifier are finer at higher pressures where more material meets the classifier cut size and circulating load is reduced, allowing more fresh feed to be introduced. In test work conducted by Reichert et al. (2014) for two iron ores, after increasing grinding pressure past a point, no further increase in production rate was achieved. Altering the grinding pressure exerted by the rollers on the particle bed has been observed to affect the specific grinding energy and the production of fines in the system (Reichert et al., 2015; Schwechten and Schonert, 1986; Tamashige et al., 1991).

Dam Ring Height

The dam ring, situated around the rim of the table, can be varied in height to affect the depth of the grinding bed as well as the table residence time (Hackländer-Woywadt, 2005; Jørgensen, 2005). Tamashige et al. (1991) and Reichert et al. (2014) indicated that the dam ring height has a significant influence on the throughput of the vertical roller mill. Data for clinker grinding collected by Tamashige et al. (1991) showed increased throughput at lower dam ring heights for two different grinding pressures. Conversely, in the work by Reichert et al. (2014) on two iron ore samples, throughput was found to be greater at increased dam ring heights. Reichert et al. (2014) and Tamashige et al. (1991) both reported observing an increase in specific grinding energy as the dam ring height was raised. Tamashige et al. (1991) stated that the reduction in energy efficiency is a result of increased bed depth and the associated decrease in grinding efficiency as the size reduction mechanism moves further from single particle breakage. Furthermore, Jørgensen (2005) and Knoflicek and Wentzel (1994) showed that increasing dam ring height causes the production of more fines and a broader particle size distribution, because of the increased residence time of particles in the grinding zone as the dam ring is raised.

3.4 Laboratory Tumbling Mill

The conventional milling test work was carried out in a laboratory scale tumbling mill, shown in Figure 3-7. The specifications of the mill are given in Table 3-1. The mill was 0.3 m in length, had a diameter of 0.3 m, an installed power of 0.75 kW and was filled with 22 - 24 mm diameter rods. It was operated on a batch basis, generating feed material for batch flotation testing, following the Centre for Minerals Research laboratory mill standard operating procedure. A grinding curve was prepared for the ore and used to determine milling times required to achieve desired target grinds, the process of which is discussed in Section 4.3.

Table 3-1: Technical specifications of the tumbling mill used for the test work.

Diameter	mm	300
Length	mm	300
Media size (rod ⌀)	mm	22-24
Media mass	kg	18
Media density	g/cm^3	7.8
Mass of ore	kg	3.3
Percent solids	%	64
Mill speed	% crit.	75
Installed mill power	kW	0.75

Figure 3-7: The 0.3 m diameter laboratory tumbling mill used for the test work.

3.5 Flotation

An 8 litre modified Leeds flotation cell manufactured under the name Barker was used for the flotation test work. The same flotation cell was used for all flotation testing in order to avoid inconsistencies in results caused by cell conditions. A photograph of the flotation test rig used in the experimental work is shown in Figure 3-8. The flotation cell was fitted with a 75 mm diameter impeller and stator, and connected to a compressed air line which allowed for control and measurement of the air flow by way of a rotameter. The impeller was connected to a 750 W Bonfiglioli Group electric motor (BC270-180-3000-750), fitted to allow for control of impeller rotational speed between 0 - 1800 rpm. The flotation cell was used to perform batch tests to

evaluate the flotation response of vertical roller mill and tumbling mill products. The details for these flotation tests are discussed in Section 4.5.

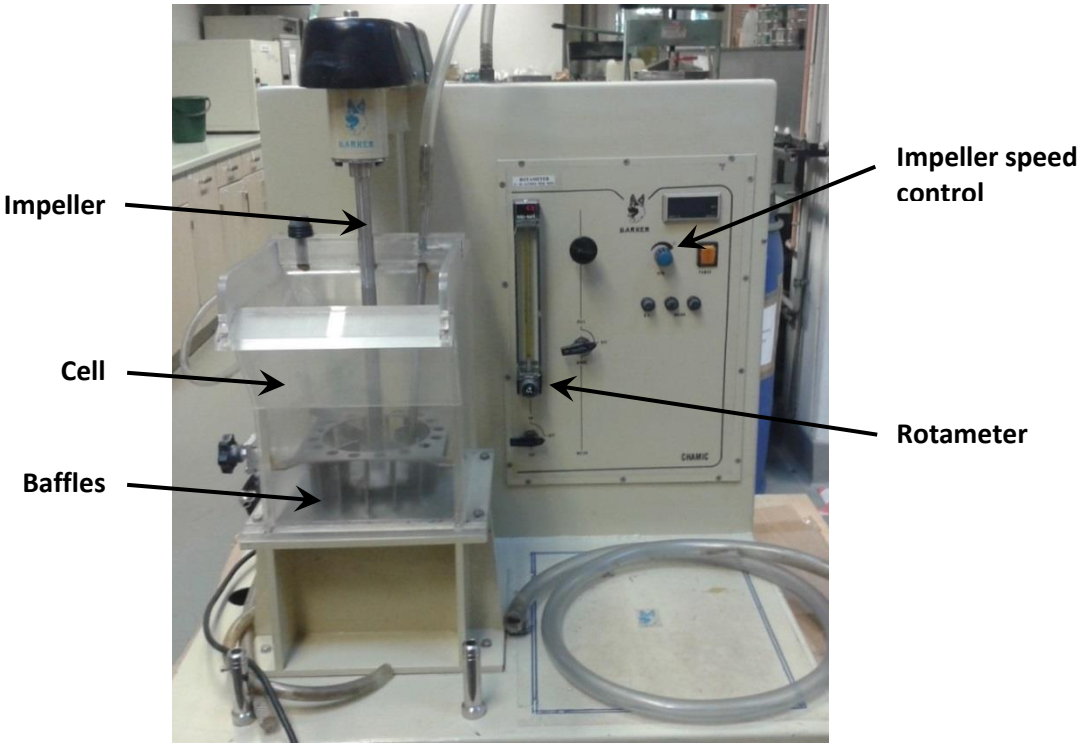

Figure 3-8: Front view of the 8l modified Leeds flotation cell.

Chapter 4

MATERIALS AND METHODS

This chapter focuses on describing the VRM and tumbling mill comminution test work performed and explains the flotation, sizing, and mineralogical analyses conducted. The experimental work involved the comminution and flotation of the platinum bearing ore, Platreef. Comminution tests consisted of grinding in a pilot scale vertical roller mill circuit at different operating conditions and with different methods of classification. Products from selected tests were floated in a batch flotation cell to determine the effects of different VRM grinding conditions on valuable mineral grade and recovery. In order to assess the flotation performance of the VRM, flotation tests were performed with a laboratory scale tumbling mill product and comparisons were made in terms of valuable mineral recoveries.

4.1 The Ore

The Platreef bulk sample was taken from the Mogalakwena North Concentrator in South Africa. The concentrator receives a blend of ore from different benches within the Mogalakwena mining operation targeting a 4E PGE plant feed head grade of 3.0 g/t (Anglo American Platinum Limited, 2015). Situated in the northern limb of the Bushveld Complex, the mine accesses the deposit by means of the Mogalakwena North, Mogalakwena Central, Sandsloot and Zwartfontein open pits. The ores mined from all these pits is observed to vary considerably in recovery potential and hardness, with Bond work indices of greater than 25 kWh/t frequently encountered (Cramer, 2001; Humphries et al., 2006; Mainza and Powell, 2006; Schouwstra et al., 2013).

Ore Preparation

A bulk 30 tonne sample was taken as a belt cut from the product of the crushing section of the plant, prior to the high pressure grinding rolls which pre-weaken the particle (Rule et al., 2008), to ensure that any efficiency benefits realised would be attributable to the VRM alone. The ore

sample was crushed at Anglo American Platinum Divisional Metallurgical Laboratory (DML) to an F_{80} of 12 mm. Figure 4-1 show a photograph of crushed material prepared for the test work. The top size of 12 mm was chosen because it is the maximum size suitable, as suggested by the Loesche, for grinding in their pilot vertical roller mill with grinding rollers of 0.3 m diameter.

Crushed material was transported to Anglo Technical Solutions where it was then blended and split into representative lots of 2 tonnes, by coning and quartering. The lots from coning and quartering were placed into drums. Twenty-four tonnes of ore were shipped to the Loesche test facilities in Germany and six tonnes remained in South Africa to be used for ball mill test work and serve as a backup sample. Prior to performing the grinding test work, drums containing the day's forecast tonnage were re-blended together using a mechanical blender to eliminate segregation caused by settling during transportation. Representative samples were taken from a drum sent to Germany and from the material kept for the ball mill test work for particle size analysis of the feed.

Figure 4-1: Platreef ore sample crushed to an F_{80} of 12 mm.

The density and moisture content of the ore sampled (prior to grinding) were calculated to be 2.88 g/cm^3 and 1.37% respectively. These values are averages calculated for 1.5 kg samples taken from the mixing unit at Loesche Test Centre. Figure 4-2 shows the particle size distribution of the feed, determined from a 90 kg sample. The top size of the material was 22.4 mm and the distribution has a P_{80} and P_{50} of 10.8 and 3.9 mm respectively.

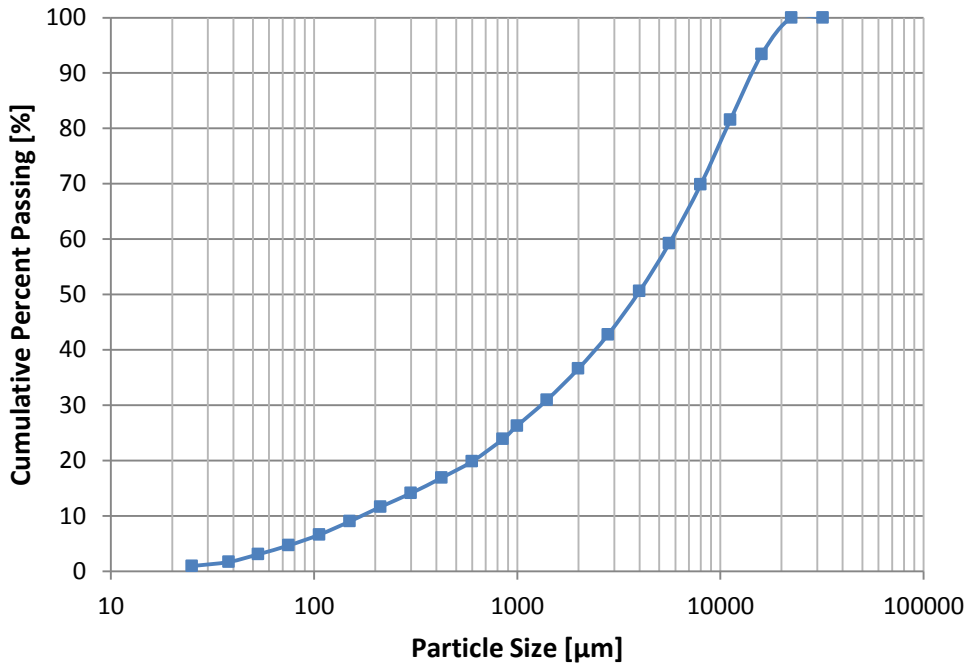

Figure 4-2: Feed particle size distribution.

Assay of flotation concentrates and tails indicated a recalculated mean head grade (Pt, Pd & Au) of 2.50 g/t for the ore and mineralogical analysis of the platinum group mineral distribution (and gold) indicated the dominant platinum group minerals groups being PGE tellurides (60%), PGE sulphides (15%) and PGE arsenides/sulpharsenides (15%), with a significant amount of gold (5%) present.

4.2 Test Matrix

The bulk of the grinding test work was carried out on a vertical roller mill operated with different classification systems. The tests with internal air classification were conducted as the standard. For test work with the internal air classifier, the system was configured to assess the influence of dam ring height and grinding pressure on attainable throughput and energy efficiency at a series of target grinds.

The testing was conducted in a three factor, three level factorial design frame work and multiple samples were collected for the factorial design central conditions for error estimations (Figure 4-3). The order in which the experiments were carried out was not randomized due to the difficulties and high ore usage associated with changing variables. Tests were performed by keeping the dam ring height constant while varying grinding pressure and the target product particle size (obtained by adjusting classifier rotor speed). The order of the tests did not affect the outcome of the work because the test preparations ensured that the ore was

representatively split and conditions were kept as close as possible to the defined test set requirements. Furthermore, tests for all possible combinations in this series of experiments were performed.

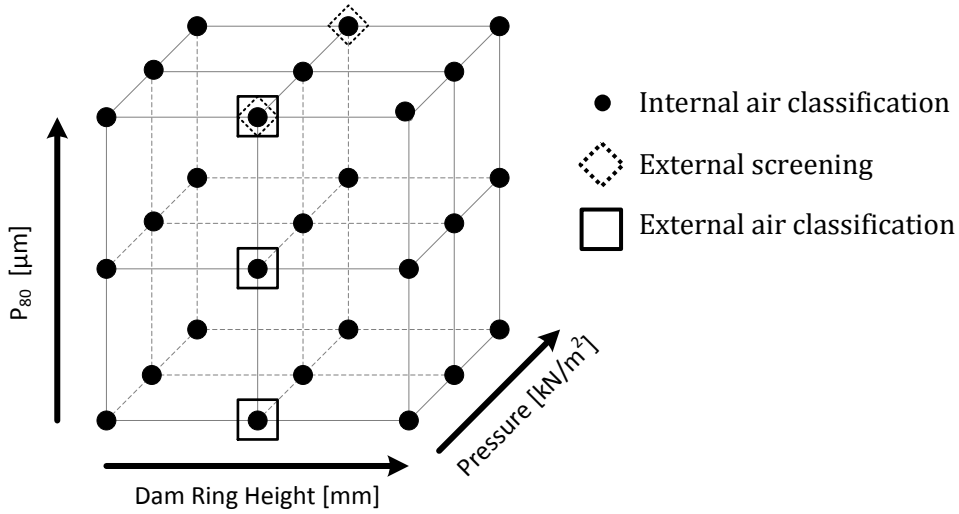

Figure 4-3: Matrix of vertical roller mill tests conducted.

The target grinds for the airflow test work were P_{80}'s of 240, 75 and 45 µm. These were defined to mimic typical grinding circuits employed in the platinum and base metal industries involving primary, secondary and tertiary grinding stages. The grinding pressures of 600, 800 and 1000 kN/m^2 spanned the range of grinding pressures available for use in the pilot scale VRM and the dam ring heights 4, 7 and 14 mm were equivalent to those typically used for the selected product sizes.

Operation of the vertical roller mill in conjunction with a dry screen (external classification) was restricted to a coarse product grind, due to throughput limitations and feasibility of continuous dry screening at the intermediate and fine grind. For this grind, the pilot mill was tested at different grinding pressures with the grinding table rotational speed which yielded the greatest throughput for the VRM-dry screen system. External air classifier tests were conducted at the intermediate dam ring height and lowest grinding pressure, yielding target grinds equivalent to those for operation with the internal air classifier. For the classification comparison, the finest target grind was revised to a P_{80} of 60 µm, so as to match the steeper internal air classification PSD more closely to that which is achieved in operations (P_{90} of 75 µm). The summary of operating conditions at which VRM grinding tests were performed are outlined in Table 4-1. Experiments involving milling the material using a laboratory scale tumbling mill were conducted to produce target grinds that have P_{50} values as close as possible to those obtained from the VRM tests.

Table 4-1: An outline of the vertical roller mill test work conducted.

Classification	Target Product P_{80} [µm]	Grinding Pressure [kN/m²]	Dam Ring Height [mm]
Airflow	45	600	4, 7, 14
		800	4, 7, 14
		1000	4, 7, 14
	75	600	4, 7, 14
		800	4, 7, 14
		1000	4, 7, 14
	240	600	4, 7, 14
		800	4, 7, 14
		1000	4, 7, 14
External Screening	240	600	7
		1000	7
Internal Air Classification*	60	600	7
	75	600	7
	240	600	7
External Air Classification	60	600	7
	75	600	7
	240	600	7

**Repeat airflow (internal air classification) test were carried out to generate fresh material for the classification comparison, targeting a revised finest grind of P_{80} 60 µm, and eliminating potential aging effects.*

4.3 Milling Test Work

The vertical roller mill tests were performed using equipment described in Section 3. The airflow circuit used for the airflow tests is illustrated in Figure 4-4 and the circuits used for the overflow testing with an external screen and an external hybrid air classifier are shown in Figure 4-5 and Figure 4-6. Prior to each test run the variables of interest were changed to the required set points. Fresh feed was introduced to the mills via a screw feeder and the rate at which material entered the system was controlled by varying the speed of the screw. For each grinding test the feed rate to the mill was maximised for the given conditions. Feed rate to the system was maximized by increasing fresh material introduced, while monitoring the retention of material in the system to avoid an overload. Once the plant had started up, the grinding and classification systems were allowed to reach steady state before the test run was started. In order to assess if the plant had reached steady state both the feed rate and rate of product discharge were measured. When these values were comparable and fluctuated around the same flow rate the system was considered to be at steady state. After the system had reached steady

state, sampling commenced and recording of the test measurements started. The specific sampling procedures for the different VRM circuit configurations are discussed in the following sections. During each testing interval as many as 37 process parameters in the pilot plant are recorded, a selection of which are shown in Table 4-2, Table 4-3 and Table 4-4. The measured roller torque was used to calculate mechanical power of the grinding components and, in conjunction with the throughput of the mill, specific grinding energy. Certain classifier and airflow parameters were measured and kept constant to ensure the system was operating consistently across the different test conditions. They are not directly used in the analyses for this project. The associated energies of classification were determined for each of the classification methods using literature.

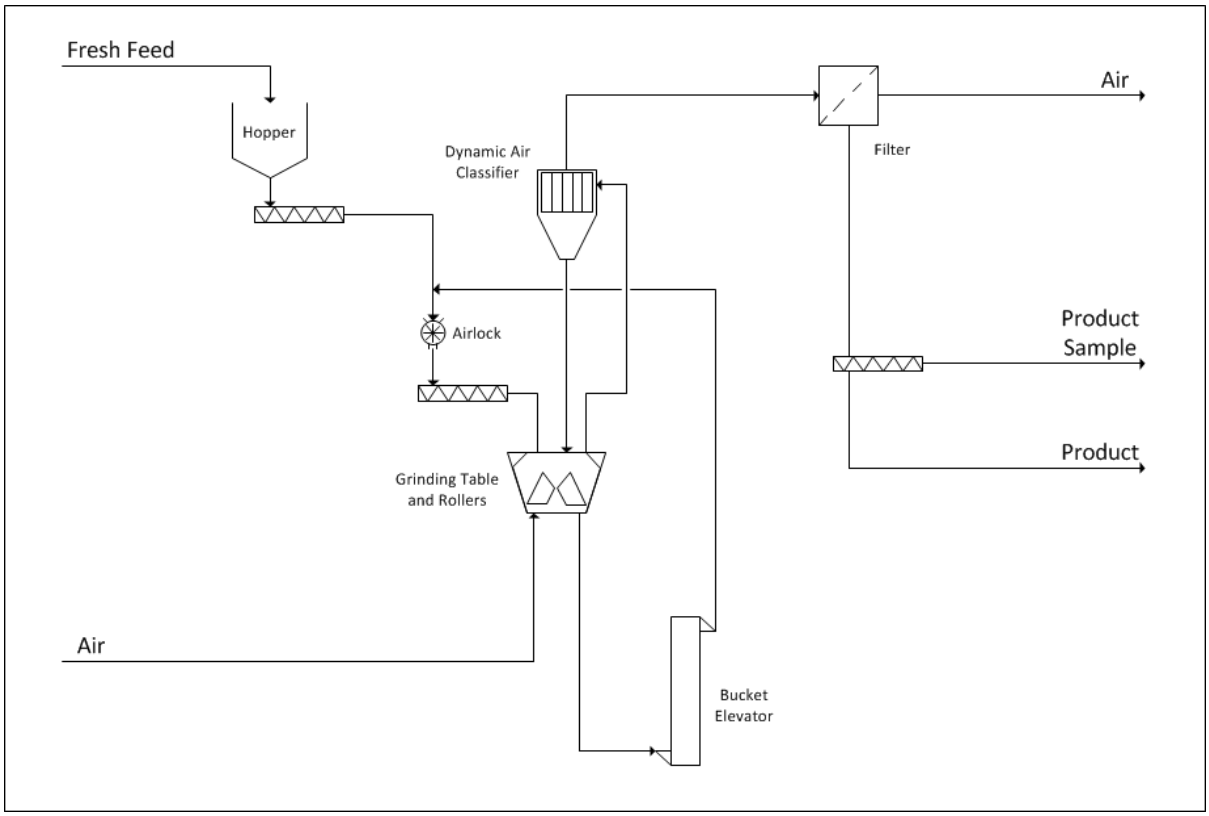

Figure 4-4: Vertical roller mill circuit in airflow mode.

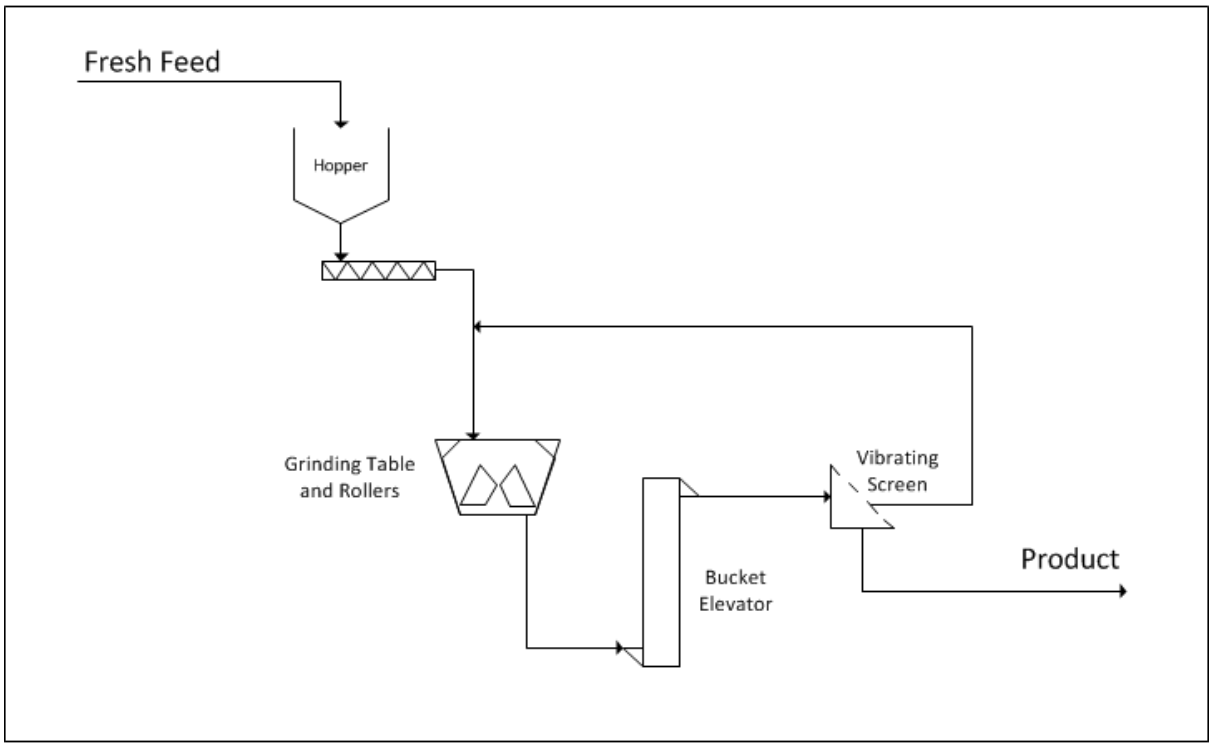

Figure 4-5: Vertical roller mill circuit in overflow mode with screening.

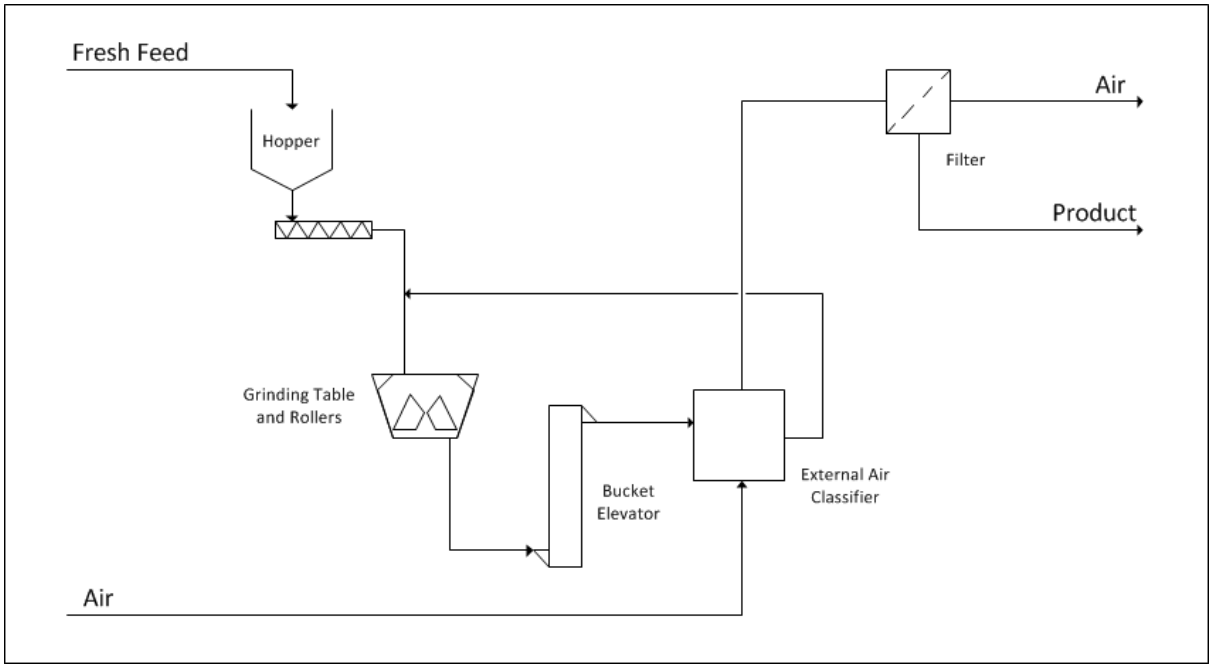

Figure 4-6: Vertical roller mill circuit in overflow mode with external air classification.

Airflow

Before each test interval the rotational speed of the dynamic air classifier was controlled to manipulate the product size. Rotational speed set points were established to produce the desired target grinds during initial calibration tests conducted at the intermediate dam ring height when determining the required air flow rate through the mill for this specific ore. Minor

changes to classifier rotor speed were required as operating variables and throughputs varied. Airflow rate and pressure drop across the system were kept constant. Before starting the actual run, samples of the mill product were taken and sized with an air jet sieve to determine the product size. The classifier speed was adjusted until the desired product size was achieved. Once the classifier set point was determined the circuit was allowed to reach steady state. Once steady state was reached, the test run commenced and sampling and recording of measurements was started. Table 4-2 indicates selected variables recorded for each test run.

Table 4-2: Important variables recorded during VRM airflow test work. Classifier and airflow parameters measured are in italics.

Measured Variable	**Units**
Grinding Pressure	bar
Classifier rotational speed (rpm)	1/min
Volumetric flowrate at filter	m^3/h
Pressure drop across mill	mbar
Feed rate	kg/h
Roller torque	Nm
Grinding bed height roller 1	mm
Grinding bed height roller 2	mm
Sample accumulated	kg
Duration of test run	s

For operation of the VRM in airflow mode, where the internal air classifier was used for final product separation, neither the stream of particles delivered to the classifier nor material recirculated to the mill could be sampled without disturbing the system. An attempt was made to sample the material returning to the table via the grit cone using a specially designed spacer which fitted between the grinding components and classifier, extending the height of the grinding chamber. The spacer had a built-in sampler which could extend into the chamber, however when using the sampler, the system immediately became unstable and unrepresentative of steady state. In the PhD thesis by Özer (2011) a method and specifically designed tools were developed for sampling within the mill shell of a plant scale vertical spindle mill. Although this is considered to be best procedure, it could not be followed in this test work because of the smaller size of the pilot scale mill used.

External Classification with Screening

The vertical roller mill was operated in overflow mode in conjunction with two external classification techniques. Both external air classification and screening were performed with material transported by the bucket elevator after passing over the grinding table. External screening VRM tests were carried out with a 1.2 m diameter Rhewum circular screen operated dry with a 500 μm aperture sieve. The circuit, illustrated in Figure 4-5, generated only a product equivalent to the coarsest airflow product size, at multiple grinding pressures. Attempts were made to operate the VRM with a finer screen aperture (300 μm) but this lead to high screen loading and reduced screening efficiency which limited the throughput in the circuit. Initial tests conducted with the VRM and screen resulted in low feed rates to the mill, high loading of material on the screen and low P_{80}'s. To alleviate this, the mill table rotational speed was decreased. Operation of the VRM at a table rotational speed of 70 rpm (Airflow 100 rpm) in conjunction with a 500 μm aperture screen was found to yield a maximum feed rate and gave a product close to the target P_{80} value of 240 μm.

The feed rate to the circuit was limited by the capacity of the screen. A maximum feed rate to the circuit was determined by repeatedly sampling the screen oversize and establishing the carryover of sub 500 μm material while increasing the feed rate. Once a dramatic increase in sub 500 μm material occurred, indicating an overloading of the circuit, the feed rate was reduced to the previous level. The system was then allowed to reach steady state and the test run started. Material passing through the screen was collected as product for the duration of the test run with the variables presented in Table 4-3 recorded. Samples were taken from the screen feed and oversize at the end of the test run to avoid disrupting the stable conditions established.

Table 4-3: Important variables recorded during test work with the VRM using external screening.

Measured Variable	Units
Table rotational speed (rpm)	1/min
Grinding Pressure	bar
Feed rate	kg/h
Grinding product rate	kg/h
Roller torque	Nm
Grinding bed height roller 1	mm
Grinding bed height roller 2	mm
Sample accumulated	kg
Duration of test run	s

External Air Classification

The external air classification tests were conducted at grinding pressure of 600 kN/m^2 and classification conditions which generated similar product size material to those produced in the airflow tests. For this configuration, the VRM was operated in overflow mode in conjunction with a hybrid air classifier which contains both static and dynamic air classification elements. Material is initially introduced into the static portion of the classifier and coarse particles are separated from intermediate and product size fractions. These fractions report to the dynamic classification component, where the product quality material exits suspended in a stream of air and intermediate size fraction is rejected. The rejected intermediate fraction is returned to the grinding table with the coarse particles. The air flow rate through the hybrid classifier and rotor speed of the dynamic component of the classifier were adjusted to vary the product size. To assess if the circuit was operated under classifier conditions that gave the desired product, samples were obtained from the final classifier product and sized with an air jet sieve. Based on these results the classifier was iteratively adjusted until a desired cut size was achieved. The external air classification circuit is illustrated in Figure 4-6 and the variables recorded presented in Table 4-4.

Table 4-4: Significant variables recorded during the VRM external air classification test work.

Measured Variable	Units
Grinding Pressure	bar
Classifier rotational speed (rpm)	1/min
Volumetric flowrate at filter	m^3/h
Feed rate	kg/h
Grinding product rate	kg/h
Roller torque	Nm
Grinding bed height roller 1	mm
Grinding bed height roller 2	mm
Rate of product accumulation	kg/h

Laboratory Milling

Tumbling mill tests were carried out using the mill described in Section 3.4 to generate feed material for flotation test work. The flotation response of the tumbling mill product was compared to that of the VRM products to assess the influence of these devices on the downstream recovery process. The flotation performance of conventional comminution circuit and vertical roller mill products was compared using laboratory scale flotation testing. Flotation tests were conducted as per procedure utilised at Anglo Technical Solutions for general

laboratory scale flotation of the Platreef ore. For these tests, the six tonnes of ore that remained in South Africa for ball mill test work was re-blended and split by coning and quartering to produce a representative 120 kg sample, which was sent to the Centre for Minerals Research laboratories at the University of Cape Town. To reduce the top size of the feed material to that acceptable for the laboratory tumbling mill, the 120 kg was passed through a Mineral Innovative Technologies, Terminator JCT1AL jaw crusher with a 2 mm closed side setting. The crusher was choke fed in batches and the material generated was sieved at 2.8 mm. The oversized particles were reintroduced to the crusher with fresh feed, and the sub 2.8 mm material was representatively split with a rotatory splitter to produce samples for milling.

In order to determine milling times required to generate products of the desired size, a grinding curve was established. The grinding curve was obtained by grinding a standard feed sample for a defined time and performing size analysis on the product. As no prior work had been undertaken on this ore in this mill, an initial scope test was conducted with grab samples taken directly from the mill at intervals during a grind. The choice of grinding curve times was guided by estimates from the scoping test, a deviation from the longer standard procedure for generating a normal milling curve. Figure 4-7 shows the particle size distributions for grinding times of 20, 45 and 55 minutes. From these the grinding curve in Figure 4-8 was established. While establishing the grinding curve, a comparison of particle size distributions for a rotatory split sample and material sampled from agitated slurry in the flotation cell was made (Figure 4-9). The particle size distributions were identical and based on this, the slurry sampling method was used for subsequent sampling of the mill product/flotation feed.

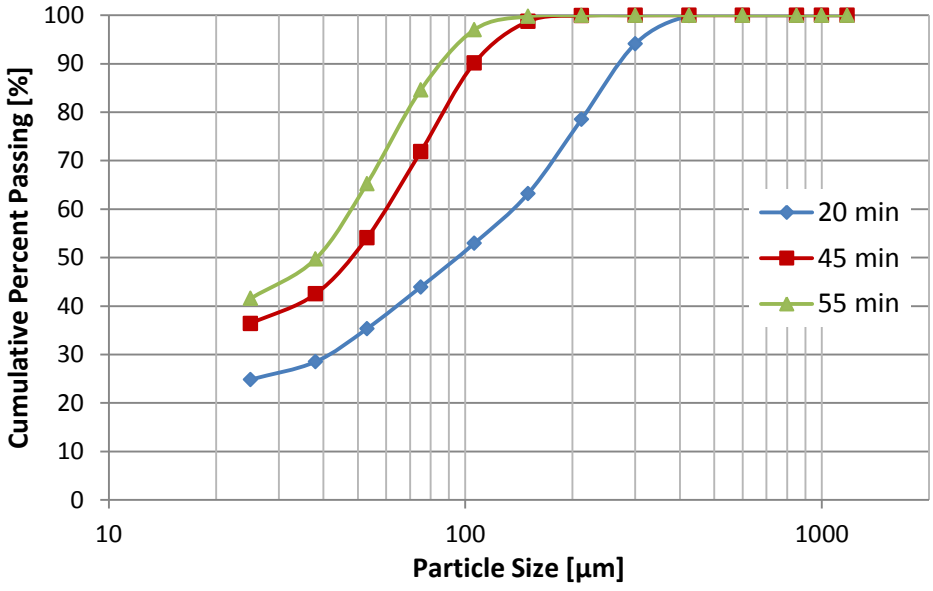

Figure 4-7: The product particle size distributions of the laboratory tumbling mill grinding tests used to establish the grinding curve.

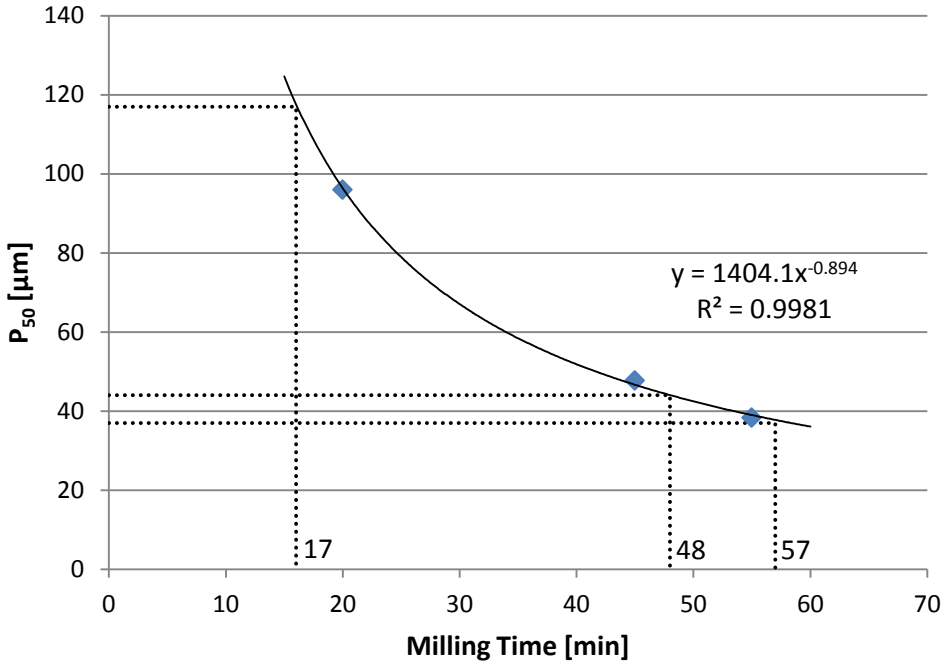

Figure 4-8: Grinding curve for the tumbling mill, showing the required times to achieve P_{50} values equivalent to thos obtained from VRM tests.

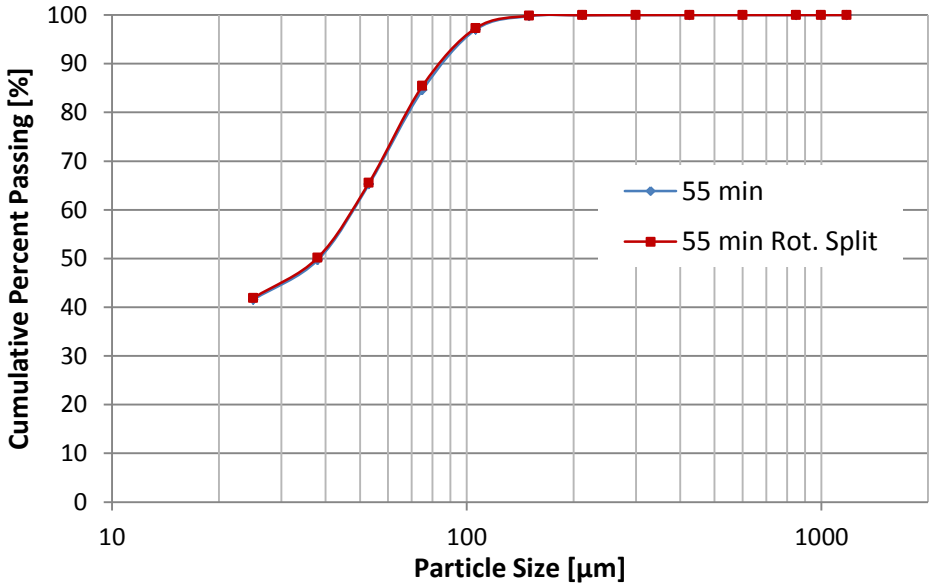

Figure 4-9: Comparison between particle size distributions of two sub-samples of the same tumbling mill product/flotation feed sample. Acquired by rotary splitting and sampling slurry directly from the agitated flotation cell.

The grinding curve was used to determine times needed to achieve equivalent P_{50} values for the tumbling mill products and it was deduced that 17, 48 and 57 minute milling times were required to generate suitable products for flotation. The samples were then taken and ground for 17, 48 and 57 minutes and the product particle size distributions from these tests compared to those from the vertical roller mill as shown in Figure 4-10. It can be seen that the P_{50} values

were comparable and the overall PSDs were close even though the P_{80} values were not exactly the same. The vertical roller mill products generated in airflow mode had a steeper PSD, and if equivalent P_{80} values were targeted with the tumbling mill, the products would have had a much greater proportion of fine particles. Hence it was decided that, since the particle size distributions would match a single point, the central P_{50} would be the better comparison.

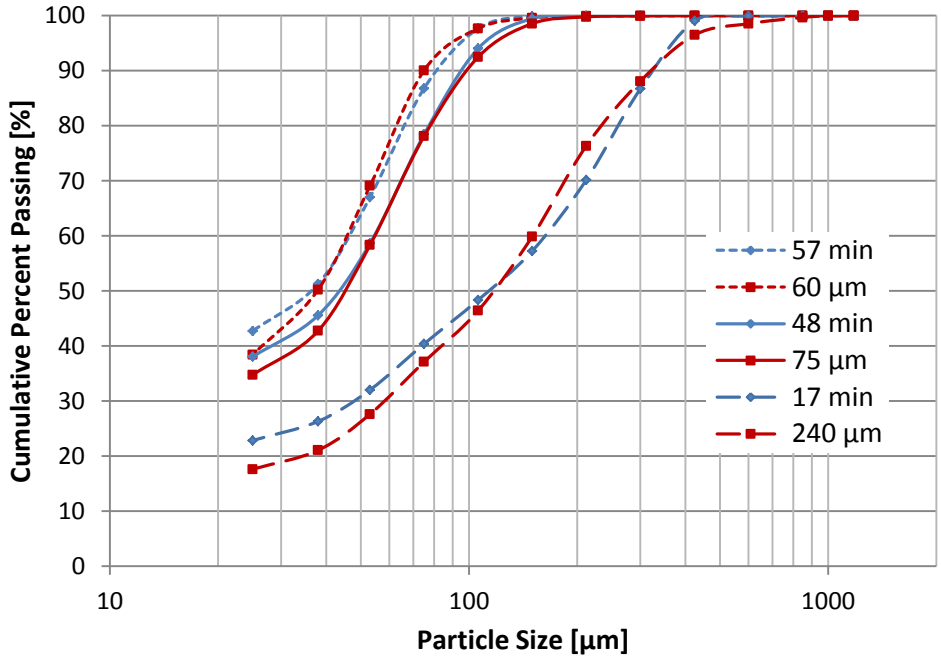

Figure 4-10: Particle size distributions of the 57, 48 and 17 minute tumbling mill products and the products for the vertical roller mill operating in airflow mode at a grinding pressure of 600 kN/m² and dam ring height of 7 mm, targeting a P_{80}'s of 60, 75 and 240 µm.

4.4 Processing Samples

The product samples collected during each comminution test were split using a series of chute rifflers and rotary splitters to produce representative sub-samples for flotation and mineralogical test work, laser particle size analysis, screening and assay. A check on the representativeness of the splitting was conducted by sizing a series of sub-samples (Figure 4-11). The samples were screened using 200 mm diameter sieves arranged in a $\sqrt{2}$ series of sieves for aperture sizes between 1.0 mm and 25 µm. For sieves of aperture size less than 75 µm, wet screening was carried out. Laser particle size analysis using a Malvern Mastersizer 2000 was performed to complement the sieving size characterisation.

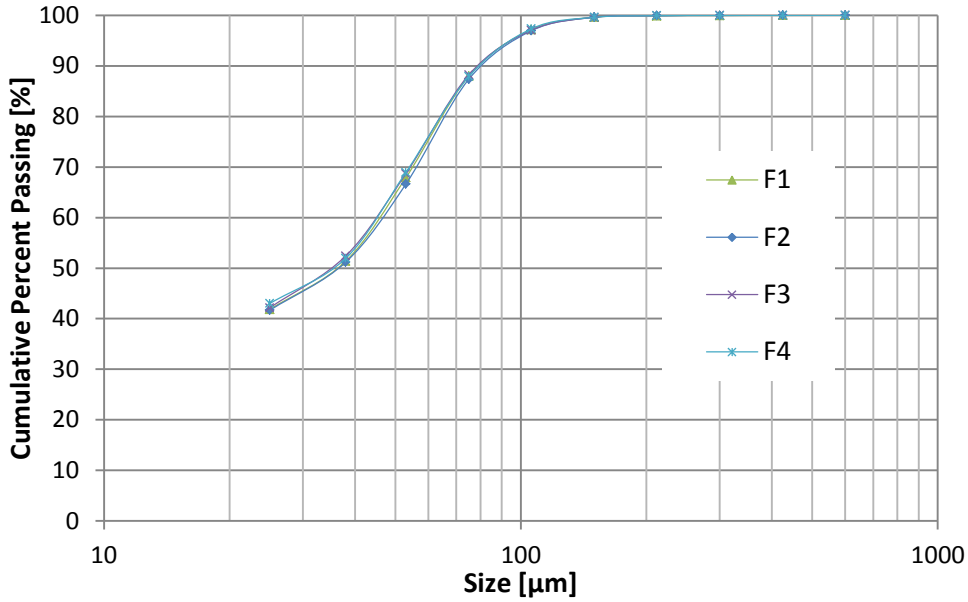

Figure 4-11: Particle size distributions of four sub-samples of flotation feed.

Where access allowed, samples were collected of the classifier feed and oversize. These samples were screened with a sieve series between 16 mm and 1 mm. The -1 mm fraction was representatively split and a 300 g portion screened with the same method used for product samples.

Batch flotation tests performed on comminution products from the various grinding circuits yielded multiple concentrates and tail samples. The concentrate samples were assayed as combined concentrates, which yielded a single assay result for all concentrate collected during a flotation test. For this, all the dried flotation concentrates collected in a float were blended together (Figure 4-12). De-lumped flotation concentrate and tails samples were divided using the series of rotary splitters to provide 30 g and 150 g samples required for assay of higher grade and lower grade samples respectively.

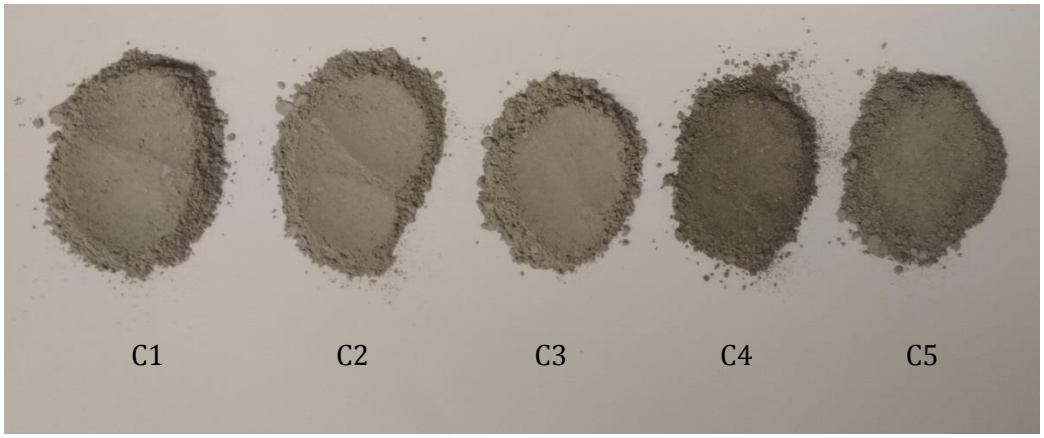

Figure 4-12: Dried flotation concentrates.

4.5 Flotation

The role of comminution and classification in minerals processing is to efficiently liberate valuable minerals so as to allow for their recovery and concentration in subsequent separation processes. As such it is important to investigate the effect on the recovery process when conducting comminution test work.

Batch flotation test work was carried out on selected vertical roller mill and tumbling mill comminution products. Figure 4-13 indicates the flotation test work experimental design for the comminution products. The selection of airflow products that were floated was based on modes of operation considered typical for the vertical roller mill and includes higher dam ring heights for finer products and lower dam ring heights for coarser products. All the VRM comminution products generated with the external air classifier and external screen, and the tumbling mill products of equivalents P_{50} were floated at the same conditions as the internal air classification products.

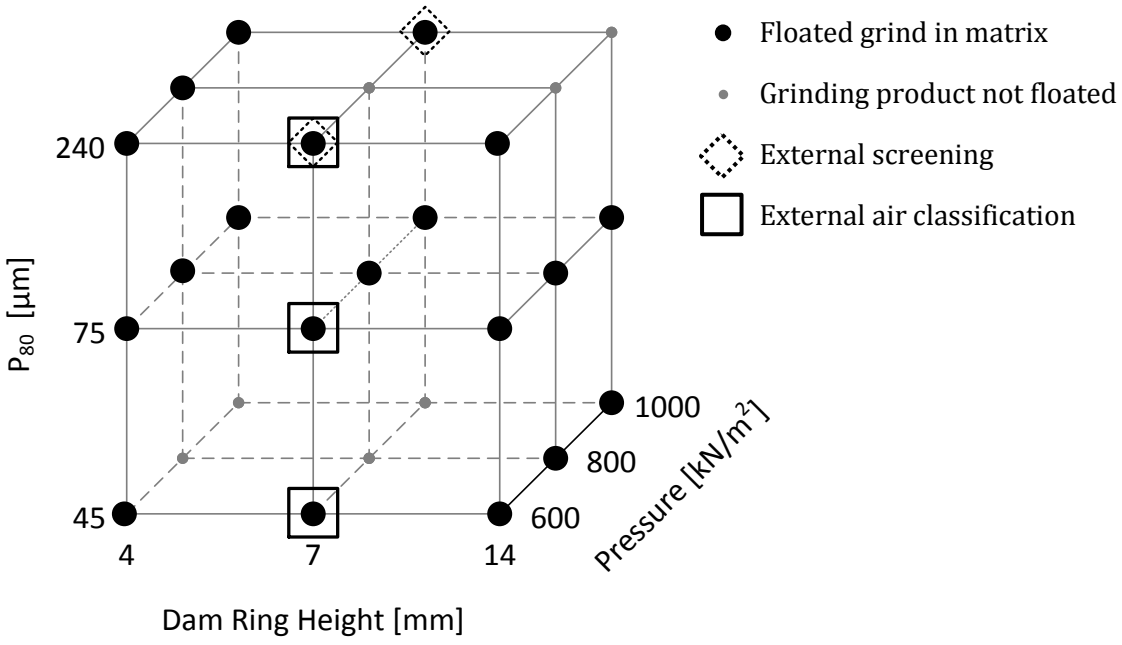

Figure 4-13: Comminution test products floated.

Reagents and Flotation Procedure

The reagent suite and flotation procedure utilised at Anglo Technical Solutions for general laboratory scale flotation of the Platreef ore was used in this test work. The reagent suite is typically for laboratory wet ball milling tests and no attempt was made within this study to optimise the flotation reagent suite for the vertical roller mill product. The reagents, dosages, pH, percent solids and conditioning and concentrate collection times are outlined in Table 4-5 and presented in Figure 4-14. A detailed step-by-step procedure is given in Appendix I. Flotation

tests were carried out using synthetic plant water as suggested by Wiese et al. (2005) and reagents for the flotation were sourced from Senmin International (PTY) Ltd.

Table 4-5: Flotation reagent dosages, conditioning and concentrate collection times as supplied by Anglo Technical Solutions.

Activity	Time (min)	% Solids	pH	Reagents (g/t)			
				SIBX	Senkol 3	Sendep 30D	XP 200
Condition 1	2	35	Natural	100	40		
Condition 2	2					80	8
Conc 1	2						
Conc 2	6						
Conc 3	12						
Condition 3	2			50	20		
Condition 4	2					40	6
Conc 4	10						
Conc 5	10						
Total	**48**			**150**	**60**	**120**	**14**

During a vertical roller mill product flotation test, the cell was initially filled with synthetic plant water to which a representatively split 3.3 kg sample of dry comminution product was added. The slurry, once mixed, was topped up to the desired level to achieve a suspension of 35% solids. The first set of reagents, the collectors sodium iso-butyl xanthate and Senkol 3, were added and conditioned for 2 minutes. The second set of reagents, the depressant Sendep 30D and frother XP200, were then added and the slurry conditioned for a further 2 minutes. After the second conditioning stage, air was introduced into the cell. Froth overflowing the lip of the flotation cell was collected as concentrate by scraping the top of the froth in 15 second intervals and using individual wash bottles to rinse material into each concentrate tray (Figure 4-15 B). The concentrate C1 was collected for 2 minutes, C2 for 6 minutes and C3 for 12 minutes. During this airflow rate, impeller speed and slurry level (Figure 4-15 A) were monitored and maintained at their respective set points. For the third and fourth conditioning stages, airflow to the flotation cell was halted. The collectors sodium iso-butyl xanthate (SIBX) and Senkol 3 were added and conditioned for 2 minutes, then the Sendep 30D and XP200 were added and the slurry conditioned for a further 2 minutes. Air flow to the cell was restored and the concentrates C4 and C5 collected for separate 10 minute intervals. Air flow to the cell and impeller rotation was stopped, and residual material, Figure 4-15 C, was drained from the flotation cell, filtered, dried and bagged as tails. The five concentrates were weighed wet, filtered, dried and weighed again, and together with the amount of wash water used in rinsing the scraper, the solids and

water recoveries for each concentrate were determined. Flotation tests were conducted in either duplicate or triplicate and dry concentrates were bagged separately for assaying.

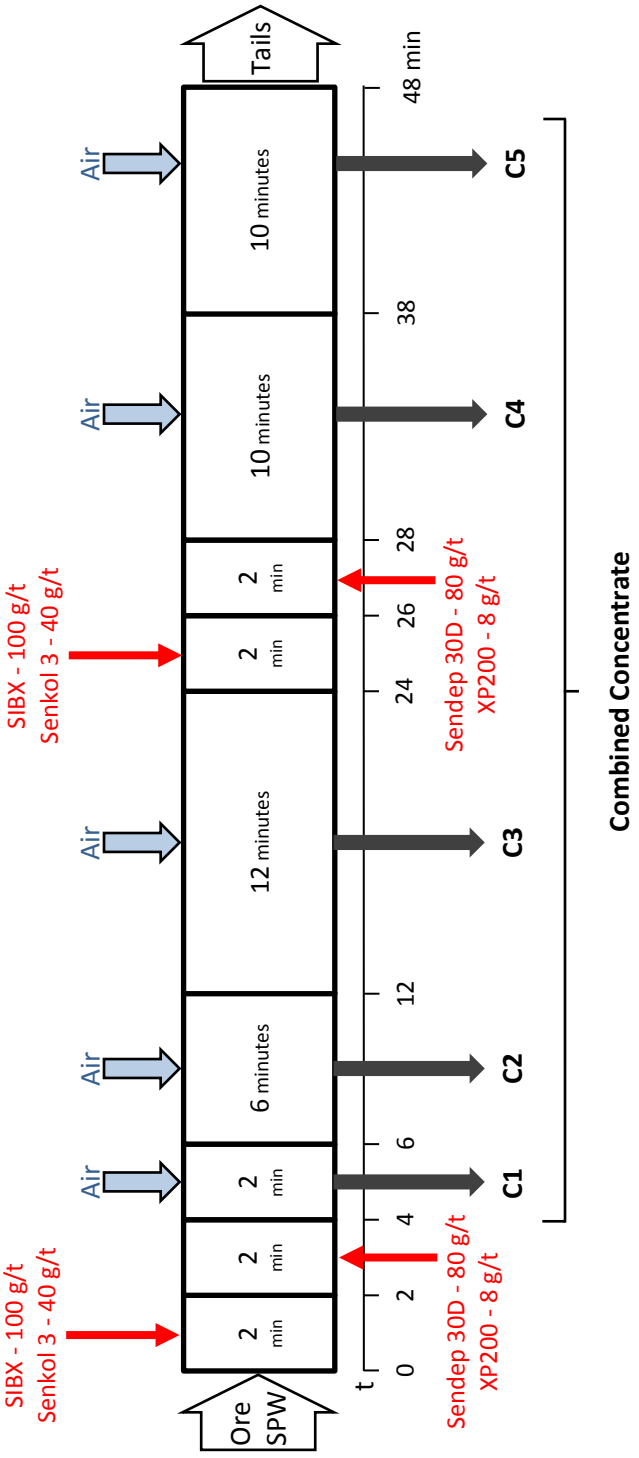

Figure 4-14: Diagram representation of flotation indicating the reagent dosages, conditioning and concentrate collection times and assayed samples.

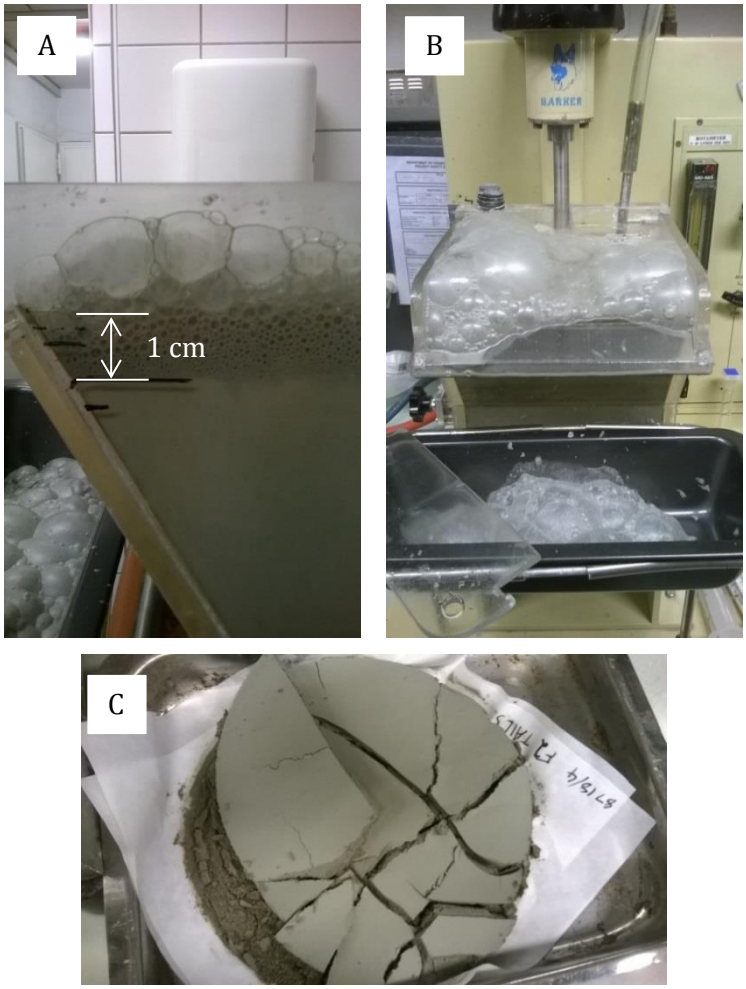

Figure 4-15: Side [A] and front [B] view of the froth in the flotation cell. Image B shows the overflow froth from the flotation cell and the scraper used to assist in froth collection. Filtered flotation tails [C].

When preparing flotation feed in the tumbling mill test work, grinding was carried out with synthetic plant water used to pulp the feed material in the mill to the desired 64% solids by mass. Synthetic plant water was also used to rinse comminuted material from the mill, which was added to the flotation cell and diluted to the required 35% solids before switching on the impeller. The procedure as laid out for VRM product flotation was then followed.

Assays

Flotation feed, tails and combined concentrate samples were sent for Pt, Pd, Au (Fire assays and ICP-AES finish), Ni, Cu (ICP-OES assays) and S (Leco sulphur analyser) assays at an independent laboratory. For the flotation feed and tails, representatively split 150 g samples were sent for assay, while 30 g samples of the combined concentrates were sent. The combined concentrate samples assayed were representative splits of the blended five concentrates collected during a flotation test. In cases where insufficient concentrate mass was generated in a single flotation test, the concentrates from a repeat were added. For flotation tests conducted in triplicate,

samples from two of the floats were sent for assay. The assay data was compiled and analysed together with the solids and water recoveries to assess flotation response to differences in grinding and classification conditions. Based on the results of this analysis, mill products from selected comminution tests were sent for mineralogical analysis.

4.6 Mineralogy

Mineralogical analyses were performed with the FEI QEMSCAN 650F and associated software, iDiscover™, at the University of Cape Town on selected vertical roller mill products. Samples were prepared as representative 1 g aliquots mounted in 30 mm epoxy resin blocks, which were polished and carbon coated prior to analysis. The blocks were analysed with a 25 kV potential and 10 nA probe current using the particle mineral analysis (PMA) and trace mineral search (TMS) routines at a pixel spacing of 1 and 0.8 µm, and field sizes of 686 and 456 µm respectively. The analyses were carried out to determine mineral grades of each sample and the mineral associations and liberation profiles of the platinum group minerals, base metal sulphides and gangue mineral species. Products selected for QEMSCAN analysis were those produced by the VRM operating in airflow mode at the combination of conditions highlighted in Figure 4-16.

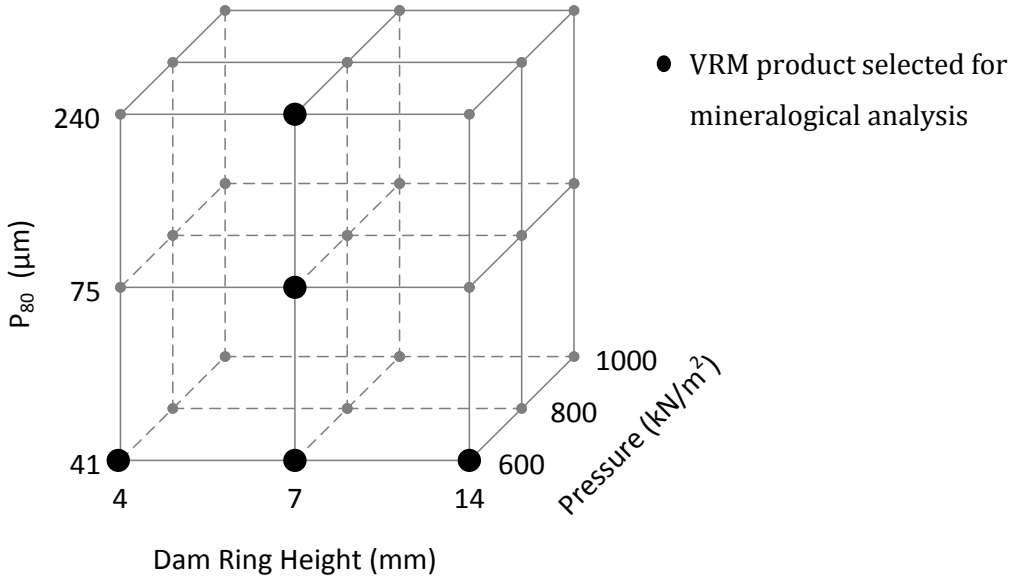

Figure 4-16: Airflow comminution test which underwent mineralogical analysis.

The TMS targeted platinum group minerals, identifying particles containing areas of high back scattered electron (BSE) counts and then using Energy Dispersive X-ray Spectroscopy (EDS) to determine the elemental composition. Multiple blocks of each sample were run for multiple

polished surfaces, in order to obtain a PGM particle count of above 100. Locating more PGMs was not considered viable because of the substantial amount of machine time required in locating the low concentration species. The combined PGM mineralogy results for all of the VRM products analysed are presented in Section 5.4.

PMAs were used to determine the mean bulk mineralogy for each of the VRM products by analysing a single surface of each resin block prepared as unsized vertical sections. The bulk mineralogy results from QEMSCAN were validated by comparison of QEMSCAN back calculated elemental assay data with X-ray fluorescence (XRF) elemental data and a Leco sulphur assay. The comparison of the chemical assay determined by XRF, Leco and QEMSCAN is shown in Figure 4-17. All elements assayed for are in reasonable agreement.

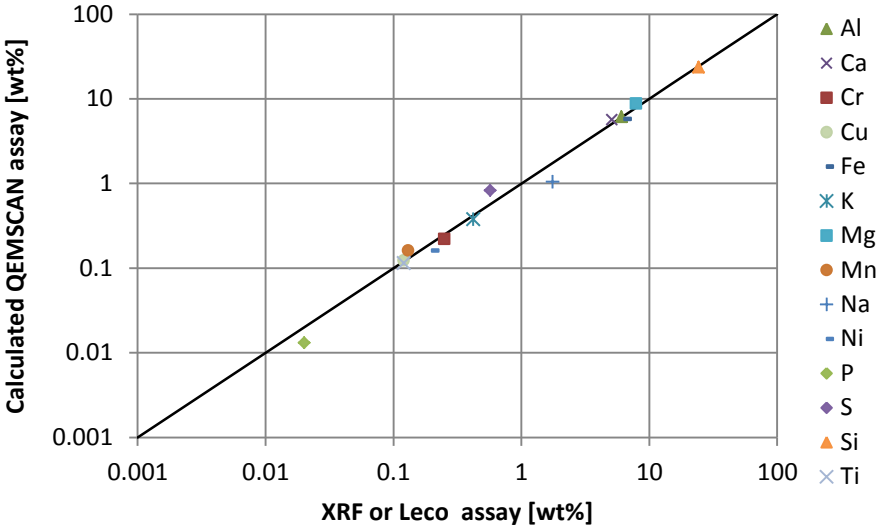

Figure 4-17: QEMSCAN data validation with chemical assay

Chapter 5

AIRFLOW OPERATION

In this chapter the performance of the vertical roller mill operated in airflow mode is investigated. The effects that the VRM variables; grinding pressure, dam ring height and classifier rotor speed had on the product fineness, throughput and energy usage of the mill are analysed. How these variables affected the grinding product particle size distribution, mineralogical characteristics and flotation response is also determined.

5.1 Circuit Product

The airflow test work was conducted with three variables arranged in a three level factorial matrix. The variables, grinding pressure, dam ring height and product size (P_{80}), were adjusted as described in Section 4 and their effect on steady state mill performance recorded. During this steady state operation, the product generated by the circuit was collected for use in further test work.

Classifier Speed (Product Size)

Before each test interval the rotational speed of the dynamic air classifier was manipulated to control the product size. Figure 5-1 illustrates the relationship between classifier rotor speed and product size, represented with P_{80}. The classifier rotor speed and the product size, at constant airflow rate, are inversely proportional with generation of a finer product requiring a higher classifier rotor speed, in line with Altun and Benzer (2014). This is because an increase in rotor speed increases the centrifugal force experienced by a particle, increasing the likelihood of the particle being rejected by the classifier. The relationship indicates that significantly higher classifier rotor speeds are required to generate finer material, these high speeds relate to a greater energy duty, increasing the specific energy usage for production of finer material.

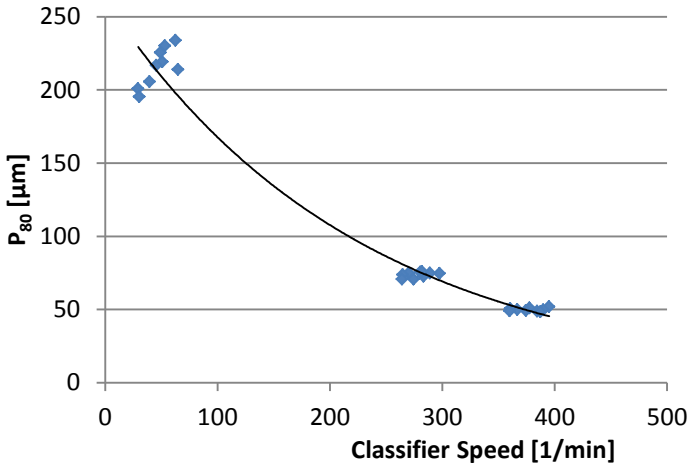

Figure 5-1: The relationship between classifier rotor rotational speed and product size (P_{80}) for all of the airflow tests.

Grinding Pressure

The vertical roller mill was operated at grinding pressures of 600, 800 and 1000 kN/m^2. Figure 5-2 illustrates the sieving product particle size distributions for operation at 4, 7 and 14 mm dam ring heights showing the differences with grinding pressure for the target grind requirement of P_{80} of 45, 75 and 240 µm. The respective laser sizing product particle size distributions can be found in Appendix II. At the coarser 240 µm grind, changing grinding pressure had a noticeable effect on product size distribution for all the tested dam ring heights. It can be seen that for the coarse grind, the product from the device became finer with an increase in grinding pressure. This is the expected response in a comminution device as in grinding at a higher roller pressure the material will experience a greater compressive force on each pass under the roller. The greater compressive force equates to an increase in energy imparted to the particles on each pass through the grinding environment, yielding a finer product (Tamashige et al., 1991). This leads to variations in the material leaving the grinding table and being presented to the classifier, affecting the final comminution product. For the targeted P_{80} of 45 and 75 µm, the variation in particle size distribution is reduced. At these grinds, the effect of variation in grinding table product on the final product has been moderated by the fine tuning of the classifier rotor speed. This is illustrated in Figure 5-1 as the horizontal scatter of points for the finer grinds. For the coarse grind, where throughput is considerably higher and the recycle rate correspondingly lower, the effectiveness of classifier to moderate the variation in grinding table product is reduced. This presents as the deviation in P_{80} at the low classifier speed in Figure 5-1.

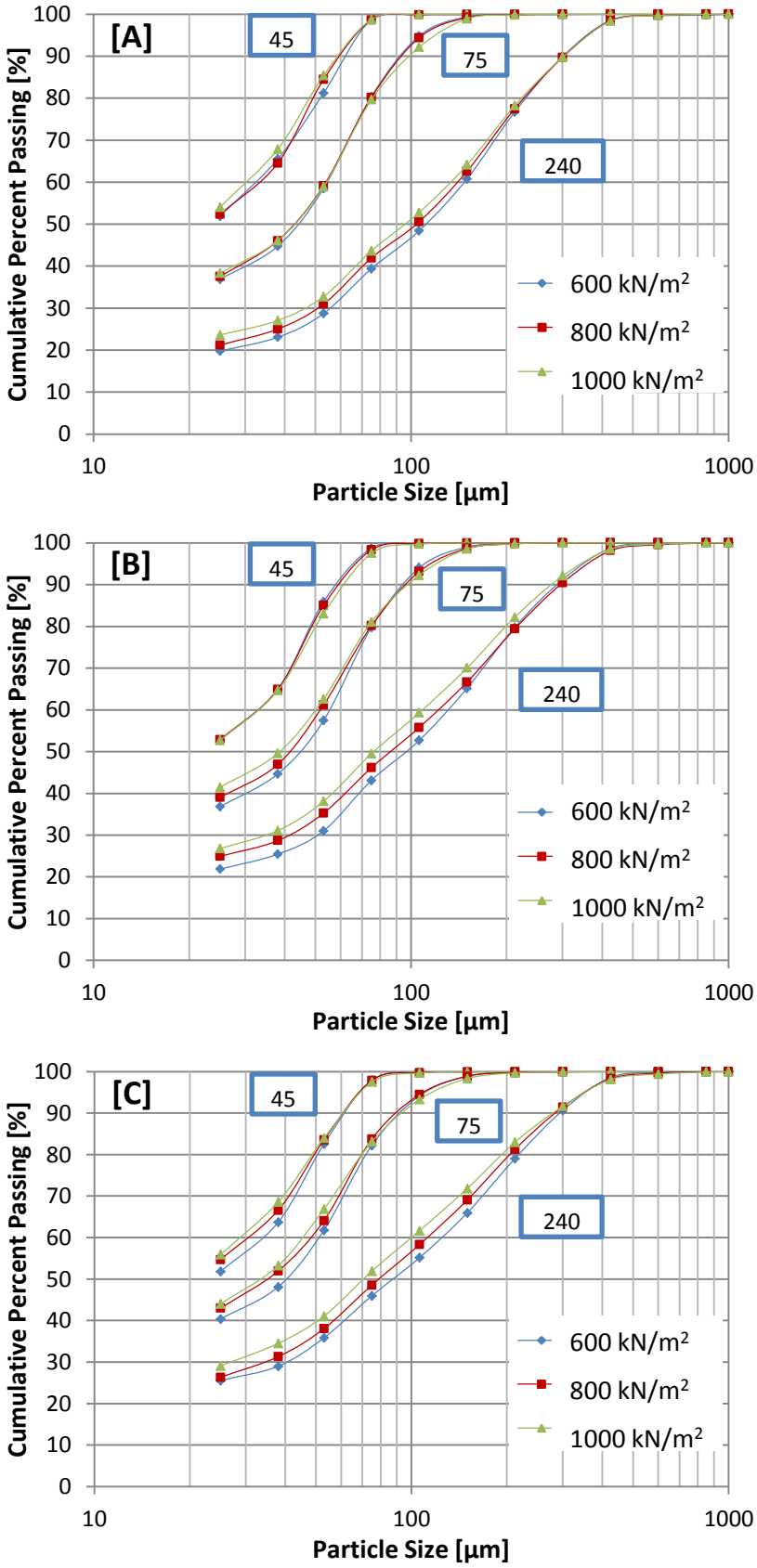

Figure 5-2: Particle size distribution generated by sieving for different target products (P_{80}: 45, 75 & 240 µm) and grinding pressures (600, 800 & 1000 kN/m²) at the dam ring heights: 4 [A], 7 [B] and 14 [C] mm.

The P_{80} and P_{50} values for the comminution products are given in Table 5-1. The measured P_{80} and P_{50} values decrease with increasing grinding pressure for the coarse 240 µm target grind. At the 75 µm targeted grind, the variation in measured P_{80} with grinding pressure is less than 1.8 µm. For the P_{50} values the differences with grinding pressure are greater. For 4, 7 and 14 mm dam ring heights, P_{50} decreased 1.1, 5.8 and 6.6 µm respectively, as the grinding pressure increased from 600 to 1000 kN/m^2. The greater difference at the higher dam ring heights suggests that the product is more susceptible to changes in grinding pressure with a larger dam ring. This can be explained by an increase in residence time on the grinding table resulting from an increase in bed depth caused by a greater dam ring height. For a greater residence time, the material experiences more successive compression events before leaving the grinding table and results in a broader particle size distribution, which presents as the differences in P_{50} values (Roy, 2002). At the 45 µm targeted grind there was less variation in both measured P_{80} and extrapolated P_{50} values, the variation present was greater for products prepared with the 14 mm dam ring height.

Table 5-1: Measured P_{80} and P_{50} values for the vertical roller mill products showing the variation with grinding pressure and dam ring height.

		P_{80}			**P_{50}**		
Target Grind	**DRH**	**Grinding Pressure [kN/m^2]**			**Grinding Pressure [kN/m^2]**		
[µm]	[mm]	600	800	1000	600	800	1000
45	4	51.9	49.7	48.4	27.1	26.4	25.3
	7	48.8	49.3	50.5	27.1	25.8	25.6
	14	51.0	49.9	49.2	26.0	24.7	23.0
75	4	74.6	74.8	76.0	43.7	42.5	42.6
	7	75.6	74.8	73.8	44.3	41.3	38.5
	14	72.6	70.8	70.8	40.1	35.2	33.5
240	4	234	230	226	111.7	104.1	96.6
	7	214	217	201	97.3	87.4	76.6
	14	219	206	195	88.7	79.7	71.1

**P_{50} values for the 45 µm target grind are determined from the laser sizing analyses.*

Dam Ring Height

The vertical roller mill was run with dam ring heights of 4, 7 and 14 mm. The variation in the sieving product particle size distribution for these dam ring heights, at the 800 kN/m² grinding pressure is illustrated in Figure 5-3. Sieving product particle size distributions for the other grinding pressures and laser sizing PSDs are shown in Appendix II and Appendix III respectively. Figure 5-3 shows that operating at a greater dam ring height yields a comminution product which is finer for the 75 and 240 µm target grinds. This difference is greater for the coarser target grinds. A selection of the P_{80} and P_{50} data given in Table 5-1 is presented in Figure 5-4. For the 45 µm target grind, the measured P_{80} values are observed to vary little with dam ring height. At the 75 and 240 µm target grinds, there is a decrease in measured P_{50} as the dam ring height increases. The magnitude of the decrease is greater for the coarser 240 µm grind.

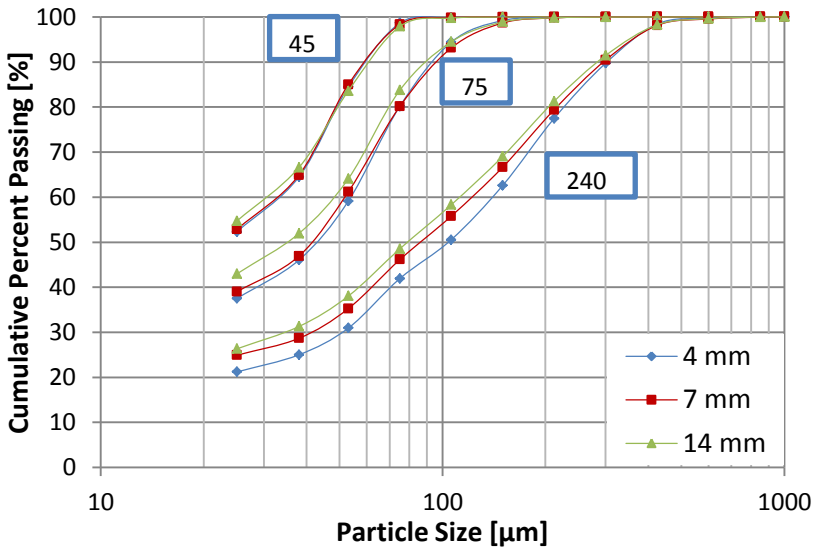

Figure 5-3: Particle size distribution generated by sieving for different target products (P_{80}: 45, 75 and 240 µm) and dam ring heights at the intermediate grinding pressure (800 kN/m²).

The difference in product particle size distribution with dam ring height can be explained in terms of bed depth. An increased bed depth results in a longer residence time for material on the grinding table and particles experience more successive compressive events before leaving the grinding table (Roy, 2002; Tamashige et al., 1991). As energy imparted to the particles on each pass through the grinding environment varies, so the material leaving the grinding table and being presented to the classifier changes, and this affects the final comminution product. Much like with varying grinding pressure, for the targeted P_{80} of 45 and 75 µm, the variation in particle size distribution with changes in dam ring height is reduced. At these grinds, the effect of variation in grinding table product on the final product has been moderated by the fine tuning of the classifier rotor speed. The bed depths are shown in Figure 5-5 and for all grinding pressures there is an increase in bed depth as dam ring height increased. Furthermore, in

comparing the separate plots, it is observed that higher grinding pressures are associated with a decrease in bed depth. It was not possible to get representative samples of the bed in steady state to assess the density of material compacted on the bed.

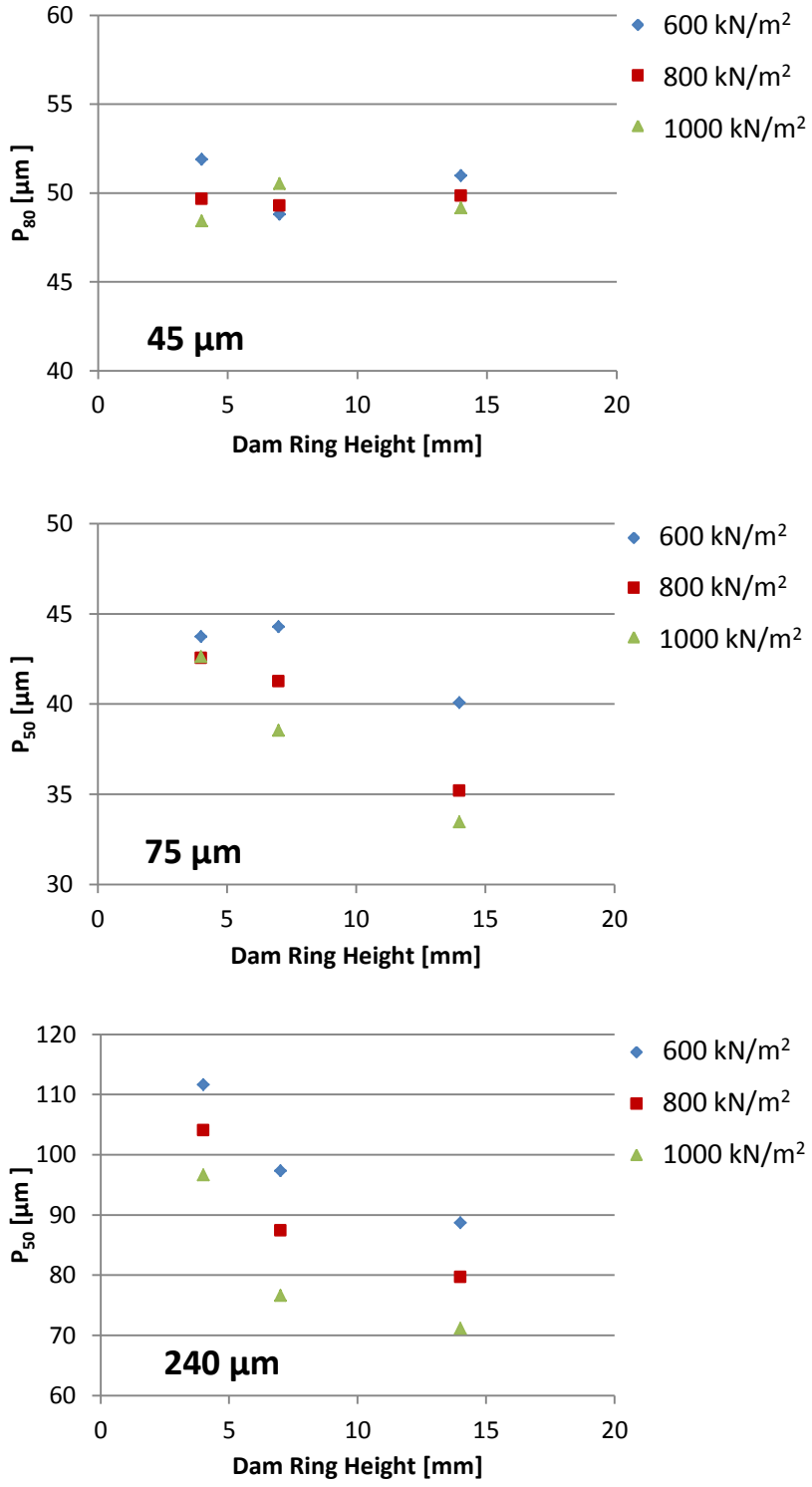

Figure 5-4: Changes in P_{80} and P_{50} as dam ring height and grinding pressure vary for the target grinds of 45, 75 and 240 µm.

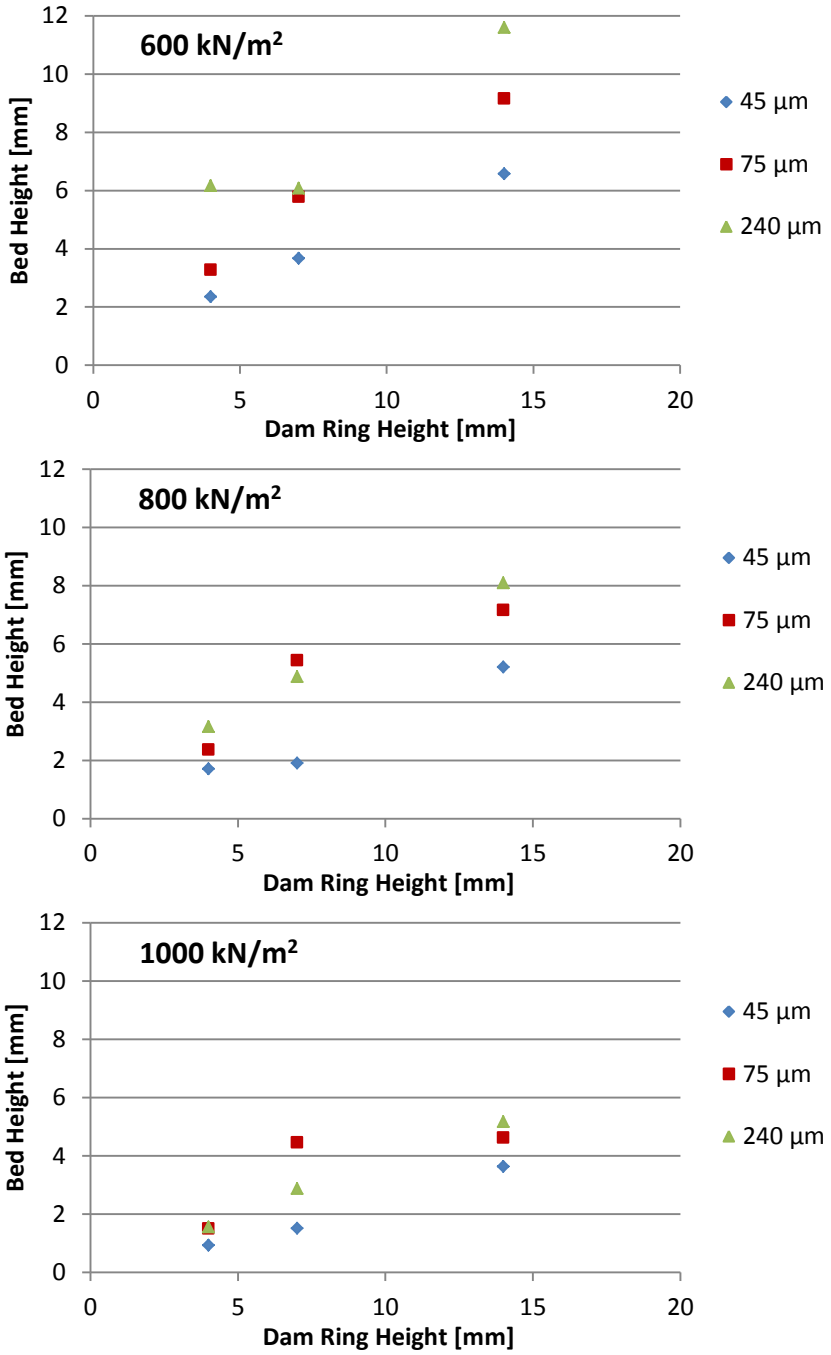

Figure 5-5: Change in bed depth as dam ring height varies at the grinding pressures 600, 800 and 1000 kN/m².

5.2 Throughput

The mill throughput was obtained from the average mass flow rate measurement of classifier product collected over a given test period, while the system was at steady state. The data obtained showed that at the set target grinds, the dam ring height and grinding pressure had a significant influence on the throughput of the vertical roller mill.

Classifier Speed

The manipulation of classifier rotor speed not only has an effect on the product size but also affects the recycle of material within grinding and classification system. Increasing the classifier rotor speed reduces the product particle size and hence increases the amount of material retained within the grinding-classification circuit. The vertical roller mill is characterised by the possibility to control and adjust this circulating load and is accomplished by monitoring the pressure drop across the mill, which is influenced by the gas flow rate and the solid loading inside the mill. When operating with a fixed pressure drop over the mill, increasing classifier rotor speed will cause solids loading in the mill to increase. Provided the gas flow rate and other milling variables are held constant, the only way to maintain the pressure drop is to reduce solids loading by introducing less feed material, reducing production rate (Altun et al., 2017). Figure 5-6 with data for the 7 mm dam ring height illustrates this relationship, with a lower classifier rotor speed achieving a higher throughput. Similar relationships were observed for the other dam ring heights and with grinding pressure (Appendix IV).

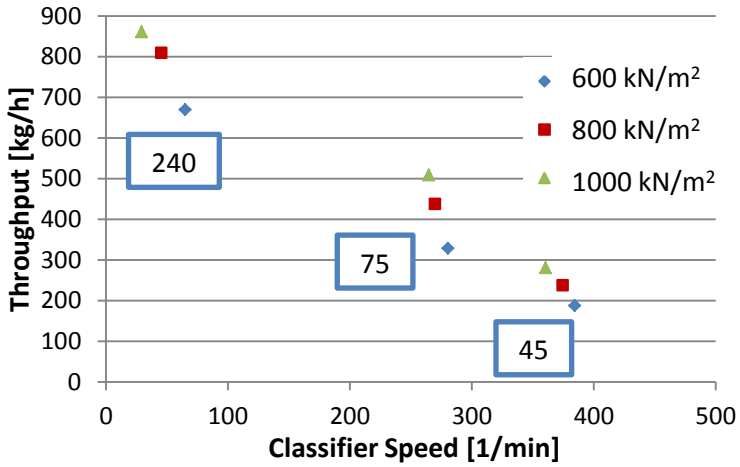

Figure 5-6: Vertical roller mill throughput - classifier rotor rotational speed relationship for tests carried out at the intermediate (7 mm) dam ring height.

Dam Ring Height and Grinding Pressure

The influence which dam ring height and grinding pressure had on throughput for the three different target grinds are shown Figure 5-7 and Figure 5-8. It was observed that for the target grind P_{80} of 45 μm, throughput increased with increase in dam ring height for the range tested. For the target grinds with P_{80} levels of 75 and 240 μm throughput increased only when the dam ring height was increased from 4 to 7 mm. Further increase in dam ring height for the 75 μm P_{80} target grind yielded no change, while for the 240 μm P_{80} target grind a reduction in throughput was observed. Similar trends were observed for all grinding pressures used in the experimental work. In the work by Reichert et al. (2014) on two iron ore samples, results indicated an increased throughput was achieved for greater dam ring heights, with the increase in throughput lower for a coarser product grind. Data collected by Tamashige et al. (1991) for grinding clinker showed that operating at a higher dam ring height decreased throughput. The conflicting results in the work Reichert et al. (2014) and Tamashige et al. (1991), together with results observed in this study suggest that there could be an ore dependent optimum dam ring height to maximise throughput for each of the target grinds. Reichert et al. (2014) could have been operating below the optimum and as a result increases in dam ring height increased throughput, while Tamashige et al. (1991) operated above the optimum, so higher dam rings yielded lower throughputs. In this study, for the coarse and intermediate target grinds a maximum throughput appears within the range of dam ring heights tested. The optimum dam ring height however cannot be adequately identified from the data. For the finest grind, throughput was not maximised and further increases may have been achievable at higher dam ring heights.

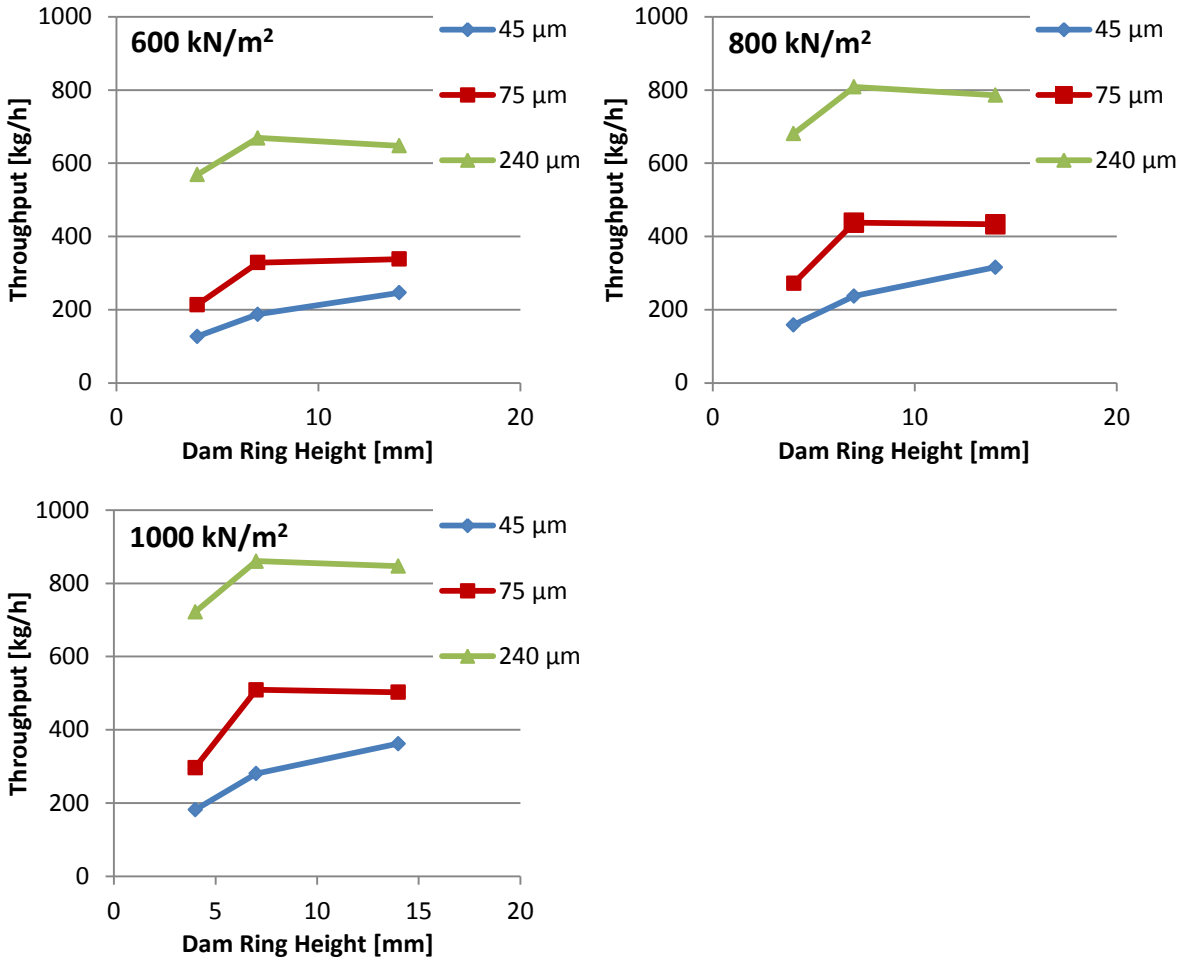

Figure 5-7: Changes in throughput with dam ring height, distinguishing between target product P_{80}. Differences in throughput at a dam ring height and product P_{80} are due to changes in grinding pressures.

The influence of grinding pressure on throughput is also shown in Figure 5-8. It was observed that throughput was greater at higher grinding pressures for all target grinds and dam ring heights evaluated. The rise in throughput with an increase in pressure can be attributed to more energy being imparted to the material on each pass under the rollers, resulting in a finer grinding table product. When this material is presented to the air classifier, more particles are finer than the classifier product top size and are discharged as product, reducing the circulating load and allowing more fresh feed to be introduced. In the work by Altun et al. (2016) similar trends were observed to those in this study, for the grinding of a gold ore to different target grinds in a pilot scale vertical roller mill. Reichert et al. (2014), however, found that for two iron ores, after increasing grinding pressure past a point no further increase in production rate was achieved. This phenomenon, while not observed in either this or the study by Altun et al. (2016), could occur above the range of grinding pressures tested for these two ores.

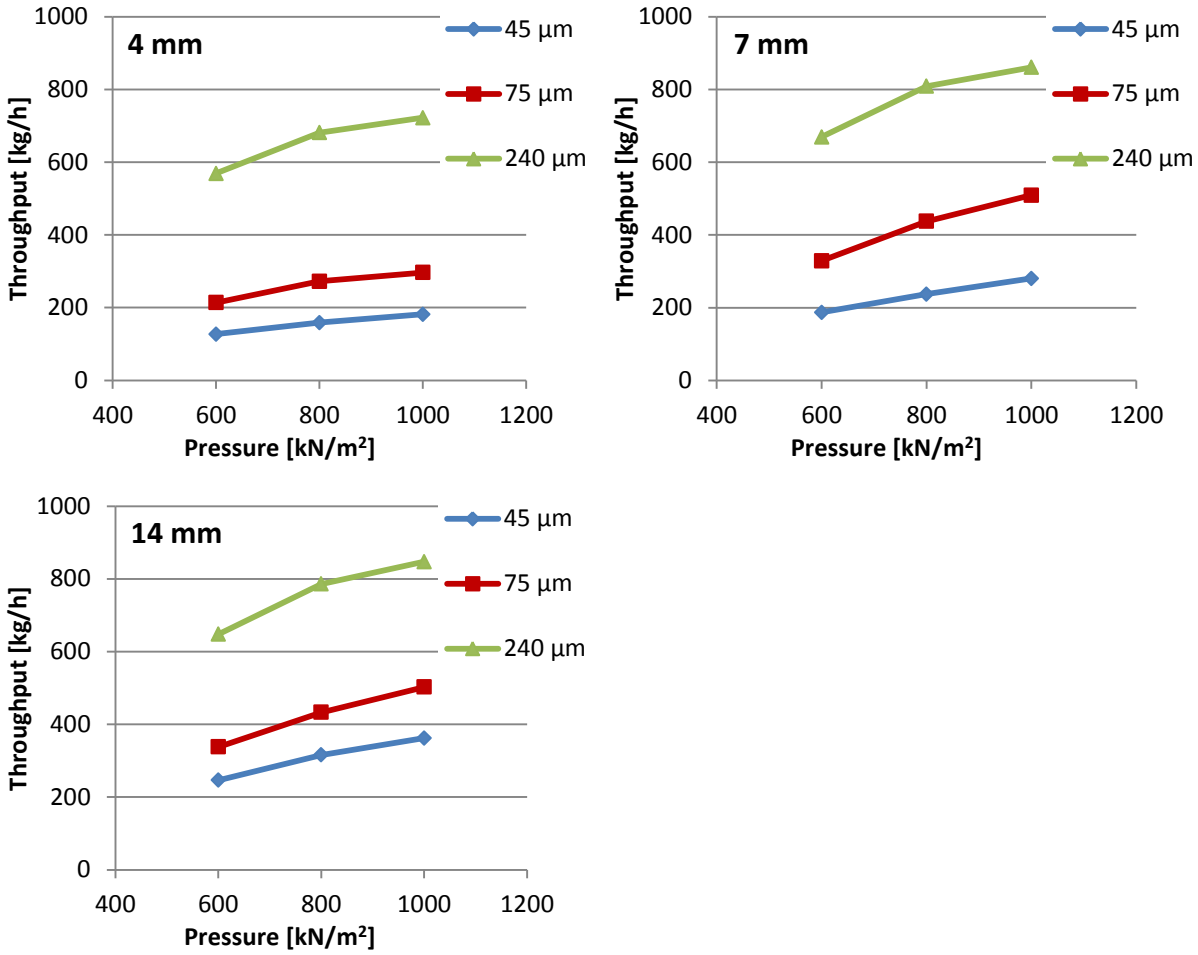

Figure 5-8: Changes in throughput with dam ring height, distinguishing between target product P_{80}. Differences in throughput at a dam ring height and product P_{80} are due to changes in grinding pressures.

5.3 Energy Utilisation

The vertical roller mill used in the airflow part of this study had instrumentation for the measurement of energy usage of the various grinding and classification components in the system. This section focuses on the measured energy usage of the grinding elements. The measured energy consumptions of the fan and dynamic air classifier are not representative of industrial scale devices and as such, are not evaluated directly. The classification energy is recalculated during scale up.

Mechanical Energy

The mechanical energy of grinding was calculated via a torque value, measured using a load cell on the gear box driving the grinding table. The data generated during each of the steady state test runs is presented in Figure 5-9. Plot A, B and C in Figure 5-9 correspond to the three target grinds of P_{80} 45, 75 and 240 µm. The mill mechanical power is in the same range for all three target grinds. Since grinding to a lower particle size requires more energy, and mechanical energy input rate is consistent, the consequence is a decrease in throughput as the target grind decreases. The mechanical power is observed to increase with an increase in dam ring height for all cases. This is explained by a greater resistance of the grinding table to rotation as dam ring height increases. A greater dam ring height causes the depth of material on the grinding table to increase (Figure 5-5), this affects the resistance experienced as the rollers travel over the material and necessitates a greater rotational force be applied to maintain the grinding table rotation. The measured mechanical power is greater for higher grinding pressures for all cases. This is because an increased pressure applied by the rollers, impedes the passing of material under the rollers and requires a greater rotational force be applied in order to maintain grinding table rotation. Analysing the mechanical power can be beneficial in gaining an understanding of the grinding environment, however, the data can be misleading when analysing the system as a whole. Because of this, the results should also be assessed in conjunction with mill throughput.

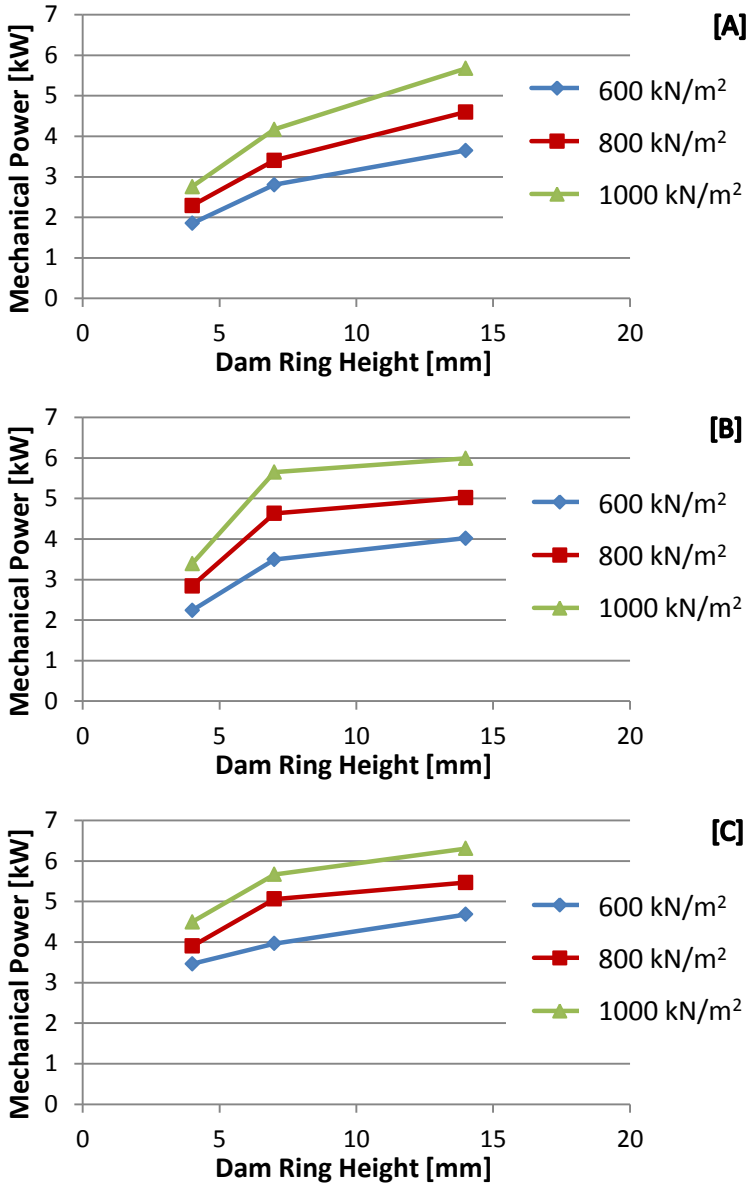

Figure 5-9: Mechanical power variation with dam ring height and grinding pressure and the three target grinds 45 [A], 75 [B] and 240 [C] µm.

Specific Grinding Energy

Using the mechanical power of grinding and mill throughput, specific grinding energy was calculated. Figure 5-10 illustrates the response of specific grinding energy in the vertical roller mill to changes in dam ring height for the different target grinds. Dam ring height was observed to have an effect on specific grinding energy, with the variation greatest at the coarse grind (P_{80} of 240 µm). The percentage changes in specific grinding energy with dam ring height are given in Table 5-2. The average percentage increase in specific grinding energy with dam ring height was 20% at the coarse grind, 9% at the intermediate grind and 2% at the finest grind. The decrease in percentage change with dam ring height for finer grinds is a consequence of the greater specific energy required when generating a finer product. Reichert et al. (2014) and

Tamashige et al. (1991) both reported observing an increase in specific grinding energy as the dam ring height was raised. Tamashige et al. (1991) stated that the reduction in energy efficiency is a result of increased bed depth and the associated decrease in grinding efficiency as the size reduction mechanism departs further from single particle breakage. Figure 5-11 illustrates the relationship between specific grinding energy and particle size for products generated in the VRM at different grinding pressures. The plot shows that an increase in specific grinding energy is required to achieve a lower product particle size, which follows general comminution theory.

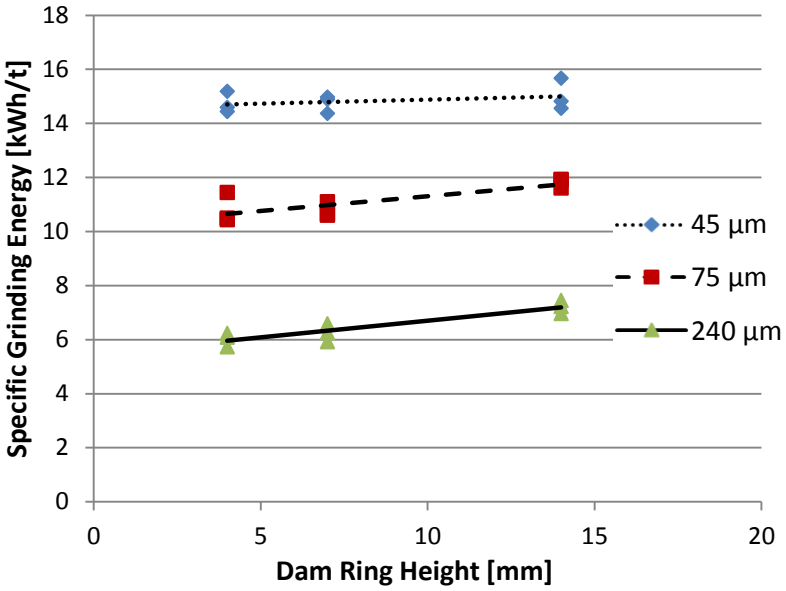

Figure 5-10: Changes in specific grinding energy of the vertical roller mill with dam ring height for different product sizes. Linear trendlines fitted only to highlight general relationship between specific grinding energy and dam ring height.

Table 5-2: Percent change in specific grinding energy with dam ring height. Percentages calculated relative to the specific grinding energy at the 4 mm dam ring height for each grinding pressure - target grind configuration.

Target Grind [µm]	**Grinding Pressure** [kN/m²]	**Dam Ring Height [mm]** 4	7	14
45	600	100	103	102
	800	100	99	101
	1000	100	98	103
75	600	100	101	113
	800	100	102	111
	1000	100	97	104
240	600	100	97	119
	800	100	109	122
	1000	100	106	120

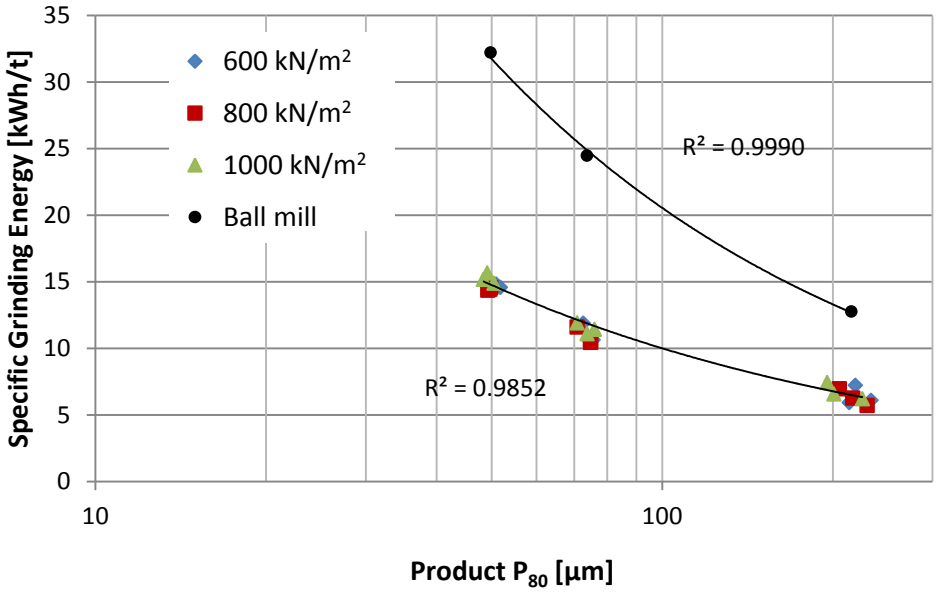

Figure 5-11: Signature plot of specific grinding energy in the vertical roller mill and theoretical ball mill, differentiating between the grinding pressures for the VRM.

An estimation of the expected energy required for ball milling is included in Figure 5-11. The estimate was calculated with the Bond formula using the Bond Work Index for Platreef of 23 kWh/t at a closing screen size of 75 µm (Mainza and Powell, 2006). The result compares well with results for the industrial plant processing Platreef ore (Rule et al., 2015). A direct comparison between the ball mill and VRM specific grinding energies should however not be made, as the classification energy requirements of the two circuits are vastly different. Ball mills are typically coupled with screens and hydroclones, while classification in the vertical roller mill in airflow mode is performed with a dynamic air classifier. Dynamic air classification consumes more energy than the pumping requirements for hydrocyclones or screens. In previous pilot scale studies the energy consumption of classification has been reported to be 60 - 80% to that for the grinding components (Altun et al., 2015; van Drunick et al., 2010). If these ratios are applied to this data the pilot VRM operates at 75 - 85% of the specific energy consumption of the ball mill. The vertical roller mill grinding and classification components scale differently from pilot to industrial units, with the ratio of classification to grinding energy in the vertical roller mill 40% lower in industrial applications (Nyakunuhwa, 2019). If this scale up factor is applied, the industrial scale vertical roller mill would have a 25 to 35% lower specific energy than that of a ball mill.

5.4 Mineralogy

Products from all three target grinds (P_{80} of 45, 75 & 240 µm) at the 7 mm dam ring height, and the intermediate products (P_{80} of 75 µm) at the 4 and 14 mm dam ring heights were selected for mineralogical analysis. All samples were milled at a grinding pressure of 600 kN/m^2. The average bulk mineralogy of the five samples is shown in Table 5-3, bulk mineralogy for the individual samples are shown in Appendix V in Figure 9-14 and Table 9-1. There was little variation in the bulk mineralogy between the different samples, confirming that the samples were representatively split to obtain sub-samples. The characterisation of the sample indicated that the ore contained the major gangue minerals: plagioclase (30%), orthopyroxene (30%) and clinopyroxene (14%), chlorite (8%), talc (4%) and quartz (4%), and the base metal sulphides: pentlandite (0.5%), pyrrhotite (1.3%) and chalcopyrite (0.4%). The proportions of major gangue constituents, which coupled with CaO levels (7.1%) measured by X-Ray Florescence (XRF), indicate that the feed material can be classified as a feldspathic pyroxenite (Schouwstra et al., 2013, 2017).

Table 5-3: Bulk mineralogy of the Platreef ore used for comminution and flotation test work.

Mineral	**[wt%]**	**SE**
Chalcopyrite	0.4	0.06
Pentlandite	0.5	0.04
Pyrrhotite	1.3	0.10
Olivine	2.5	0.05
Pyroxene	43.9	1.08
Chlorite	7.3	0.26
Talc	3.5	0.23
Amphibole	1.8	0.16
Serpentine	0.7	0.07
Plagioclase	29.7	0.52
Mica	2.0	0.09
Carbonate	0.7	0.07
Quartz	4.0	1.12
Chromite	1.1	0.11
Other	0.6	0.05

**Chlorite, talc, amphibole and serpentine are grouped as alteration silicates.*

The combined PGM mineralogy for all of the VRM products analysed is presented in Table 5-4. More than half of the platinum group elements (PGE) were found to be present as PGE tellurides (dominantly kotulskite and moncheite). The PGE sulphides (mostly cooperite and laurite) and PGE arsenides/sulpharsenides (sperrylite) accounted for 18 and 13% of the platinum group minerals respectively, with smaller amounts of gold and PGE alloys also present.

Table 5-4: PGM distribution (where the number of PGM containing particles (n) is 536).

Mineral Group	**[Area%]**
PGE Tellurides	57.4
PGE Sulphides	17.9
PGE Arsenides/Sulpharsenides	13.2
PGE Alloys	4.6
PGE Bismuthides	2.6
PGE Antimonides	0.02
Gold	4.3

Size by Size Mineral Distribution

Figure 5-12, Figure 5-13 and Figure 5-14 display bulk mineral distribution by size for the three target grinds (P_{80} of 45, 75 & 240 μm) at a dam ring height of 7 mm. Analysis of a single surface was carried out for each of the products and sizing was done based on the 2-D particle image data collected. The samples were unsized prior to mounting in resin and because of this results should be viewed as more qualitative. When comparing the bulk mineral deportment by size there is a shift as the target grind increased, with more material reporting to the coarser size classes. There is minimal consistent variation in the deportment of most of the minerals between the different size classes. The exception to this is the alteration silicates, for which there is a trend for the mineral class to deport preferentially to the smaller size classes. Figure 5-15 shows the deportment of alteration silicates by size for different target grinds, prepared at different dam ring heights (4, 7 and 14 mm). The figure illustrates the preferential deportment of alteration silicates to the smaller particle size classes for all target grinds and at all three dam ring heights.

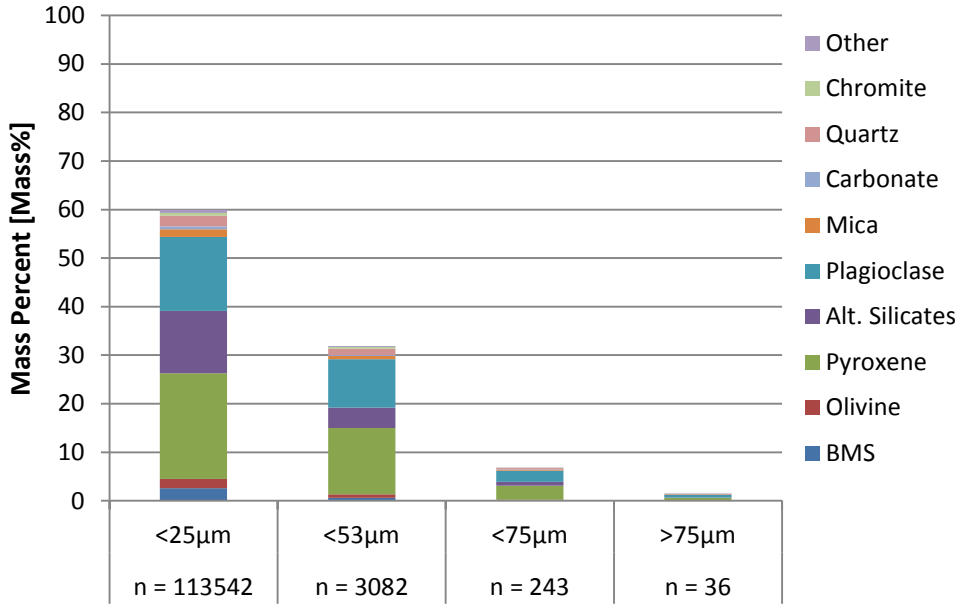

Figure 5-12: Bulk mineral deportment by size for the fine target grind (P_{80} 45 µm) at a dam ring height of 7 mm, where n is the number of particles analysed.

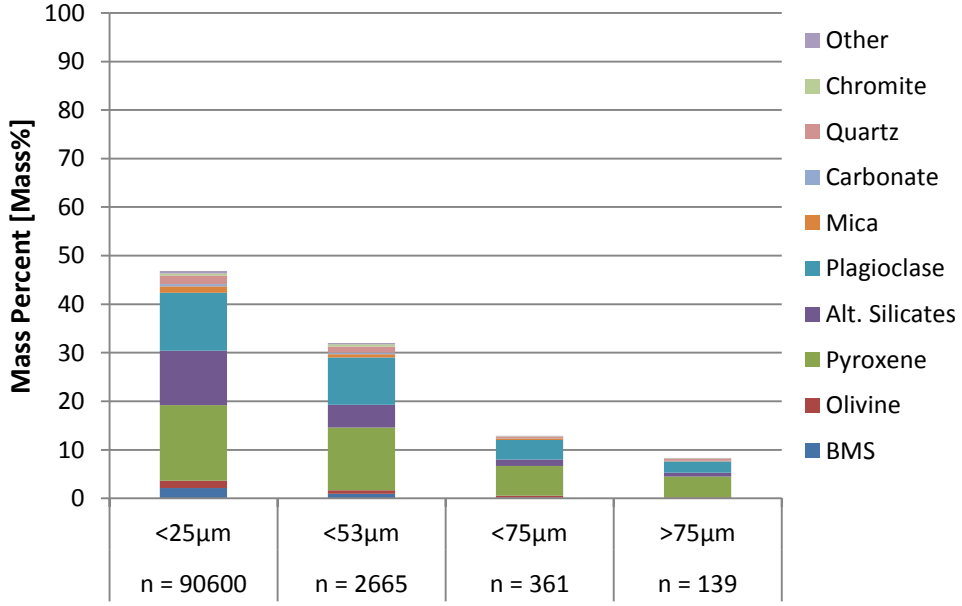

Figure 5-13: Bulk mineral deportment by size for the intermediate target grind (P_{80} 75 µm) at a dam ring height of 7 mm, where n is the number of particles analysed.

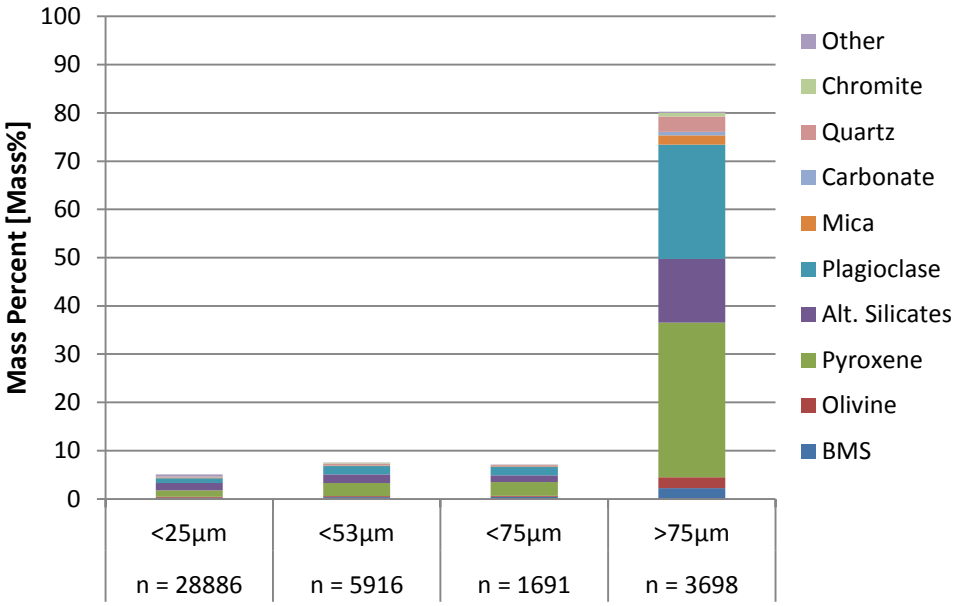

Figure 5-14: Bulk mineral deportment by size for the coarse target grind (P_{80} 240 µm) at a dam ring height of 7 mm, where n is the number of particles analysed.

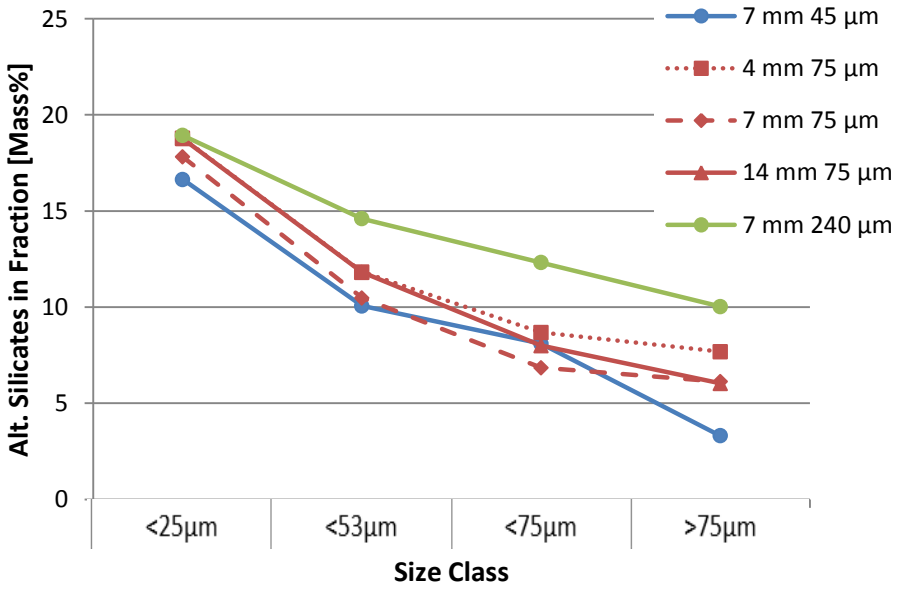

Figure 5-15: Deportment of alteration silicates by size for different target grinds (P_{80} 45, 75, 240 µm) and dam ring heights (4, 7, 14 mm).

The variable deportment of the alteration silicates with size can be further analysed by looking at the individual mineral components which make up this mineral grouping. The alteration silicates class contains the minerals amphibole, chlorite, serpentine and talc. Of these, talc, serpentine and chlorite are known to be problematic naturally floating gangue species (Baum, 2013) and preferential deportment of these minerals could lead to variation in valuable mineral recoveries and concentrate grades (Wiese et al., 2005). Profiles of the liberation of the talc and chlorite are given in Figure 5-16 and Figure 5-17.

The amount of liberated talc in Figure 5-16 varies with both target P_{80} and dam ring height. As is expected, a greater proportion of the talc is liberated as the target P_{80} decreased and the vertical roller mill product as a whole becomes finer. With respect to dam ring height, the intermediate dam ring height of 7 mm had an appreciably lower proportion of liberated talc than the 4 and 14 mm dam ring heights. Furthermore, the 75 µm P_{80} products generated at the 4 and 14 mm dam ring heights both had a greater amount of liberated talc than the 45 µm P_{80} product. This variation in liberation with dam ring height for a mineral which is known to be naturally floating, could lead to differences in flotation performance. In Figure 5-17 the liberation profile of chlorite only varies with product P_{80} and not dam ring height. Similar to that seen for talc, as the target P_{80} reduced, a greater proportion of the chlorite is liberated.

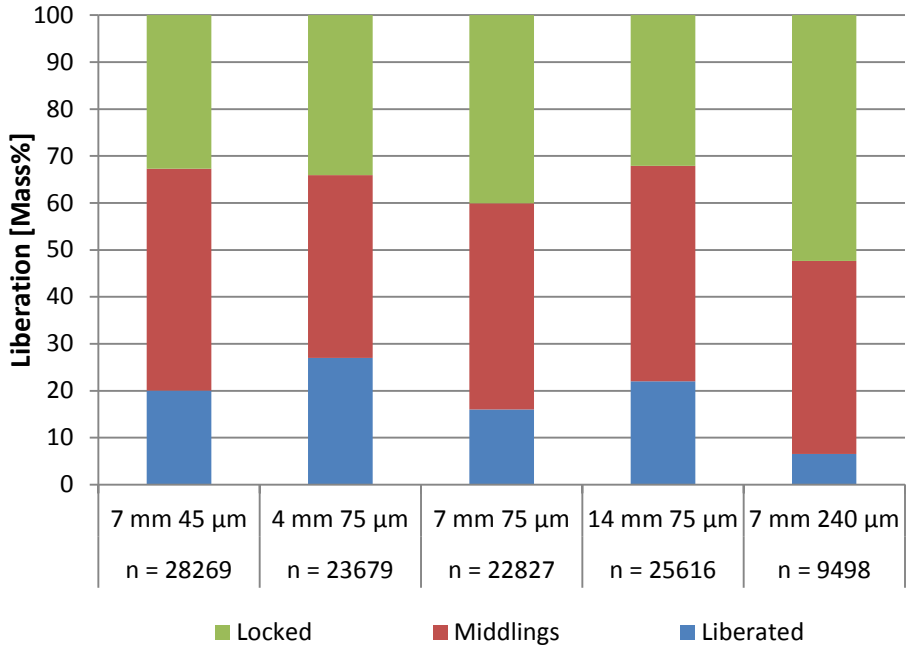

Figure 5-16: Liberation and size based profile of talc, where liberated, middlings and locked equate to >80%, 80-30% and <30% association with background. Where n is the number of particles analysed.

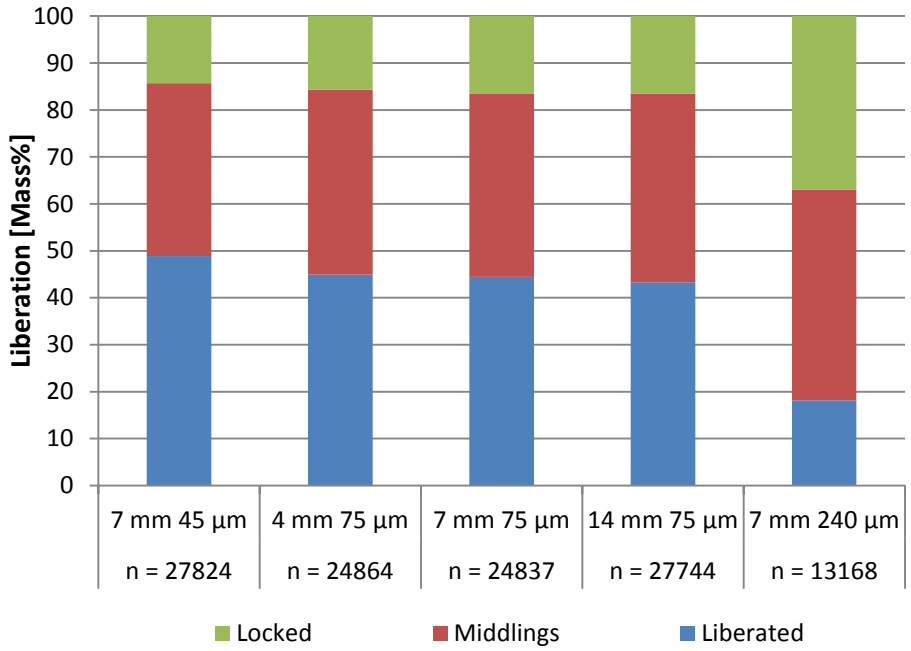

Figure 5-17: Liberation and size based profile of chlorite, where liberated, middlings and locked equate to >80%, 80-30% and <30% association with background. Where n is the number of particles analysed.

Base Metal Sulphides

Figure 5-18, Figure 5-19 and Figure 5-20 focus specifically on the base metal sulphide (BMS) containing portion of the particles analysed using the particle mineral analysis (PMA) routine. The measurements are based on 2D image analysis of unsized polished blocks and hence results should be viewed as more qualitative. Figure 5-18 and Figure 5-19 display the size distributions for the BMS grains and BMS containing particles, respectively. The size distribution of both the BMS grains and BMS containing particles are observed to shift left, becoming finer as the target P_{80} decreases. This is expected as the whole particle size distribution will become finer when grinding to a lower P_{80}. There are no significant differences in BMS grain size distribution for the different dam ring heights. For the BMS containing particles there is a slight shift in size distribution, with higher dam rings being marginally coarser.

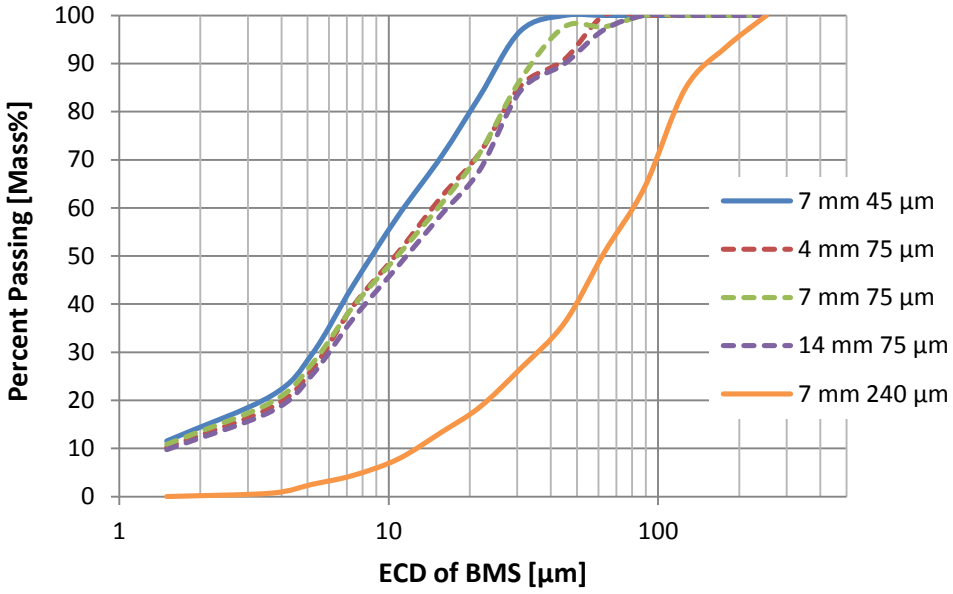

Figure 5-18: Base metal sulphide grain size distribution (equivalent circle diameters). Number of particles analysed: 5264, 4785, 4894, 3812 & 2370 respectively.

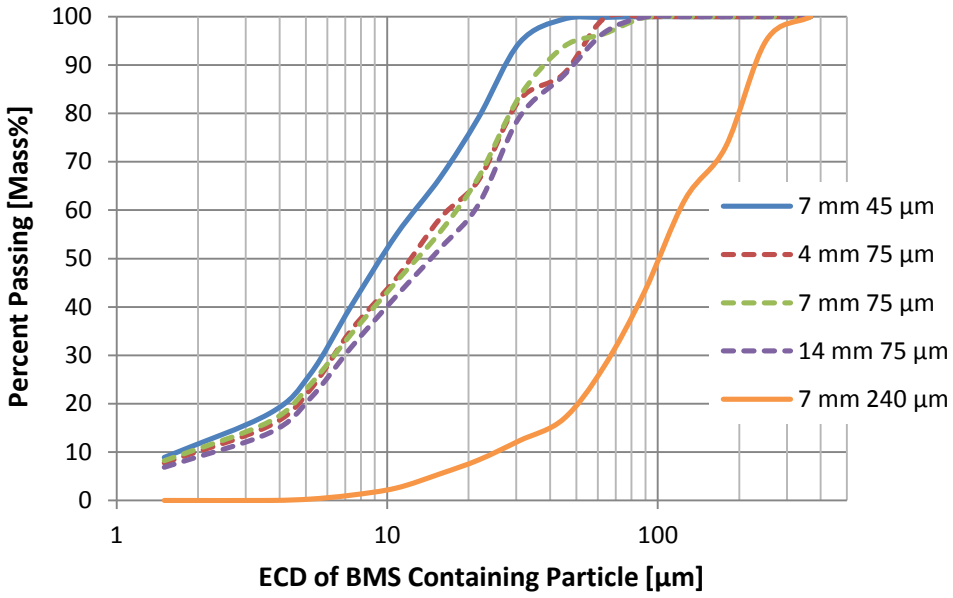

Figure 5-19: Particle size distribution of particles containing base metal sulphide (equivalent circle diameters). Number of particles analysed: 5264, 4785, 4894, 3812 & 2370 respectively.

The base metal sulphide liberation data is presented in Figure 5-20. The amount of liberated BMS increases for the finer grinds, going from 40% at the coarse target grind (P_{80} of 240 µm) to 85% at the finest target grind (P_{80} of 45 µm). Changing dam ring height does not cause large differences in the BMS liberation profile. The proportion of locked BMS may be marginally greater when operating with higher dam rings. This matches the observed slightly coarser size distribution for BMS containing particles at the higher dam ring in Figure 5-19. This variability

in base metal sulphide liberation with dam ring height could lead to differences in copper and nickel recoveries in product flotation response.

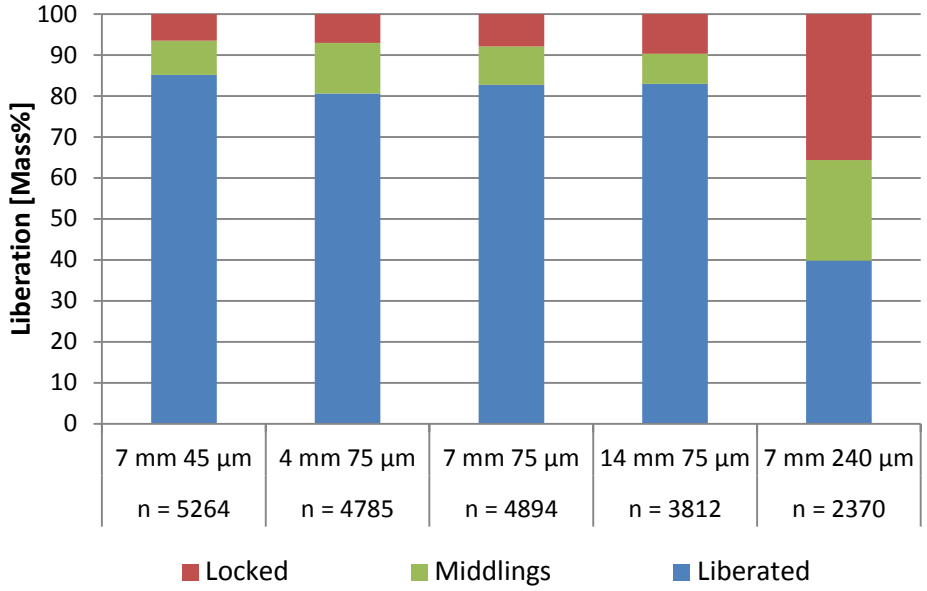

Figure 5-20: Base metal sulphide mineral liberation profile at different P_{80} and dam ring heights, where n is the number of particles analysed and liberated, middlings and locked equate to >90%, 90-30% and <30% association with background.

Platinum Group Minerals

The platinum group mineral mineralogy resulting from the trace mineral search (TMS) analysis of the selected vertical roller mill products is presented in Figure 5-21 and Figure 5-22. Figure 5-21 shows a breakdown of the gold and platinum group element (PGE) mineral distributions and there is significant amount of variation between the different products. Most of the variation is due to the low sample sizes of the platinum group minerals as suggested by van de Plas and Tobi (1965). The low PGM sample sizes are a consequence of the low concentration of PGMs in the ore, in spite of longer machine run times for analysis. Due to this, only ~100 PGMs for each product were analysed. To illustrate this, for base metal sulphides over 2000 BMS containing particles were located in the PMA of a single surface of a single block, whereas the 100 PGMs located for a sample were distributed over 120 000 fields, spanning multiple surfaces on multiple blocks. Although the low sample numbers lead to the variation in the measured PGM speciation, when analysing the PGM grouping as a whole, trends in liberation characteristics do emerge. Figure 5-22 shows a breakdown of only the PGMs in the samples and overall, the PGE tellurides contained the highest proportion of the PGMs present, with the second most abundant PGMs varying between PGE sulphides, PGE arsenides/sulpharsenides and PGE alloys. The PGM mineralogy for this ore is similar to that for the reef feldspathic pyroxenite presented in the work by Holwell and McDonald (2016).

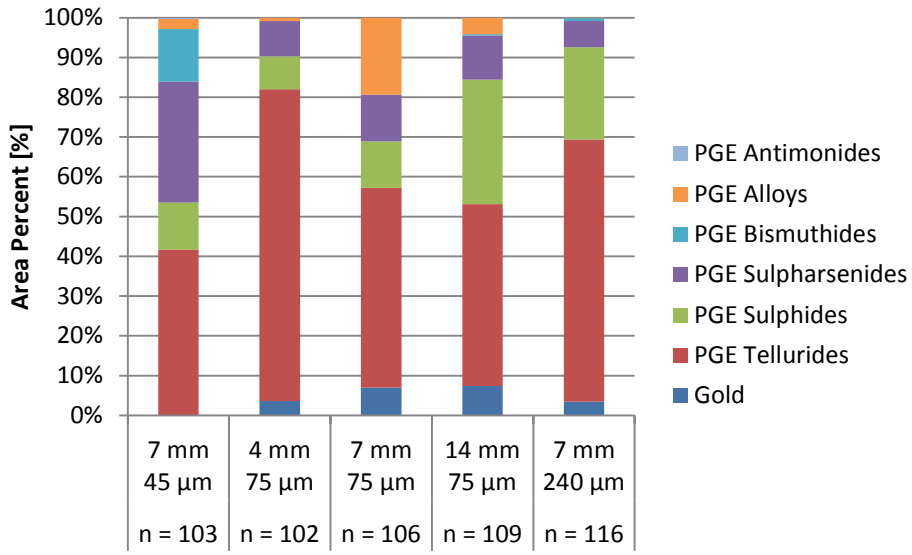

Figure 5-21: Precious metal (platinum group minerals and gold) mineralogy for three different target grinds and dam ring heights, where n is the number of particles analysed.

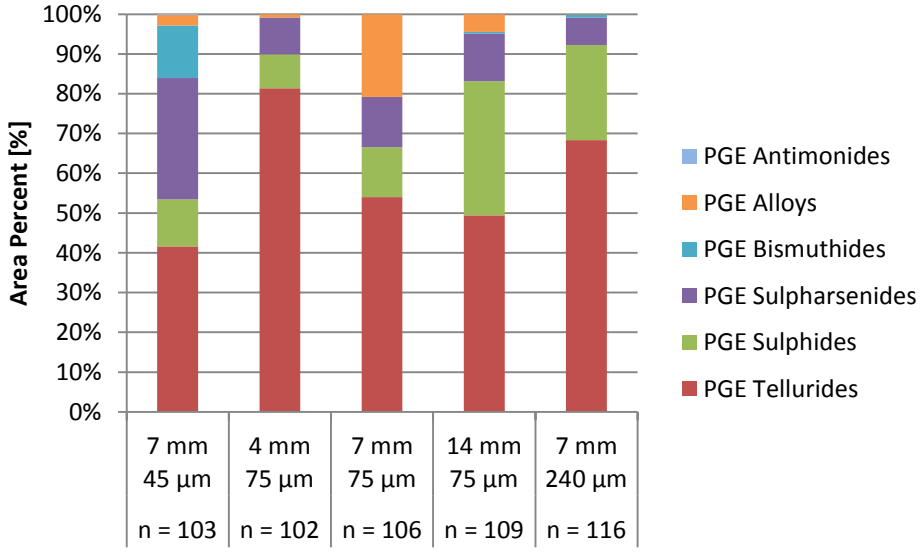

Figure 5-22: Platinum group mineral mineralogy (gold excluded) for three different target grinds and dam ring heights, where n is the number of particles analysed.

The PGM grain size distributions of the samples are shown in Figure 5-23. The platinum group mineral grain size is less than 30 µm. There is some variation between the different product sizes and dam ring heights, particularly at the coarser end of the distributions. Most of the variation is due to the low platinum group mineral sample sizes, with individual large PGMs causing a skewing effect on the rest of the grain size distribution.

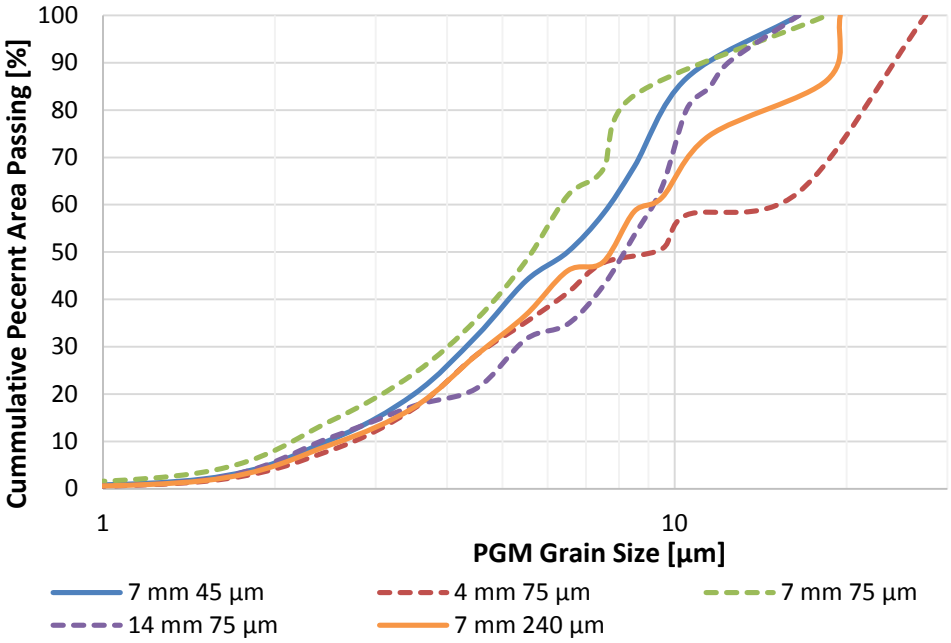

Figure 5-23: Platinum group mineral grain size distributions. Number of particles analysed: 103, 102, 106, 109 & 116 respectively.

The PGM liberation profiles for the three different grinds and dam ring heights are given in Figure 5-24. At the coarse grind, close to 60% of the PGMs are classified as locked. This reduces to around 30 and 22% when grinding to P_{80} of 75 and 45 µm respectively. Dam ring height did not appear to have a large effect on PGM liberation, with only marginally less liberated PGMs generated at higher dam ring heights.

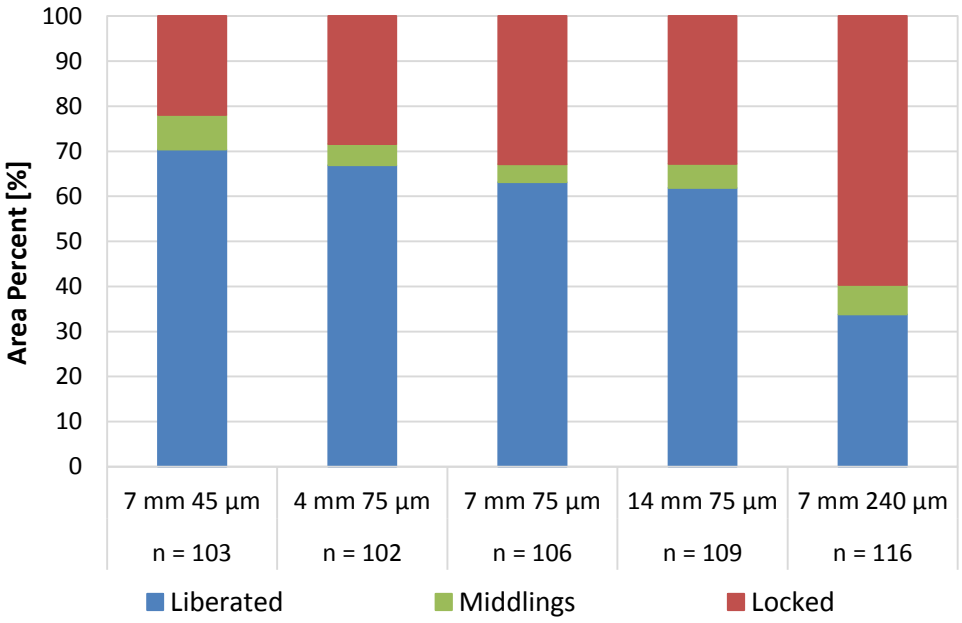

Figure 5-24: PGM liberation data for different P_{80} and dam ring heights, where n is the number of particles analysed and liberated, middlings and locked equate to >80%, 80-30% and <30% perimeter association with background.

The liberation and mineral association profiles of the PGM containing particles scanned during the trace mineral search are presented in Figure 5-25. A significant portion of the locked and middling PGMs are associated with liberated base metal sulphides, and these should be recovered during flotation. For the 75 µm target grind, there is an increase in effective PGM liberation (liberated PGMs and PGMs associated with liberated BMS) with dam ring height. The associated PGMs are also classed based on the dominant associated gangue mineral (silicate, alteration silicate or oxide) and as either attached (exposed at the particle surface) or enclosed (no exposure to the particle surface). There is a large amount of variation in the proportion of associated PGMs in each of the gangue classes across the different target grinds and dam ring heights, with no clear trends observed.

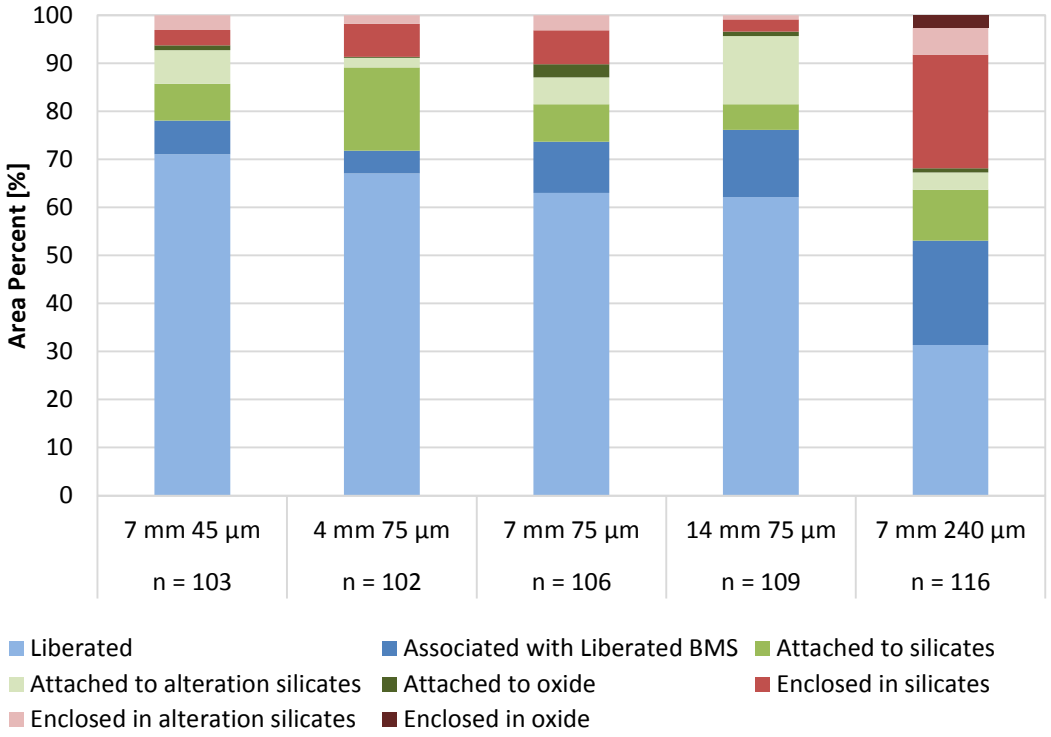

Figure 5-25: PGM liberation with base metal sulphide and gangue mineral association for different P_{80} and dam ring heights, where n is the number of particles analysed and liberated equates to >80% association with background.

5.5 Flotation Response

After grinding, the flotation response of selected vertical roller mill products generated during airflow operation was determined with a series of batch flotation tests. The flotation response was evaluated in terms of platinum, palladium, gold (3E PGE) and base metal (Cu, Ni) grade and recovery. The 3E PGE grade and recovery data has been normalised for confidentiality, such that the proportional differences are maintained but the values presented are not the true data.

Target Grind

The flotation performance of vertical roller mill products of different target grinds, generated at various dam ring heights and grinding pressures were evaluated in terms of valuable metal recovery and flotation kinetics. Figure 5-26, Figure 5-29 and Figure 5-30 display the PGE flotation recovery and grade data for vertical roller mill products of different grind, generated at different dam ring heights and a single grinding pressure of 600 kN/m^2.

Figure 5-26 [A] displays the trends in the flotation performance as target grind is changed for vertical roller mill products generated at a dam ring height of 4 mm. As the mill product decreases in size from a product P_{80} of 240 to 45 μm, the cumulative platinum, palladium and gold (3E PGE) recovery increases. A similar trend is seen in Figure 5-26 [B], for a dam ring height of 7 mm, with 62, 81 and 88% 3E PGE recoveries for the 240, 75 and 45 μm P_{80} products respectively. This increase in recovery as the grind gets finer matches the increase in valuable mineral liberation reported in Section 5.4. At a dam ring height of 14 mm there is an increase in recovery when reducing the target product P_{80} from 240 to 75 μm, however the recovery did not increase further for the finest product (P_{80} of 45 μm). For all conditions tested the cumulative platinum, palladium and gold (3E PGE) concentrate grade is observed to decrease as the particle size of the grinding product decreases.

The trends in cumulative solids recovery presented in Figure 5-27 and Figure 5-28 match those for the 3E PGE recovery. The products of finer target grind have a greater solids recovery. The cumulative solids recovery incorporates particle recovery by both true flotation and entrainment, which relates to concentrate grade. The decrease in concentrate grade with target grind observed in Figure 5-26 is caused by a greater recovery of gangue material for grinding products of a finer size. This corresponds to an increase in the non-selective recovery of material through entrainment. The entrainment of gangue is dependent on stability of the froth and directly proportional to water recovery (Liu et al., 2018; Morar et al., 2006; Neethling and Cilliers, 2002). An indication of froth stability can be inferred from the water recovery in a cell operated at a constant froth height (Wiese et al., 2011, 2006). The cumulative solids - water recovery plots are presented in Figure 5-27. The solids - water recovery plots can be found in

Figure 9-15 in Appendix VI. There are greater water recoveries for the finer grinds, indicating a more stable froth and a greater recovery of material through entrainment, diluting the concentrate grade. Entrainment is also affected by particle size, with the rate of entrainment greater for finer particles (Wang et al., 2015). This is displayed in Figure 5-28, which shows cumulative solids recovery plotted against concentrate collection time. A greater rate of entrainment of finer particles is observed as a higher rate of solids recoveries at the finer target grinds. Furthermore, at finer grinds the exposed surface area of naturally floating gangue is greater but because reagent dosing is kept constant, the ratio of depressant to surface area decreases, resulting in lower depressant coverage of the naturally floating gangue and consequently higher recovery of these species.

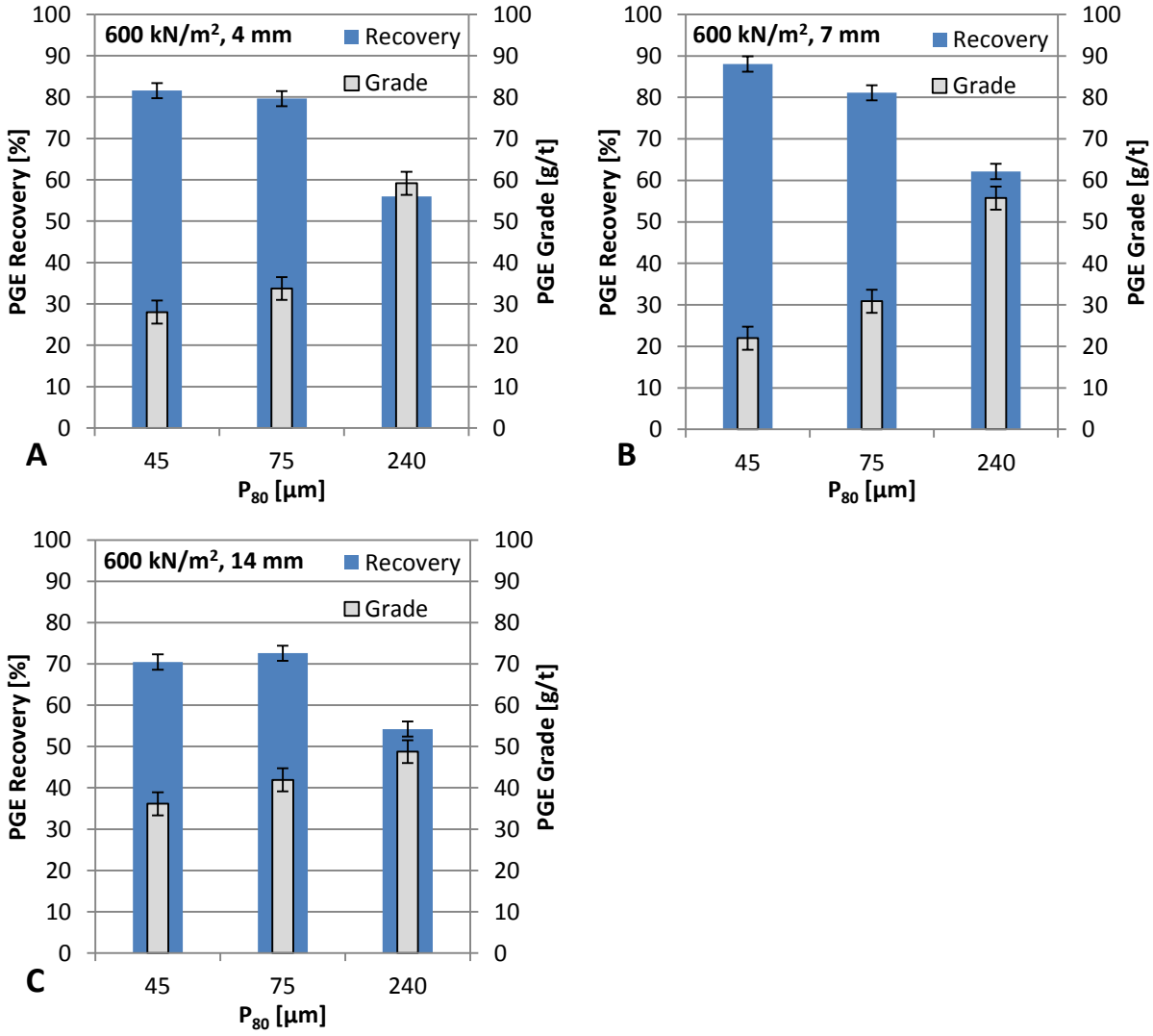

Figure 5-26: Normalised 3E PGE (Pt, Pd, Au) cumulative grade and recovery plots for batch flotation tests performed on VRM products, illustrating the variation with product size for grinding pressure of 600 kN/m² and dam ring heights of 4 mm [A], 7 mm [B] and 14 mm [C].

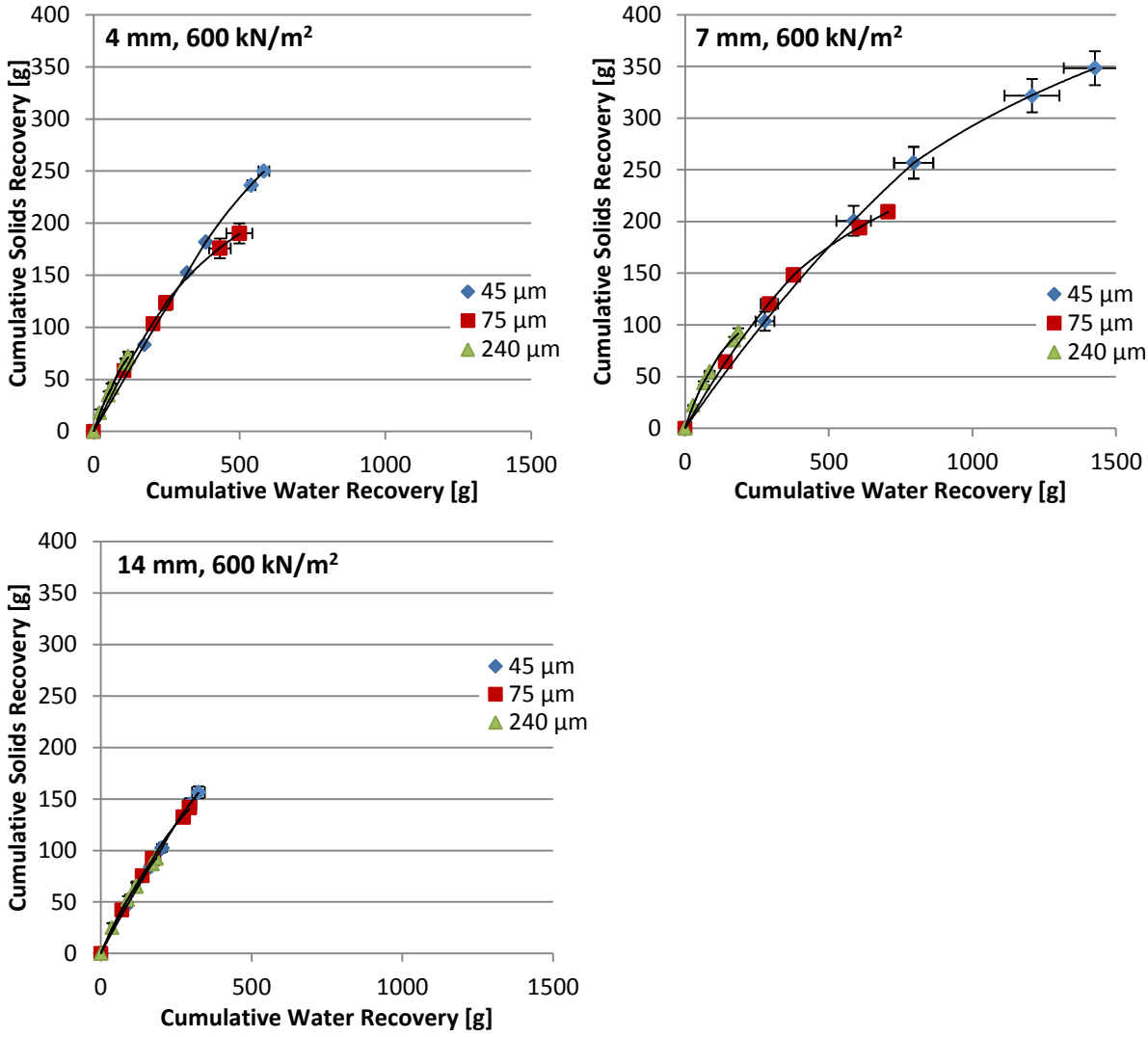

Figure 5-27: Cumulative solids - water recovery plots for batch flotation tests performed on VRM products, illustrating the variation with product size for grinding pressure of 600 kN/m² and dam ring heights of 4, 7 and 14 mm.

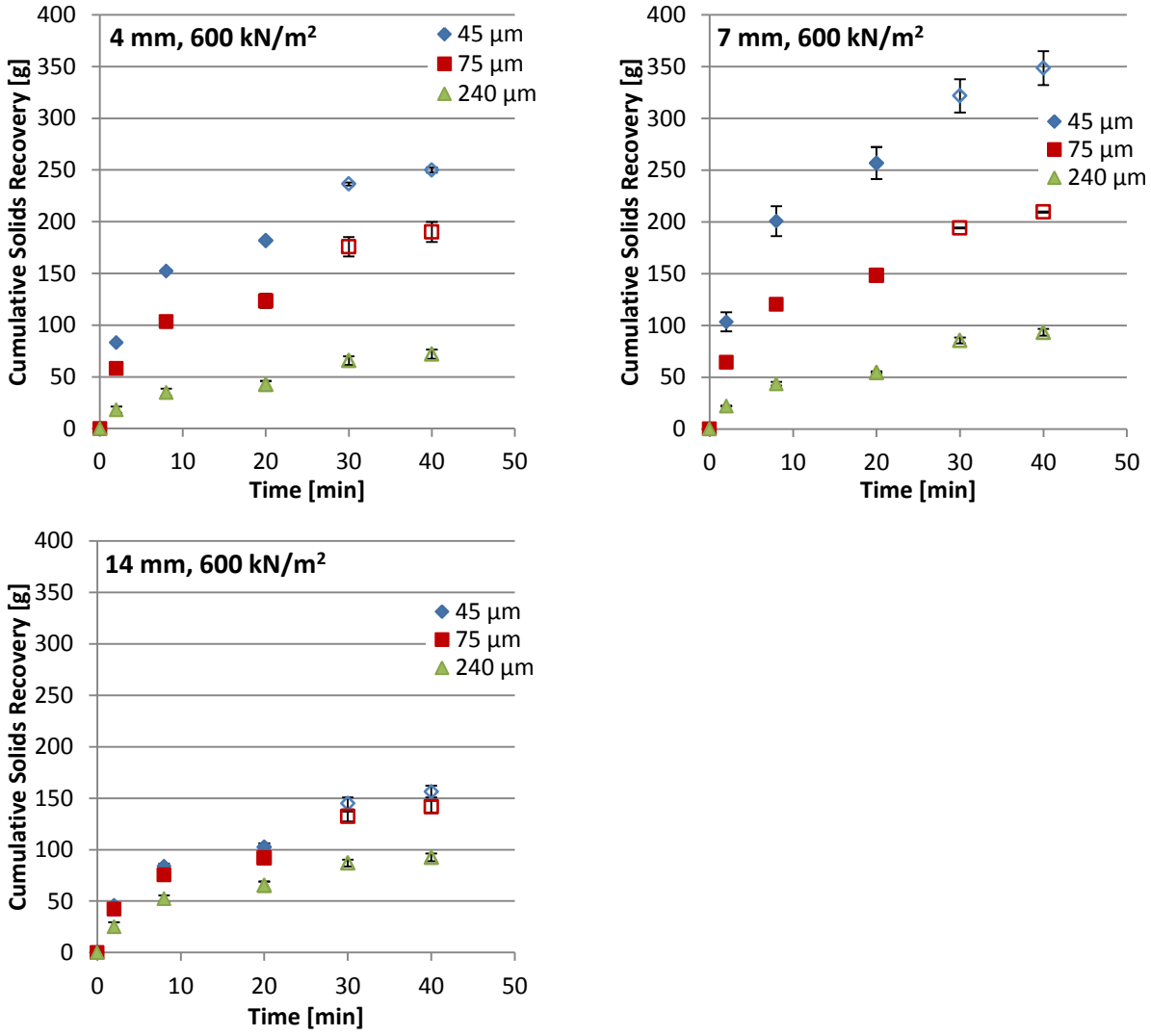

Figure 5-28: Cumulative solids recovery with time for batch flotation tests performed on VRM products, illustrating the variation with product size for grinding pressure of 600 kN/m² and dam ring heights of 4, 7 and 14 mm.

Individual platinum, palladium and gold recoveries are plotted in Figure 5-29. The precious metal recoveries are generally observed to be greater as the fineness of the grind increases, matching the increase in valuable mineral liberation reported in Section 5.4. However, for the grinding product generated with a 14 mm dam ring, the product of P_{80} 45 µm yielded a lower palladium recovery than the product of P_{80} 75 µm. The deviation does not correspond to an observed variation in mineralogy and is the reason for the lower combined 3E PGE recovery observed in Figure 5-26 [C].

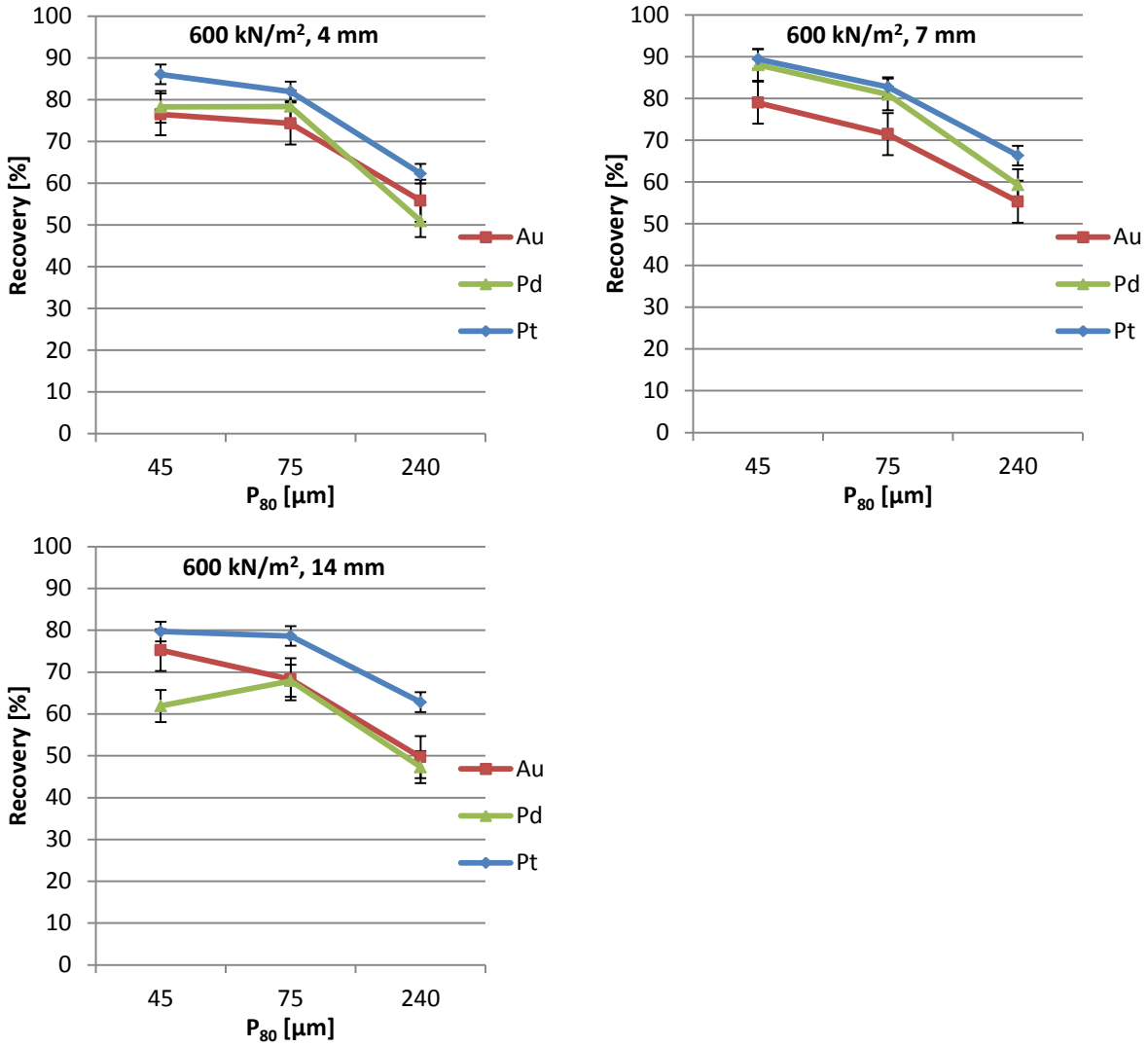

Figure 5-29: Platinum, palladium and gold recovery plots for batch flotation tests performed on VRM products, illustrating the variation with product size for grinding pressure of 600 kN/m² and dam ring heights of 4, 7 and 14 mm.

The copper and nickel recoveries for different dam ring heights at a grinding pressure of 600 kN/m² are plotted in Figure 5-30. Base metal cumulative grade and recovery plots are shown in Figure 9-25 in Appendix VII. The copper recoveries increase as the grind becomes finer for all dam ring heights. The nickel recoveries vary with target grind but are generally higher at the 75 µm grind target. There is a consistent increase when reducing the grinding product size from P_{80} 240 to 75 µm, however when reducing the grinding product size to a P_{80} of 45 µm, the effect on recoveries differ. The highest nickel recovery for a product prepared with a dam ring height of 7 mm was at the target grind of 45 µm. However for dam ring heights of 4 and 14 mm, nickel recovery for a grinding product of P_{80} 45 µm was lower than that for a P_{80} of 75 µm. The response in nickel recoveries is similar to what was observed for palladium in Figure 5-29. The correlation between palladium recovery and nickel recoveries is expected in Platreef ore where significant amounts of palladium are found in solid solution in pentlandite, the dominant nickel

sulphide mineral (Hutchinson and McDonald, 2005; Junge et al., 2014; Smith et al., 2014). In Figure 5-30 the overall nickel recoveries are lower than copper recoveries for all conditions. The lower nickel recoveries are due in part to some nickel in the ore being associated with some of the silicate gangue material, which is unrecoverable by flotation (Cramer, 2001; Wiese et al., 2006). Lower nickel recoveries may also be linked with the oxidation of the pentlandite mineral surfaces causing a decrease in flotation kinetics and recovery (Corin et al., 2013; Kelebek and Nanthakumar, 2007; Mishra et al., 2013; Peng et al., 2011).

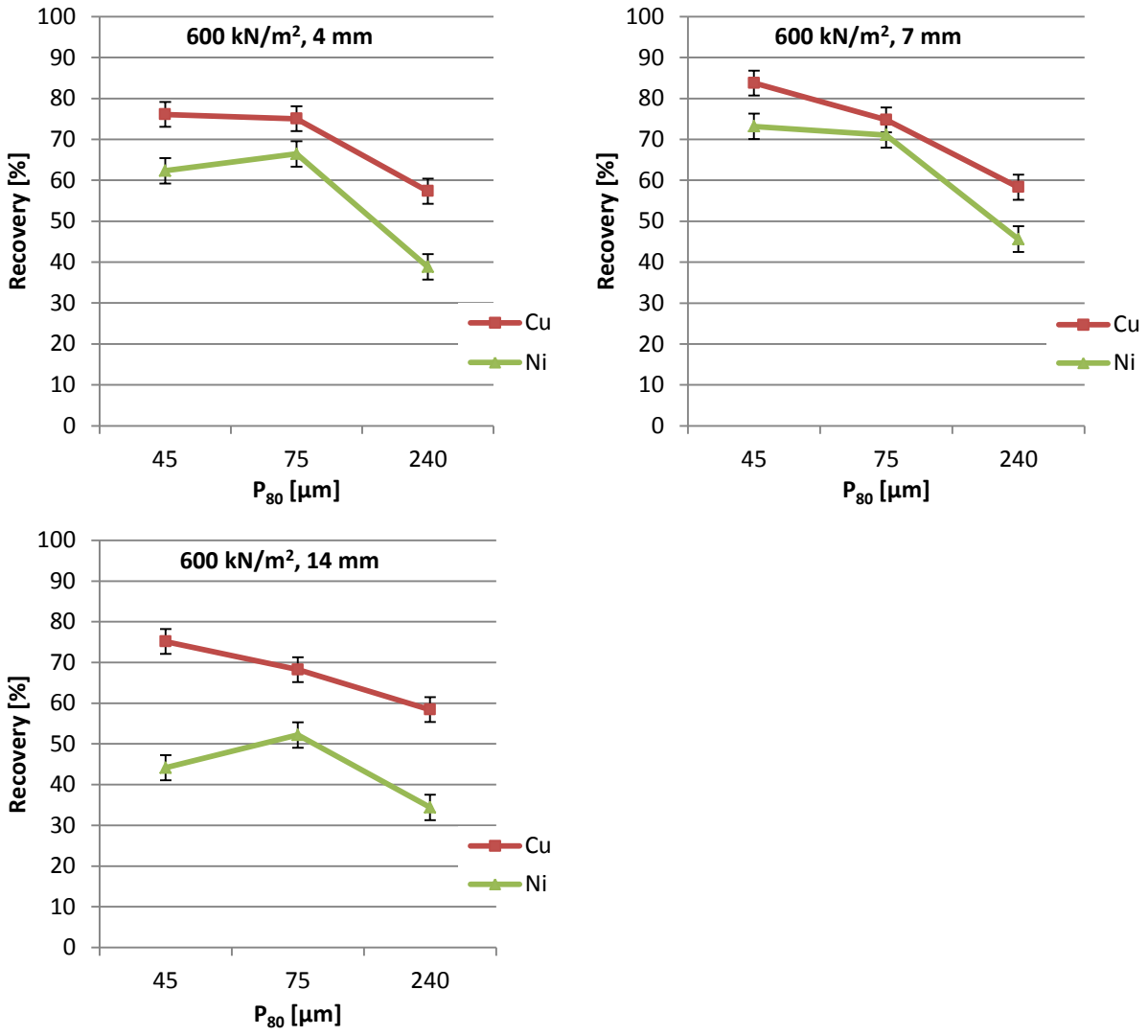

Figure 5-30: Copper and nickel recovery plots for batch flotation tests performed on VRM products, illustrating the variation with product size for grinding pressure of 600 kN/m² and dam ring heights of 4, 7 and 14 mm.

Grinding Pressure

This section focuses on the flotation response to operating the vertical roller mill at different grinding pressures. The assessment considers the variation in copper and nickel recoveries, cumulative solids - water recoveries and 3E PGE grades and recoveries. Figure 5-31 shows the

cumulative 3E PGE recoveries and grades for vertical roller mill grinding products generated at different grinding pressure. Figure 5-32 displays the individual platinum, palladium and gold recoveries and Figure 5-33 the copper and nickel recoveries. Base metal cumulative grade and recovery plots are shown in Figure 9-26 in Appendix VII. The solids - water recoveries for the flotation tests are presented in Figure 5-34. The flotation testing favoured the target grind - dam ring height configurations considered typical for vertical roller mill operation, with higher dam ring heights used when generating a finer product and lower dam ring heights used for coarser products.

The data presented in Figure 5-31 for a dam ring height of 7 mm and P_{80} of 75 µm, showed a 4% difference in 3E PGE recovery for products generated at 600 and 1000 kN/m^2 grinding pressures. For a dam ring height of 14 mm and P_{80} of 45 µm there was a 9% difference in 3E PGE recovery and for a dam ring height of 4 mm and P_{80} of 240 µm, the difference was 3%. While not all of these individual differences are significant, across the full data set there is a trend of increased grinding pressure in the vertical roller mill resulting in lower cumulative 3E PGE recoveries and higher 3E PGE grades. ANOVA statistical analysis of the 3E PGE grade and recovery data with regards to grinding pressure confirmed the significance of the trends, with F and p values of 12.715 and 0.002 for 3E PGE grade and 24.293 and <0.001 for 3E PGE recovery. To put the trend in recovery in perspective, a 2% increase in PGE recovery for the Mogalakwena Platinum Mine in 2018, would have equated to additional production of 28 000 PGM ounces, an increase in $33 million in sales revenue and ~7% increase in earnings before interest and tax, assuming no change in operating costs (Anglo American Platinum Limited, 2018). The individual platinum and palladium recoveries displayed in Figure 5-32 match the cumulative 3E PGE recovery trend, decreasing as grinding pressure increases. For gold however, the effect of grinding pressure on recovery was not found to be significant. Nickel and copper recoveries in Figure 5-33 show a decrease with an increase in grinding pressure for all dam ring height and target grind combinations. The solids and water recoveries decrease with an increase in grinding pressure for all dam ring height and target grind configurations. The decrease in solids recoveries with grinding pressure, matches the trends for 3E PGE and base metal recoveries. Solids - water recovery plots for the other dam ring height and target grind combinations and other supporting data can be found in Figure 9-16 and Figure 9-17 in Appendix VI.

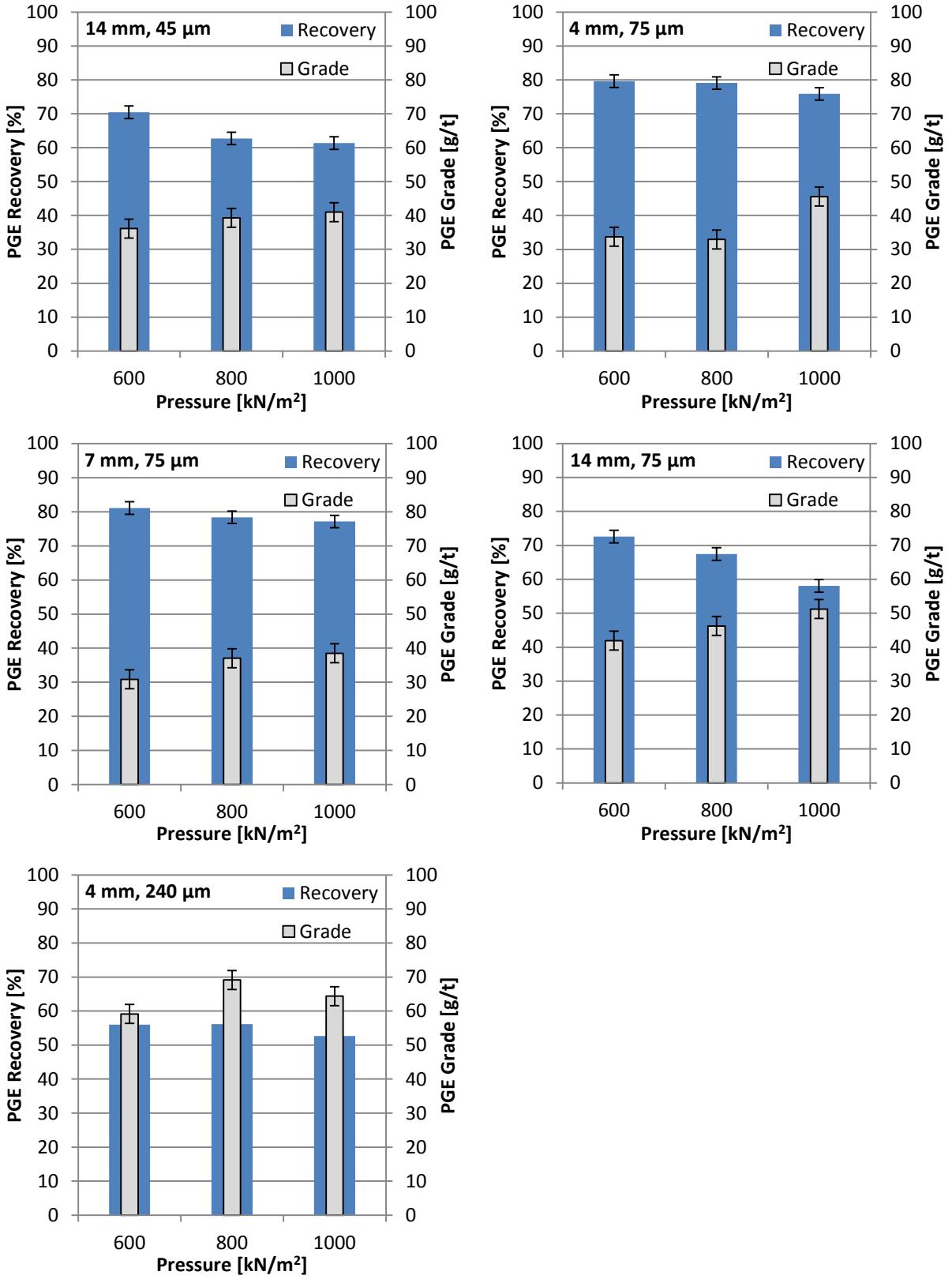

Figure 5-31: Normalised 3E PGE (Pt, Pd, Au) cumulative grade and recovery plots for batch flotation tests performed on VRM products, illustrating the variation with grinding pressure for product size and dam ring heights of 45 µm & 14 mm, 75 µm & 4 mm, 75 µm & 7 mm, 75 µm & 14 mm and 240 µm & 4 mm.

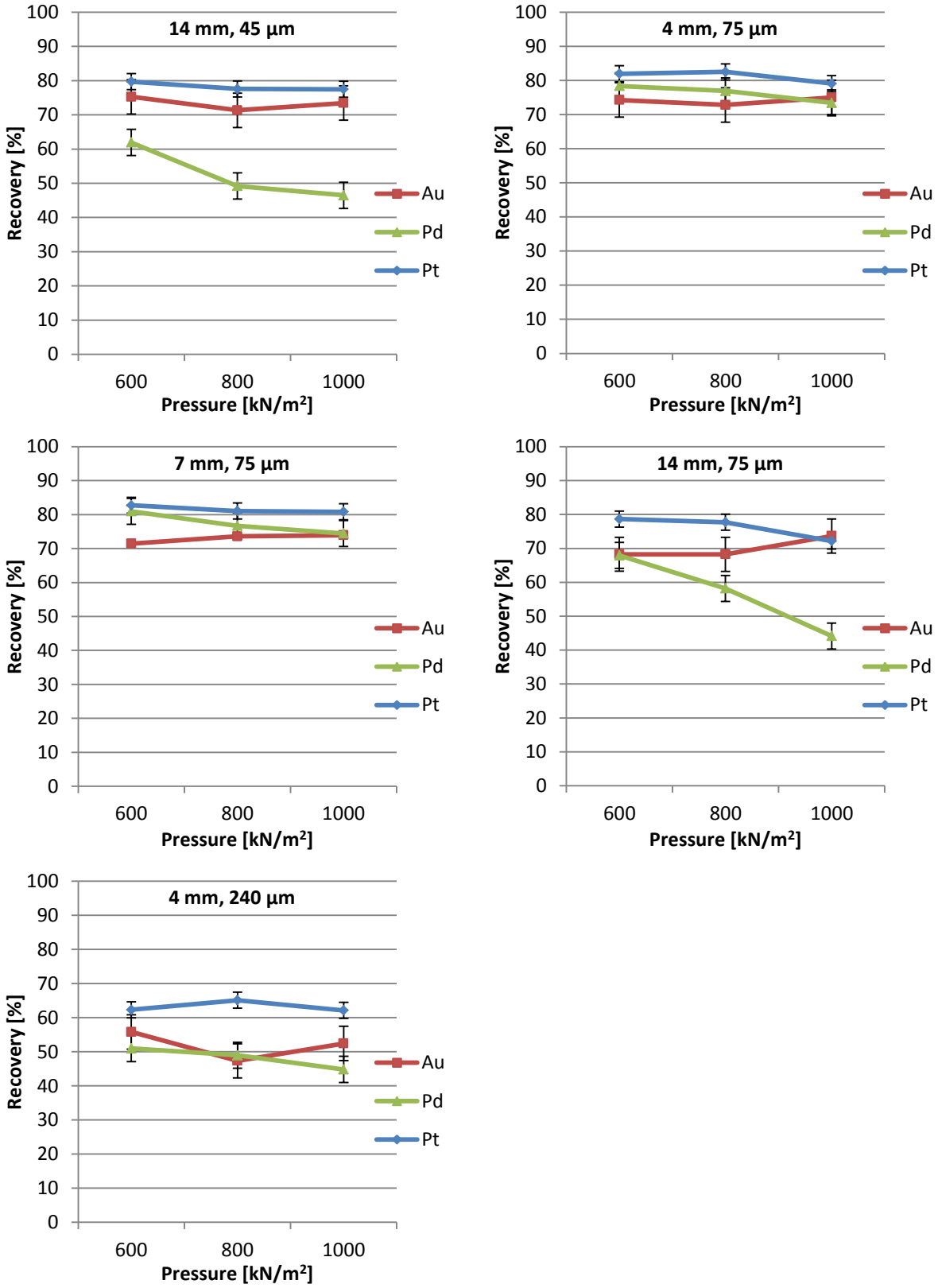

Figure 5-32: Platinum, palladium and gold recovery plots for batch flotation tests performed on VRM products, illustrating the variation with grinding pressure for product size and dam ring heights of 45 µm & 14 mm, 75 µm & 4 mm, 75 µm & 7 mm, 75 µm & 14 mm and 240 µm & 4 mm.

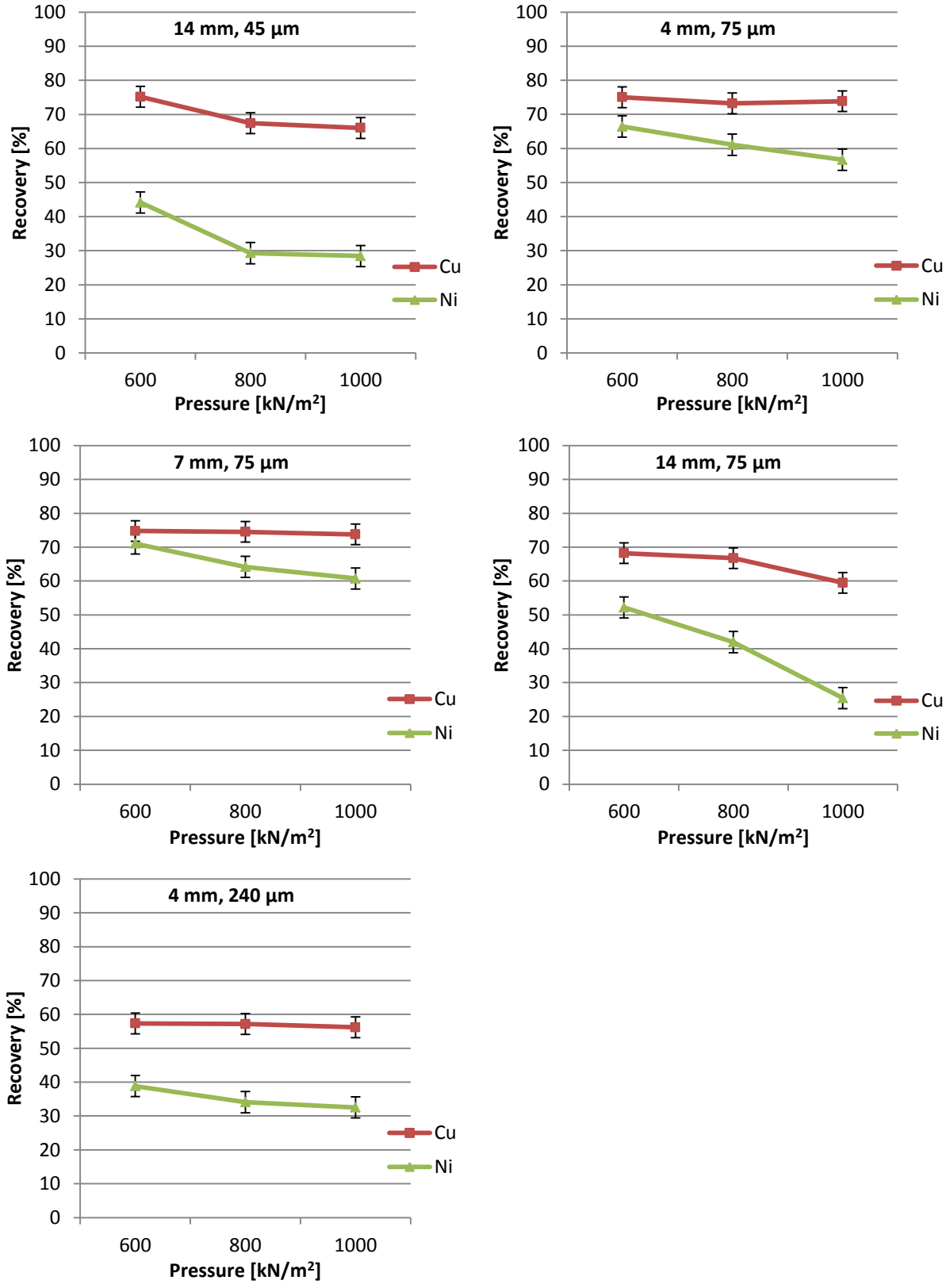

Figure 5-33: Copper and nickel recovery plots for batch flotation tests performed on VRM products, illustrating the variation with grinding pressure for product size and dam ring heights of 45 µm & 14 mm, 75 µm & 4 mm, 75 µm & 7 mm, 75 µm & 14 mm and 240 µm & 4 mm.

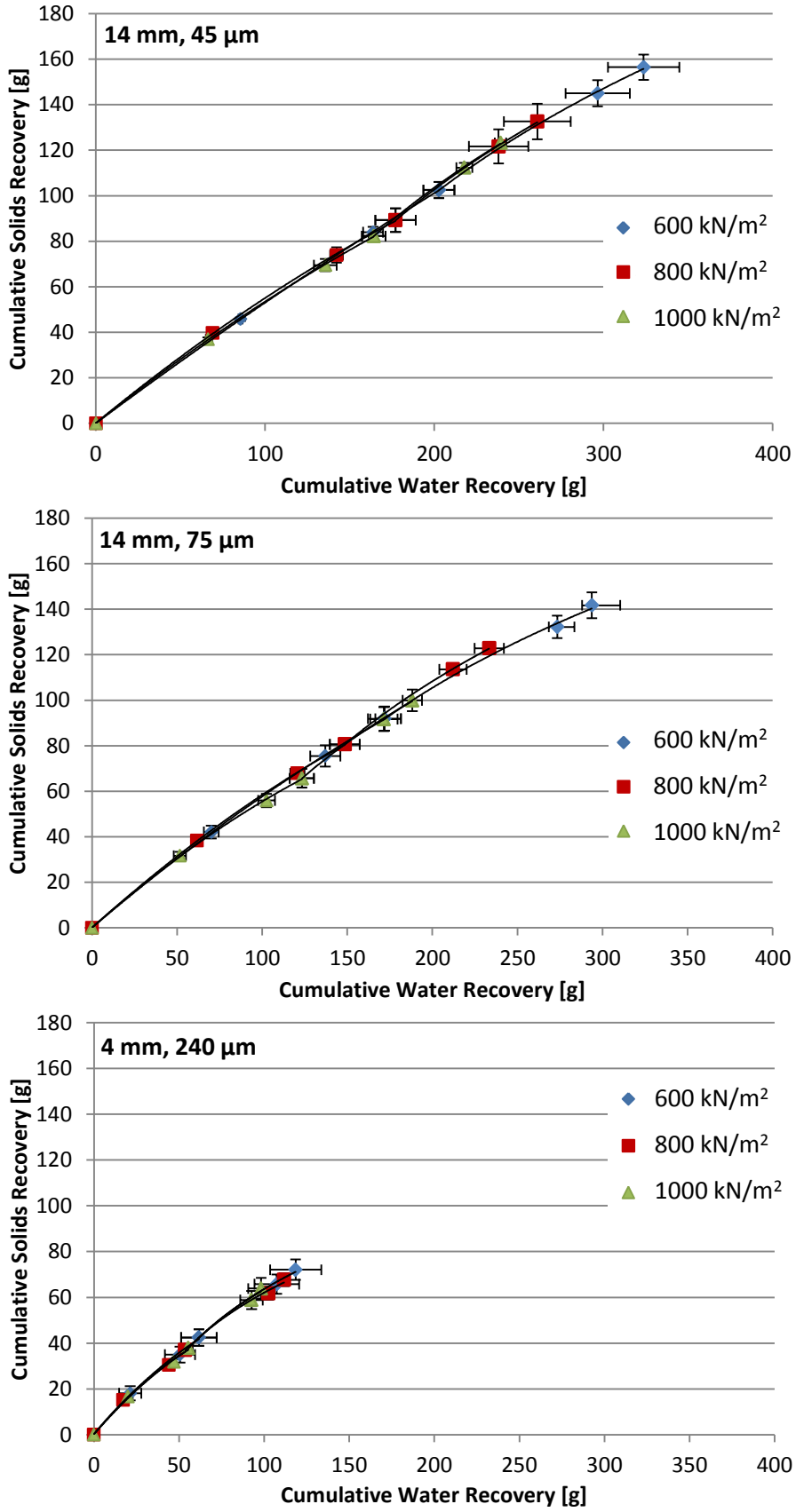

Figure 5-34: Cumulative solids - water recovery plots for batch flotation tests performed on VRM products, illustrating the variation with grinding pressure for product sizes and dam ring heights of 45 µm & 14 mm, 75 µm & 14 mm and 240 µm & 4 mm.

A variation in platinum group mineral and base metal sulphide liberation profiles with changes in grinding pressure may explain the differences in 3E PGE and base metal recoveries. It is recommended that mineralogical analysis be carried out on VRM products generated at different grinding pressures to assess if the observed changes are due to differences in the liberation profiles. One difference that was observed as the grinding pressure increased was an increase in the proportion of fine material in the grinding product (Figure 5-2). A shift in the particle size distribution is expected to affect flotation performance (Ata, 2012; Feng and Aldrich, 1999; Runge et al., 2013; Trahar, 1981; Wang et al., 2015), however typically increasing the proportion of fine material in a flotation cell would correspond to an increase in the rate of entrainment, which would reflect as greater solids recoveries. This however is opposite to what occurred in this test work, as an increased amount of fine material generated at higher grinding pressures, corresponded to lower solids and water recoveries. The lower water recoveries at higher grinding pressures indicates there is a decrease in froth stability (Wiese et al., 2011, 2006). Froth stability is affected by both the composition (hydrophobicity) and size of particles in the froth (Achaye, 2017; Feng and Aldrich, 1999). Particle composition in the froth would change if the size distribution of the grinding product/floatation feed was to change, because the recovery of particles to the froth is affected by particle size (Wang et al., 2015). Wiese et al. (2011) stated that an increase in concentration of strongly hydrophobic particles in the froth can lead to froth destabilisation, with particles bridging the froth films and allowing the rapid movement of the bubble interface over the particle surface, resulting in bubble collapse. During the batch flotation testing this was seen as a difference in bubble size and solids loading of the bubbles, illustrated in Figure 5-35. In the work by Achaye (2017), particles of high hydrophobicity (contact angle of >68°) led to a lower froth stability and lower solids recoveries. A destabilisation of the froth through an increased concentration of strongly hydrophobic particle, brought about by a higher transfer of fine particles to the froth could explain the lower valuable mineral recoveries at higher grinding pressures. A further contributor to the destabilisation of the froth could be the liberation and deportment of naturally floating gangue species but these were not assessed in this study. Bulk mineralogical analysis should be considered for future test work involving grinding pressure in the vertical roller mill.

Figure 5-35: Pictures indicating the differences in the froth collected during the first minute of flotation for products of P_{80} 75 µm generated at a dam ring height of 7 mm at grinding pressures of 600 [A] and 800 [B] kN/m².

Dam Ring Height

In this section the flotation response of vertical roller mill products generated with different dam ring heights is assessed in terms of copper and nickel recoveries, cumulative solids - water recoveries and 3E PGE grades and recoveries. The 3E PGE recovery results are shown in Figure 5-36. Comminution products generated at a 14 mm dam ring height consistently yielded lower 3E PGE recoveries than those produced at 4 and 7 mm dam ring heights. The difference in flotation recovery between the 4 and 7 mm dam ring heights varied within a 5% range, the recovery for the 7 mm dam ring height grinding product was however generally higher. Figure 5-36 also shows the 3E PGE grades, which were higher when the 3E PGE recoveries were lower. The individual platinum, palladium and gold recoveries shown in Figure 5-37 match the trends observed for cumulative 3E PGE recoveries. In addition, the magnitude of the response to changing dam ring height was greater for palladium recovery than gold or platinum.

Mineralogical analysis was carried out on grinding products generated at different dam ring heights, for a target grind of 75 μm at a grinding pressure of 600 kN/m^2, corresponding to the top right plot in Figure 5-36. There were some differences in the PGM mineralogy and grain size distribution, as well as a small decrease in liberation as the dam ring height increased. These variations may account for some of the differences in recovery. The effective PGM liberation (liberated PGMs and PGMs associated with liberated BMS) however was seen to increase with an increase in dam ring height. This does not fit with the observed recovery profile, indicating another flotation factor is also affecting the recovery of valuable minerals.

Figure 5-38 shows the copper and nickel flotation recoveries. Base metal cumulative grade and recovery plots are shown in Figure 9-27 in Appendix VII. The base metal recoveries are similar to the individual PGE and cumulative 3E PGE recoveries, with recoveries lowest for products generated at a 14 mm dam ring height. Recoveries of copper are consistently higher than those for nickel, which is due to the presence of non-recoverable nickel hosted in the gangue material (Cramer, 2001; Wiese et al., 2006). Base metal sulphide liberation data from bulk mineral analysis indicated that the proportion of locked BMS is slightly greater when operating with higher dam rings (Figure 5-20). This could contribute to the lower BMS recoveries observed at higher dam ring heights but does not explain the similar recoveries at the intermediate and lowest dam ring heights.

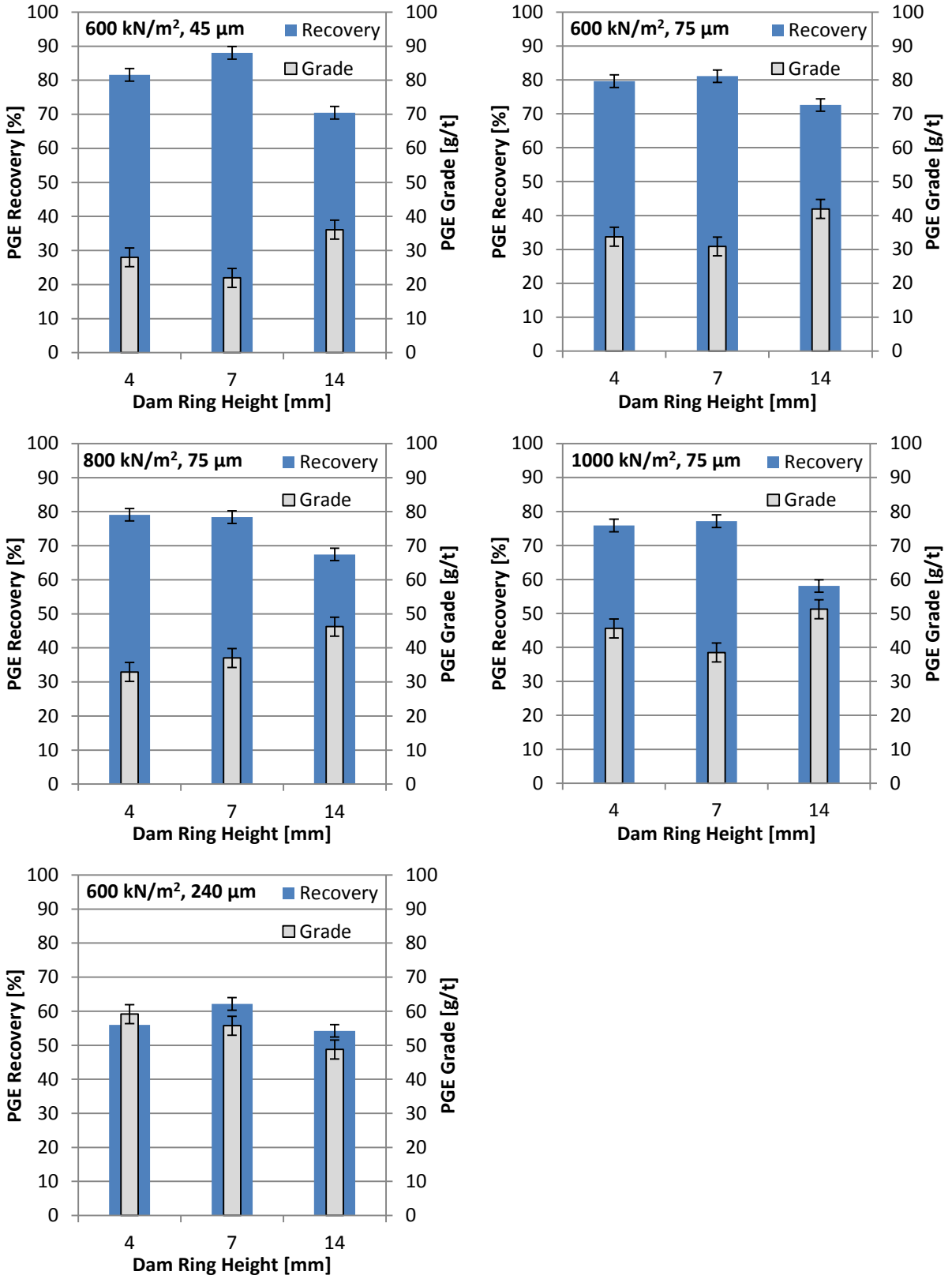

Figure 5-36: Normalised 3E PGE (Pt, Pd, Au) cumulative grade and recovery plots for batch flotation tests performed on VRM products, illustrating the variation with dam ring height for product size and grinding pressures of 45 µm & 600 kN/m², 75 µm & 600 kN/m², 75 µm & 800 kN/m², 75 µm & 1000 kN/m² and 240 µm & 600 kN/m².

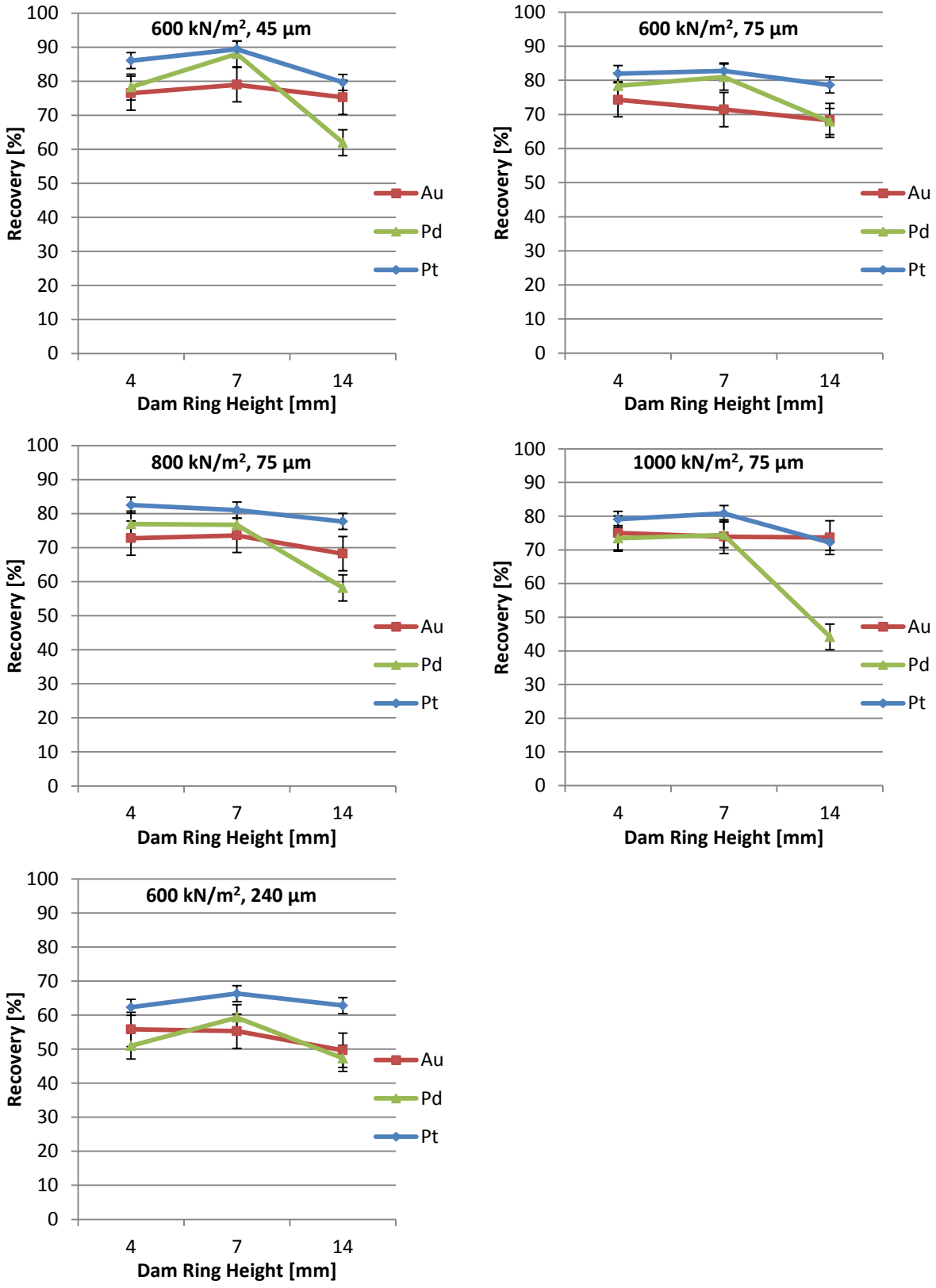

Figure 5-37: Platinum, palladium and gold recovery plots for batch flotation tests performed on VRM products, illustrating the variation with dam ring height for product size and grinding pressures of 45 µm & 600 kN/m², 75 µm & 600 kN/m², 75 µm & 800 kN/m², 75 µm & 1000 kN/m² and 240 µm & 600 kN/m².

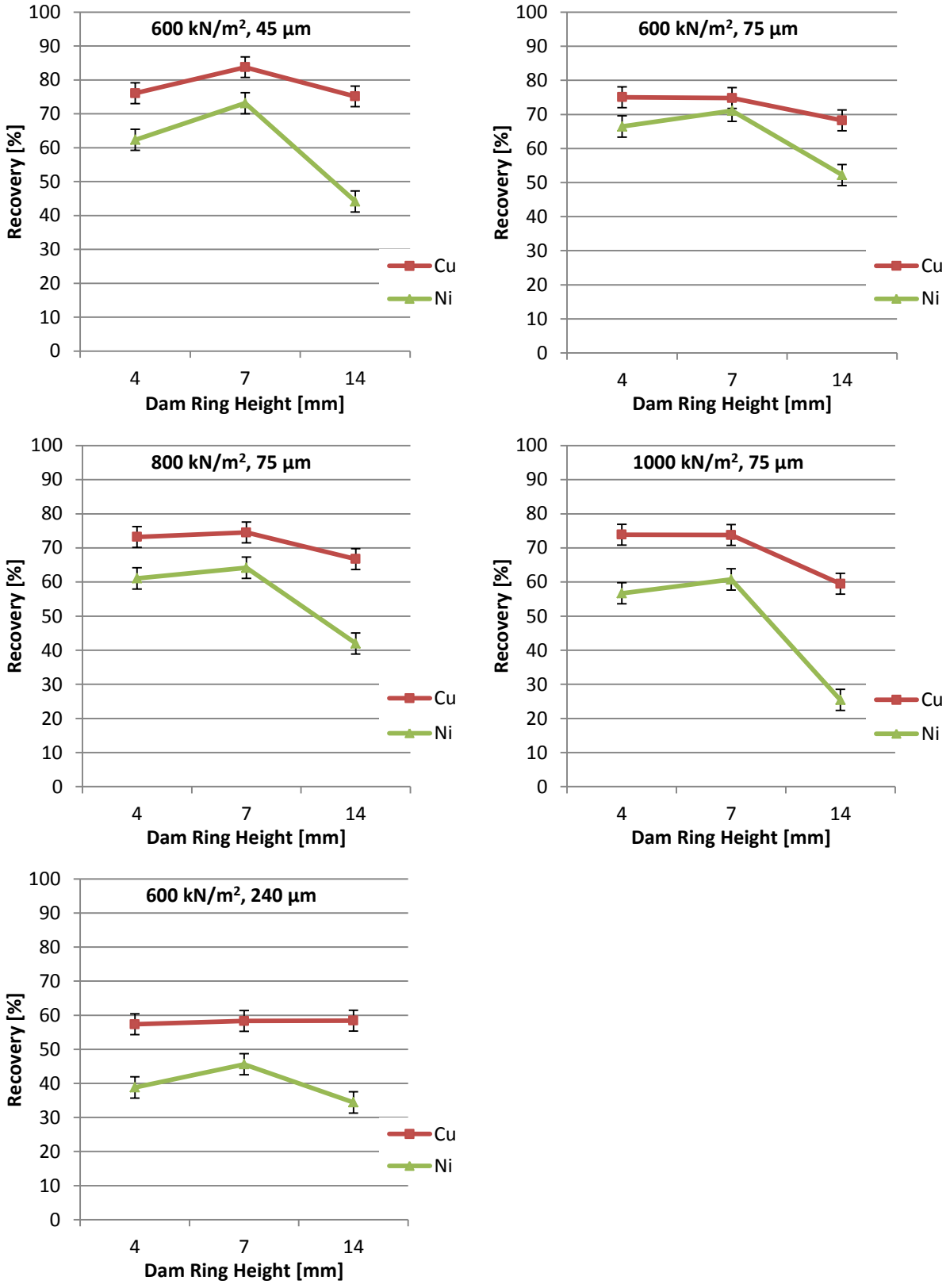

Figure 5-38: Copper and nickel recovery plots for batch flotation tests performed on VRM products, illustrating the variation with dam ring height for product size and grinding pressures of 45 µm & 600 kN/m², 75 µm & 600 kN/m², 75 µm & 800 kN/m², 75 µm & 1000 kN/m² and 240 µm & 600 kN/m².

Cumulative solids and water recoveries for varying dam ring heights at constant target grinds and grinding pressures are given in Figure 5-39. The solids and water recoveries for the 4 and 7 mm dam ring height were greater than that for the 14 mm dam ring height. This is consistent with the observations for the 3E PGE recovery profiles. Solids - water recovery plots for the other grinding pressures are given in Figure 9-18 and Figure 9-19 in Appendix VI. As with grinding pressure, the lower solids and water recoveries observed could be due to a decrease in froth stability associated with a change in product particle size distribution (Wang et al., 2015; Wiese et al., 2011, 2006). Products generated with higher dam rings had a greater proportion of fine material, similar to those prepared at higher grinding pressures which likewise had lower flotation recoveries. This variation may have led to an increase in concentration of strongly hydrophobic particles in the froth, causing increased bubble coalescence (Achaye, 2017; Wiese et al., 2011).

At higher dam ring heights there was a decrease in PGM liberation but an overall increase in amount of recoverable PGMs (Liberated PGMs + PGMs in Liberated BMS). The flotation recoveries do not correlate to the measured increase in recoverable PGMs, as recoveries should be higher for greater dam ring heights. The decrease in flotation recovery across the range of dam ring heights tested was caused by an increase in proportion of fines in the products prepared at higher dam ring heights. The deviation in flotation recovery of the 7 mm dam ring products from the expected trend is possibly due to variation in liberation of talc (Figure 5-16). Liberation of talc was appreciably lower for the 7 mm dam ring height, 600 kN/m^2 grinding pressure product for which mineralogical analysis was conducted. Talc is a strongly hydrophobic mineral and variation in its liberation would have an effect on froth stability.

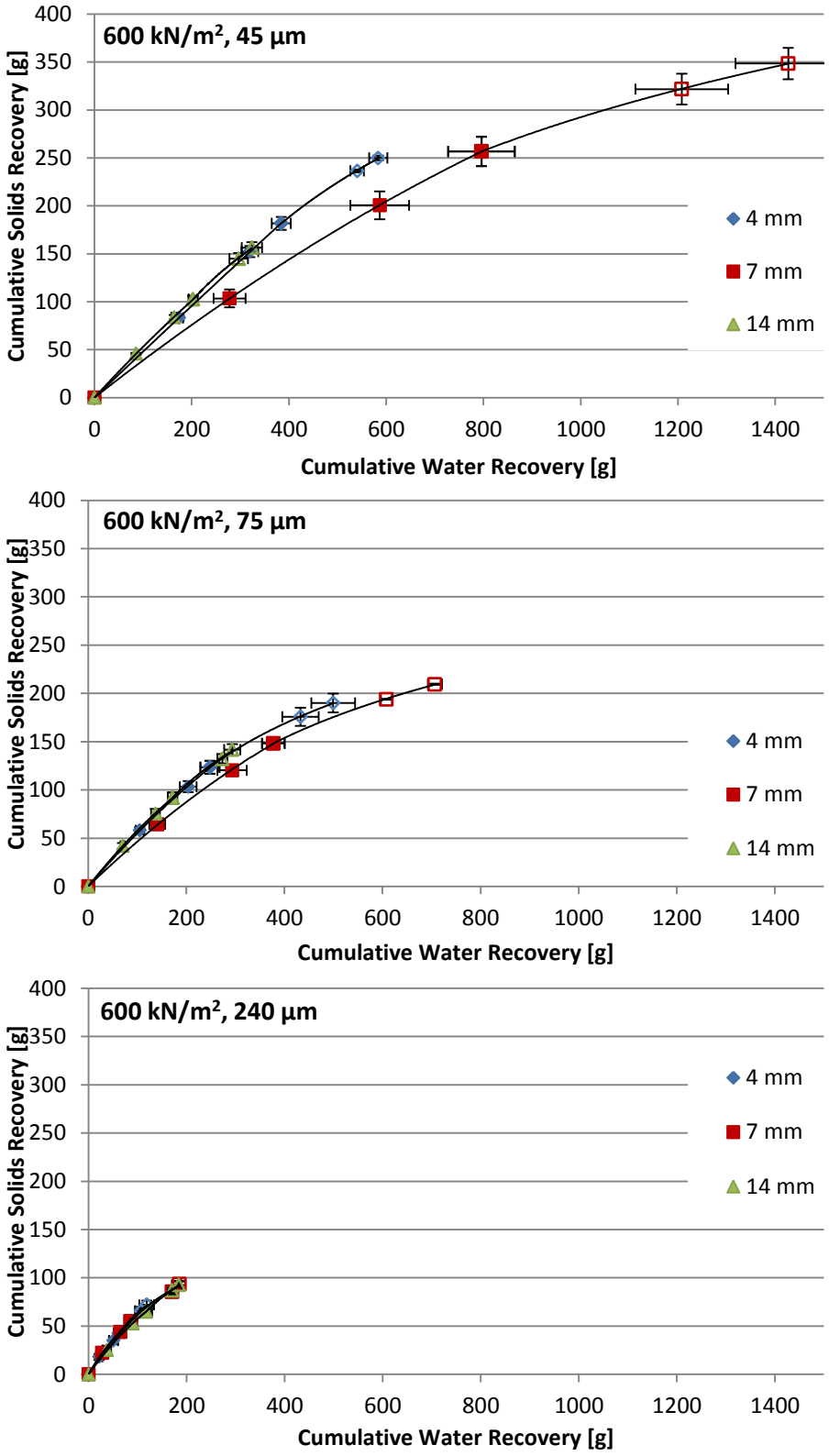

Figure 5-39: Cumulative solids - water recovery plots for batch flotation tests performed on VRM products, illustrating the variation with dam ring height for product sizes of 45, 75 and 240 µm at a grinding pressures 600kN/m².

5.6 Summary

In this chapter comminution results for a vertical roller mill operated in airflow mode were analysed alongside mineralogical and batch flotation data generated for the grinding products. The test work was conducted with the three variables: grinding pressure, dam ring height and target grind size. The product size was manipulated through the rotational speed of the built-in dynamic air classifier, with P_{80} values of 45, 75 and 240 μm targeted. Mineralogical analysis of grinding products at the three different target sizes showed that grinding finer yielded a material with more liberated platinum group minerals, base metal sulphides and other gangue species. This increase in liberation was seen as an increase in 3E PGE and Cu, Ni flotation recoveries.

Operating the vertical roller mill at higher grinding pressures generated products with a less steep particle size distribution, which had a greater proportion of fine material for an equivalent P_{80}. Throughput for the VRM increased as grinding pressure was increased. The specific grinding energy of the system did not vary with changes in grinding pressure and although the mechanical energy usage was greater for higher grinding pressures it was offset by increases in VRM throughput. The 3E PGE and Cu, Ni flotation recoveries were greater for products generated at lower grinding pressures. This was due to a decrease in froth stability for products generated at higher grinding pressures caused by the change in fines content of the comminution product.

Operating at increased dam ring heights generated products which had a less steep particle size distribution, which had a greater proportion of fine material for an equivalent P_{80}. The response of throughput to changes in dam ring height was observed to vary and results indicated that there is an optimum dam ring height where throughput can be maximised for each target grind. For higher dam rings, the mechanical energy usage was greater and this translated to an increase in the specific grinding energy. Mineralogical analysis of products generated at different dam ring heights showed differences in the liberation and deportment profiles of the PGMs, BMS and naturally floating gangue species. Products generated at a 14 mm dam ring height had lower 3E PGE and Cu, Ni flotation recoveries than those generated at a 4 and 7 mm dam ring height. The variation in flotation recovery results did not follow the trend in effective PGM liberation but could be explained by changes in froth stability, resulting from variation in particle size distribution and liberation of naturally floating gangue species.

Chapter 6

MEANS OF CLASSIFICATION

This chapter considers the performance of the vertical roller mill operated with different classification methods. The comparison is made in terms of comminution performance, focusing on throughput, specific energy and product quality, and downstream flotation response. Results for the vertical roller mill operated in closed circuit with different classifiers are compared and assessed alongside batch tumbling mill grinding and flotation data.

6.1 Circuits and Particle Size Distributions

The vertical roller mill was operated in closed circuit with three different classification devices. The dynamic air classifier, which is used for the standard 'airflow mode' operation, was used as a baseline. Two external classification methods were employed with the vertical roller mill operated in 'overflow mode', where there is no suspension of particles within the unit and material falling from the grinding table is transported mechanically to the classifier. The external classification devices used were a vibrating screen with a 500 μm aperture sieve, and a hybrid dynamic/static air classifier. Testing on each circuit was carried out for various grinding pressures and target product sizes (P_{80}), with their effect on steady state mill performance recorded. The finest grind was adjusted to target P_{80} of 60 μm from the original 45 μm, as this corresponded better to the grind targeted on the industrial plant (P_{90} of 75 μm). Over the test period, classifier products from each circuit were collected for use in flotation test work and at the end of test periods, internal stream samples were collected for the two overflow circuits. For the external screening circuit, the screen oversize was collected, and for the external air classification, the classifier feed was collected. Sampling internal streams was not possible in airflow mode as not only is sampling internal streams difficult for the enclosed vertical roller mill, but sampling disrupts circulation of material between the grinding and classification components, destabilising the system. Table 6-1 contains an outline of the testing carried out

with the different classification setups and shows the grinding pressure and target P_{80} for each test. The original internal air classification tests were replicated at the same time as the external air classification tests, in order to generate fresh material and eliminate potential aging effects in the classification flotation test work. Figure 6-1 shows a comparison of the particle distributions for the classification experiments and original airflow tests. A close match was observed for the 60 and 75 µm P_{80} target; however, there was a notable deviation for the 240 µm P_{80} target grind. The product particle size distribution for 240 µm target grind in the classification test work was coarser than the corresponding particle size distribution for the original airflows tests. The coarser grind in the repeated test work corresponded with an increased throughput.

Table 6-1: Outline of the vertical roller mill test work conducted with different methods of classification.

Classification	**Product P_{80}** [µm]	**Grinding Pressure** [kN/m²]
External Screening	240	600 1000
Internal Air Classification	60 75 240	600 600 600
External Air Classification	60 75 240	600 600 600

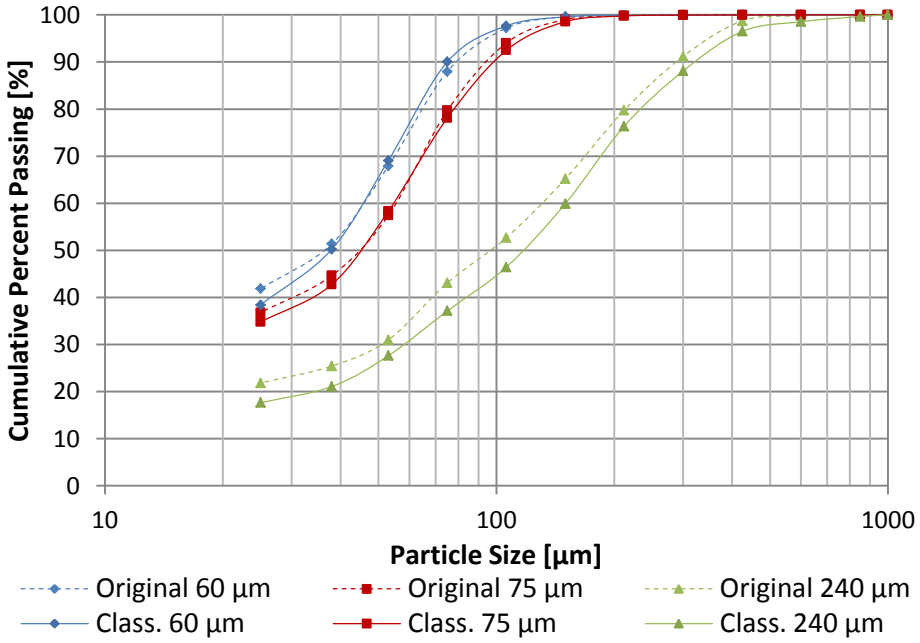

Figure 6-1: Particle size distributions for the original airflow and classification focused tests with different target products sizes (P_{80}: 60, 75 and 240 µm) produced at a grinding pressure of 600 kN/m² and dam ring height of 7 mm.

Mass Balancing

During the external classification tests the mass flow of grinding product was measured as the mass transported to the classifier. Together with the circuit throughput, and a product and an internal stream PSD, the streams around the classifier were able to be balanced. Stream summaries for the VRM operated in closed circuit with an external screen are presented in Table 6-2 and the corresponding particle size distributions are plotted in Figure 6-2. The VRM in the external screening circuit was operated at two different grinding pressures, targeting a product of P_{80} 240 µm. Both the grinding and overall circuit products generated at the 1000 kN/m² grinding pressure had slightly lower P_{80} values than those produced at the 600 kN/m² grinding pressure. The production rate of the VRM circuit with the external screen was greater at the higher grinding pressure, and circulation of material between the grinding and classification components was higher.

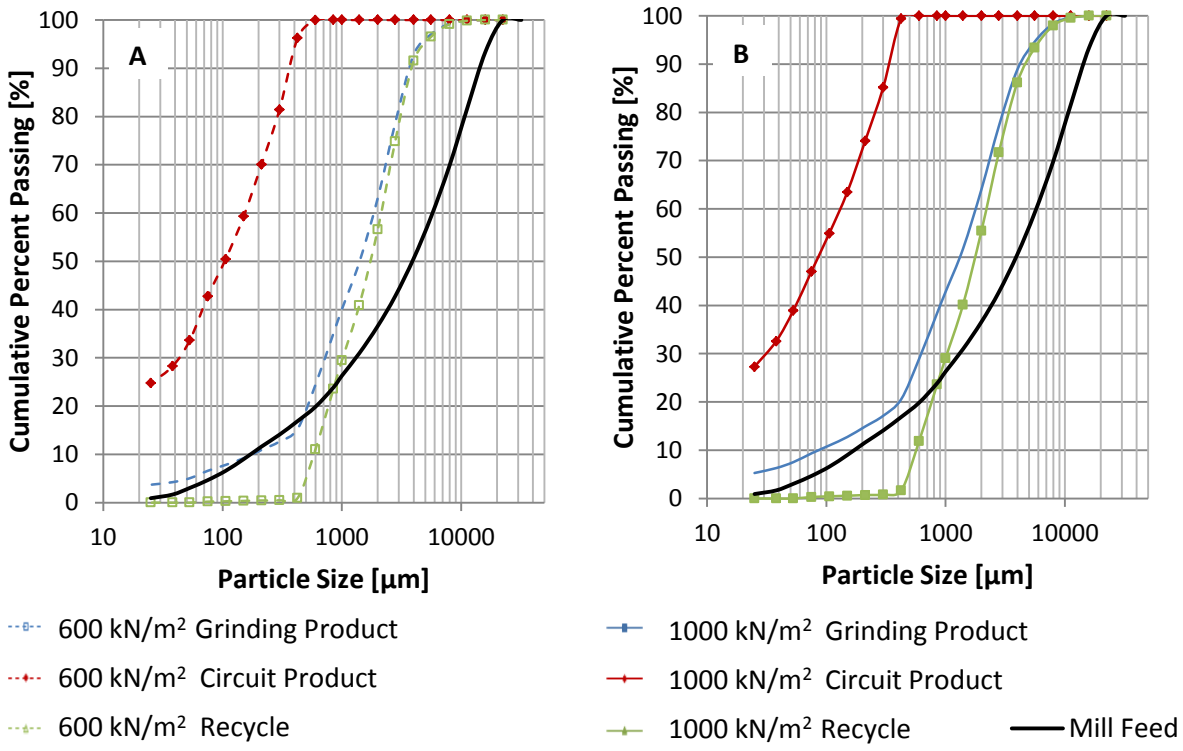

Figure 6-2: Measured and mass balanced (Grinding Product) particle size distributions for the external screening vertical roller mill circuit at grinding pressures of 600 [A] and 1000 [B] kN/m² with target product sizes of P_{80} 240 µm.

Table 6-2: Experimental and balanced data for the external screening vertical roller mill circuit at grinding pressures of 600 and 1000 kN/m² for a 240 µm P_{80} target grind.

Stream	Grinding Pressure [kN/m²]	Flow Rate [kg/h]		P_{80} [µm]		Sub 75 µm [%]	
		Exp	Bal	Exp	Bal	Exp	Bal
Grinding Product	600	2260	-	-	2900	-	6.6
Recycle		-	1920	3200	-	0.2	-
Circuit Product		340	-	289	-	47.7	-
Grinding Product	1000	3095	-	-	3090	-	9.4
Recycle		-	2495	3490	-	0.3	-
Circuit Product		600	-	259	-	47.0	-

The stream summaries and particle size distributions for the VRM operated in closed circuit with external air classification, are given in Table 6-3 and Figure 6-3. The test work with the external hybrid air classifier was conducted with the vertical roller mill operated only at a grinding pressure of 600 kN/m². The testing was however conducted to target three different product sizes. Products of P_{80} 60, 75 and 240 µm were targeted by manipulating air flow rate to the external classifier and the rotor speed in the dynamic portion of the classifier. For the external air classifier, the experimental and balanced P_{80} values of the classifier streams were greater for the coarser target grinds. Additionally, the proportion of material less than 75 µm in the classifier streams was lower for coarser target grinds.

Table 6-3: Experimental and balanced data for the external air classifier vertical roller mill circuit for the different target products sizes (P_{80}: 60, 75 and 240 µm) at a 600 kN/m² grinding pressure.

Stream	Target P_{80} [µm]	Flow Rate [kg/h]		P_{80} [µm]		Sub 75 µm [%]	
		Exp	Bal	Exp	Bal	Exp	Bal
Grinding Product	60	2975	-	1020	-	4.0	-
Recycle		-	2845	-	1070	-	0.3
Circuit Product		130	-	70	-	84.1	-
Grinding Product	75	5940	-	1200	1190	1.8	2.6
Recycle		-	5740	-	1220	-	0
Circuit Product		200	-	78	-	79.8	-
Grinding Product	240	4080	-	1400	1370	0.9	4.6
Recycle		-	3750	-	1450	-	0
Circuit Product		330	-	162	-	57.1	-

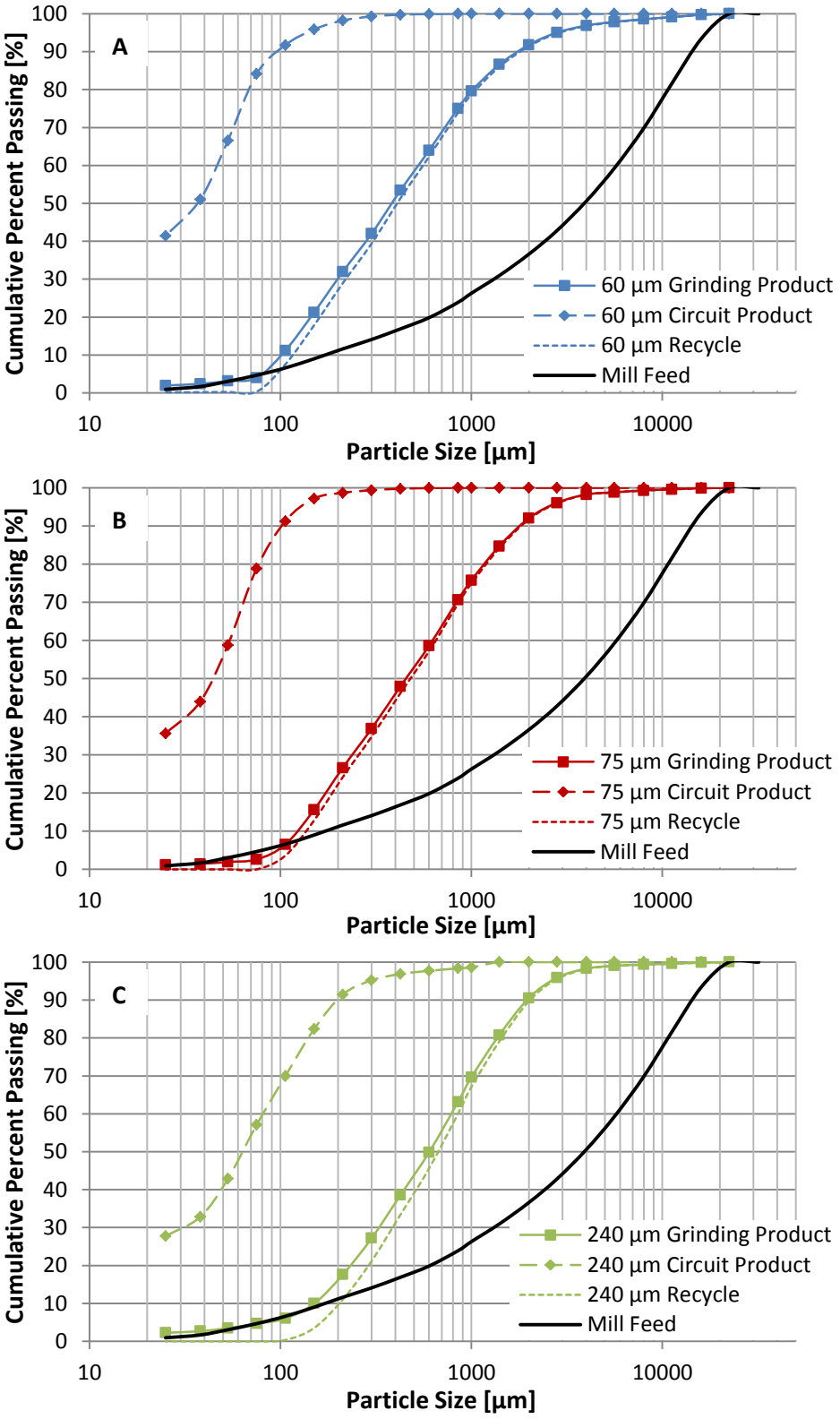

Figure 6-3: Measured and mass balanced (Recycle) particle size distributions for the external air classifier vertical roller mill circuit for the different target products sizes (P_{80}: 60 [A], 75 [B] and 240 [C] µm) at a 600 kN/m² grinding pressure.

For the internal air classification circuit, because no internal streams could be sampled, a mass balance for the system could only be conducted with some assumptions and estimations. The

circuit is shown in Figure 6-4 and the balance was conducted for the overall classification occurring in the system. This overall classification includes both the classification occurring in the mill body, as suspended larger/denser particles fall back to the grinding table, and that occurring in the dynamic air classifier. The balance around classification is under specified, with only the product PSD and flow rate known. In order to obtain an approximation for the system, addition information was included. The classifier feed particle size distribution was approximated by the measured PSDs obtained during VRM operation with external air classification and circulating load of 1100, 2000 and 2200% were assumed based on the ranges obtained for the external air classifier. The stream summaries and particle size distribution approximations for the internal air classification circuit for the three targeted grinds are shown in Table 6-4 and Figure 6-5. As with external air classification circuit, the particle size distributions for internal air classification are coarser for the coarser target grinds.

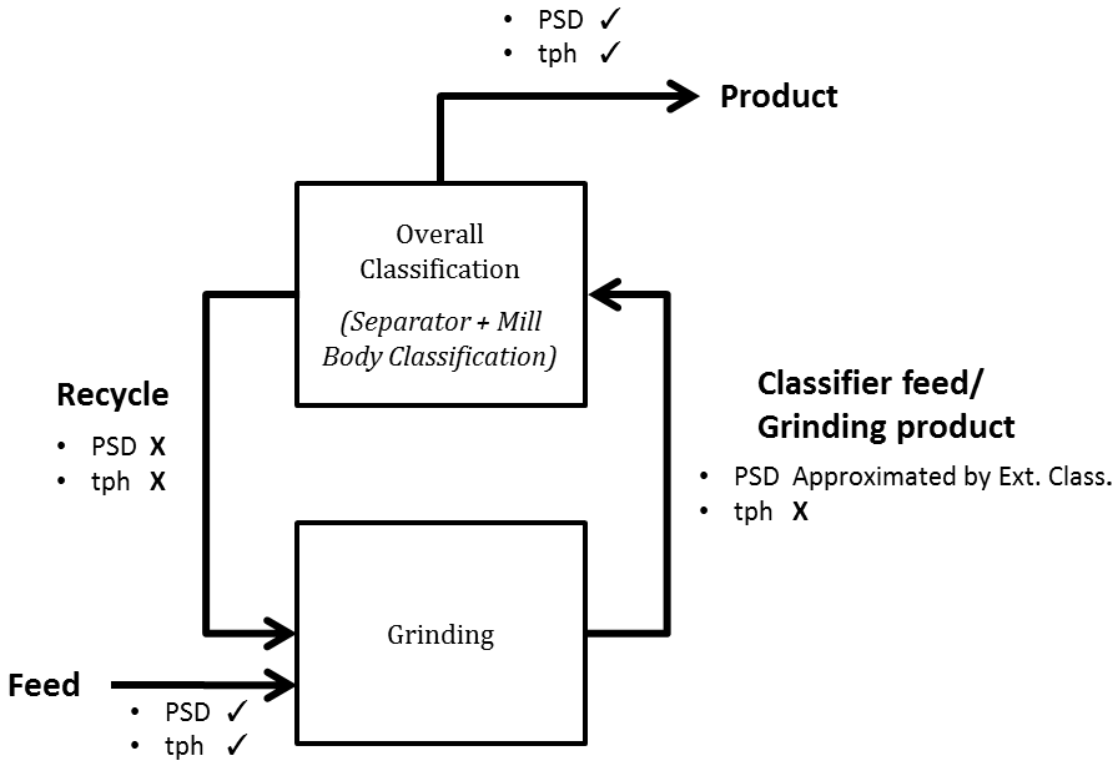

Figure 6-4: Representation of the internal air classification circuit describing the measured data and approximation used to balance the system.

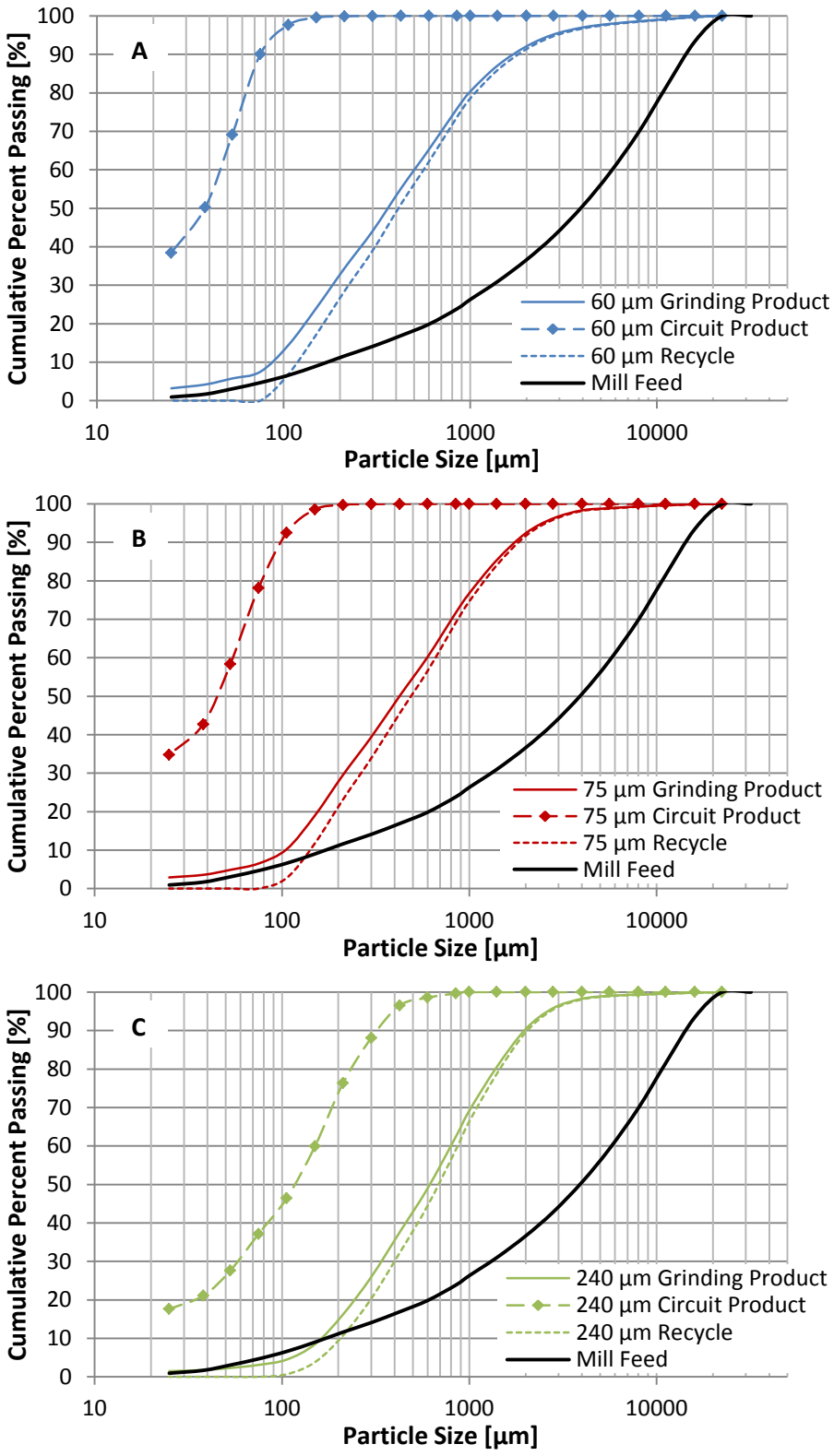

Figure 6-5: Measured (Circuit Product) and estimated mass balanced particle size distributions for the internal air classifier vertical roller mill circuit for the different target products sizes (P_{80}: 60 [A], 75 [B] and 240 [C] µm).

Table 6-4: Experimental and balanced date for the internal air classifier vertical roller mill circuit for the different target products sizes (P_{80}: 60, 75 and 240 µm).

Stream	Target P_{80} [µm]	Flow Rate [kg/h]		P_{80} [µm]		Sub 75 µm [%]	
		Exp	Bal	Exp	Bal	Exp	Bal
Grinding Product	60	-	6260	*1020**	1010	*4.0**	3.9
Recycle		-	5988	-	1070	-	0
Circuit Product		270	-	64	-	90.1	-
Grinding Product	75	-	6937	*1200**	1180	*1.8**	3.7
Recycle		-	6607	-	1220	-	0
Circuit Product		330	-	79	-	78.1	-
Grinding Product	240	-	9165	*1400**	1380	*0.9**	3.1
Recycle		-	8400	-	1470	-	0
Circuit Product		765	-	239	-	37.1	-

**The classifier feed PSD was approximated by that for external air classification*

Partition Curves

The balanced classification data was used to generate partition curves for the three classification setups. The partition curves for the two external screening experiments are plotted in Figure 6-6, and the calculated and fitted classification parameters for the system are shown in Table 6-5. The bypass of the screens in the 600 and 1000 kN/m² grind pressure tests were 2 and 4% respectively. This low carryover of fines to the oversize indicates the screen was not overloaded during the testing. The cut sizes for the 600 and 1000 kN/m² grinding pressures tested with the external screen were 423 and 414 µm, and the corrected cut sizes were marginally coarser at 424 and 417 µm respectively.

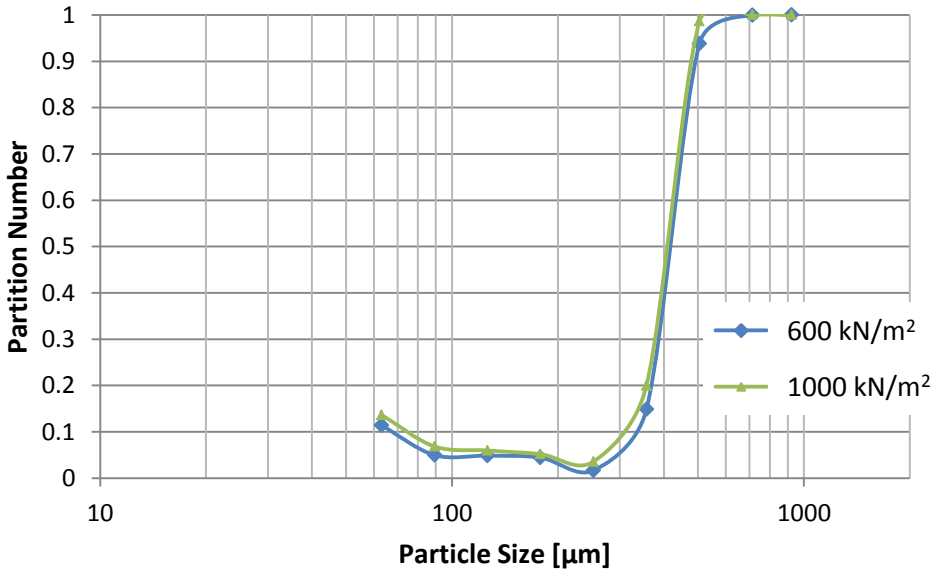

Figure 6-6: Partition curves for the external screening vertical roller mill circuit at grinding pressures of 600 and 1000 kN/m².

The partition curves for the three grinds targeted with the external air classification circuit are plotted in Figure 6-7. In the figure, a bypass is only observed for the 60 µm P_{80} grind. The absence of a bypass for the 75 and 240 µm P_{80} grinds is due to the correction of balanced classifier data. A correction to the data was required because the back-calculated PSDs for the recycle streams yielded negative values at sizes 75 µm and below. To negate this, the classifier feed PSDs were allowed to change so that the sub 75 µm fractions were constrained to zero values. For the external air classification tests shown in Figure 6-7, the sharpness of separation is observed to vary with the target grind.

The partition curves for the three target grinds with the internal air classification circuit are presented in Figure 6-8. No bypass is seen for the internal air classification partition curves and this is due to the correction applied to the sub 75 µm particle mass balance. Similar to the external air classification partition curves, the sharpness of separation for the internal air classifier is observed to vary with the target grind. Both the classifier feed PSDs and circulating loads for these curves are assumed.

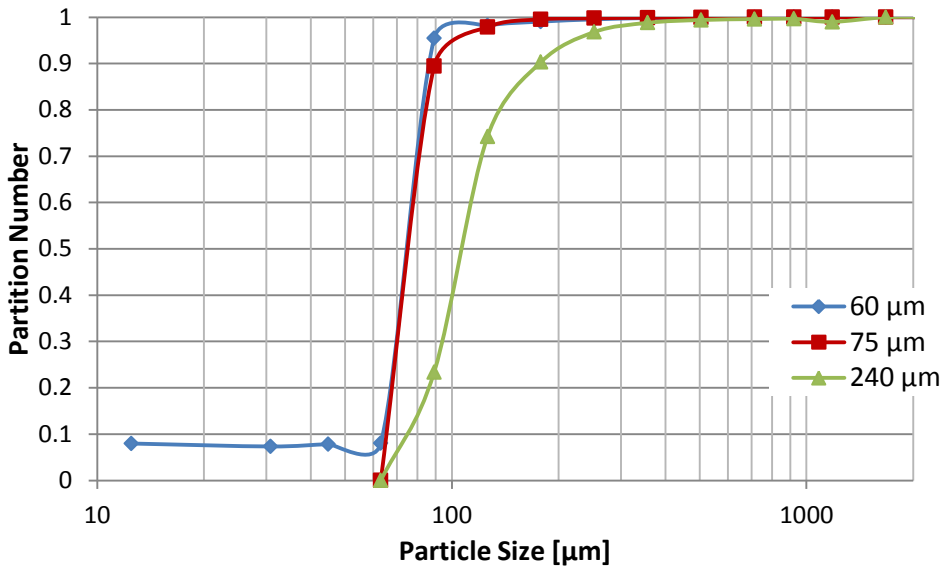

Figure 6-7: Partition curves for the external air classifier vertical roller mill circuit for the different target products sizes (P_{80}: 60, 75 and 240 µm). Mass balance corrected for the 75 and 240 µm curves.

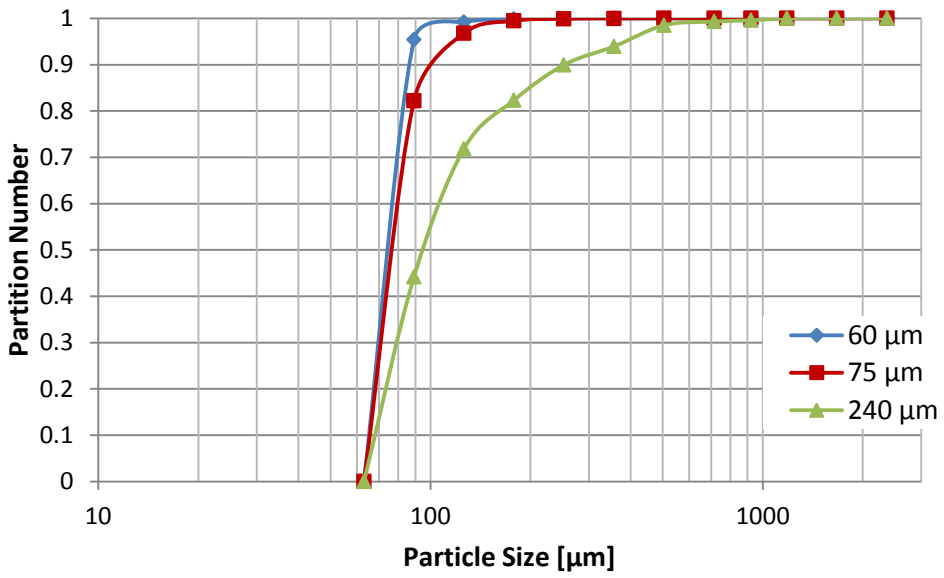

Figure 6-8: Partition curves for the internal air classifier vertical roller mill circuit for the different target products sizes (P_{80}: 60, 75 and 240 µm). Based on corrected mass balance data with the assumption of a 1100% circulating load.

The separation efficiencies (α) for the three classifier setups are displayed in Table 6-5. The separation efficiency is related to the sharpness of separation, with more ideal separations/partition curves of steeper slope having greater separation efficiencies (α). For both the internal and external air classification systems separation efficiency decreases as the target grind coarsened. The 75 µm external air classification target grind is the anomaly to this trend and related to the unusually high circulating load for this test. The separation efficiency for classification with the screen was greater than both air classifier setups at the coarse target grind. The circulating loads for three classification systems are also displayed in Table 6-5. For internal air classification, a constant circulating load was assumed for mass balancing purposes. Variation in this assumption could have large consequences on the results. The circulating load varied with target grind for the external air classifier, with the 240 µm P_{80} grind having a circulating load around half of that for the two finer target grinds. The circulating load for the screen - VRM circuit was significantly less than that for the external hybrid air classifier circuit.

Table 6-5: Calculated and fitted classification parameters for internal air classifier, external air classifier and external screening vertical roller mill circuits for the different target products sizes (P_{80}: 60, 75 and 240 µm) and grinding pressures of 600 and 1000 kN/m².

Classifier	**Internal Dynamic Air**			**Screen**		**External Hybrid Air**		
Grinding Pressure [kN/m²]	600	600	600	**600**	**1000**	600	600	600
Target P_{80} [µm]	**60**	**75**	**240**	240	240	**60**	**75**	**240**
Throughput [kg/h]	272	330	764	340	699	129	197	332
Circulating load	*2200%*	*2000%*	*1100%*	560%	420%	2200%	2900%	1100%
D_{50c} [µm]	77	79	97	424	417	77	78	108
α	21.6	14.3	5.2	12.7	13.0	15.0	16.8	6.9

Circuit Product Comparison

The comminution product is highly dependent on classification in the circuit. The product is not only affected by the operation of the classification device, but also by type of classification device utilised. Because of this it is important to compare the products generated by the different circuits tested.

A comparison of particle size distributions for the vertical roller mill products of target P_{80} 240 µm generated with external screening, external hybrid air classification and internal air classification is given in Figure 6-9. The screening and internal air classification products have comparable P_{50} of 104 and 97 µm at a 600 kN/m² grinding pressure and a P_{50} of 87 and 77 µm at a grinding pressure of 1000 kN/m². The P_{80} values of the product do however differ, with the external screening product having greater P_{80} values. The coarse target grind (P_{80} of 240 µm) product produced by the external air classifier is significantly finer than both the internal air classification and external screening products. The measured P_{80} for the external air classifier product was only 162 µm and the P_{50} was 64 µm.

The external air classification and internal air classification product particle size distributions for the 60 and 75 µm target grinds are plotted together in Figure 6-10. The product particle size distributions for the internal and external air classification tests with a 75 µm P_{80} target grind were closely comparable. For the finest target grind (P_{80} of 60 µm) the P_{50} values for the internal and external air classification were the same (37 µm), however the product particle size distribution for the internal air classifier was steeper than that for external air classification and the P_{80} values differed (63 and 70 µm respectively). The variation in the product size, liberation

profile, generated by the different VRM - classification circuits will influence the downstream recovery process.

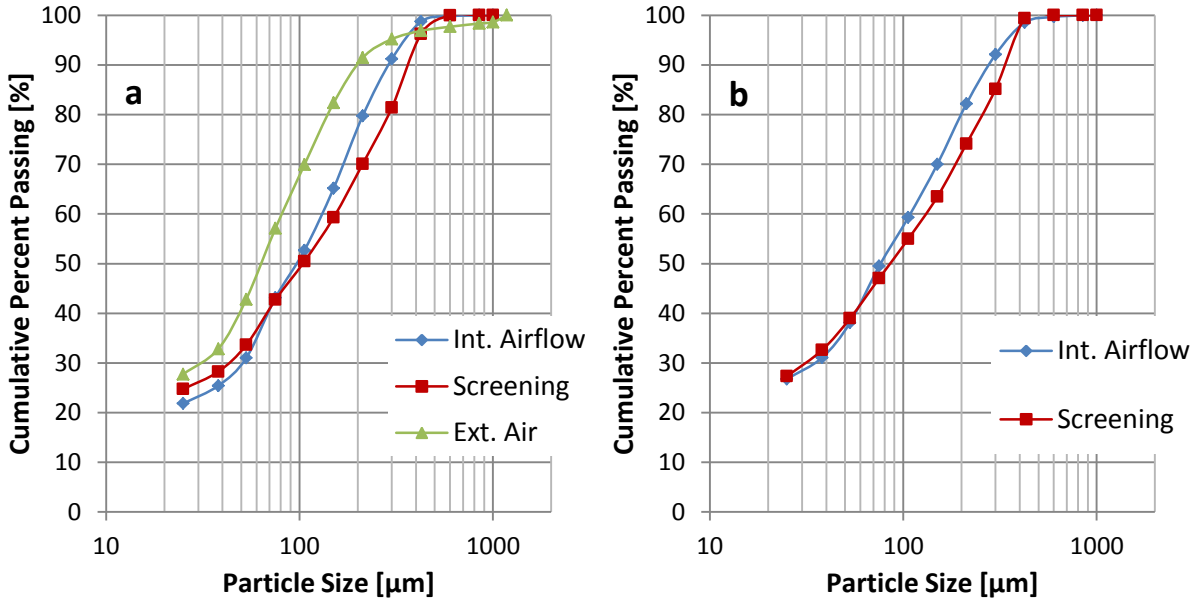

Figure 6-9: Particle size distributions for external screening, external air classification and internal air classification products generated at a grinding pressure of 600 [a] and 1000 [b] kN/m² with a target P_{80} of 240 µm.

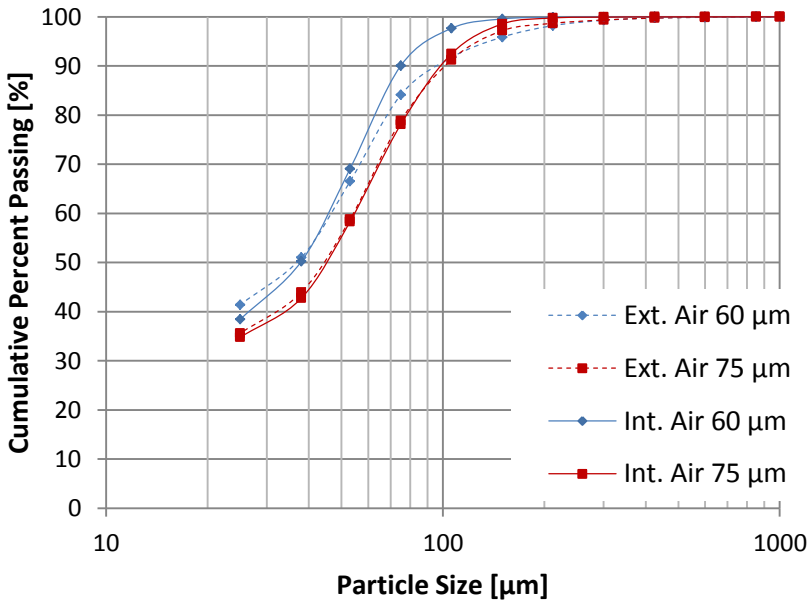

Figure 6-10: Particle size distributions for external air classification and repeated airflow tests with different target products sizes (P_{80}: 60 and 75 µm).

6.2 Grinding Parameters

The vertical roller mill setups used to perform the experiments with the three different classification devices were equipped to measure various grinding and classification parameters including; torque, power, bed height, classifier rotor speed and airflow rates. Parameters were continuously monitored and averaged for each test period and the mill throughput was obtained from the mass of classifier product accumulated during a test.

Throughput and Energy Utilisation

In both the internal and external air classification test work, the classifier rotor speed was used as the primary control to vary the product particle size. Figure 6-11 shows this data and illustrates the inverse relationship between classifier rotor speed and product P_{80}. Manipulation of classifier rotor speed not only has an effect on the product size but also throughput and the recycle of material within the system. At higher classifier rotor speeds a smaller product particle size is produced, however the rate of generation of product material decreases, as the classifier retains more material within the circuit.

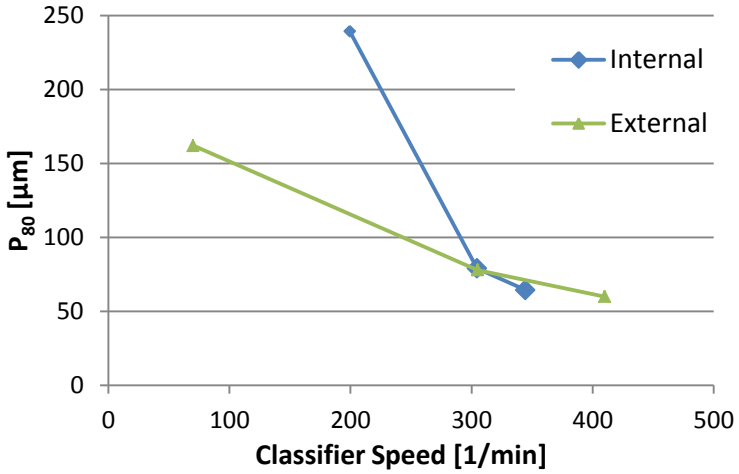

Figure 6-11: Vertical roller mill product size - classifier rotor rotational speed relationship for the internal and external air classification tests.

Throughputs for the external and internal air classification test work are plotted against product particle size in Figure 6-12. For both circuits, higher throughputs are achieved for coarser grinds. Figure 6-13 shows specific grinding energies for the vertical roller mills in the external and internal air classification circuits. The trends show that an increase in specific grinding energy is required to achieve a lower product particle size, which follows with general comminution theory.

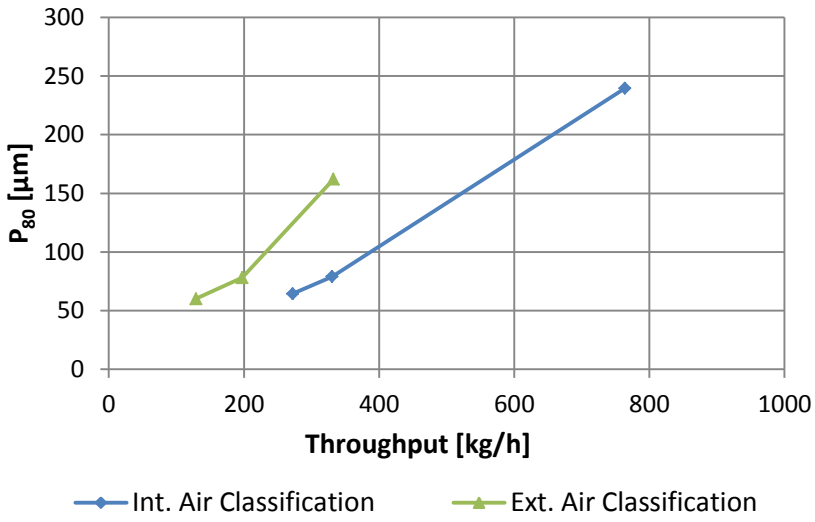

Figure 6-12: Relationship between vertical roller mill throughput and product size, distinguishing between the internal and external air classification tests.

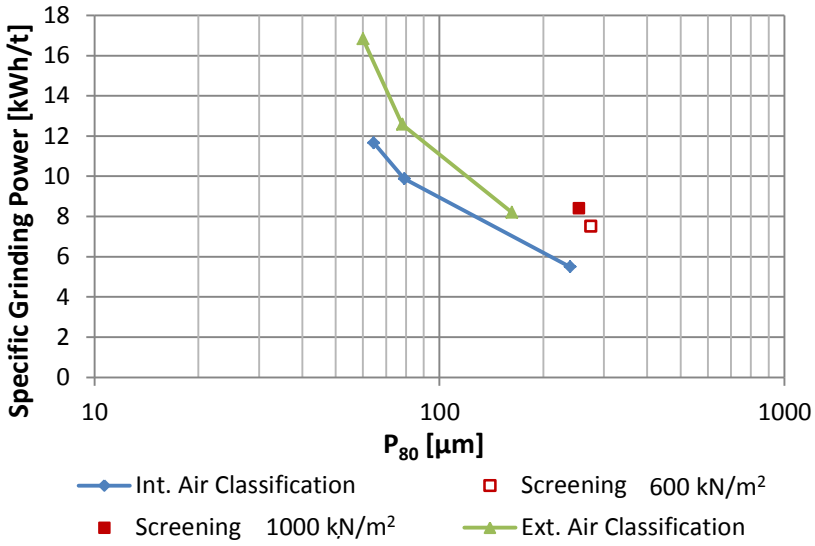

Figure 6-13: Changes in specific grinding energy for the vertical roller mill with product size, distinguishing between the screening, and internal and external air classification tests.

Figure 6-14 displays the throughput and specific grinding energy for the vertical roller mill operated in closed circuit with a vibrating screen. Higher throughput was observed at a grinding pressure of 1000 kN/m^2 compared to a grinding pressure of 600 kN/m^2. The greater throughput at the higher grinding pressure can be attributed to more energy being imparted to the material on each pass under the rollers, resulting in a finer grinding table product. This finer product, when presented to the classifier, contains more particles able to pass through the screen and be discharged as product, reducing the circulating load and allowing more fresh feed to be introduced to the system. A similar response was found for airflow test work carried out in this study as well as in the studies by Altun et al. (2016) and Reichert et al. (2014). Specific

grinding energy for the vertical roller mill in the screening circuit also varied with grinding pressure. The specific grinding energy was greater at the 1000 kN/m² grinding pressure and corresponds to an increased mechanical power (Figure 9-29 in Appendix VIII) which is not completely offset by the increase in throughput. This lower grinding efficiency at the higher grinding pressure is explained by the generation of a finer product (Figure 6-2). A bed depth comparison between the classification systems is given in Figure 9-30 in Appendix VIII.

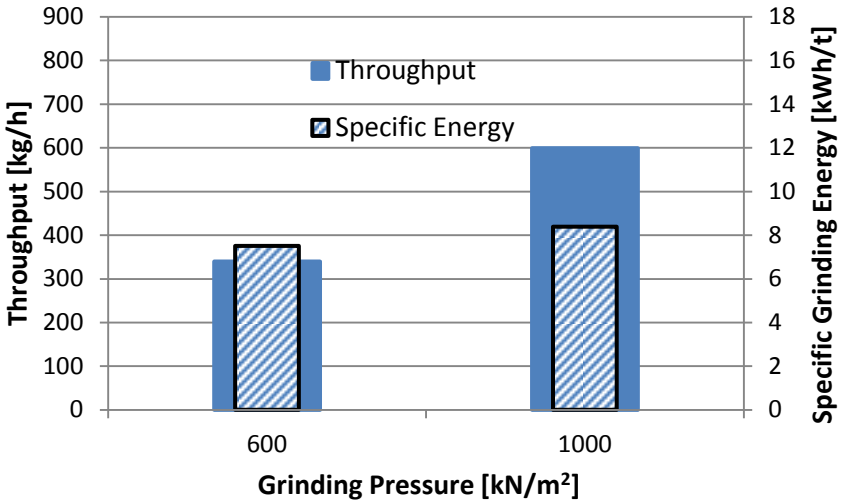

Figure 6-14: Throughputs and specific grinding energies for the vertical roller mill operated in circuit with an external screen, at the grinding pressures 600 and 1000 kN/m².

Estimations of the overall specific energies for the internal and external air classification circuits are presented in Figure 6-15. Estimations of the classification energy are based on data from the study by van Drunick et al. (2010), for the processing of Gamsberg ore, fed as a cone crusher product to a pilot scale vertical roller mill. The estimated overall specific energies for the external classification circuit are lower than those of the internal air classification circuit at the coarser grinds. Whether these differences will be observed for industrial size machines remains to be seen.

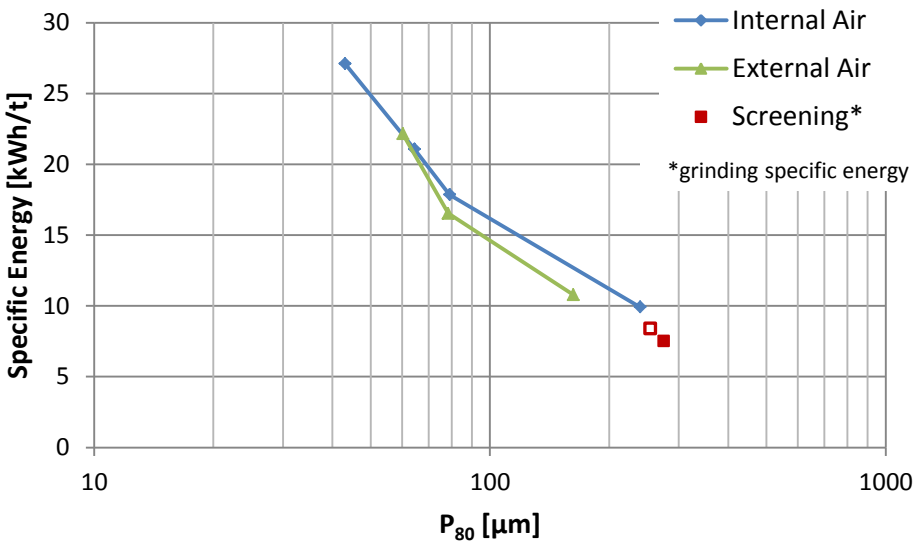

Figure 6-15: Hypothetical pilot scale specific energy comparison for different classification circuits based on comminution specific energy from this test work and energy split between grinding and classification presented by van Drunick et al. (2010).

6.3 Flotation Response

The VRM comminution circuit products obtained from different classification devices were representatively split and subjected to batch flotation tests similar to those conducted for the airflow operation products. Internal air classification flotation tests conducted at the same time as the external screening and external air classification tests were used for two comparisons. The 3E PGE grade and recovery data has been normalised, such that the proportional differences are maintained but the values presented are not the true data.

Airflow Classification Product

A subset of the original airflow tests was redone in order to generate fresh comminution product for use in comparative flotation tests focusing on changes in the classification configuration. The vertical roller mill was operated at a grinding pressure of 600 kN/m^2, with a dam ring height of 7 mm, targeting product P_{80} of 60, 75 and 240 µm. Figure 6-16 displays the flotation response of the repeated 75 µm P_{80} product, alongside the flotation response of the original 75 µm P_{80} product floated as part of the airflow operation test work and later as part of classification test work. The 3E PGE recovery and grade for the repeated and original products, floated as part of the classification test work are similar, indicating aging effects are not significant.

Figure 6-17 and Figure 6-18 show the flotation performance results for airflow products of different target grinds. In Figure 6-17 as the particle size of the grinding product decreases the cumulative 3E PGE recovery is observed to increase, while the grade of the concentrate decreases. This increase in recovery as the grind gets finer follows an expected increase in valuable mineral liberation. The decrease in grade is caused by a greater recovery of gangue material. The greater recovery of gangue at the finer target grind corresponds to an increase in entrainment. The individual platinum, palladium and gold recoveries in Figure 6-18 match the cumulative 3E PGE recovery trend, increasing as target grind decreases in size, with platinum recoveries consistently higher than those for palladium and gold.

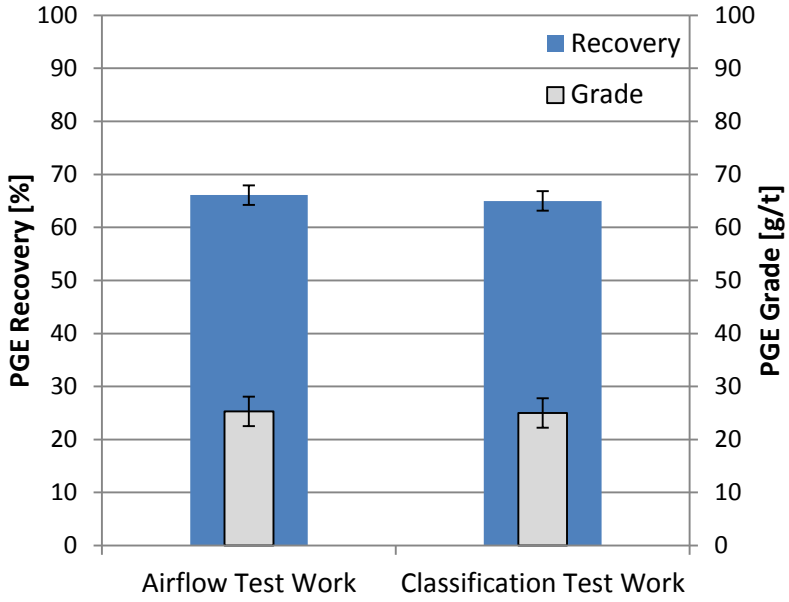

Figure 6-16: Comparison of normalised 3E PGE (Pt, Pd, Au) cumulative grades and recoveries for target P_{80} of 75 µm generated at a grinding pressure of 600 kN/m² and dam ring height of 7 mm in airflow operation. The 'Airflow Test Work' flotation results are for samples generated during the initial airflow test matrix and refloated during the later classification test work. The 'Classification Test Work' flotation results are for newly generated comminution product floated in the classification test work.

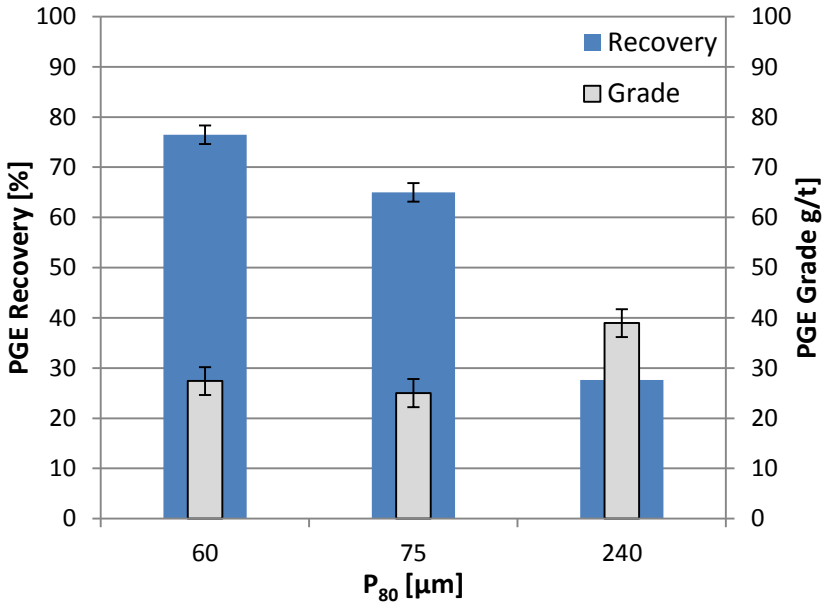

Figure 6-17: Variation of the normalised 3E PGE (Pt, Pd, Au) cumulative grades and recoveries with target grind for mill products generated at a grinding pressure of 600 kN/m² and dam ring height of 7 mm.

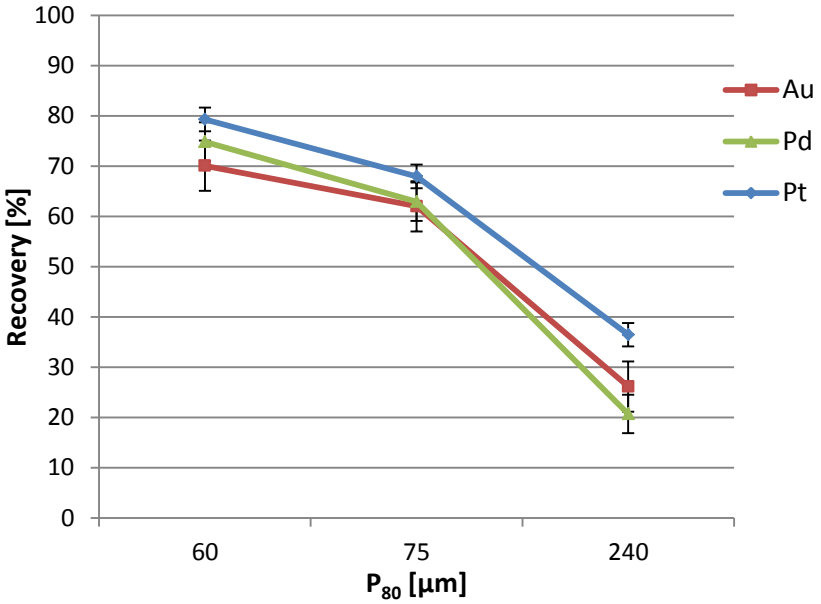

Figure 6-18: Variation of the platinum, palladium and gold recovery with target grind for mill products generated at a grinding pressure of 600 kN/m² and dam ring height of 7 mm.

Screening Classification Product

The screening comminution tests were conducted at the same time as the original airflow test work. To discount potential effects of aging in the comparison, the screening products were floated at the same time as the original airflow products. Figure 6-19 shows a comparison of the combined 3E PGE grades and recoveries from flotation tests performed on material prepared using the VRM with external screening and the VRM in airflow mode. At a 600 kN/m² grinding pressure, the 3E PGE recovery was lower for material prepared by the VRM with an external screen than that generated with the internal air classifier. A significantly higher grade concentrate was however produced for the VRM - screen circuit. An improved response was observed at a 1000 kN/m² grinding pressure, where a recovery of 43% was obtained for the VRM - screen circuit and the VRM in airflow mode was 48%. This represents a 12% improvement compared to the same system operated at a grinding pressure of 600 kN/m². The increase in recovery correlates to an increase in solids - water recovery, Figure 9-20 and Figure 9-21 in Appendix VI. This difference in recovery is partly a result of differences in particle size distribution between the two classification products (Figure 6-9). The screening and airflow products have similar P_{50} values however their P_{80} values differ appreciably at 289 and 214 µm for the 600 kN/m² grinding pressure and 259 and 201 µm for the 1000 kN/m² grinding pressure. This greater proportion of coarse material would indicate lower levels of liberation, for both gangue and valuable minerals in the screening products. Less liberation of base metal sulphides and PGMs would result in a lower recovery of these species during flotation. For the screening circuit products, 3E PGE flotation recovery was better at a higher grinding pressure as

opposed to the trends observed for airflow (Figure 5-31). This difference in recovery with grinding pressure is contrary to what was observed in the original airflow test work and the difference is likely due to the finer particle size distribution associated with the higher grinding pressure (P_{80} of 289 and 259 for the 600 and 1000 kN/m² grinding pressures respectively). At the 1000 kN/m² grinding pressure the difference in 3E PGE grade between the VRM - screen and internal air classification circuits was not found to be significant at a 95% confidence interval. The individual platinum, palladium and gold recoveries in Figure 6-20 and the copper and nickel recoveries in Figure 6-21 follow the same trend as the cumulative 3E PGE recovery observations. Cumulative base metal grade and recovery are plotted in Figure 9-28 in Appendix VII. The data shows platinum recoveries consistently higher than those for palladium and gold, and the copper recoveries greater than those of nickel. The copper and nickel recovery data indicates that material prepared in the VRM - screen circuit at a grinding pressure of 600 kN/m² has lower recoveries than that prepared in the VRM - airflow circuit. For operation at 1000 kN/m² however, the copper and nickel recoveries are improved and not significantly different to those for the VRM in airflow mode.

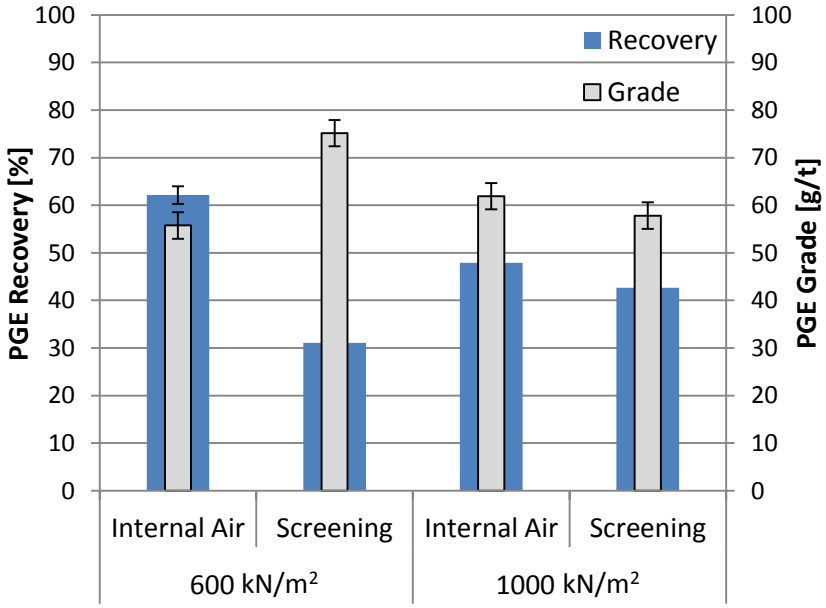

Figure 6-19: Normalised 3E PGE (Pt, Pd, Au) cumulative grade and recovery plots for batch flotation tests performed on VRM products generated when operated in conjunction with the internal air classifier and an external screen, illustrating the variation with grinding pressure for a target P_{80} of 240µm.

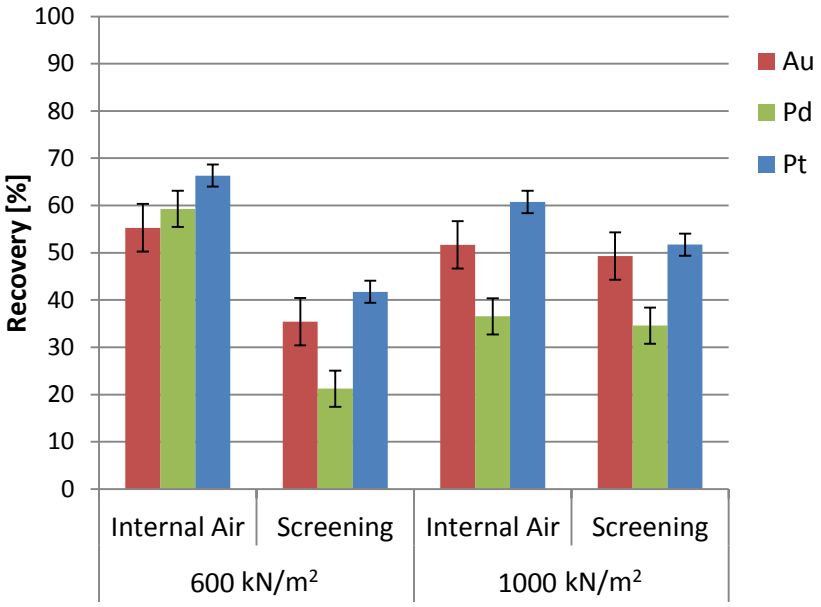

Figure 6-20: Platinum, palladium and gold recovery plots for batch flotation tests performed on VRM products generated when operated in conjunction with the internal air classifier and an external screen, illustrating the variation with grinding pressure.

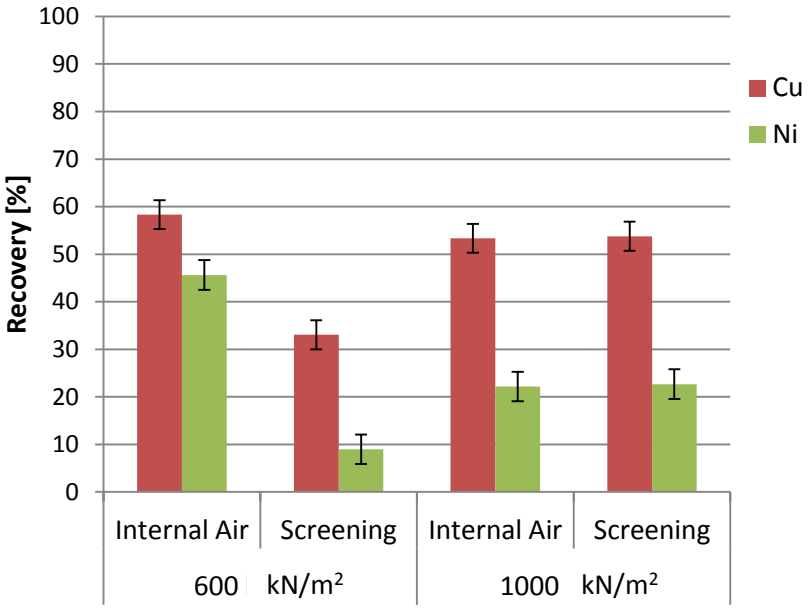

Figure 6-21: Copper and nickel recovery plots for batch flotation tests performed on VRM products generated when operated in conjunction with the internal air classifier and an external screen, illustrating the variation with grinding pressure.

External Air Classification Product

A comparison of flotation response for the VRM with internal and external air classification systems is given in Figure 6-22. Solids and water recovery graphs and plots are found in Appendix VI. The cumulative recovery data presented in Figure 6-22 shows 3E PGE flotation recoveries decrease as the grind coarsens for both internal and external air classification vertical roller mill circuits. The VRM - external air classifier setup showed superior flotation

recovery compared to that for the VRM - internal air classifier at the target grind of 240 µm P_{80}. The difference in flotation recovery at this target grind however cannot be attributed to the method of classification because the actual external air classification P_{80} (162 µm) was significantly lower than that of the internal air classifier. This reduced P_{80} would be associated with greater platinum group mineral (PGM) liberation, for which there would be an expected better PGM (and hence PGE) flotation recovery. For the 75 µm P_{80} target grind, particle size distributions of both external and internal air classification products were similar and the PGE recoveries for the different products were not significantly different. At the finest target grind the 3E PGE recovery was higher for internal air classification products. For this grind there was a difference in particle size distribution between the external and internal air classification products. Both products had similar P_{50} values however the product particle size distribution for the internal air classifier was steeper than that for external air classification (Figure 6-10). A greater proportion of external air classifier product was coarser, which is associated with lower liberation of PGMs and subsequently, reduced flotation recoveries. The individual platinum, palladium and gold recoveries in Figure 6-23 generally match the cumulative 3E PGE recovery observations, with platinum recoveries consistently higher than those for palladium and gold.

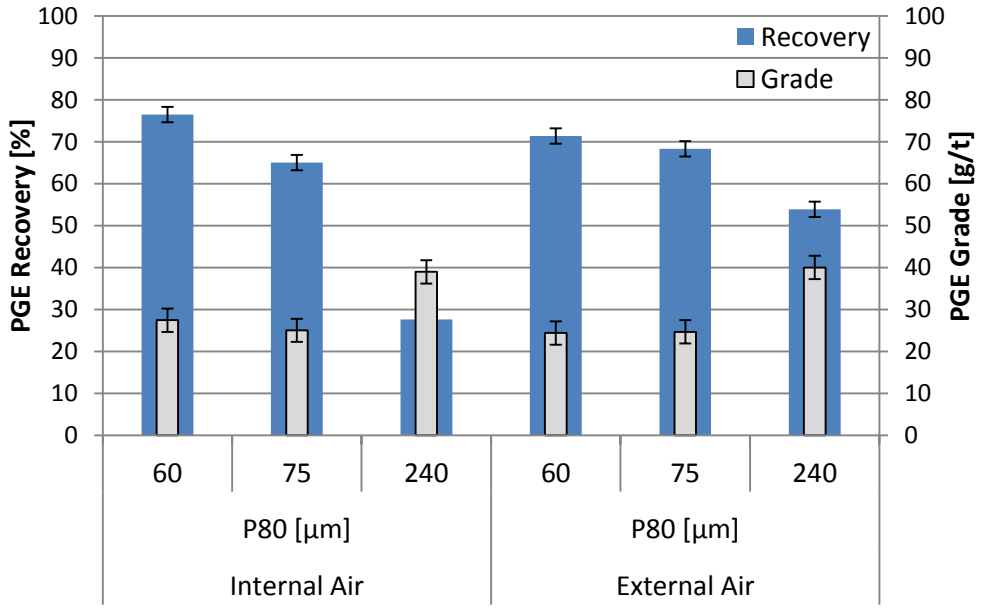

Figure 6-22: Normalised 3E PGE (Pt, Pd, Au) cumulative grade and recovery plots for batch flotation tests performed on VRM products of different target P_{80} values, generated when operated in conjunction with the internal air classifier and an external air classifier.

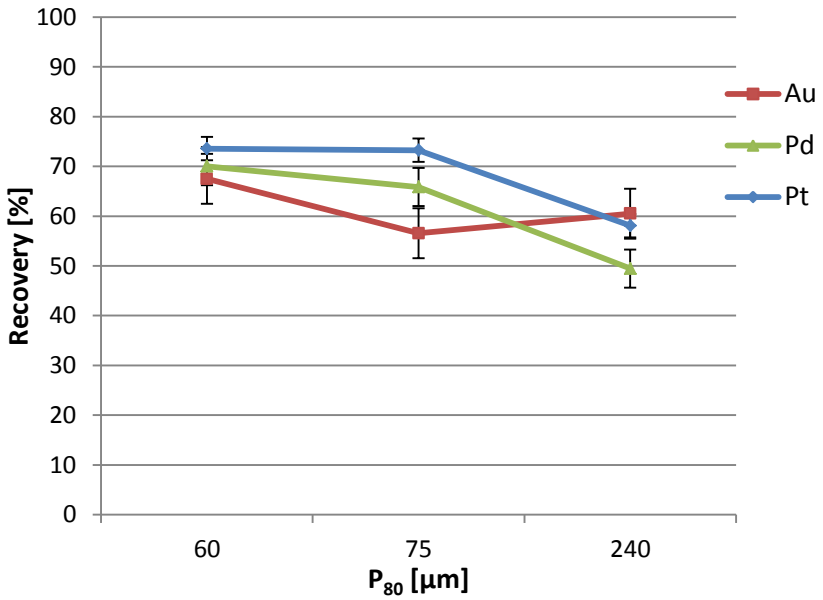

Figure 6-23: Platinum, palladium and gold recovery plots for batch flotation tests performed on VRM products of different target P_{80} values, generated when operated in conjunction with an external air classifier.

Tumbling Mill

Since most milling in the mining industry is carried out in tumbling mills, the vertical roller mill flotation response was compared with the performance of products prepared in a tumbling mill. A laboratory scale rod mill, described in Chapter 3, was used to grind material in batches to the desired target grind before flotation. The tumbling mill grinds targeted equivalent airflow product P_{50} values because of the difference in steepness of particle size distribution between the two comminution devices (Figure 4-10). The tumbling mill flotation response was compared with airflow tests performed at the same time to eliminate potential aging effects. Figure 6-24 shows the 3E PGE recovery and grade data for the flotation of tumbling mill and VRM - internal air classification products. It can be seen from Figure 6-24 that the tumbling mill had lower PGE recoveries compared to those obtained for material prepared using the vertical roller mill for all target grinds. The 3E PGE grades for the VRM internal classification circuit are however lower than those for the tumbling mill products.

The tumbling mill flotation solids and water recoveries are compared with those obtained for the VRM internal classification circuit products in Figure 6-25. The tumbling mill solids recoveries are only a quarter of those for VRM - internal classifier products at the 60 and 75 µm target grinds and a half at the 240 µm target grind. The differences in flotation water recoveries between the tumbling mill and VRM - internal classifier products are even greater. These results corresponds to what Nyakunuhwa (2019) and Feng and Aldrich (2000) observed, with dry grinding products yielding more stable froths, manifesting as higher flotation solids recoveries

for dry grinding products. The previously observed lower 3E PGE flotation recoveries correspond to these lower solids and water recoveries for the tumbling mill products.

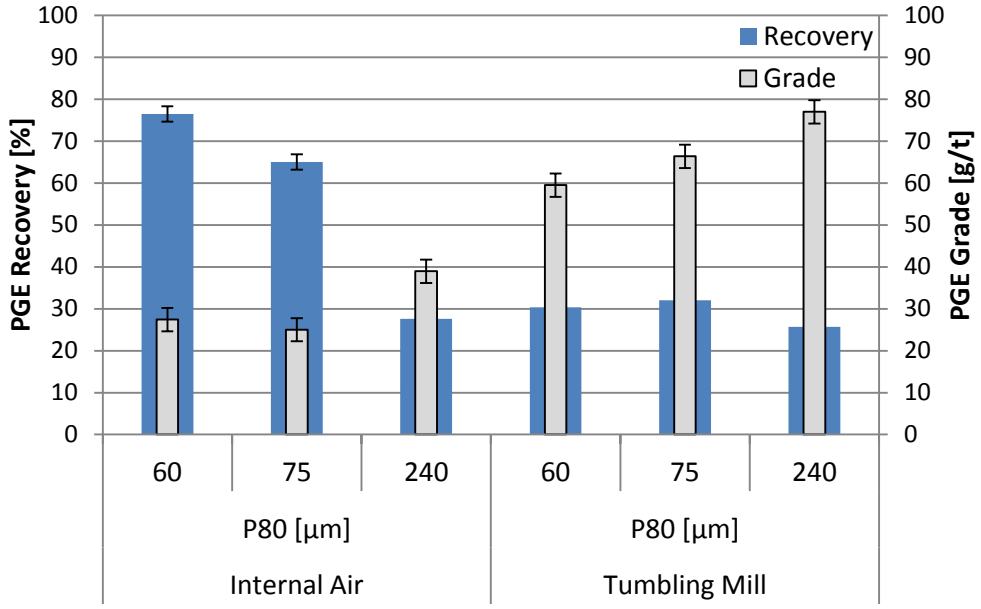

Figure 6-24: Normalised 3E PGE (Pt, Pd, Au) cumulative grade and recovery plots for batch flotation tests performed on products of different target P_{80} values, generated in a vertical roller mill operated with the built-in dynamic air classifier and a batch laboratory tumbling mill.

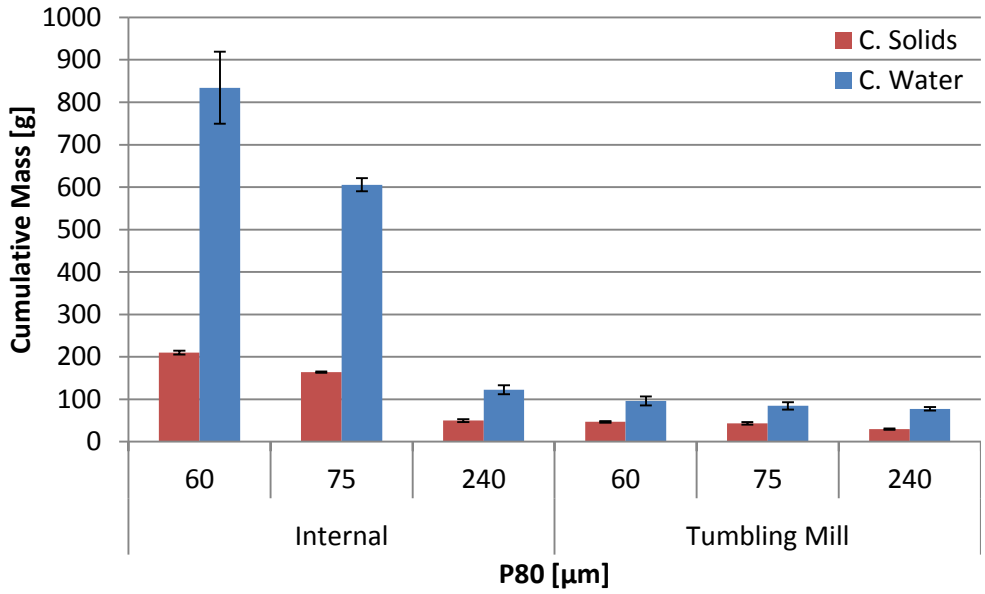

Figure 6-25: Solids and water recoveries plots for batch flotation tests performed on products of different target P_{80} values, generated in a vertical roller mill operated with the built-in dynamic air classifier and a batch laboratory tumbling mill.

Individual platinum, palladium and gold flotation recoveries are plotted for the tumbling mill products in Figure 6-26 and correspond to the cumulative 3E PGE recovery. The relative individual recoveries for the tumbling mill products are however unlike those for the vertical

roller mill. For VRM products, platinum recoveries were typically higher than those for palladium and gold, but for flotation of tumbling mill products the gold recoveries were higher.

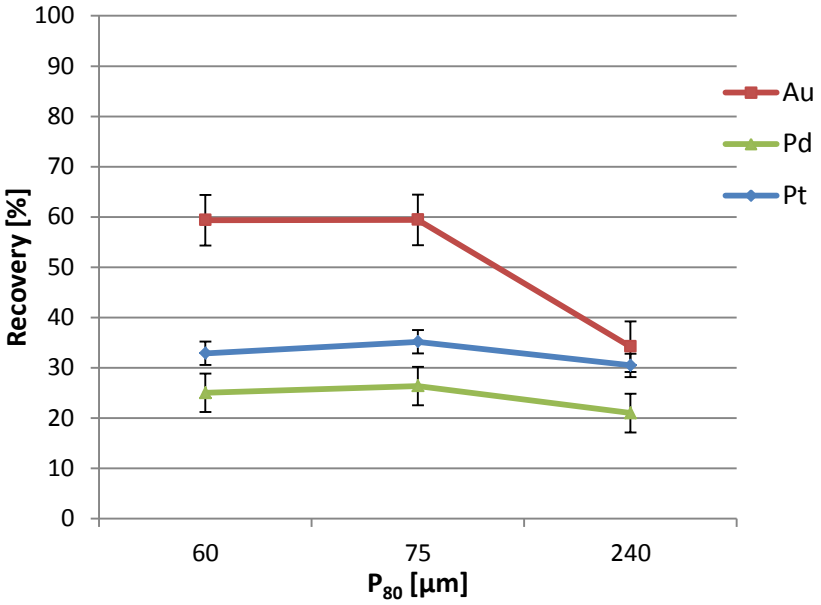

Figure 6-26: Platinum, palladium and gold recovery plots for batch flotation tests performed on products of different target P_{80} values, generated in a batch laboratory tumbling mill.

There are a few studies in literature where the flotation performance of vertical roller mill products has been compared to that for conventional milling products. In the work presented by Crosbie et al. (2005), better copper and nickel recoveries were observed for vertical roller mill products, with the difference attributed to a steeper particle size distribution and better valuable mineral liberation. In the work carried out by Katzmarzyk et al. (2019) and Nyakunuhwa (2019) however, no difference was observed in valuable mineral recoveries for the different comminution devices. In the study by Nyakunuhwa (2019), liberation of BMS was higher in VRM products, but no difference in particle size distribution for the comminution devices was observed.

For this study, the difference in 3E PGE flotation recovery would have been affected by the observed differences in particle size distribution between the tumbling mill and VRM products. Vertical roller mill products are expected to have better flotation responses, with higher valuable mineral recoveries because of their steeper particle size distributions (Crosbie et al., 2005; Erkan et al., 2012; Gerold et al., 2012b). Furthermore, there is potential that the liberation profiles of either or both the valuable and gangue minerals differed for the different comminution devices. Any variation would influence the flotation response and would contribute to differences in 3E PGE flotation recovery between the tumbling mill and VRM products.

Because of the large variation in flotation recovery between tumbling mill and VRM products, the oxidation potential (Eh) was measured during select flotation tests. The data presented in Figure 6-27 indicates there was a significant difference in oxidation potential during flotation for the tumbling mill and VRM products. The lower oxidation potential of the flotation pulp for the wet grinding tumbling mill product match those in the literature and has been linked with lower recoveries of valuable minerals (Katzmarzyk et al., 2019; Koleini et al., 2012; Palm et al., 2010; Seke and Pistorius, 2006). The higher oxidation potential for the dry milling products promotes the oxidation of xanthates to dixanthogens (Bruckard et al., 2011; Gonçalves et al., 2003) and leads to better adsorption rates for xanthate collectors (Feng and Aldrich, 2000).

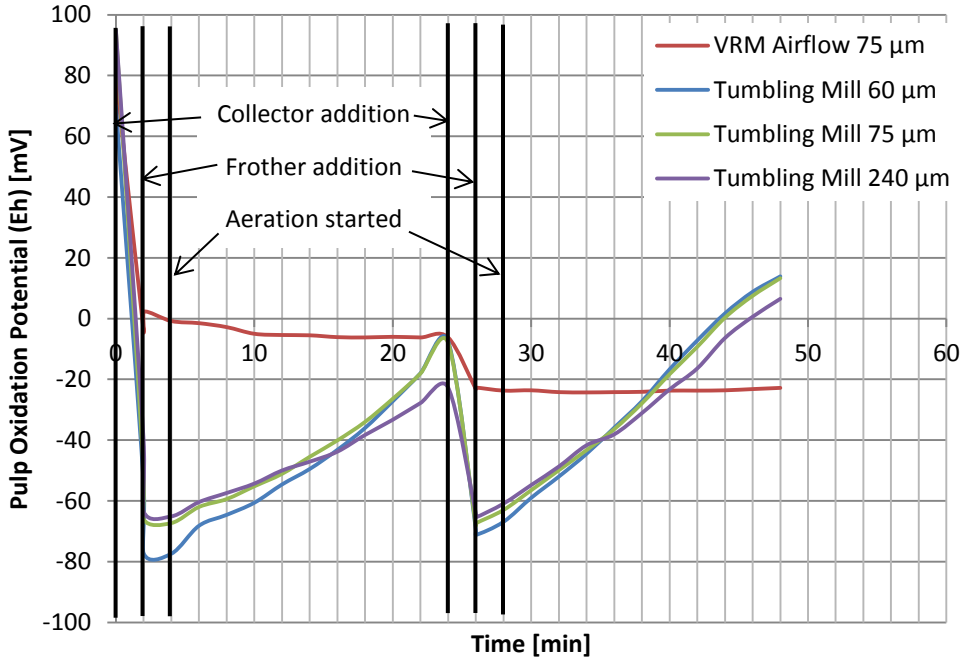

Figure 6-27: Oxidation potential (Eh) measured during batch flotation tests on tumbling mill and vertical roller mill products, indicating the different target P_{80} values.

6.4 Summary

This chapter contained the comminution results and batch flotation data for products generated by a vertical roller mill operated in conjunction with different classification devices. Operating the VRM in closed circuit with the three different classifiers had an effect on comminution throughput and energy utilization, product particle size distribution and flotation performance.

Vertical roller mill tests performed with the air classifiers indicated that classifier separation efficiencies were higher when operating at higher classifier rotor speeds to obtain a finer product. The separation efficiencies for the screening circuit at the 240 μm target grind were greater than those for the internal and external air classifiers. While in closed circuit with a screen, operating the VRM at a higher grinding pressure resulted in a greater throughput and a finer product. The products generated by the vertical roller mill operated in airflow mode, with the internal dynamic air classifier, had steeper particle size distributions than those generated by the external screening circuit or external air classification circuit.

The specific grinding energies for the external screening and external hybrid air classifier circuit were higher than those for the internal air classifier circuit at all target grinds. However, when incorporating classification energy estimates for the air classifiers, the overall specific energy for the external air classification circuit was lower than that of the internal air classifier at the coarse and intermediate grind.

For both internal and external air classification circuits, as the product particle size decreases the cumulative 3E PGE flotation recovery increased and the grade of the concentrate decreased. This increase in flotation recovery is due to higher liberation of valuable minerals in finer products, while the decrease in grade was caused by increased amounts of gangue material recovered to the concentrate. For the finest target grind, the 3E PGE flotation recovery for the external classifier was lower than that of the internal classifier. This corresponded to a less steep particle size distribution of the external air classifier product. At the 75 μm P_{80} target grind however, particle size distributions of both air classification products were similar and 3E PGE flotation recovery was comparable. For the products from the circuit containing the VRM and screen, batch flotation recoveries were lower than those of products generated in the internal air classification configuration. The difference in recovery was a result of differences in the particle size distribution.

The tumbling mill products yielded lower 3E PGE flotation recoveries than those of the corresponding vertical roller mill products. The greater vertical roller mill 3E PGE recoveries resulted from the increased adsorption of xanthate collectors caused by higher oxidation pulp potential in the dry grinding VRM products.

Chapter 7

CONCLUDING DISCUSSION

In this chapter, the aim and work undertaken as part of this thesis are outlined. The important results and key findings obtained are highlighted and recommendations are made for future work based on questions arising during this thesis.

The aim of this study was to investigate the performance of the vertical roller mill with different classification configurations when used for the comminution of a hard rock ore, while considering the influence that the device would have on the downstream valuable mineral recovery process of flotation. A graphical summary of what was considered in this study is given in Figure 7-1. The platinum group element (PGE) bearing Platreef ore, a highly competent ore which requires a fine grind for the liberation of the PGMs was used for the test work. The comminution performance was assessed in terms of the vertical roller mill specific energy, throughput and product fineness. The flotation response of the vertical roller mill products was evaluated in terms of grade and recoveries achieved. The vertical roller mill variables: grinding pressure (an online control used for maintaining product quality), and dam ring height (a design variable affecting residence time and bed depth on the grinding table), were investigated at the target grinds of P_{80} 240, 75 and 45 μm, typical of grinding stages employed in the circuit processing Platreef. The vertical roller mill was tested with the internal dynamic air classifier, an external hybrid air classifier (containing both static and dynamic air classification components) and an external vibrating screen to evaluate the influence of classification on VRM operation and the product generated.

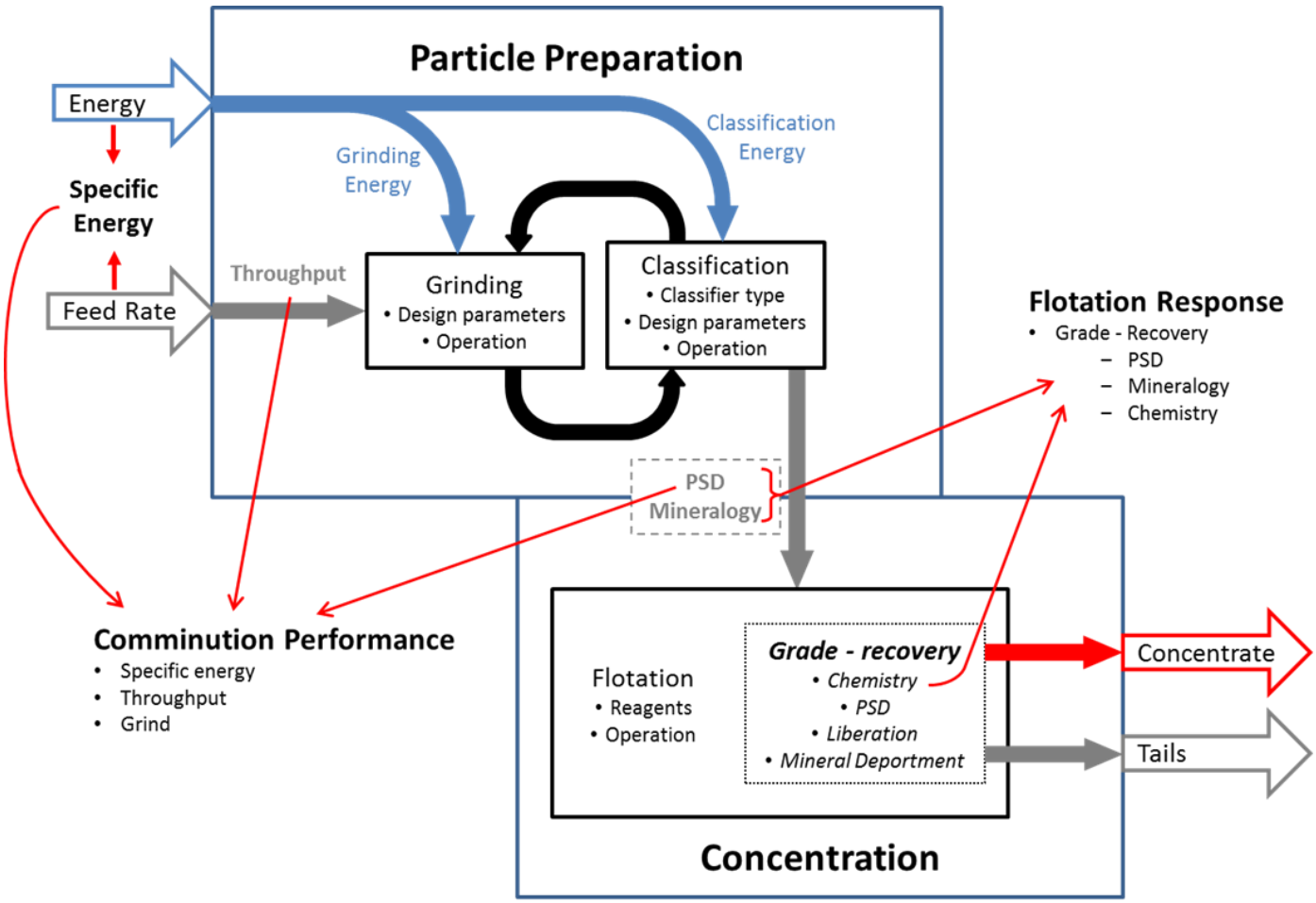

Figure 7-1: Illustration of a minerals processing circuit overlaid with factors of interest, drawing together the aspects on which the vertical roller mill applicability to minerals processing is determined.

7.1 Comminution Circuit Performance

Assessment of the vertical roller mill comminution circuit performance was guided by two hypotheses. The conclusions are directed at addressing these hypotheses and answering the associated key questions. The first hypothesis focuses on mechanisms in the grinding mill and the second on how classification affects operation.

Hypothesis 1

The VRM will be able to efficiently generate a suitable comminution product because the method of achieving breakage in this device is through the direct application of a force to a bed of particles.

This hypothesis was tested by comparison of the specific energy used by the VRM with that expected for a conventional tumbling mill, achieving equivalent target grinds.

The key question related to this hypothesis and the operation of the vertical roller mill was:

> How does performance of the VRM vary when grinding pressure alters the compressive forces particles experience and adjusting the dam ring height changes residence time on the grinding table?

Grinding Pressure

Operating the vertical roller mill at higher grinding pressures resulted in a throughput increase of up to 50%. A higher grinding pressure meant a greater force was applied to the particles on each pass under the rollers, resulting in a finer grinding table product. Sending a finer grinding table product to the classifier resulted in a greater fraction of material discharged as the final product, which reduced the recycle, creating the capacity to introduce more fresh feed to the system.

The mechanical energy usage for the vertical roller mill was greater for higher grinding pressures however this did not translate into higher specific grinding energies because of the increase in throughput.

For a given target grind, operating at higher grinding pressures yielded products which had less steep particle size distributions, with a 1-5% greater fraction of sub 25 μm particles. The differences in product particle size distribution were more pronounced for the coarser grinds and at greater dam ring heights. The generation of more fines, sub 25 μm particles, at the higher pressures was a result of the greater forces experienced by the material on the grinding table.

Dam Ring Height

The response of throughput to changes in dam ring height was observed to vary. The results in this study, together with those in literature, indicate that optimising throughput with dam ring height is target grind and ore dependent.

Increasing dam ring height resulted in higher energy usage for a given target grind. For increased dam rings heights, the depth of the material on the grinding table was greater causing greater resistance to motion for the rollers, translating into an increase in the mechanical energy. The higher mechanical energy resulted in an up to 20% increase in the specific grinding energy for the VRM at greater dam ring heights.

Operating at greater dam ring heights yielded products with less steep particle size distributions because higher dam rings increase bed depth, increasing the residence time of the material on the grinding table. Increased residence times result in particles experiencing more successive compressive events before leaving the grinding table, changing the grinding table product/classifier

feed, which affects the final comminution product. The variation in particle size distribution with dam ring was greater for the coarser target grinds.

Conclusion

The vertical roller mill can be used to efficiently comminute ore to different product sizes, suitable for valuable mineral recovery through flotation. Products were generated at a variety of grinding pressures and dam ring heights for the target grinds: 240, 75 and 45 μm, which are associated with primary, secondary and tertiary grinding stages in the platinum industry. When comparing the specific grinding energy of the vertical roller mill to that of a ball mill, the VRM specific grinding energies were less than half of those for the ball mill. If classification energy and scale up estimations are included, the vertical roller mill overall specific energy is potentially 25-35% lower than that of a ball mill. Altering the grinding pressure and dam ring height yielded differences in the product particle size distribution and caused discernible changes in throughput and energy usage (127-362 kg/h and 14.4-15.7 kWh/t at the finest target grind). Generating products of a finer particle size led to lower throughputs in the vertical roller mill and greater specific grinding energies.

Hypothesis 2

Using a VRM in conjunction with an external classifier will improve the unit's overall energy utilisation because the energy used for material transportation and separation mechanisms will reduce, while energy contributed towards breakage in the system is not altered.

The key question associated with this hypothesis was:

> What effects does changing the classification device used in conjunction with the vertical roller mill have on circuit performance and the particle size distribution of the product?

The throughputs achieved for the external screening and external hybrid air classification circuits were around 50% lower than those attained with the standard internal dynamic air classifier, and the circulating load, which could be calculated for the external classification circuits, was two times greater for the external air classifier than the screen. The sharpness of separation of the screen was better than either air classifier, with the screen achieving a corrected cut size of around 400 μm compared with the ~100 μm realised by the external air classifiers and internal air classifiers (with assumptions) when targeting the coarse product grind.

The specific grinding energies for the vertical roller mill in circuit with the external hybrid air classifier were 20-40% higher than those with the internal air classifier at the same target grinds,

and for the coarse product target grind, the specific grinding energy of the VRM - external screening circuit was greater than that of both air classification circuits. Incorporating classification energies for the air classification circuits indicated that at the pilot scale, overall specific energy of the VRM with external air classification was lower than that for the VRM with internal air classifier at the coarse and intermediate grind.

The products generated by the vertical roller mill operated with internal air classification had a steeper particle size distribution when compared to those generated with both the external screening circuit and the external air classification circuit.

Conclusion

The vertical roller mill can be used with different classification devices to generate products of suitable particle size distribution for downstream processing. VRM operation with the internal dynamic air classifier or an external air classifier was able to prepare products comparable to the primary, secondary and tertiary grinding stages in the platinum industry. The screening circuit generated an equivalent primary grinding product. For internal and external air classification circuits, specific grind energy increased and throughput decreased as the target grind size became smaller. The specific grinding energies were greater in the external classification circuits. The estimated overall specific energy, however, which includes that for grinding and classification, was lower for the external air classification at pilot scale.

7.2 Flotation Response

The flotation response of vertical roller mill product prepared under different milling circuit operating conditions with different classification devices was assessed to address the third and fourth hypotheses and associated key questions. Flotation performance was measured in terms of platinum, palladium, gold (3E PGE) and copper, nickel (Cu, Ni) grades and recoveries. The analysis also considered the liberation profile of the platinum group minerals (PGMs) and base metal sulphides (BMS).

Hypothesis 3

During comminution in the vertical roller mill, increasing the compressive forces acting on the particle bed and the degree of confinement of the particles in a bed will improve the flotation recovery for products, because energy absorbed by the particles increases, leading to higher breakage rates within the system, which increases liberation of particles.

The key questions associated with this hypothesis are:

Do the liberation profiles and flotation performance of products vary depending on the compressive force and degree of bed confinement experienced during comminution in the VRM?

Grinding Pressure

Flotation results in terms of 3E PGE and base metal grade indicated that recoveries were 3-14% lower for products generated at higher grinding pressures at the dam ring heights and target grinds investigated. Lower 3E PGE and base metal recoveries corresponded to a decrease in solids and water recoveries for products generated at higher grinding pressures, which indicated lower froth stability. The greater proportion of fine material in the grinding products generated at higher grinding pressures would influence the concentration and size of particles in the froth, affecting the froth stability. The increased grinding pressure is thought to have increased the liberation of the valuable minerals, although the potential recovery benefit of this improved liberation was not realised because of the froth stability limitation.

Dam Ring Height

The 3E PGE and base metal flotation recoveries for the lowest dam ring height were 2-17% greater than those of the highest dam ring for the target grinds and grinding pressures investigated. The decrease in flotation recoveries between the lowest and highest dam ring height is linked to a decrease in PGM liberation and lower froth stability. Products prepared at greater dam ring heights had worse liberation of discrete PGMs and contained an increase in proportion of fines, which caused the lower froth stabilities. The effective PGM liberation (considering PGMs locked in floatable BMS) was however greater for the higher dam rings. It is thought that reagent optimisation targeting improved froth stability could allow for better recoveries at the higher dam ring height products, to the extent that valuable mineral recovery would follow the trends in valuable mineral liberation.

Products prepared at the intermediate dam ring height generally had greater 3E PGE and Cu, Ni flotation recoveries than those generated with lower or higher dam rings. The intermediate dam ring height product does follow the overall trend in PGM and BMS liberation and variation in the proportion of fines, and hence should have an intermediate recovery; however, recovery was generally highest for these products. The anomaly in flotation performance for the intermediate dam ring height product may have resulted from lower liberation of talc at that dam ring height, which would have a disproportionate effect on froth stability as talc is a strongly hydrophobic mineral.

Conclusion

Increasing the compressive force through the application of higher grinding pressures led to higher fines production within the system, which caused a decrease in flotation recovery. Increasing the degree of confinement of the bed of particles through altering the dam ring height increased the rate of breakage within the system, and led to a decrease in valuable mineral liberation but increase in effective PGM liberation. The variation in flotation recovery was related to changes in froth stability, caused by differences in the proportion of fines in the VRM products. Optimisation of the flotation reagent suite could address the issues with froth stability, allowing for improvements in valuable mineral liberation to be realised as increased flotation recoveries.

Hypothesis 4

Changing the classification method used in conjunction with the VRM will affect the flotation response of the ore because different classifiers yield comminution products of different particle size distribution. Classifiers which yield a narrower particle size distribution, at the same grind, will have an increased proportion of valuable minerals in the optimum flotation range.

The key questions associated with this hypothesis are:

> *Does the flotation response for particles comminuted with the VRM change when the classification method is altered? Are changes in flotation response due to differences caused by the different classifiers employed?*

For the intermediate target grind, the 3E PGE flotation recovery for both external and internal air classification products was similar and the particle size distributions of the products were closely comparable. At the finest target grind, the external air classifier 3E PGE flotation recovery was 5% lower than that for the internal air classifier product. This was attributed to the wider product particle size distribution generated by the external air classifier, which, despite having the same P_{50} as the internal air classifier product, had a P_{80} of 70 µm as compared to the 63 µm P_{80} for the internal air classifier.

For the coarse target grind, the flotation recoveries for vertical roller mill screening circuit product were half of those of the internal air classification circuit. The difference in response was due to differences in particle size distribution. The screen and internal air classification product particle size distributions had similar P_{50} values, but the screen product P_{80} values were greater, indicating a wider PSD with a larger proportion of coarse particles.

Conclusion

In both internal and external air classification circuits, as the product particle size decreases the cumulative 3E PGE flotation recovery was observed to increase, while the grade of the concentrate decreased. This increase in flotation recovery relates to greater valuable mineral liberation for finer products, while lower grades are due to increased recovery of gangue material into the concentrate. Variation was observed in particle size distribution for products of the same target grind generated with different classification devices. The classification devices which yielded products with narrower particle size distributions generated products which had better flotation recoveries.

7.3 Recommendations for Future Work

The work presented in this thesis focused on evaluating the performance of the vertical roller mill as a comminution device to prepare a hard rock ore for flotation when operating with different classification devices. Based on the results, conclusions and observations in this study the following aspects have been identified as those which would merit further investigation.

1. The energy comparison of the vertical roller mill circuits with different classification devices was derived from calculated classifier energy values for other pilot scale units. The ratio of grinding to classification energy is known to change with scale up and as such further assessment of the different circuits is required. The scale up for the standard internal dynamic air classifier configuration is established, however, how external air classification scales up is not known. A study is required, once industrial scale units become available, to obtain scale up information for the vertical roller mill - external air classifier circuit.
2. This study has shown that the dam ring height has an influence on throughput, and it indicates that throughput could be optimised with dam ring height. More information is however required, with a test structure assessing dam ring height at closer intervals and for a wider range, to properly understand the throughput profile.
3. Mineralogical analysis was carried out for selected products of different target grind generated at different dam ring heights but not different grinding pressures. Further mineralogical analysis for different grinding pressure products would deepen the understanding of the link between comminution and flotation.
4. The reagent suite and dosages used for the flotation testing was standard for the flotation of Platreef ore as a wet, tumbling mill product. However, as was seen in the VRM - tumbling mill flotation comparison, chemistry during flotation was markedly different with recoveries for the two comminution device products also varying significantly. The reagent suite should be adapted for the dry grinding vertical roller mill product, considering differences in mineral surfaces and differences in particle size distribution. The optimised reagent suite could address issues with froth stability, allowing for the improvements in valuable mineral liberation to be realised as increased flotation recoveries. Furthermore, the study could look at the mineral surfaces with XPS and ToF-SIMS for better understanding of surface oxidation and collector adsorption in VRM products.
5. The work in this thesis was performed on a single ore and the flotation results indicated VRM products yield better valuable mineral recoveries than those prepared with a tumbling mill. Flotation performance is, however, known to be ore dependent, so further work is required to see the range of ores which show similar benefits.

Chapter 8

REFERENCES

Achaye, I., 2017. Effect of particle properties on froth stability. PhD Thesis. University of Cape Town. doi:10.1007/s10008-007-0419-9

Ahluwalia, S.C., Hackländer-Woywadt, C., Abraham, P.C., 2006. Operating experience with the first Loesche mill with the 3+3 system for grinding clinker and blastfurnace slag. Cem. Int. 4, 90–98.

Albuquerque, L., Wheeler, J., Valine, S., 2013. High frequency vibrating screens in closed grinding circuits, in: XXV Encontro Nacional de Tratamento de Minérios e Metalurgia Extrativa & VIII Meeting of the Southern Hemisphere on Mineral Technology, 20-24 October, Goiania, Brazil. pp. 417–424.

Altun, D., Gerold, C., Benzer, H., Altun, O., Aydogan, N., 2015. Copper ore grinding in a mobile vertical roller mill pilot plant. Int. J. Miner. Process. 136, 32–36. doi:10.1016 /j.minpro.2014.10.002

Altun, D., Benzer, H., Aydogan, N., Gerold, C., 2017. Operational parameters affecting the vertical roller mill performance. Miner. Eng. 103–104, 67–71. doi:10.1016/j.mineng.2016.08.015

Altun, O., Benzer, H., Dundar, H., Aydogan, N.A., 2011. Comparison of open and closed circuit HPGR application on dry grinding circuit performance. Miner. Eng. 24, 267–275. doi:10.1016/j.mineng.2010.08.024

Altun, O., Benzer, H., 2014. Selection and mathematical modelling of high efficiency air classifiers. Powder Technol. 264, 1–8. doi:10.1016/j.powtec.2014.05.013

Anglo American Platinum Limited, 2015. Annual Results Booklet 2015.

Anglo American Platinum Limited, 2018. Annual Results 2018.

Apling, A., Bwalya, M., 1997. Evaluating high pressure milling for liberation enhancement and energy saving. Miner. Eng. 10, 1013–1022.

Ata, S., 2012. Phenomena in the froth phase of flotation - A review. Int. J. Miner. Process. 102–103, 1–12. doi:10.1016/j.minpro.2011.09.008

Aydoğan, N., Ergün, L., Benzer, H., 2006. High pressure grinding rolls (HPGR) applications in the cement industry. Miner. Eng. 19, 130–139. doi:10.1016/j.mineng.2005.08.011

Aydoğan, N.A., Benzer, H., 2011. Comparison of the overall circuit performance in the cement industry: High compression milling vs. ball milling technology. Miner. Eng. 24, 211–215.

doi:10.1016/j.mineng.2010.08.005

Ballantyne, G.R., Powell, M.S., Tiang, M., 2012. Proportion of energy attributable to comminution in: Proceedings of the 11th AusIMM Mill Operators' Conference. pp. 25–30.

Batra, V.K., Mittal, P.K., Kumar, K., Chhangani, P.N., 2005. Modern processing techniques to minimize cost in cement industry [WWW Document]. URL www.holtecnet.com/web/content/references/.../p_2005_2.pdf (accessed 3.12.15).

Baum, W., 2013. Ore characterization, process mineralogy and lab automation a roadmap for future mining. Miner. Eng. 60, 69–73. doi:10.1016/j.mineng.2013.11.008

BCS Incorportated, 2007. Mining industry energy bandwidth study, US Department of Energy [WWW Document]. URL www..energy.gov/sites/prod/files/2013/11/f4/mining_bandwidth.pdf (accessed 7.18.21)

Becker, M., Mainza, A.N., Powell, M.S., Bradshaw, D.J., Knopjes, B., 2008. Quantifying the influence of classification with the 3 product cyclone on liberation and recovery of PGMs in UG2 ore. Miner. Eng. 21, 549–558. doi:10.1016/j.mineng.2007.11.001

Becker, M., Wightman, E.M., Evans, C.L., 2016. Process Mineralogy. Julius Kruttschnitt Mineral Research Centre, University of Queensland. Brisbane, Austrailia.

Benzer, H., Aydoğan, N., Dündar, H., 2011. Investigation of the breakage of hard and soft components under high compression: HPGR application. Miner. Eng. 24, 303–307. doi:10.1016/j.mineng.2010.09.012

Benzer, H., Gerold, C., Schmitz, C., 2018. First application of a vertical roller mill in a sulphide copper - gold ore project, in: 11th International Comminution Symposium (MEI Comminution '18), 16-19 April 2018, Cape Town, South Africa. pp. 1–14.

Bhardwaj, O.P., Bandyopadhyay, A., Khare, R.N., Rao, T.C., 1985. Improvement in grinding and classification circuit by the use of Hydrocone at Rakha concentrator, in: Proceedings of National Seminar on Mineral Processing and IX Annual Technical Convention of Indian Institute of Mineral Engineers, 11-12 March 1985, Jamshedpur, India. pp. 58-63.

Bradshaw, D., 2014. The role of 'process mineralogy' in improving the process performance of complex sulphide ores, in: XXVII International Mineral Processing Congress (IMPC), 20-24 October 2014, Santiago, Chile. pp. 1-17

Bruckard, W.J., Sparrow, G.J., Woodcock, J.T., 2011. A review of the effects of the grinding environment on the flotation of copper sulphides. Int. J. Miner. Process. 100, 1–13. doi:10.1016/j.minpro.2011.04.001

Brundiek, H., 1995. Newly developed Loesche roller grinding mill system for cement clinker and blast furnace slag, Turkish Cement Manufactures' Association. 26-28 April, Anakara, Turkey.

Brundiek, H., Poeschl, F., 1995. A roller mill for cement and blast furnace slag in theory and practice, in: IEEE Cement Industry Technical Conference, 4-9 June 1995, San Juan, USA. pp. 197–223. doi: 10.1109/citcon.1995.514335

Brundiek, H., Poeschl, H.J., 1997. Roller mill application for high moisture feed, in: IEEE Cement Industry Technical Conference, 20-24 April 1997, Hershey, USA. pp. 213–225. doi:10.1109/citcon.1997.599302

Cawthorn, R.G., 1999. The platinum and palladium resources of the Bushveld Complex. S. Afr. J.

Sci. 95, 481–489.

Cepuritis, R., Jacobsen, S., Onnela, T., 2015. Sand production with VSI crushing and air classification: Optimising fines grading for concrete production with micro-proportioning. Miner. Eng. 78, 1–14. doi:10.1016/j.mineng.2015.03.025

Chapman, N.A., Shackleton, N.J., Malysiak, V., O'Connor, C.T., 2011. The effect of using different comminution procedures on the flotation of Platinum Group Minerals. Miner. Eng. 24, 731–736. doi:10.1016/j.mineng.2011.01.001

Chelgani, S.C., Parian, M., Parapari, P.S., Ghorbani, Y., Rosenkranz, J., 2019. A comparative study on the effects of dry and wetgrinding on mineral flotation separation-a review. J. Mater. Res. Technol. 8, 5004–5011. doi:10.1016/j.jmrt.2019.07.053

Chongo, C., Ngosa, K., Bepswa, P.A., Mainza, A.N., 2018. A study into the merit of optimised milling configuration on process performance – A case study of the mixed ore circuit at Kansanshi, in: 11th International Comminution Symposium (MEI Comminution '18), 16-19 April 2018, Cape Town, South Africa. pp. 1–19.

Clarke, B., Uken, R., Reinhardt, J., 2009. Structural and compositional constraints on the emplacement of the Bushveld Complex, South Africa. Lithos. 111, 21–36. doi:10.1016/j.lithos.2008.11.006

Cordonnier, A., 1996. A new grinding process: HOROMILL®. Int. J. Miner. Process. 44–45, 597–606. doi:10.1016/0301-7516(95)00068-2

Corin, K.C., Mishra, J., O'Connor, C.T., 2013. Investigating the role of pulp chemistry on the floatability of a Cu-Ni sulfide ore. Int. J. Miner. Process. 120, 8–14. doi:10.1016 /j.minpro.2013.02.001

Cramer, L.A., 2001. The extractive metallurgy of South Africa's platinum ores. J. Met. 53, 14–18.

Cropp, A., Goodall, W., 2013. The influence of rock texture on mineral processing [WWW Document]. MinAssit. URL http://www.minassist.com.au/site/downloads/The-Influence-of-Rock-Texture-on-Processing (accessed 4.23.20).

Crosbie, R., Robertson, C., Smit, I., Ser, V., 2005. The benefits of inter-particle comminution on flotation, in: Centenary of Flotation Symposium, 6-9 June 2005, Brisbane, Australia. pp. 823–828.

Drozdiak, J.A., Klein, B., Nadolski, S., Bamber, A., 2011. A pilot-scale examination of a high pressure grinding roll / stirred mill comminution circuit, in: 5th International Conference on Autogenous, Semiautogenous and High Pressure Grinding Technology, 25-28 Sepember 2011, Vancouver, Canada. pp. 2–27.

Erkan, E., Umurhan, S., Sayiner, B., Cankurtaran, M., Benzer, H., Aydogan, N., Demir, H.K., Langel, J., Carsten, G., 2012. Comparison of the vertical roller mill and rod-ball mill circuit on the gold extraction, in: XIII International Mineral Processing Symposium, 10-12 October 2012, Bodrum, Mugla, Turkey. pp 1-7

Farrokhpay, S., Manouchehri, H.R., 2012. Flotation characteristics of a complex copper ore: A comparison between wet and dry grinding, in: XXVI International Mineral Processing Congress (IMPC), 24-28 September 2012, New Delhi, India. pp. 1370–1377.

Feng, D., Aldrich, C., 1999. Effect of particle size on flotation performance of complex sulphide ores. Miner. Eng. 12, 721–731. doi:10.1016/S0892-6875(99)00059-X

Feng, D., Aldrich, C., 2000. A comparison of the flotation of ore from the Merensky Reef after wet and dry grinding. Int. J. Miner. Process. 60, 115–129. doi:10.1016/S0301-7516(00)00010-7

Folsberg, J., Smidth, F.L., 1997. The air-swept ring roller mill for clinker grinding, in: IEEE Cement Industry Technical Conference, 20-24 April 1997, Hershey, USA. pp. 157–176. doi:10.1109/CITCON.1997.599284

Fuerstenau, D.W., Gutsche, O., Kapur, P.C., 1996. Confined particle bed comminution under compressive loads. Int. J. Miner. Process. 44–45, 521–537. doi:10.1016/0301-7516(95)00063-1

Fuerstenau, D.W., Lutch, J.J., De, A., 1999. The effect of ball size on the energy efficiency of hybrid high-pressure roll mill/ball mill grinding. Powder Technol. 105, 199–204.

Gao, M., Forssberg, E., 1995. Prediction of product size distributions for a stirred ball mill. Powder Technol. 84, 101–106.

Gerold, C., Schmitz, C., Stapelmann, M., 2012a. Latest installations and developments of Loesche vertical roller mills in the ore industry, in: XXVI International Mineral Processing Congress (IMPC), 24-28 September 2012, New Delhi, India. pp. 1018–1029.

Gerold, C., Schmitz, C., Stapelmann, M., Dardemann, F., 2012b. Recent installations and developments of Loesche vertical roller mills in the ore industry, in: 8th International Comminution Symposium (MEI Comminution '12), 17-20 April 2012, Cape Town, South Africa. pp. 1–22.

Ghorbani, Y., 2012. On the progression of leaching from large particles in heaps. PhD Thesis. University of Cape Town.

Ghorbani, Y., Mainza, A.N., Petersen, J., Becker, M., Franzidis, J.P., Kalala, J.T., 2013. Investigation of particles with high crack density produced by HPGR and its effect on the redistribution of the particle size fraction in heaps. Miner. Eng. 43–44, 44–51. doi:10.1016/j.mineng.2012.08.010

Gonçalves, K.L.C., Andrade, V.L.L., Peres, A.E.C., 2003. The effect of grinding conditions on the flotation of a sulphide copper ore. Miner. Eng. 16, 1213–1216. doi:10.1016/j.mineng.2003.05.006

Gu, Y., Schouwstra, R.P., Rule, C., 2014. The value of automated mineralogy. Miner. Eng. 58, 100–103. doi:10.1016/j.mineng.2014.01.020

Hackländer-Woywadt, C., 2005. Granulated blastfurnace slag grinding with Loesche mills. ZKG Int. 58, 44–51.

Hackländer-Woywadt, C., 2006. Slag grinding with Loesche vertical roller mills. Glob. Slag Mag. July 2006. 25–29.

Harder, J., 2010. Grinding trends in the cement industry. ZKG Int. 63, 46–58.

Hayes, P.C., 2003. Process principles in minerals and materials production, 3rd ed. Hayes Publishing Co, Brisbane.

He, S., Fornasiero, D., Skinner, W., 2005. Correlation between copper-activated pyrite flotation and surface species: Effect of pulp oxidation potential. Miner. Eng. 18, 1208–1213. doi:10.1016/j.mineng.2005.07.016

Holwell, D.A., Boyce, A.J., McDonald, I., 2007. Sulfur isotope variations within the Platreef Ni-Cu-PGE deposit: Genetic implications for the origin of sulfide mineralization. Econ. Geol. 102, 1091 – 1110.

Holwell, D.A., McDonald, I., 2016. Distribution of platinum-group elements in the Platreef at Overysel, northern Bushveld Complex: A combined PGM and LA-ICP-MS study. Contrib. to Mineral. Petrol. 154. doi:10.1007/s00410-007-0185-9

Hosten, C., Cimilli, H., 2009. The effects of feed size distribution on confined-bed comminution of quartz and calcite in piston-die press. Int. J. Miner. Process. 91, 81–87. doi:10.1016/j.minpro.2009.01.002

Hu, Y., Wu, M., Liu, R., Sun, W., 2020. A review on the electrochemistry of galena flotation. Miner. Eng. 150, 106272. doi:10.1016/j.mineng.2020.106272

Hukki, R.T., 1961. Proposal for a Solomonic settlement between the theories of von Rittinger, Kick and Bond. Trans AIME. 220, 403–410.

Humphries, G., Rule, C., Wolmarans, E., 2006. The development of a process flowsheet for the new Anglo Platinum , PPRust north concentrator, incorporating HPGR, in: International Platinum Conference 'Platinum Surges Ahead.' pp. 129–136.

Hutchinson, D., McDonald, I., 2005. Breaking the rules. Divergent behavior of platinum and palladium in the Northern Limb of Bushveld Complex, RSA, in: 10th International Platinum Symposium, 8-11 August 2005, Oulu, Finland. pp. 118–121.

Jacobs, P., Seopa, G., Mofokeng, M., Nienhaus, D., Gerold, C., Mersmann, M., 2016. 16 Years of successful operation of a Loesche vertical roller mill type LM 50.4 in a hard rock application at Foskor Pty (Ltd) in Phalaborwa, in: 10th International Comminution Symposium (MEI Comminution '16), 11-14 April 2016, Cape Town, South Africa. pp. 1-13.

Jankovic, A., Valery, W., 2012. The impact of classification on the energy efficiency of grinding circuits – The hidden opportunity, in: 11th AusIMM Mill Operator's Conference, 29-31 October 2012, Hobart, Tasmania. pp. 65–69.

Jensen, L.R.D., Friis, H., Fundal, E., Møller, P., Brockhoff, P.B., Jespersen, M., 2010. Influence of quartz particles on wear in vertical roller mills. Part I: Quartz concentration. Miner. Eng. 23, 390–398. doi:10.1016/j.mineng.2009.11.014

Jensen, L.R.D., Fundal, E., Møller, P., Jespersen, M., 2011. Wear mechanism of abrasion resistant wear parts in raw material vertical roller mills. Wear 271, 2707–2719. doi:10.1016/j.wear.2011.03.018

Johansson, G., Pugh, R.J., 1992. The influence of particle size and hydrophobicity on the stability of mineralized froths. Int. J. Miner. Process. 34, 1–21. doi:10.1016/0301-7516(92)90012-L

Jørgensen, S.W., 2005. Cement grinding - A comparison between vertical roller mill and ball mill. Cem. Int. 3. pp.54-63

Junge, M., Wirth, R., Oberthür, T., Melcher, F., Schreiber, A., 2014. Mineralogical siting of platinum-group elements in pentlandite from the Bushveld Complex, South Africa. Miner. Depos. 50, 41–54. doi:10.1007/s00126-014-0561-0

Kanda, Y., Takahasi, S., Sakaguti, N., 1990. A compressive crushing of powder bed - A consideration of size distribution of product and specific energy to produce fine particles. Powder Technol. 63, 221–227. doi:10.1016/0032-5910(90)80047-3

Katzmarzyk, J., Silin, I., Hahn, K.M., Wotruba, H., Gerold, C., Stapelmann, M., 2019. Investigation on flotation behavior of a copper sulfide ore after dry grinding by Loesche vertical roller mill, in: Conference of Metallugists Copper 2019, 18-21 August 2019, Vancouver, Canada. pp. 1–11.

Kelebek, S., Nanthakumar, B., 2007. Characterization of stockpile oxidation of pentlandite and pyrrhotite through kinetic analysis of their flotation. Int. J. Miner. Process. 84, 69–80. doi:10.1016/j.minpro.2007.03.005

Kellerwessel, H., 1990. High-pressure material-bed comminution in practice. ZKG Int. 43, 71–75.

Klimpel, 1984. Froth flotation: The kinetic approach. Int. J. Miner. Process. 12, 323–324.

Knoflicek, M.J., Wentzel, W.C., 1994. Experiences with clinker grinding in roller mills. in: IEEE Cement Industry Technical Conference, 29 May - 2 June 1994, Seattle, USA. pp. 139–157. doi:10.1109/CITCON.1994.343435

Koleini, S.M.J., Abdollahy, M., Soltani, F., 2012. Wet and dry grinding methods effect on the flotation of Taknar cu-zn sulphide ore using a mixed collector, in: XXVI International Mineral Processing Congress (IMPC). pp. 5113–5119. doi:10.13140/2.1.3508.9606

Kou, S.Q., Liu, H.Y., Lindqvist, P.A., Tang, C.A., Xu, X.H., 2001. Numerical investigation of particle breakage as applied to mechanical crushing - Part II: Interparticle breakage. Int. J. Rock Mech. Min. Sci. 38, 1163–1172.

Laskowski, J.S., 2004. Testing flotation frothers. Physicochem. Probl. Miner. Process. 38, 13–22.

Lehloenya, P.B., Roelofse, F., 2013. Mercury distribution amongst co-existing silicates within the Bushveld Complex. Chemie der Erde 73, 261–266. doi:10.1016/j.chemer.2013.07.003

Little, L., 2016. The development and demonstration of a practical methodology for fine particle shape characterisation in minerals processing. PhD Thesis. University of Cape Town.

Little, L., Mainza, A.N., Wiese, J.G., Becker, M., 2016. Using mineralogical and particle shape analysis to investigate enhanced mineral liberation through phase boundary fracture. Powder Technol. 301, 794–804. doi:10.1016/j.powtec.2016.06.052

Liu, H.Y., Kou, S.Q., Lindqvist, P.A., 2005. Numerical studies on the inter-particle breakage of a confined particle assembly in rock crushing. Mech. Mater. 37, 935–954. doi:10.1016/j.mechmat.2004.10.002

Liu, J., Long, H., Corin, K.C., O'Connor, C.T., 2018. A study of the effect of grinding environment on the flotation of two copper sulphide ores. Miner. Eng. 122, 339–345. doi:10.1016/j.mineng.2018.03.031

Livshits, A.K., Dudenkov, S.V., 1965. Some factors in flotation froth stability, in: VII International Mineral Processing Congress (IMPC), 20-24 September 1965, New York, USA. pp. 367–371.

Loesche, E.G., 1964. The development and application of large grinding mills of the roller type, in: Annual Meeting of the America Institute of Mining, Metallurgical, and Petroleum Engineers, 16-20 February 1964, New York, USA.

Loesche GmbH, 2006. Mills for the world – 100 years Loesche | 1906 – 2006. ZKG Int. 59, 54-74.

Loesche GmbH, 2013. Saving energy with the new Loesche Dynamic Classifier (LDC) [WWW Document]. URL http://www.loesche.com/assets/PageContent/Data/Multimedia/Brochures/Service-News/pdf/185_flyer_saving_energy_classifier_E.pdf (accessed 5.29.13).

Loesche GmbH, 2014a. Loesche Mills for cement and granulated blast furnace slag [WWW Document]. URL https://www.loesche.com/sites/default/files/list-content/brochure/2017-08/143-LOESCHE-Mills-for-cement-and-granulated-blast-furnace-slag-E-2016.pdf (accessed 6.24.14).

Loesche GmbH, 2014b. Loesche Mills for metal recovery and filler production from steel slag [WWW Document]. URL https://www.loesche.com/sites/default/files/list-content/brochure/2017-08/205_Loesche-Mills-for-Metal-Recovery-and-Filler-Production-from-Steel-Slag_GB.pdf (accessed 6.27.14).

Lotter, N.O., 2011. Modern Process Mineralogy: An integrated multi-disciplined approach to flowsheeting. Miner. Eng. 24, 1229–1237. doi:10.1016/j.mineng.2011.03.004

Lynch, A., Ed. 2015. Comminution Handbook. The Australasian Institute of Mining and Metallurgy, Victoria, Australia.

Lynch, A.J., Rowland, C.A., 2005. The History of Grinding. Society for Mining, Metallurgy, and Exploration, Inc., Littleton, Colorado.

Mainza, A., Powell, M.S., Knopjes, B., 2004. Differential classification of dense material in a three-product cyclone. Miner. Eng. 17, 573–579. doi:10.1016/j.mineng.2004.01.023

Mainza, A.N., Powell, M.S., 2006. RoM Ball mills - a comparison with AG/SAG milling, in: 4th International Autogenous and Semiautogenous Grinding Technology, 23-27 September 2006, Vancouver, Canada. pp. 314–325.

Mainza, A.N., Evertsson, M., Benzer, H., Tavares, L.M., Powell, M.S., Rule, C., Lomdard, M., Knopjes, B., 2013. The role of classification in an evolving comminution circuit, in: 13th European Symposium on Comminution and Classification, 9-12 September 2013, Braunschweig, Germany. pp. 1–5.

Mainza, A.N., 2016. The contribution of the classifiers to comminution and separation processes in mineral processing, in: XXVIII International Mineral Processing Congress (IMPC), 11-15 September 2016, Quebec City, Canada. pp. 1-11.

Mainza, A., 2017. Incorporating classification in the design of mineral processing plants – An afterthought!, in: 15th European Symposium on Comminution and Classification, 11-14 September 2017, Izmir, Turkey. pp. 1–10.

Marchal, G., 1997. Industrial experience with clinker grinding in the HOROMILL®, in: IEEE Cement Industry Technical Conference, 20-24 April 1997, Hershey, USA. pp. 195–211. doi:10.1109/CITCON.1997.599299

McDonald, I., Harmer, R.E.J., Holwell, D.A., Hughes, H.S.R., Boyce, A.J., 2017. Cu-Ni-PGE mineralisation at the Aurora Project and potential for a new PGE province in the Northern Bushveld Main Zone. Ore Geol. Rev. 80, 1135–1159. doi:10.1016/j.oregeorev.2016.09.016

Michaelis, H. Von, 2005. Real and potential metallurgical benefits of HPGR in hard rock ore processing, in: Randol Innovative Metallurgy Forum, 21-244 August 2005, Perth, Australia. pp. 1-9.

Mishra, G., Viljoen, K.S., Mouri, H., 2013. Influence of mineralogy and ore texture on pentlandite flotation at the Nkomati nickel mine, South Africa. Miner. Eng. 54, 63–78. doi:10.1016/j.mineng.2013.04.009

Morar, S.H., Hatfield, D.P., Barbian, N., Bradshaw, D.J., Cilliers, J.J., Triffett, B., 2006. A comparison of flotation froth stability measurements and their use in the prediction of concentrate

grade, in: XXIII International Mineral Processing Congress (IMPC), 11-15 September 2016, Quebec City, Canada. pp. 739–744.

Morley, C., 2010. HPGR - FAQ. J. South. African Inst. Min. Metall. 110, 107–115.

Mudd, G.M., 2010. Key trends in the resource sustainability of platinum group elements. Ore Geol. Rev. 46, 106–117. doi:10.1016/j.oregeorev.2012.02.005

Muscolino, J., 2010. Mechanical centrifugal air classifiers. Chem. Eng. 117, 48–50.

Mwale, A.N., 2015. A mathematical model for predicting classification performance in wet fine screens. Masters Thesis. University of Cape Town.

Naldrett, T., Kinnaird, J., Wilson, A., Chunnett, G., 2008. Concentration of PGE in the Earth's crust with special reference to the Bushveld Complex. Earth Sci. Front. 15, 264–297. doi:10.1016/S1872-5791(09)60006-3

Neethling, S.J., Cilliers, J.J., 2002. The entrainment of gangue into a flotation froth. Int. J. Miner. Process. 64, 123–134. doi:10.1016/S0301-7516(01)00067-9

Nel, E., Valenta, M., Naude, N., 2005. Influence of open circuit regrind milling on UG2 ore composition and mineralogy at Impala's UG2 concentrator. Miner. Eng. 18, 785–790. doi:10.1016/j.mineng.2005.01.031

Nguyen, A.Q., Husemann, K., Oettel, W., 2002. Comminution behaviour of an unconfined particle bed. Miner. Eng. 15, 65–74. doi:10.1016/S0892-6875(01)00201-1

Norgate, T., Haque, N., Wright, S., Jahanshahi, S., 2010. Opportunities and technologies to reduce the energy and water impacts of deteriorating ore reserves, in: Sustainable Mining Conference, 17-19 August 2010, Kalgoorlie, Australia. pp. 128–137.

Nyakunuhwa, H.S., 2019. Effect of VRM on a polymetallic sulfide ore and the flotation response as compared to conventional wet and dry rod milling. Masters Thesis. University of Cape Town.

Oesch, C., Jurko, B., 2002. Finish grinding with vertical roller mills - Operating data, in: IEEE Cement Industry Technical Conference, 5-9 May 2002, Jacksonville, USA. pp. 187–192. doi:10.1109/citcon.2002.1006505

Oettel, W., Nguyen, A.Q., Husemann, K., Bernhardt, C., 2001. Comminution in confined particle beds by single compressive load. Int. J. Miner. Process. 63, 1–16. doi:10.1016/S0301-7516(00)00066-1

Özer, C., Whiten, W., Shi, F., Dixon, T., 2010. Investigation of the classification operation in a coal pulverising vertical spindle mill, in: XXV International Mineral Processing Congress (IMPC), 6-10 September 2010, Brisbane, Australia. pp. 1065–1076.

Özer, C.E., 2011. A new multi-component model for the vertical spindle mill. PhD Thesis. University of Queensland.

Padhi, M., Mangadoddy, N., Sreenivas, T., Vakamalla, T.R., Mainza, A.N., 2019. Study on multi-component particle behaviour in a hydrocyclone classifier using experimental and computational fluid dynamics techniques. Sep. Purif. Technol. 229, 1–14. doi:10.1016/j.seppur.2019.115698

Palm, N.A., Shackleton, N.J., Malysiak, V., O'Connor, C.T., 2010. The effect of using different comminution procedures on the flotation of sphalerite. Miner. Eng. 23, 1053–1057.

doi:10.1016/j.mineng.2010.08.001

Patzelt, N., 1992. High pressure grinding rolls, a survey of experience, in: IEEE Cement Industry Technical Conference 10-14 May 1992, Dallas, USA. pp. 149–181. doi:10.1109/citcon.1992.687614

Pease, J.D., Curry, D.C., Young, M.F., 2006. Designing flotation circuits for high fines recovery. Miner. Eng. 19, 831–840. doi:10.1016/j.mineng.2005.09.056

Peng, Y., Wang, B., Bradshaw, D., 2011. Pentlandite oxidation in the flotation of a complex nickel ore in saline water. Miner. Eng. 24, 85–87. doi:10.1016/j.mineng.2010.09.002

Petruk, W., 2000. Applied mineralogy in the mining industry. Elsevier Science. doi: 10.1016/B978-0-444-50077-9.X5000-7

Phala, N., 2012. Innovation Drivers and opportunities across the gold metallurgy value stream, in: XXVI International Mineral Processing Congress (IMPC) 24-28 September 2012, New Delhi, India.

Powell, M.S., Mainza, A.N., 2012. Step change – A staircase rather than a giant leap, in: XXVI International Mineral Processing Congress (IMPC) 24-28 September 2012, New Delhi, India.

Prakash, R., Majumder, S.K., Singh, A., 2018. Flotation technique: Its mechanisms and design parameters. Chem. Eng. Process. - Process Intensif. 127, 249–270. doi:10.1016/j.cep.2018. 03.029

Reichert, M., Gerold, C., Fredriksson, A., Adolfsson, G., Lieberwirth, H., 2015. Research of iron ore grinding in a vetical roller mill. Miner. Eng. 73, 109–115. doi:10.1016/j.mineng.2014. 07.021

Robinson, G.F., 1985. A model of the transient operation of a coal pulverizer. J. Inst. Energy 58, 51–63.

Roy, G., 2002. Increasing cement grinding capacity with vertical roller mill technology, in: IEEE Cement Industry Technical Conference 5-9 May 2002, Jacksonville, USA . pp. 205–211. doi:10.1109/citcon.2002.1006507

Rule, C., 2008. Energy considerations in the current PGM processing flowsheet utilizing new technologies. J. South. African Inst. Min. Metall. 109, 39–46.

Rule, C., Fouchee, R., Swart, W., 2015. HPGR Operation at Mogalakwena Concentrators, in: 6th International Conference on Autogenous, Semiautogenous and High Pressure Grinding Technology, 20-23 September 2015, Vancouver, Canada.

Rule, C., Minnaar, D.M., Sauermann, G.M., 2008. HPGR - Revolution in Platinum?, in: Third International Platinum Conference 'Platinum in Transformation', 5-9 October 2008, Sun City, South Africa. pp. 21–28.

Rule, C., Schouwstra, R.P., 2011. Process mineralogy delivering significant value at Anglo Platinum concentrator operations, in: 10th International Congress for Applied Mineralogy, 1-5 August 2011, Tronheim, Norway. pp. 1–5.

Rule, C.M., 2011. Stirred milling - New comminution technology in the PGM industry. J. South African Inst. Min. Metall. 111, 101–107.

Runge, K.C., Tabosa, E., Jankovic, A., 2013. Particle size distribution effects that should be

considered when performing flotation geometallurgical testing, in: 2nd AusIMM International Geometallurgy Conference, 30 September - 2 October 2013, Brisbane, Australia. pp. 335–344.

Sabbagh, R., Lipsett, M.G., Koch, C.R., Nobes, D.S., 2016. Predicting equivalent settling area factor in hydrocyclones: A method for determining tangential velocity profile. Sep. Purif. Technol. 163, 341–351. doi:10.1016/j.seppur.2016.03.009

Salewski, G., 2005. Vertical Versatility. World Cem. 36, 97-101.

Saramak, D., Krawczykowska, A., Młynarczykowska, A., 2014. Effects of high pressure ore grinding on the efficiency of flotation operations. Arch. Min. Sci. 59, 731–740. doi:10.2478/amsc-2014-0051

Schaefer, H., 2001. Loesche vertical roller mills for the comminution of ores and minerals. Miner. Eng. 14, 1155–1160.

Schonbach, B.H., 1988. High efficiency separators in roller mills. World Cem. 19, 436-444.

Schönert, K., 1988. A first survey of grinding with high-compression roller mills. Int. J. Miner. Process. 22, 401–412.

Schönert, K., 1996. The influence of particle bed configurations and confinements on particle breakage. Int. J. Miner. Process. 44–45, 1–16. doi:10.1016/0301-7516(95)00017-8

Schönert, K., Sander, U., 2002. Shear stresses and material slip in high pressure roller mills. Powder Technol. 122, 136–144. doi:10.1016/S0032-5910(01)00409-0

Schouwstra, R.P., Kinloch, E.D., Lee, C.A., 2000. A short geological review of the Bushveld Complex. Platin. Met. Rev. J. 44, 33–39.

Schouwstra, R., Vaux, D. De, Muzondo, T., Prins, C., 2013. A geometallurgical approach at Anglo American Platinum's Mogalakwena Operation, in: 2nd AusIMM International Geometallurgy Conference, 30 September - 2 October 2013, Brisbane, Australia. pp. 85–92.

Schouwstra, R.P., De Vaux, D. V., Snyman, Q., 2017. Further development of a chemistry proxy for geometallurgical modelling at the Mogalakwena Mine. J. South. African Inst. Min. Metall. 117, 719–726. doi:10.17159/2411-9717/2017/v117n7a13

Schwechten, D., Schonert, K., 1986. Wet operation of high compression roller mills, in: World Congress on Particle Technology, 16-18 April 1986, Nurenberg, Germany. pp. 443–457.

Seke, M.D., Pistorius, P.C., 2006. Effect of cuprous cyanide, dry and wet milling on the selective flotation of galena and sphalerite. Miner. Eng. 19, 1–11. doi:10.1016/j.mineng.2005.03.005

Shapiro, M., Galperin, V., 2005. Air classification of solid particles: A review. Chem. Eng. Process. Process Intensif. 44, 279–285. doi:10.1016/j.cep.2004.02.022

Shoji, K., Meguri, N., Sato, K., Kanemoto, H., 1998. Breakage of coals in ring-roller mills Part 2. An unsteady-state simulation model. Powder Technol. 99, 46–52.

Simmons, M., Gorby, L., Terembula, J., 2005. Operational experience from the United States' first vertical roller mill for cement grinding, in: IEEE Cement Industry Technical Conference 15-20 May 2005, Kansas City, USA. pp. 241–249. doi:10.1109/CITCON.2005.1516366

Smith, J.W., Holwell, D.A., McDonald, I., 2014. Precious and base metal geochemistry and mineralogy of the Grasvally Norite–Pyroxenite–Anorthosite (GNPA) member, Northern

Bushveld Complex, South Africa: Implications for a multistage emplacement. Miner. Depos. 49, 667–692. doi:10.1007/s00126-014-0515-6

Solomon, N., Becker, M., Mainza, A., Petersen, J., Franzidis, J.P., 2011. Understanding the influence of HPGR on PGM flotation behavior using mineralogy. Miner. Eng. 24, 1370–1377. doi:10.1016/j.mineng.2011.07.015

Tamashige, T., Obana, H., Hamaguchi, M., 1991. Operational results of OK series roller mill. IEEE Trans. Ind. Appl. 27, 416–424. doi:10.1109/28.81821

Tavares, L.M., 2005. Particle weakening in high-pressure roll grinding. Miner. Eng. 18, 651–657. doi:10.1016/j.mineng.2004.10.012

Thiel, J., Schössow, C., 2001. Shot coke grinding in ball race mills. ZKG Int. 54, 630–637.

Trahar, W.J., 1981. A rational interpretation of the role of particle size in flotation. Int. J. Miner. Process. 8, 289–327. doi:10.1016/0301-7516(81)90019-3

Tromans, D., 2008. Mineral comminution: Energy efficiency considerations. Miner. Eng. 21, 613–620. doi:10.1016/j.mineng.2007.12.003

Valine, S.B., Wheeler, J.E., Albuquerque, L.G., 2009. Fine sizing with Derrick Stack Sizer Screen, in: Recent Advances in Mineral Processing Plant Design. D. Malhotra, P.R. Taylor, E. Spiller & M. LeVier, Eds. Society for Mining, Metallurgy, and Exploration., Littleton, Colorado. pp. 433–443.

van der Plas, L., Tobi, A.C., 1965. A chart for judging the reliability of point counting results. Am. J. Sci. 263, 87–90.

van der Meer, F.P., Maphosa, W., 2012. High pressure grinding moving ahead in copper, iron, and gold processing. J. South. African Inst. Min. Metall. 112, 637–647.

van Drunick, W., Gerold, C., Palm, N., 2010. Implementation of an energy efficient dry grinding technology into an Anglo American zinc beneficiation process, in: XXV International Mineral Processing Congress (IMPC), 6-10 September 2010, Brisbane, Australia. pp. 1333–1341.

Verrelli, D.I., Bruckard, W.J., Koh, P.T.L., Schwarz, M.P., Follink, B., 2012. Influence of particle shape and roughness on the induction period for particle-bubble attachment, in: XXVI International Minerals Processing Congress, 24-28 September, New Delhi, India. pp. 5665–5676.

Viljoen, R., Smit, J., Du Plessis, I., Ser, V., 2001. The development and application of in-bed compression breakage principles. Miner. Eng. 14, 465–471.

Wahl, W., 1994. Improving the wear protection on the grinding rollers in roller grinding mills. ZKG Int. 47, 167–170.

Wang, G., Nguyen, A. V., Mitra, S., Joshi, J.B., Jameson, G.J., Evans, G.M., 2016. A review of the mechanisms and models of bubble-particle detachment in froth flotation. Sep. Purif. Technol. 170, 155–172. doi:10.1016/j.seppur.2016.06.041

Wang, L., Peng, Y., Runge, K., Bradshaw, D., 2015. A review of entrainment: Mechanisms, contributing factors and modelling in flotation. Miner. Eng. 70, 77–91. doi:10.1016/j.mineng.2014.09.003

Wiese, J., Harris, P., Bradshaw, D., 2005. The influence of the reagent suite on the flotation of

ores from the Merensky reef. Miner. Eng. 18, 189–198. doi:10.1016/j.mineng.2004.09.013

Wiese, J., Harris, P., Bradshaw, D., 2006. The role of the reagent suite in optimising pentlandite recoveries from the Merensky reef. Miner. Eng. 19, 1290–1300. doi:10.1016/j.mineng.2006.04.003

Wiese, J., Harris, P., Bradshaw, D., 2011. The effect of the reagent suite on froth stability in laboratory scale batch flotation tests. Miner. Eng. 24, 995–1003. doi:10.1016/j.mineng.2011.04.011

Wills, B.A., Napier-Munn, T.J., 2006. Wills' Mineral Processing Technology: An Introduction to the Practical Aspects of Ore Treatment and Mineral Recovery, Rev. 7th ed. Elsevier Science & Technology Books. doi: 10.1016/B978-0-7506-4450-1.X5000-0

Wüstner, H., 1986. Energy-saving with the roller press comminution process. World Cem. 17, 94–96.

Xiao, Z., Laplante, A., 2004. Characterizing and recovering the platinum group minerals - A review. Miner. Eng. 17, 961–979. doi:10.1016/j.mineng.2004.04.001

Ye, X., Gredelj, S., Skinner, W., Grano, S.R., 2010. Regrinding sulphide minerals - Breakage mechanisms in milling and their influence on surface properties and flotation behaviour. Powder Technol. 203, 133–147. doi:10.1016/j.powtec.2010.05.002

Young, M.F., Pease, J.D., Johnson, N.W., Munro, P.D., 1997. Developments in milling practice at the lead/zinc concentrator of Mount Isa Mines Limited from 1990, in: 6th AusIMM Mill Operators' Conference 6-8 October 1997, Madang, Papua New Guinea. pp. 1-20

Zanin, M., Lambert, H., du Plessis, C.A., 2019. Lime use and functionality in sulphide mineral flotation: A review. Miner. Eng. 143, 105922. doi:10.1016/j.mineng.2019.105922

Zhou, G., Si, J., Taft, C.W., 2000. Modeling and simulation of C-E deep bowl pulverizer. IEEE Trans. Energy Convers. 15, 312–322. doi:10.1109/60.875498

Zhu, G., Wang, Y., Liu, X., Yu, F., Lu, D., 2015. The cleavage and surface properties of wet and dry ground spodumene and their flotation behavior. Appl. Surf. Sci. 357, 333–339. doi:10.1016/j.apsusc.2015.08.257

Chapter 9

APPENDICES

I. Flotation Procedure

The following list provides a detailed description of the vertical roller mill product flotation procedure:

1. Synthetic plant water added to the cell.
2. Impeller is started and adjusted to desired 1200 rpm rotational speed.
3. Dry 3.3 kg VRM products added to the flotation cell to make 35% solids.
4. The reagents SIBX and Senkol 3 added to the slurry and conditioned for 2 minutes.
5. The reagents Sendep 30D and XP200 added to the slurry and conditioned for 2 minutes.
6. Air flow to the cell was opened and adjusted to the desired rotameter reading (62.5).
    - Concentrate was collected as material overflowing the launder and with the assistance of a scraper, passing of the froth in 15 second intervals.
    - Slurry levels were maintained to retain a 1 cm froth layer.
    - Impeller rotational speed and air flow rate were monitored and maintained at the desired values.
7. The first concentrate was collected over 2 minutes. An associated wash bottle was used to rinse concentrate into the concentrate tray from the launder and scraper.
8. Concentrate tray and wash bottle were changed.
9. The second concentrate was collected over 6 minutes. An associated wash bottle was used to rinse concentrate into the concentrate tray from the launder and scraper.
10. Concentrate tray and wash bottle were changed.
11. The third concentrate was collected over 12 minutes. An associated wash bottle was used to rinse concentrate into the concentrate tray from the launder and scraper.
12. Air flow to the flotation cell was stopped.
13. The reagents SIBX and Senkol 3 were added to the slurry and conditioned for 2 minutes.
14. Concentrate tray and wash bottle were changed.
15. The reagents Sendep 30D and XP200 were added to the slurry and conditioned for 2 minutes.
16. Air flow to the cell was opened.
17. The fourth concentrate was collected over 10 minutes. An associated wash bottle was used to rinse concentrate into the concentrate tray from the launder and scraper.

18. Concentrate tray and wash bottle were changed.
19. The fifth concentrate was collected over 10 minutes. An associated wash bottle was used to rinse concentrate into the concentrate tray from the launder and scraper.
20. Air flow to the flotation cell and impeller were stopped.
21. Slurry was drained from the flotation cell, filtered and dried.
22. Concentrates, wash bottles and trays were weighed.
23. Concentrates were individually filtered on weighed filter paper, dried in an oven and reweighed.
24. Dried samples were individually bagged.
25. Assay samples were delumped as required.

For the tumbling mill flotation test work the steps 1 - 3 involve adding the slurry for the batch milling test to the flotation cell and then adding plant water to achieve the required 35% solids before switching on the impeller.

II. Laser Sizing Particle Size Distributions

Grinding Pressure

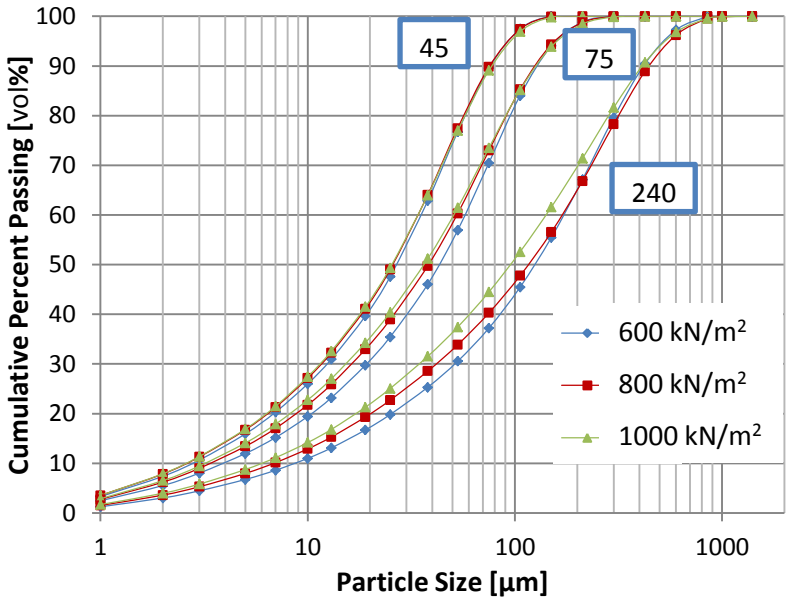

Figure 9-1: Particle size distribution generated by laser particle sizing for different target products (P_{80}: 45, 75 and 240 µm) and grinding pressures at the lowest dam ring height (4 mm).

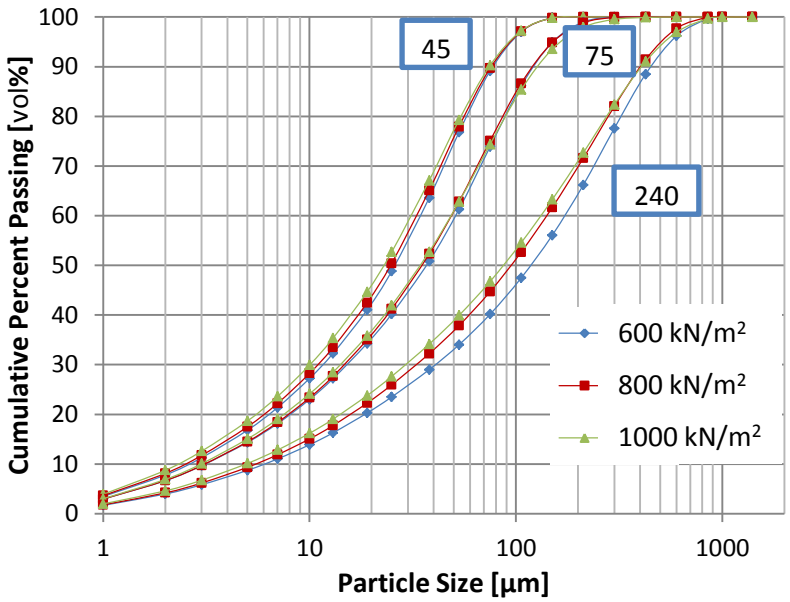

Figure 9-2: Particle size distribution generated by laser particle sizing for different target products (P_{80}: 45, 75 and 240 µm) and grinding pressures at the intermediate dam ring height (7 mm).

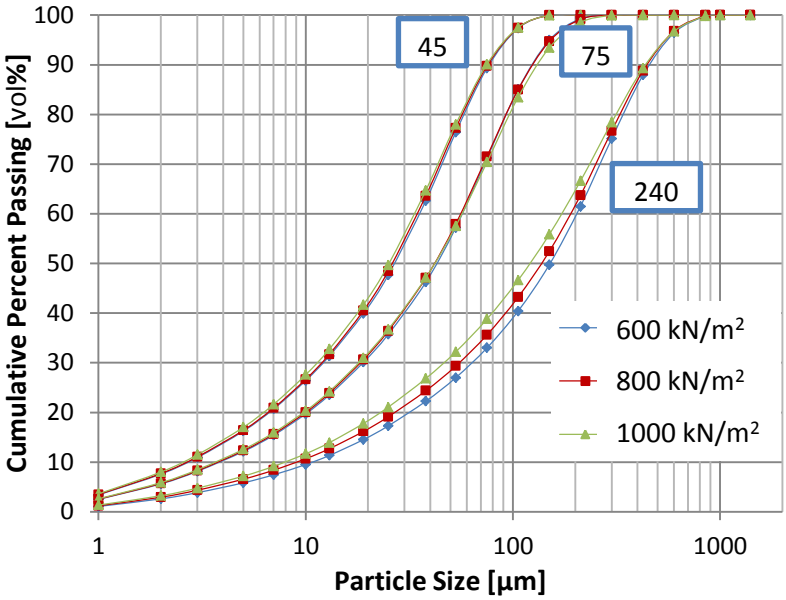

Figure 9-3: Particle size distribution generated by laser particle sizing for different target products (P_{80}: 45, 75 and 240 µm) and grinding pressures at the largest dam ring height (14 mm).

Dam Ring Height

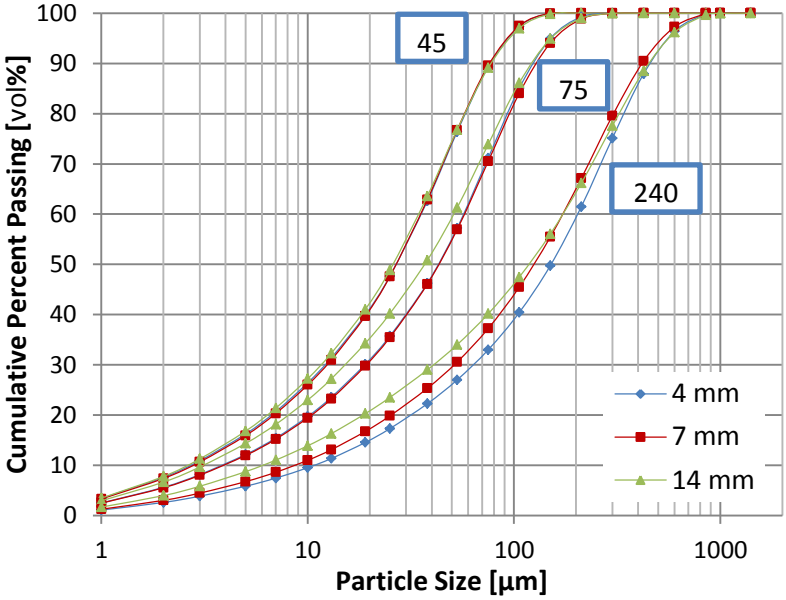

Figure 9-4: Particle size distribution generated by laser particle sizing for different target products (P_{80}: 45, 75 and 240 µm) and dam ring heights at the lowest grinding pressure (600 kN/m²).

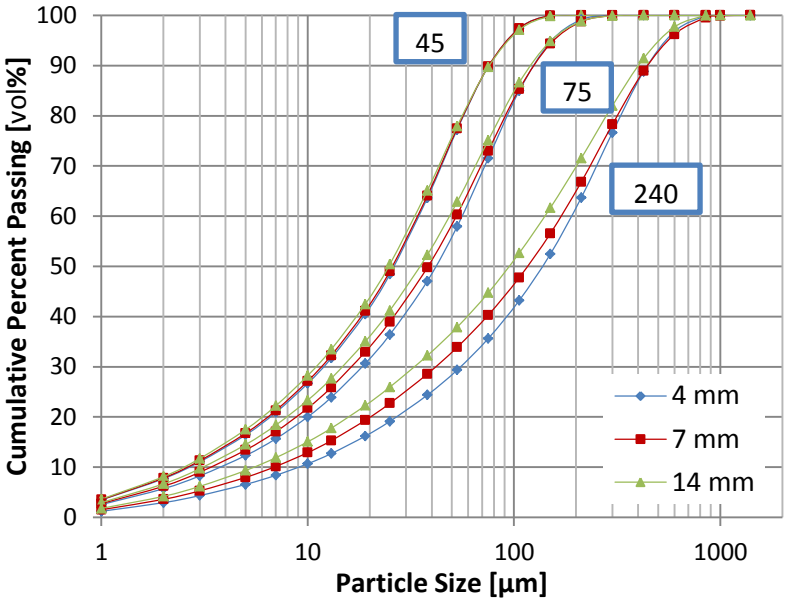

Figure 9-5: Particle size distribution generated by laser particle sizing for different target products (P_{80}: 45, 75 and 240 µm) and dam ring heights at the intermediate grinding pressure (800 kN/m²).

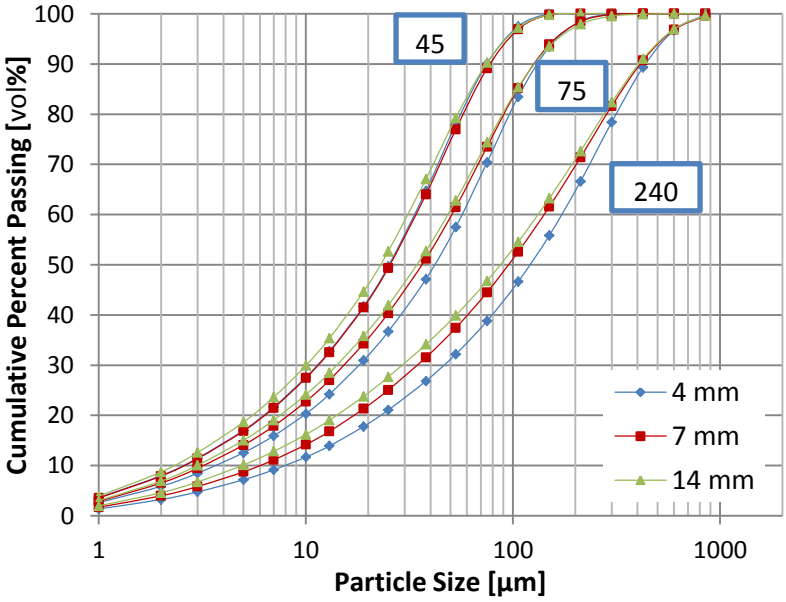

Figure 9-6: Particle size distribution generated by laser particle sizing for different target products (P_{80}: 45, 75 and 240 µm) and dam ring heights at the highest grinding pressure (1000 kN/m²).

III. Particle Size Distributions

Dam Ring Height

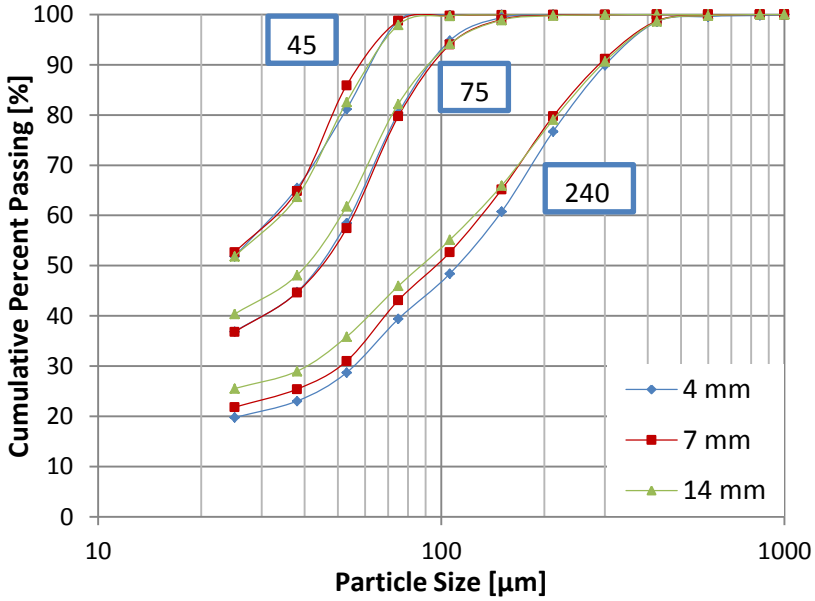

Figure 9-7: Particle size distribution generated by sieving for different target products (P_{80}: 45, 75 and 240 µm) and dam ring heights at the lowest grinding pressure (600 kN/m²).

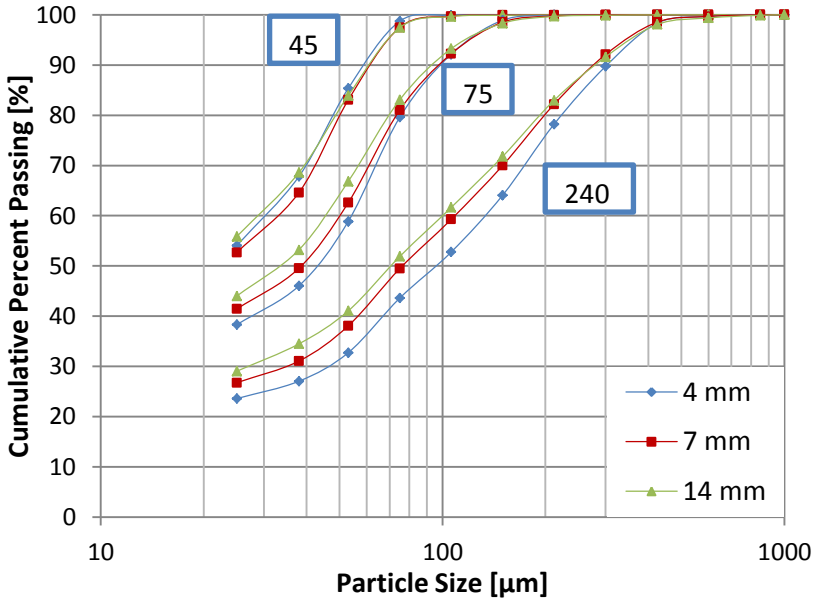

Figure 9-8: Particle size distribution generated by sieving for different target products (P_{80}: 45, 75 and 240 µm) and dam ring heights at the highest grinding pressure (1000 kN/m²).

IV. Classifier Speed - Throughput Plots

Grinding Pressure

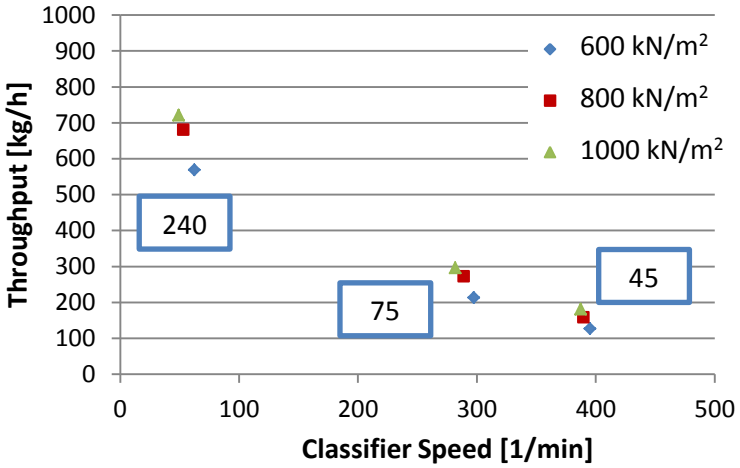

Figure 9-9: Vertical roller mill throughput - classifier rotor rotational speed relationship for tests carried out at the lowest (4 mm) dam ring height.

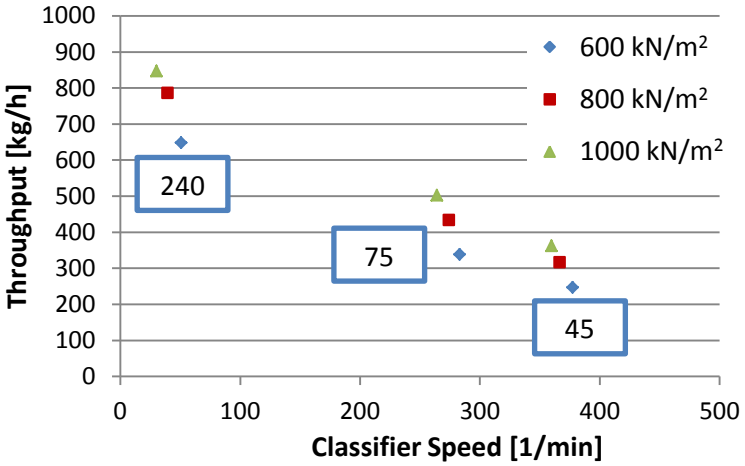

Figure 9-10: Vertical roller mill throughput - classifier rotor rotational speed relationship for tests carried out at the highest (14 mm) dam ring height.

Dam Ring Height

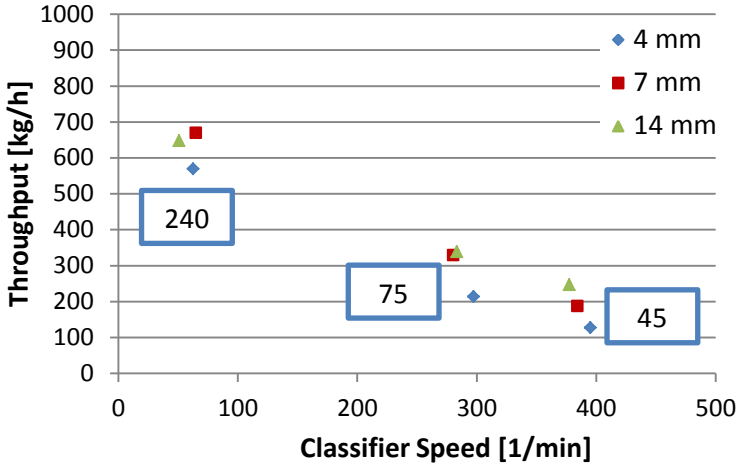

Figure 9-11: Vertical roller mill throughput - classifier rotor rotational speed relationship for tests carried out at the lowest (600 kN/m²) grinding pressure.

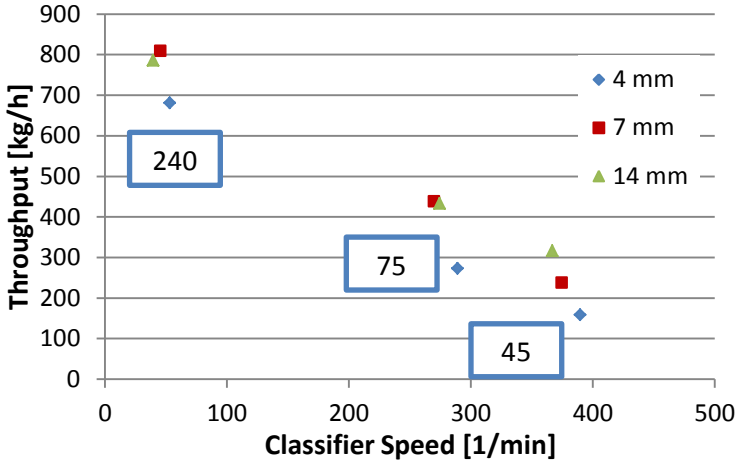

Figure 9-12: Vertical roller mill throughput - classifier rotor rotational speed relationship for tests carried out at the intermediate (800 kN/m²) grinding pressure.

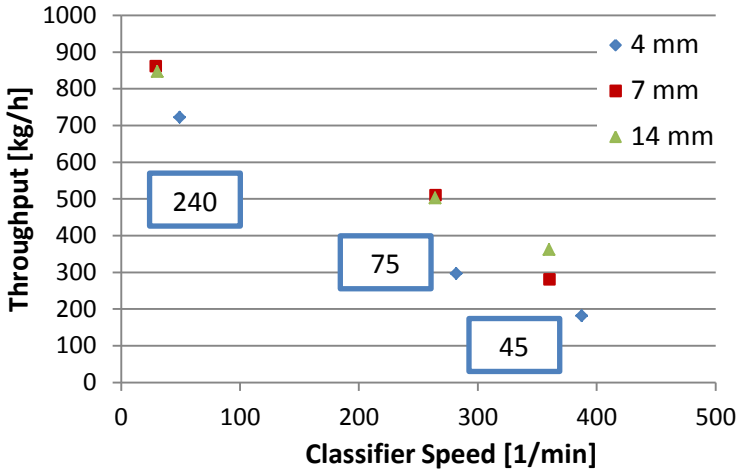

Figure 9-13: Vertical roller mill throughput - classifier rotor rotational speed relationship for tests carried out at the highest (1000 kN/m²) grinding pressure.

V. Bulk Mineralogy

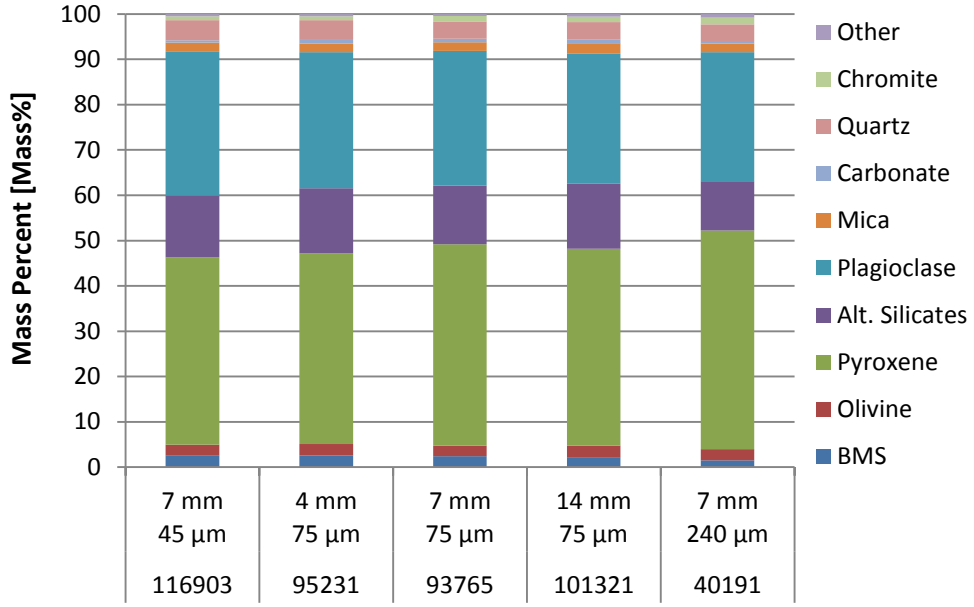

Figure 9-14: Bulk mineralogy for the samples analysed, where n is the number of particles analysed.

Table 9-1: Bulk mineralogy for the samples analysed.

Number of particles	116903	95231	93765	101321	40191
Dam Ring Height [mm]	7 mm	4 mm	7 mm	14 mm	7 mm
P_{80} [µm]	45 µm	75 µm	75 µm	75 µm	240 µm
Mineral			**wt%**		
Chalcopyrite	0.46	0.61	0.46	0.33	0.24
Pentlandite	0.52	0.55	0.45	0.50	0.30
Pyrrhotite	1.59	1.36	1.49	1.21	0.94
Other BMS	0.03	0.00	0.01	0.00	0.00
Olivine	2.39	2.57	2.36	2.67	2.52
Talc	3.99	3.89	3.31	3.80	2.59
OPX	29.27	28.22	30.80	30.03	33.34
CPX	12.01	13.94	13.60	13.48	14.88
Amphibole	1.96	1.99	1.85	2.01	1.04
Serpentine	0.66	0.58	0.49	0.62	0.98
Chlorite	7.07	7.86	7.27	7.88	6.31
Plagioclase	31.71	30.00	29.76	28.67	28.49
Mica	2.02	1.96	1.88	2.38	1.85
Carbonate	0.55	0.93	0.80	0.79	0.57
Quartz	4.46	4.17	3.81	3.83	3.71
Chromite	0.84	0.86	1.19	1.23	1.47
Other	0.48	0.52	0.46	0.57	0.79

VI. Solids and Water Recovery Plots

Product Size

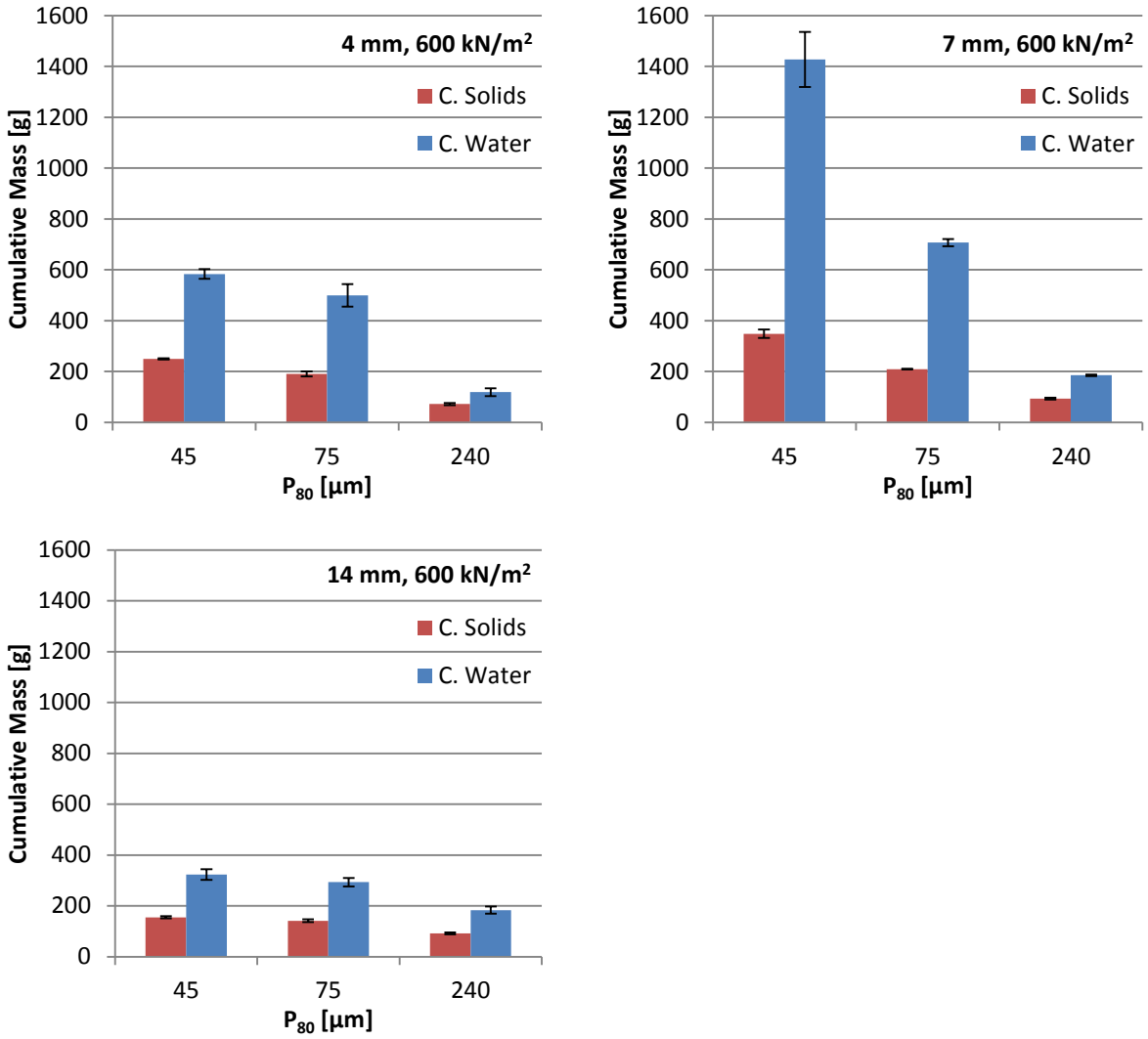

Figure 9-15: Solids and water recoveries plots for batch flotation tests performed on VRM products, illustrating the variation with product size for grinding pressure and dam ring heights of 600 kN/m² & 4 mm, 600 kN/m² & 7 mm and 600 kN/m² & 14 mm.

Grinding Pressure

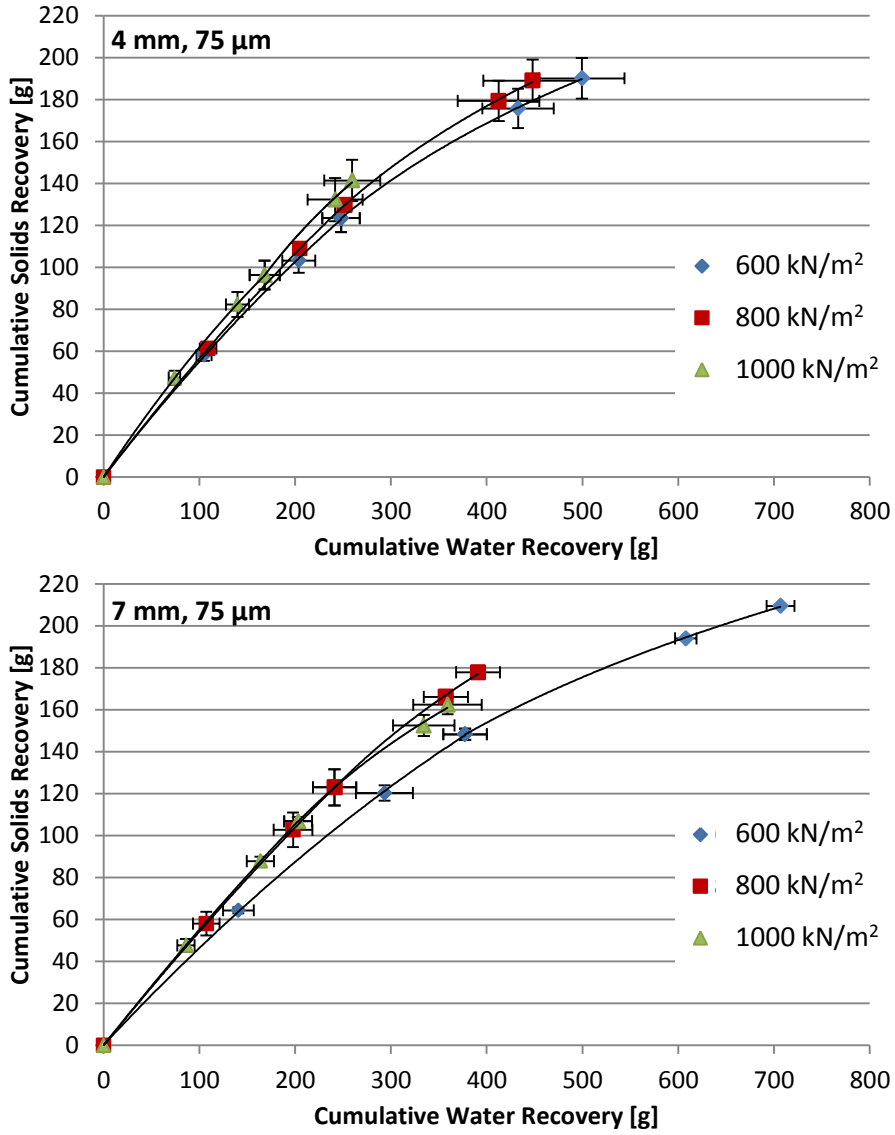

Figure 9-16: Cumulative solids - water recovery plots for batch flotation tests performed on VRM products, illustrating the variation with grinding pressure for product sizes of 75 µm and dam ring heights 4 mm and 7 mm.

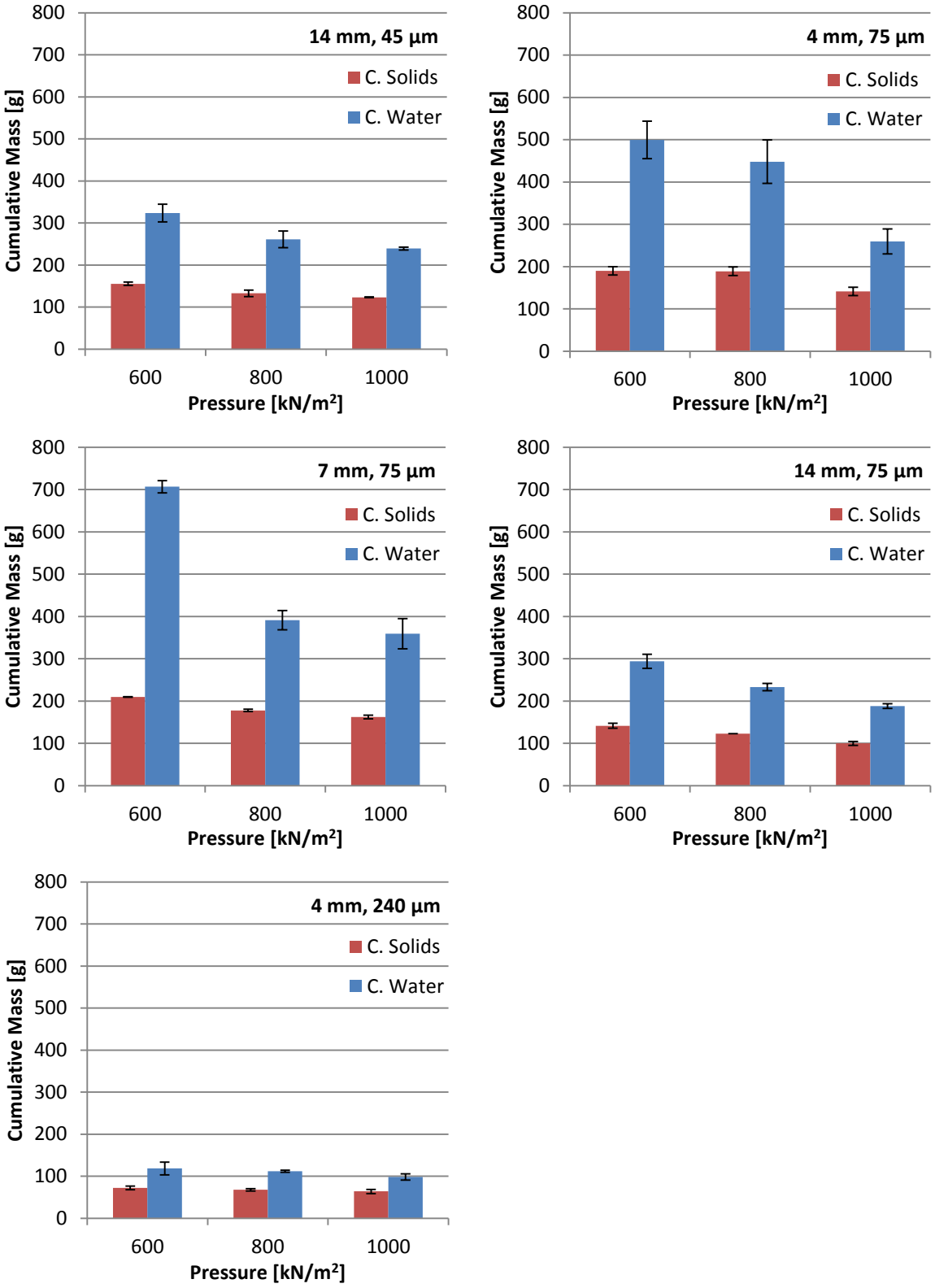

Figure 9-17: Solids and water recoveries plots for batch flotation tests performed on VRM products, illustrating the variation with grinding pressure for product size and dam ring heights of 45 µm & 14 mm, 75 µm & 4 mm, 75 µm & 7 mm, 75 µm & 14 mm and 240 µm & 4 mm.

Dam Ring Height

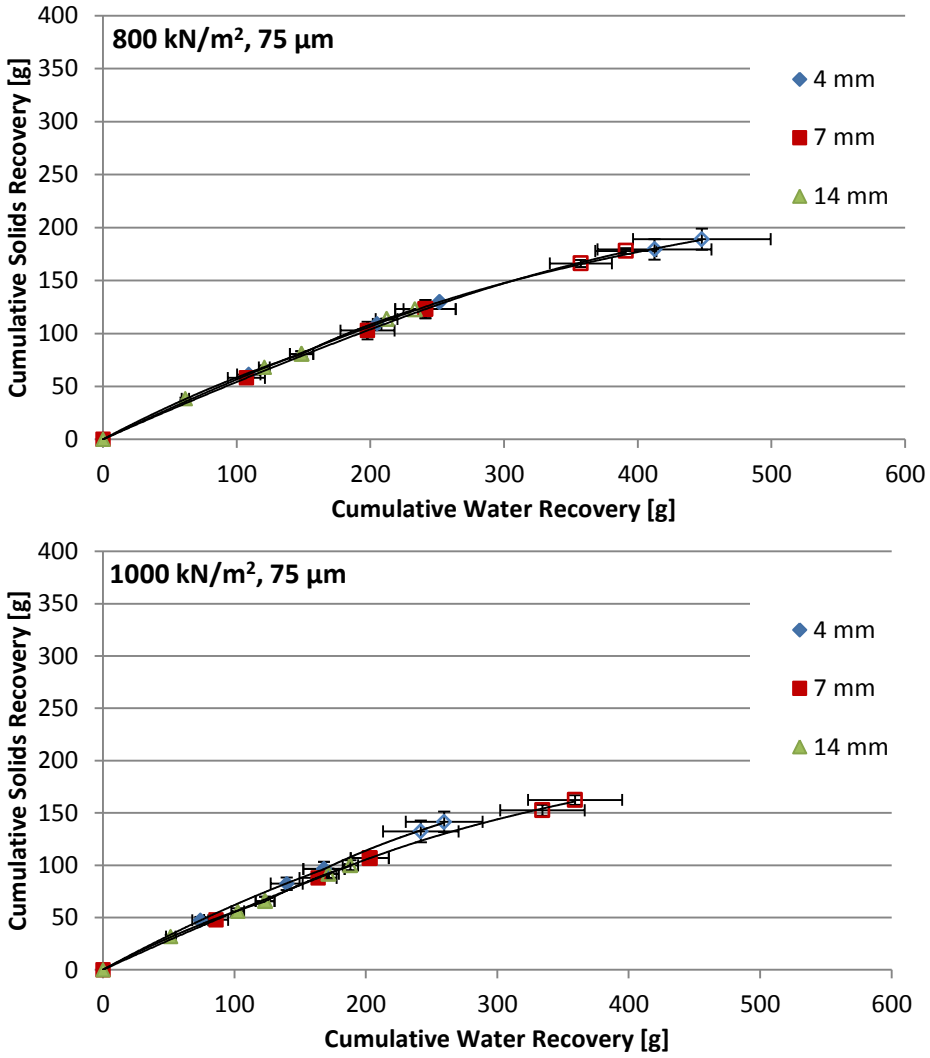

Figure 9-18: Cumulative solids - water recovery plots for batch flotation tests performed on VRM products, illustrating the variation with dam ring height for product sizes of 75 µm at grinding pressures of 800 and 1000kN/m².

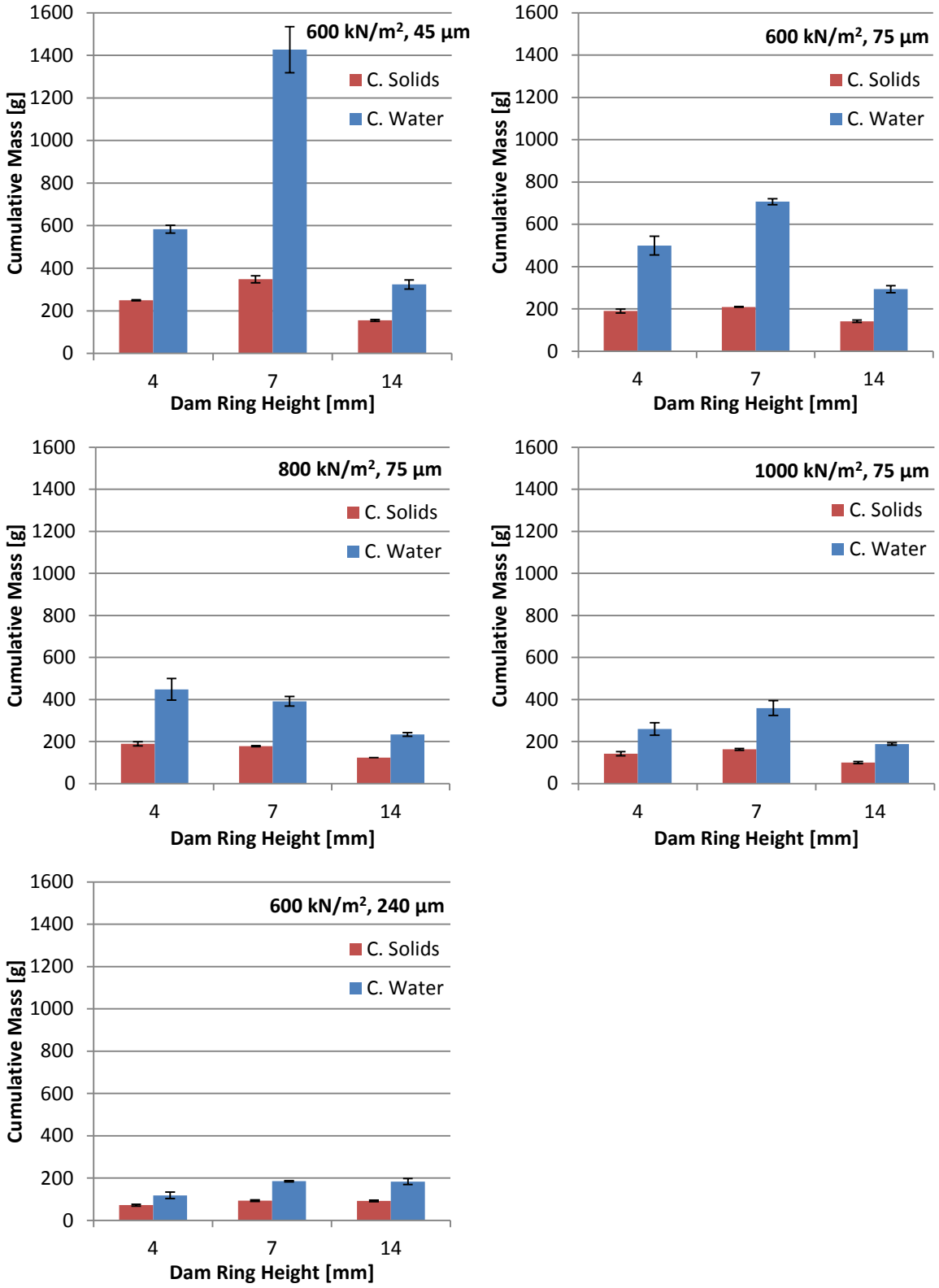

Figure 9-19: Solids and water recoveries plots for batch flotation tests performed on VRM products, illustrating the variation with dam ring height for product size and grinding pressures of 45 µm & 600 kN/m², 75 µm & 600 kN/m², 75 µm & 800 kN/m², 75 µm & 1000 kN/m² and 240 µm & 600 kN/m².

Screening

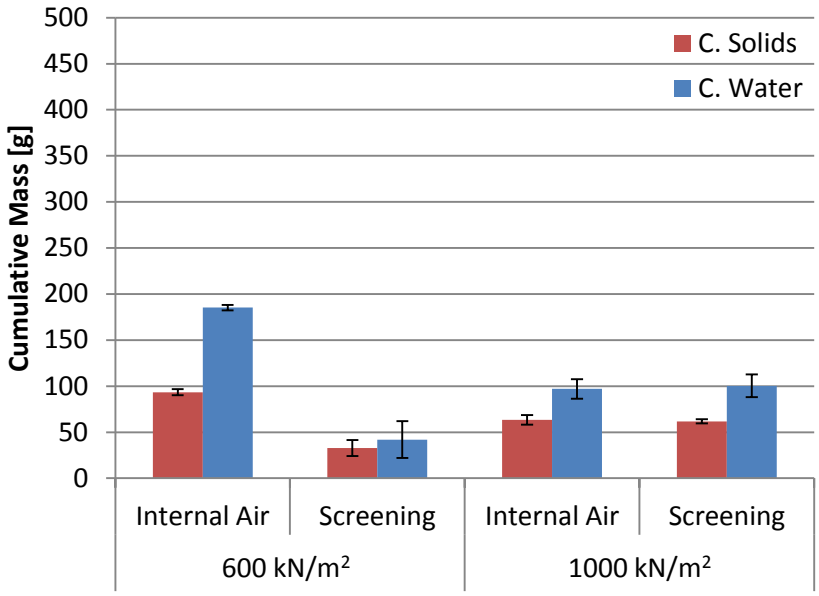

Figure 9-20: Solids and water recoveries plots for batch flotation tests performed on VRM products generated when operated in conjunction with the internal air classifier and an external screen, illustrating the variation with grinding pressure.

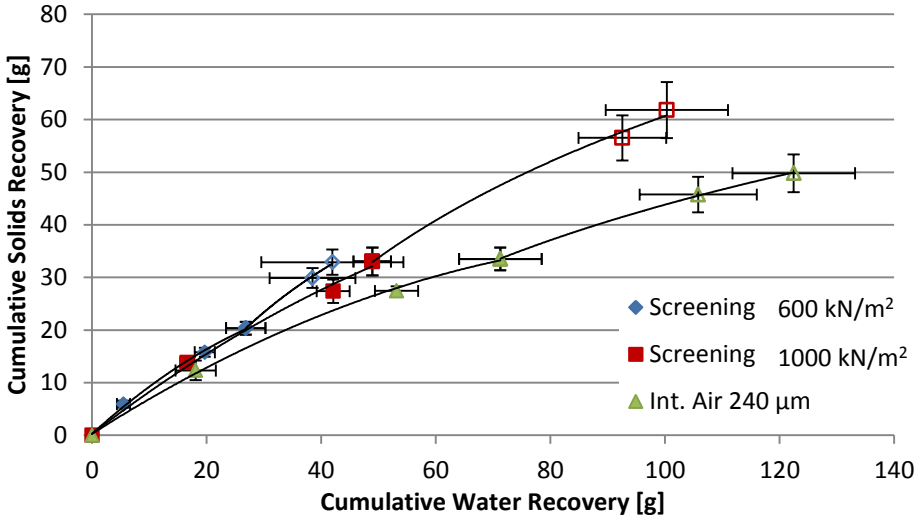

Figure 9-21: Cumulative solids - water recovery plots for batch flotation tests performed on VRM products prepared with the internal air classifier and an external screen, illustrating the variation with grinding pressure.

Internal and External Air Classification

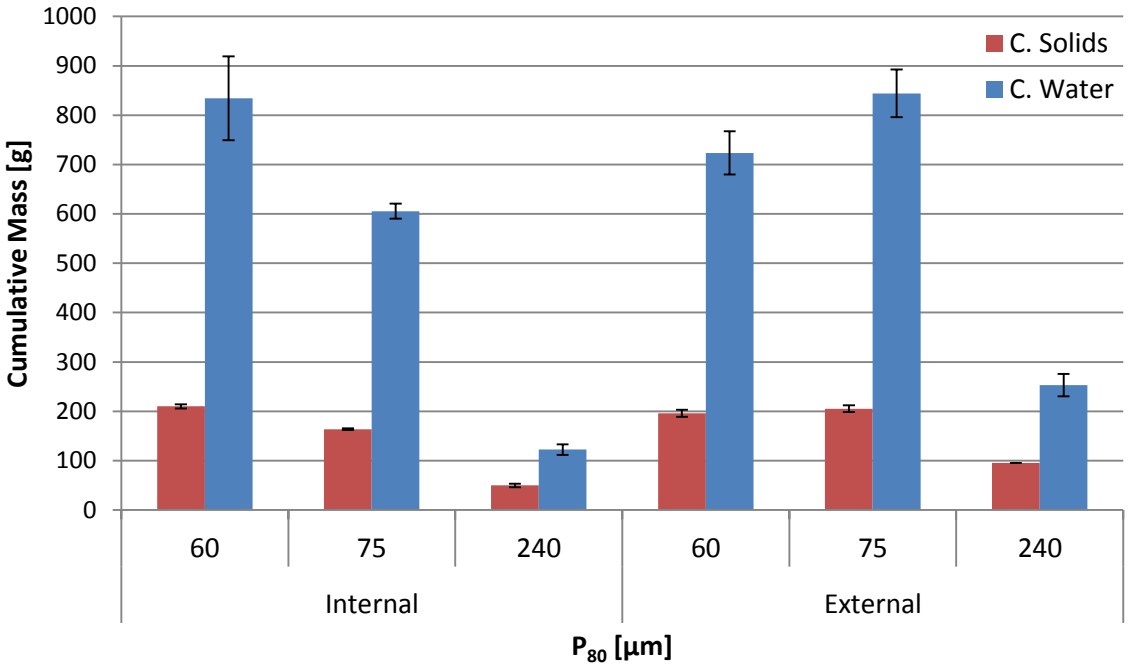

Figure 9-22: Solids and water recoveries plots for batch flotation tests performed on VRM products of different target P_{80} values, generated when operated in conjunction with the internal air classifier and an external air classifier.

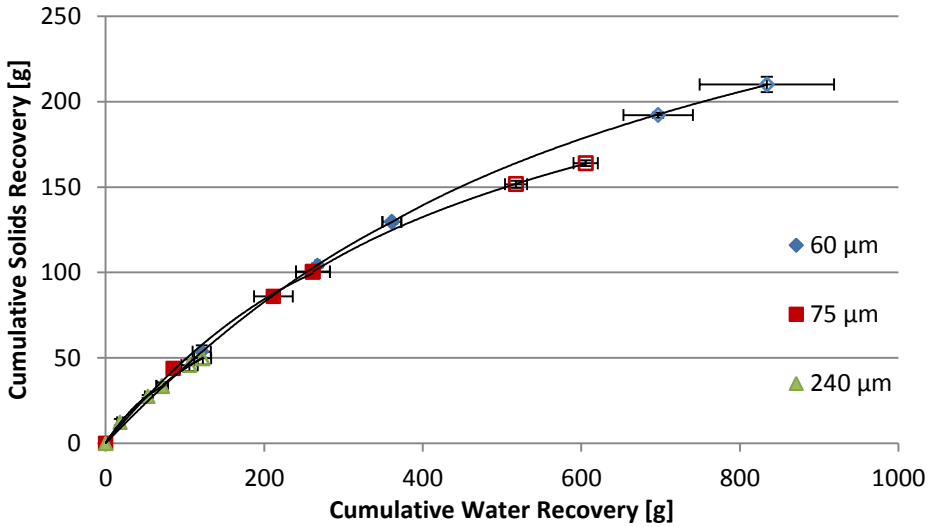

Figure 9-23: Cumulative solids - water recovery plots for batch flotation tests performed on VRM products of different target P_{80} values, generated when operated in conjunction with the internal air classifier.

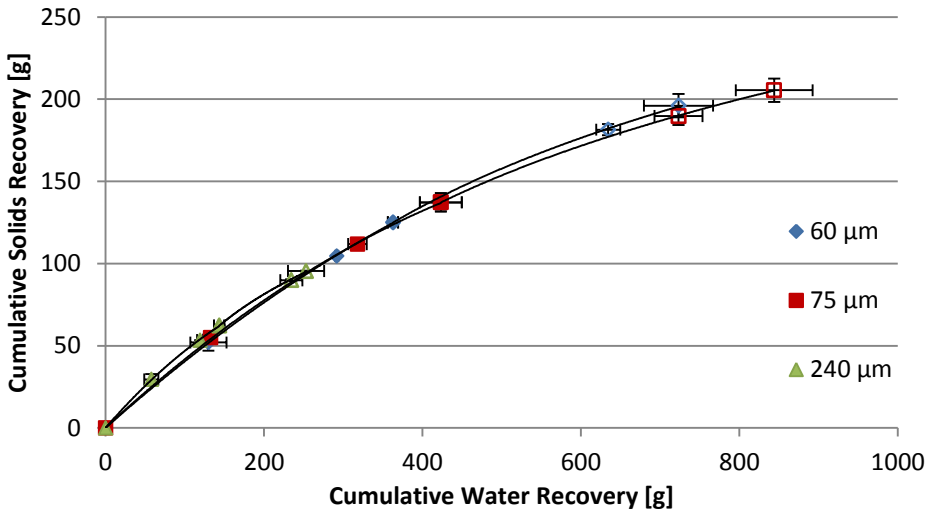

Figure 9-24: Cumulative solids - water recovery plots for batch flotation tests performed on VRM products of different target P_{80} values, generated when operated in conjunction with the external air classifier.

VII. Flotation Base Metal Grade and Recovery Plots

Product Size

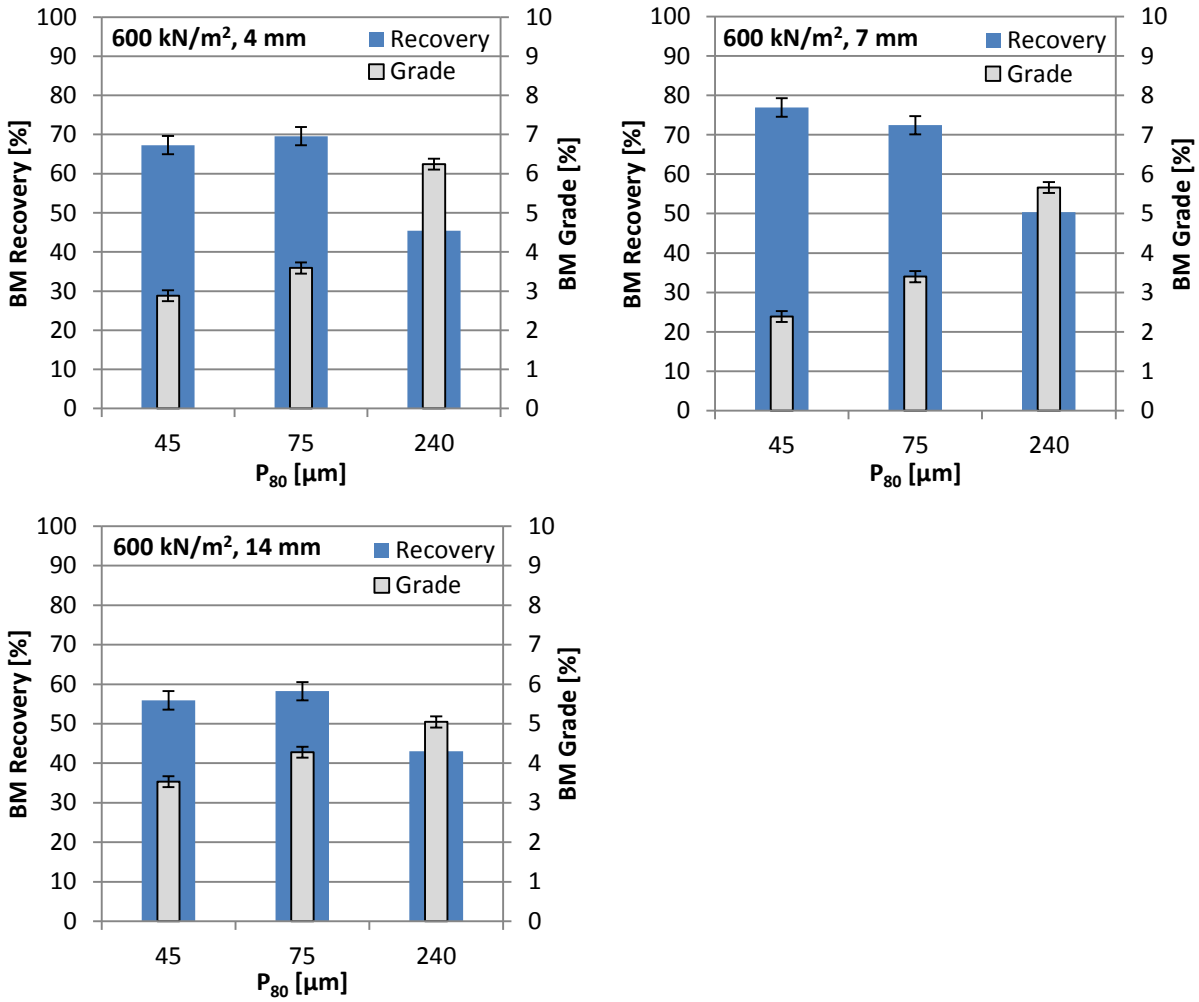

Figure 9-25: Base metal (Ni, Cu) cumulative grade and recovery plots for batch flotation tests performed on VRM products, illustrating the variation with product size for grinding pressure and dam ring heights of 600 kN/m² & 4 mm, 600 kN/m² & 7 mm and 600 kN/m² & 14 mm.

Grinding Pressure

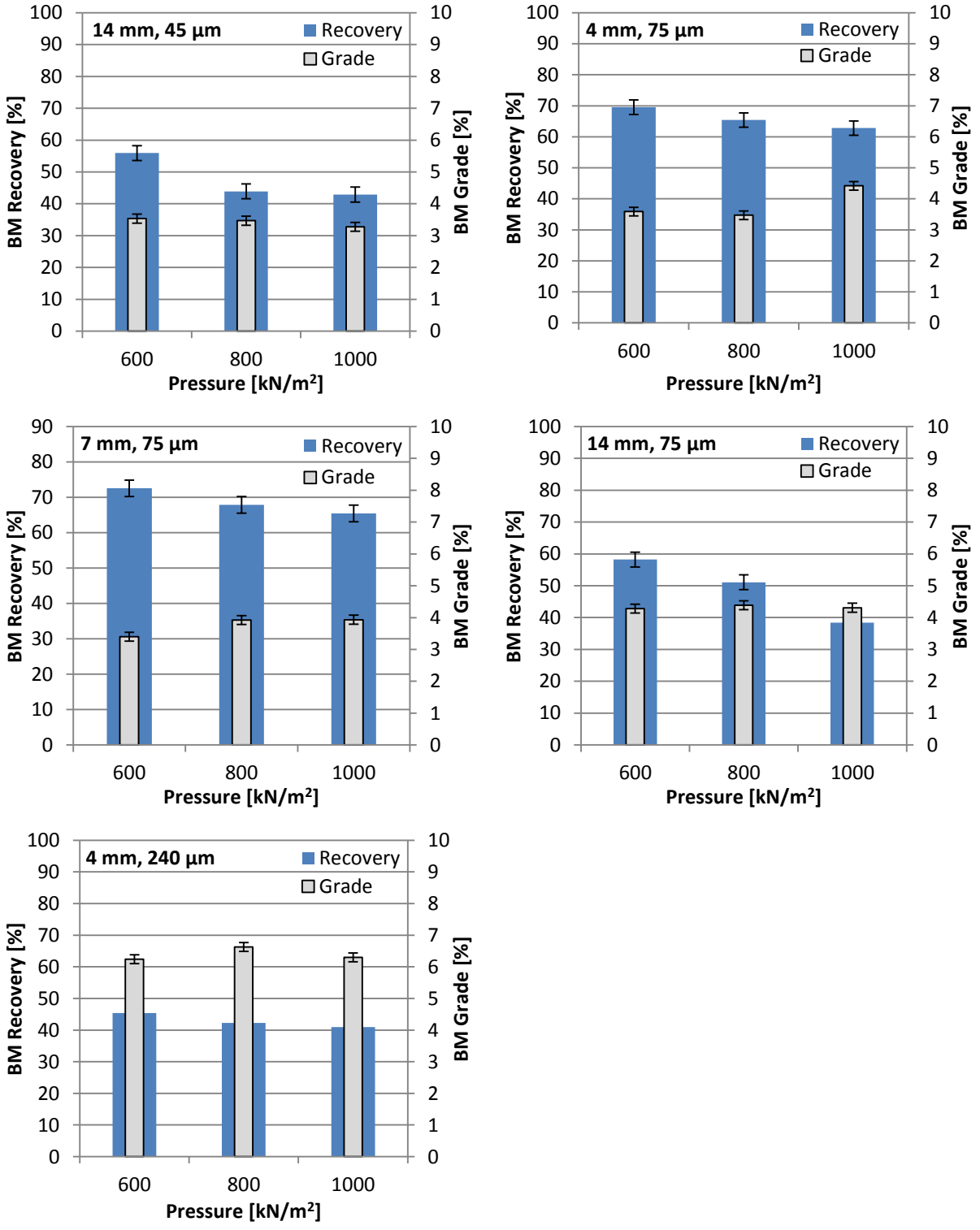

Figure 9-26: Base metal (Ni, Cu) cumulative grade and recovery plots for batch flotation tests performed on VRM products, illustrating the variation with grinding pressure for product size and dam ring heights of 45 µm & 14 mm, 75 µm & 4 mm, 75 µm & 7 mm, 75 µm & 14 mm and 240 µm & 4 mm.

Dam Ring Height

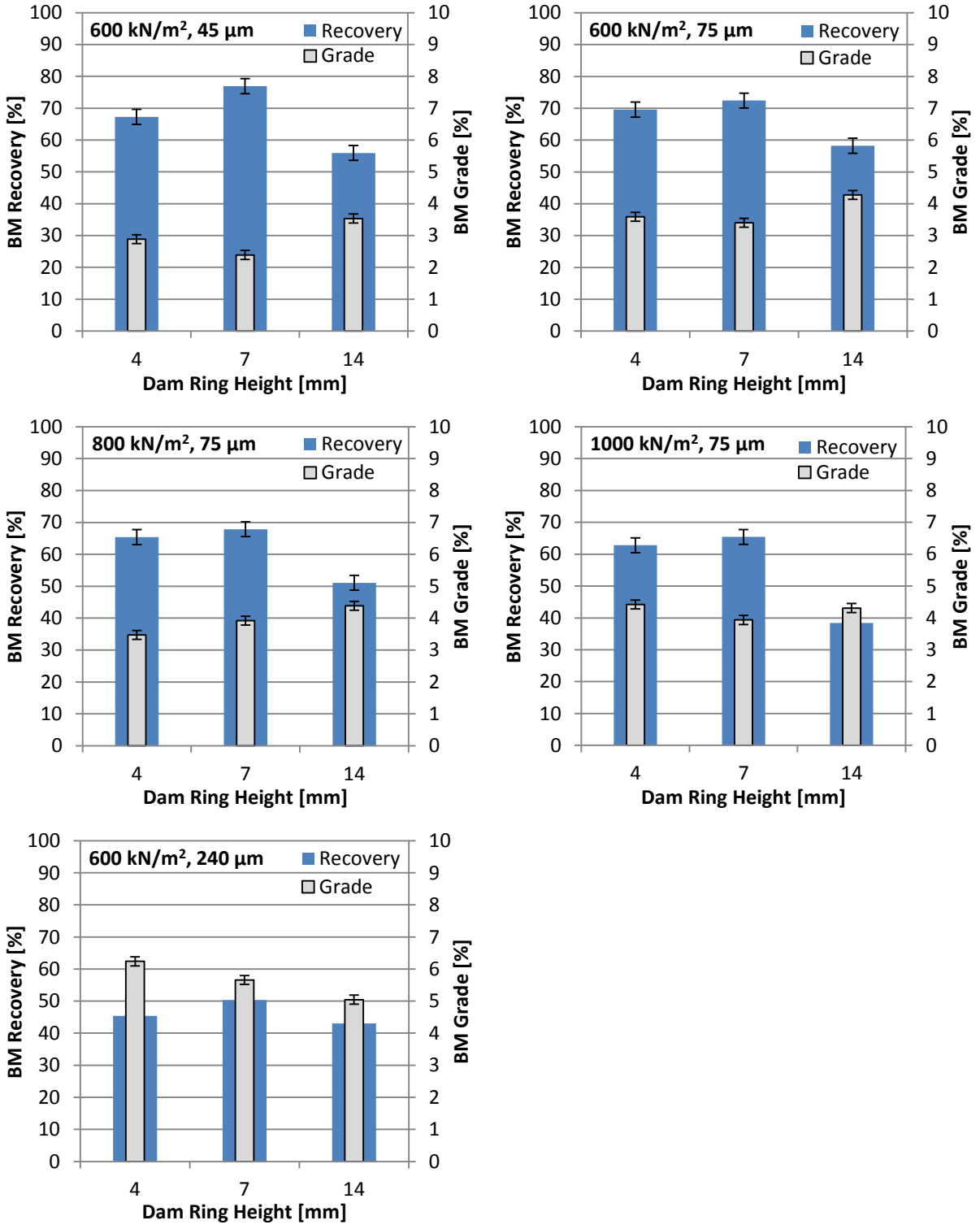

Figure 9-27: Base metal (Ni, Cu) cumulative grade and recovery plots for batch flotation tests performed on VRM products, illustrating the variation with dam ring height for product size and grinding pressures of 45 µm & 600 kN/m², 75 µm & 600 kN/m², 75 µm & 800 kN/m², 75 µm & 1000 kN/m² and 240 µm & 600 kN/m².

Screening

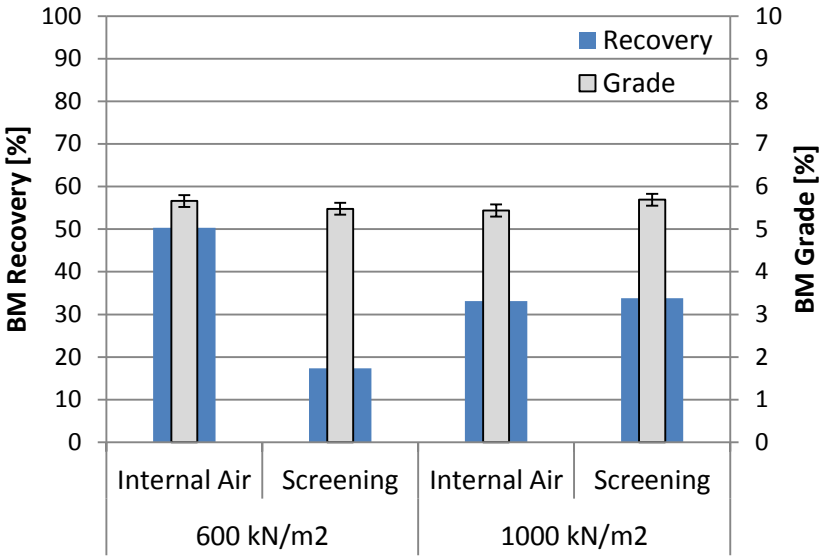

Figure 9-28: Base metal (Ni, Cu) cumulative grade and recovery plots for batch flotation tests performed on VRM products generated when operated in conjunction with the internal air classifier and an external screen.

VIII. Grinding Parameter in External Classification

Mechanical Power

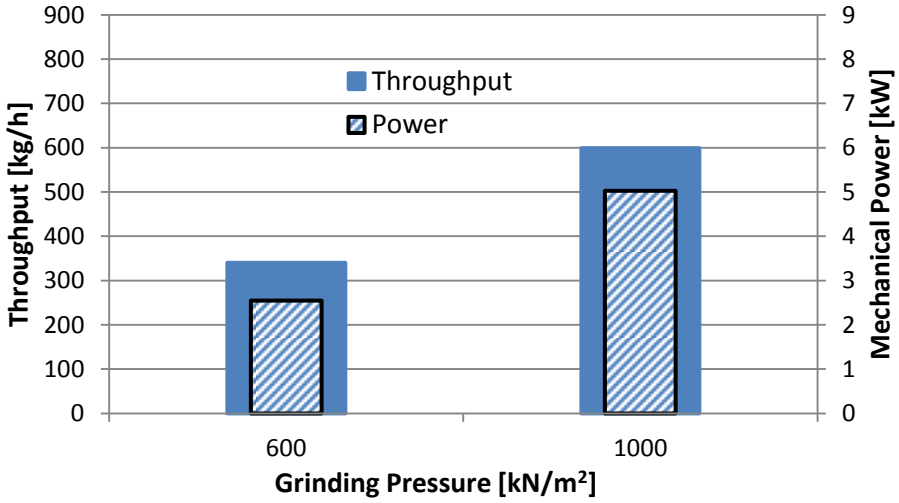

Figure 9-29: Throughputs and mechanical power for the vertical roller mill operated in circuit with an external screen, at the grinding pressures 600 and 1000 kN/m².

Bed Height

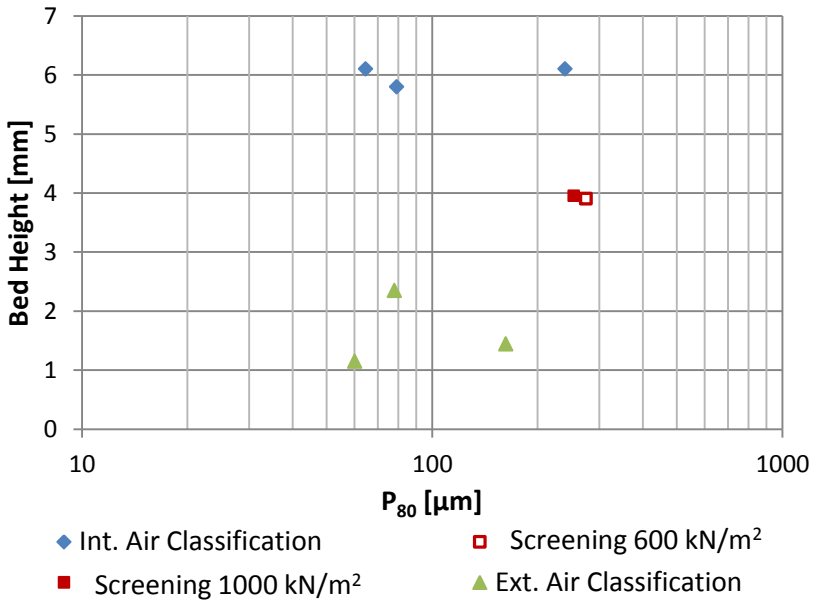

Figure 9-30: Variation in bed depth with product size for the internal and external air classification tests.